80AP

PROJECT URP72; STUDY 4
ASSESSMENT OF DAMAGE TO OFFSHORE STRUCTURES, PIPELINES AND SUBSEA SYSTEMS

FINAL REPORT

REPORT NO WOL 109/86A OCTOBER 1986

PREPARED FOR UEG, BY
WIMPEY OFFSHORE ENGINEERS & CONSTRUCTORS LIMITED

PROJECT URP72; STUDY 4
ASSESSMENT OF DAMAGE TO OFFSHORE STRUCTURES, PIPELINES AND SUBSEA SYSTEMS

FINAL REPORT

CONTENTS

PROJECT URP72; STUDY 4

ASSESSMENT OF DAMAGE TO OFFSHORE STRUCTURES, PIPELINES AND SUBSEA SYSTEMS

FINAL REPORT

REPORT NO WOL 109/86A MAY 1986

1. INTRODUCTION

This study addresses the assessment of damage to steel offshore structures, pipelines and subsea systems. In addition, it relates the significance of damage to the philosophy of inspection planning. The study is one of several on various inspection related topics which form the UEG Project on Underwater Inspection (Project URP72).

The Draft version of this report was presented to the project steering group in June 1986. Comments made at that time and in subsequent communication between project participants and UEG have been collated by UEG and are incorporated into this final report where appropriate.

There were two broad areas of comment. Firstly, it was felt that the methods recommended were too complex for general use. It remains the opinion of the contractor, as stated at the steering group meeting, that any simplification which is also to be 'safe' would introduce unnecessary conservatism and much of the power of the techniques for cost saving would be lost. In comparison with the very high cost of obtaining the relevant data from a defect site, the cost difference between using a complex rather than a simple assessment technique is negligible. It is the aim of Section 6 of this report to bring the more sophisticated techniques within reach of the non-specialist engineer.

The second area of comment concerned the document layout and consequently its ease of use. Section 2 of the draft report has undergone minor changes in this final revision. Sections 3 and 4 of the draft have been amalgamated so that the objectives and the methods used in this study are now all contained in Section 3.

Section 5 of the Draft, entitled 'Information from the Industry' has been replaced by two Sections which treat the industry's experience of damage (Section 4 of this Volume) separately from the engineering data necessary for using the assessment techniques presented in Section 6. An important addition to Section 4 is a discussion on locations and modes of failure (Subsection 4.3). Apart from layout changes to give better integration with Section 6, the data capture Section (Section 5) is not significantly altered in content.

Section 6 is unaltered since the Draft.

Section 7, Development of an Optimised Inspection Strategy, has been rewritten. The methodology is unchanged but the presentation is simplified and additional flowcharts have been introduced to assist the user.

Section 8, which discusses the application of optimised inspection strategies, includes an additional section, 8.3, which attempts an evaluation of the benefit of adopting the methodologies described in Section 7.

2. THE ROLE OF DAMAGE ASSESSMENT IN OFFSHORE INSPECTION PLANNING

The ultimate objective of an inspection plan is to provide a level of reliability in each structural component commensurate with the consequences of its failure. For an offshore installation the possible consequences of failure include:

1. Loss of life.
2. Damage to the environment.
3. Lost production.
4. Costs of recovery/replacement of the facility.

The overriding philosophy in developing an inspection plan is to satisfy the relevant reliability objectives at minimum cost. The interests of the Certifying Authorities concern items 1. and 2.; the Operator is also concerned with items 3 and 4 and frequently applies more stringent inspection criteria on himself than those enforced by legislation. Nevertheless, inspection is generally based on a regular cycle; for example, in the North Sea, inspection is planned in step with 4 year (Norwegian) or 5 year (British Sector) recertification requirements. Many operators bias their routine inspection towards the components which, from structural analysis or historical information, are most likely to show premature damage.

Currently, then, an inspection plan is geared to respond to items susceptable to damage and a typical decision tree is given in Figure 2.1.

There are two ways in which it may be possible to refine the current philosophy to give a more cost effective inspection programme without increasing the risk to the structure. These two avenues form the basis of this study.

The first avenue concerns knowledge of defect behaviour. Currently, when a survey identifies damage, assessment of the damage is carried out and a decision is taken on remedial action. In fact, many compenents may be highly tolerant of defects. Using modern assessment techniques, understanding of the behaviour of crack-like defects has improved. If it can be shown that:

1. A crack of a given size is certain to develop very slowly under fatigue loading;

2. The defect will not cause catastrophic (brittle) or static failure of the component under maxinum storm loading;

then it may be possible to increase the period between inspections. This approach can be applied to any subsea component susceptable to fatigue damage, and parallel rationales could be applied to other types of damage. A review of the available techniques is the subject of Section 6.

The second avenue concerns a modified inspection philosophy and applies in particular to structures with built-in redundancy. Steel jackets fall into this category and much of the discussion on this approach is directed particularly to jacket inspection. Applicability in other areas is discussed in Section 8.

The modified approach to inspection starts from the question "what would be the impact of failure of component "j" on the integrity of the overall structure?" It can be seen that this is significantly different from the basis of current philosophy which asks "which of the components is most likely to show damage?"

An inspection programme based on this approach would start by classifying the components of a structure according to the following criteria:

- Consequence of damage in a specific component to the integrity of the installation.

- Possible failure modes (eg. fractures are most likely in tension members with significant fatigue loading, whereas buckling failures may occur in compression members exposed to impact damage).

- Likelihood of failure (quantified by a damage assessment), even when some damage has been identified.

- Cost and reliability of structural inspection.

Figures 2.2 and 2.3 show decision trees for this approach, and the topics above are discussed more fully in the following sections.

An "optimised" inspection programme would make use of the above techniques together with the current criteria for inspection. The hierarchy of questions to be addressed in the optimised strategy is:

- What are the effects of damage in component 'j' on the whole installation?
- Is component 'j', which is known to be defect critical, likely to show premature failure? (from analysis results, previous history, susceptibility to impact or corrosion damage).
- How stable is a small defect at site 'j'?
- What is the cost of ensuring that defects at site 'j' are identified in the field before they reach critical size?

In the context of inspection planning, damage assessment techniques are employed as follows:

- possible component failure modes are identified
- theoretical damage is postulated
- assessment techniques are used to indicate the criticality of the damaged component
- inspection is planned accordingly

It is not implied that inspection programmes developed on these lines will necessarily lead to instant and dramatic reductions in the amount of inspection carried out each year. Reliability of inspectors and techniques, coupled with service experience (which has shown that defects occur at unexpected sites), highlights the imprudence of dramatic reduction. Nevertheless, the greatest proportion of effort would be concentrated on defect critical components with some reductions elsewhere. It is envisaged that a well planned programme would reduce both the risk associated with and the cost of inspection.

Before the effectiveness of the strategy can be quantified it is necessary to review the reliability of available assessment techniques and those still being developed. These are the topics of subsequent sections. The cost effectiveness of this approach is influenced by:

- Cost of subsea inspection, and particularly DSV rates.
- Increased cost of analysis in developing the strategy.

Broadly, if one day of diving can be saved at the cost of a man year of engineering effort then the approach is economically worthwhile.

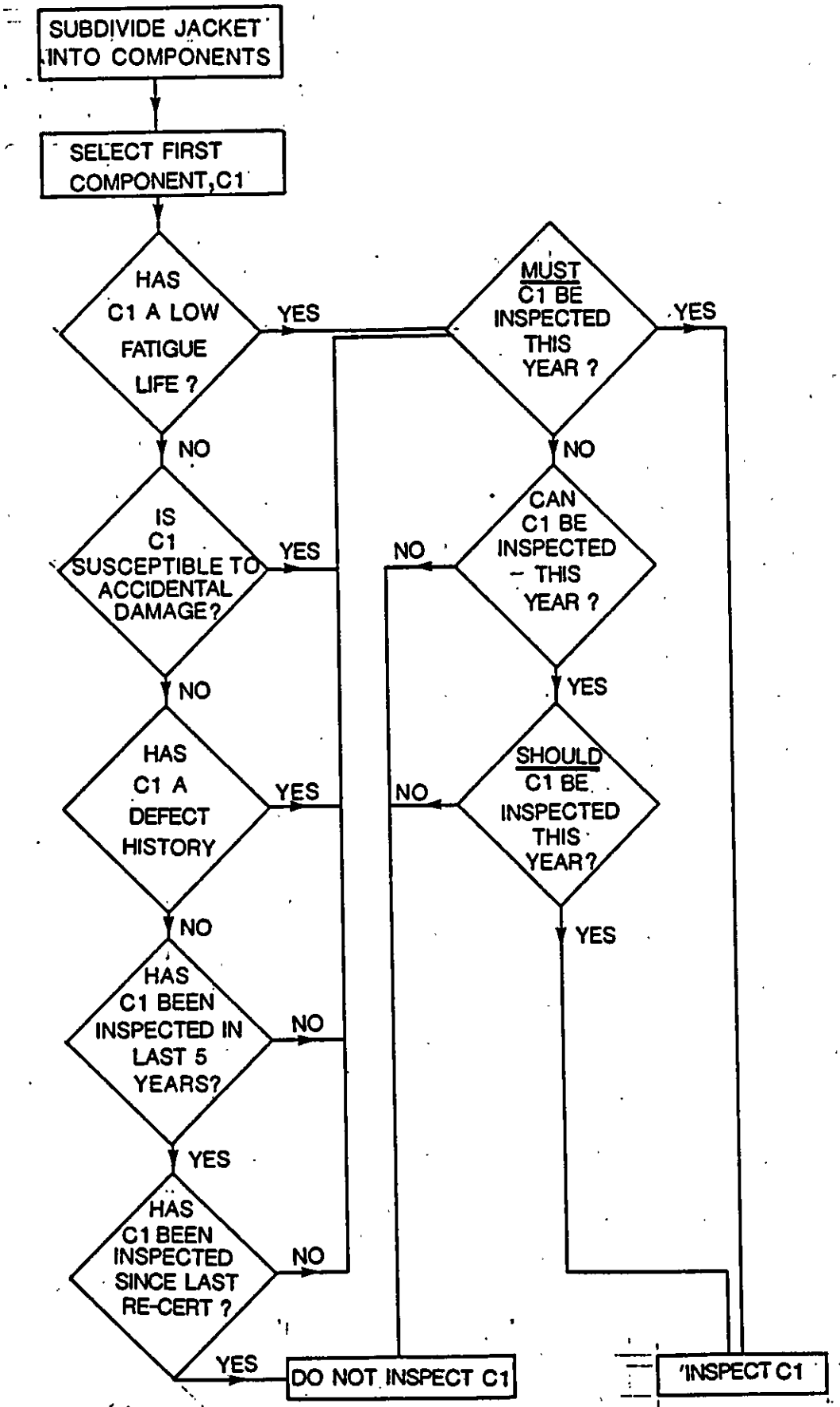

JACKET STRUCTURE: TYPICAL (SIMPLIFIED) PHILOSOPHY FOR INSPECTION PLANNING YEAR, 'n' CURRENT PRACTICE

PROJECT URP 72 : STUDY 4 INSPECTION PLANNING , THE ROLE OF DAMAGE ASSESSMENT	REPORT No. WOL109/86 FIG. 2·1

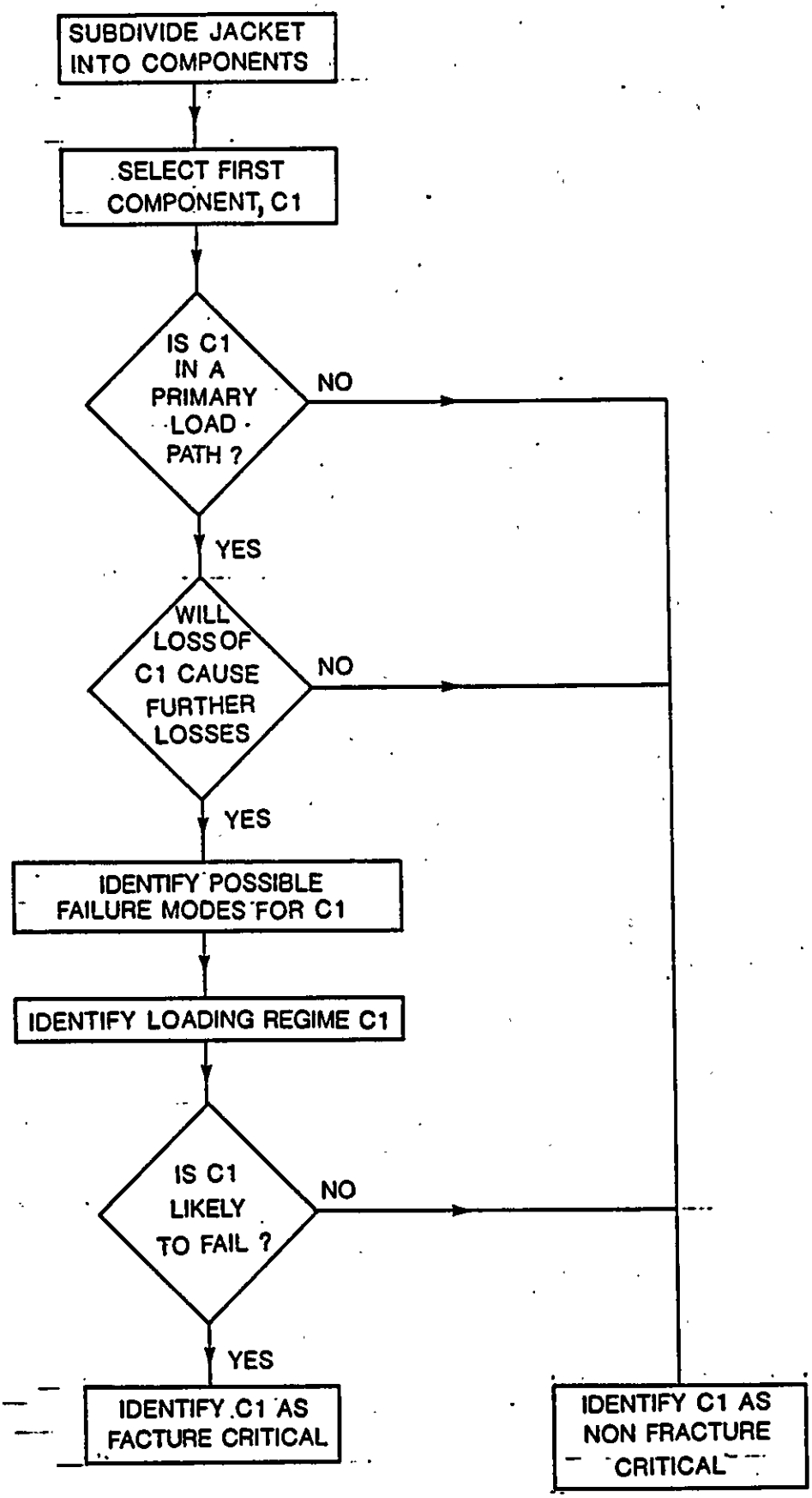

PART OF DECISION TREE FOR DEVELOPMENT OF AN OPTIMISED INSPECTION STRATEGY

PROJECT URP 72 : STUDY 4 INSPECTION PLANNING , THE ROLE OF DAMAGE ASSESSMENT	REPORT No. WOL109/86 FIG. 2·2

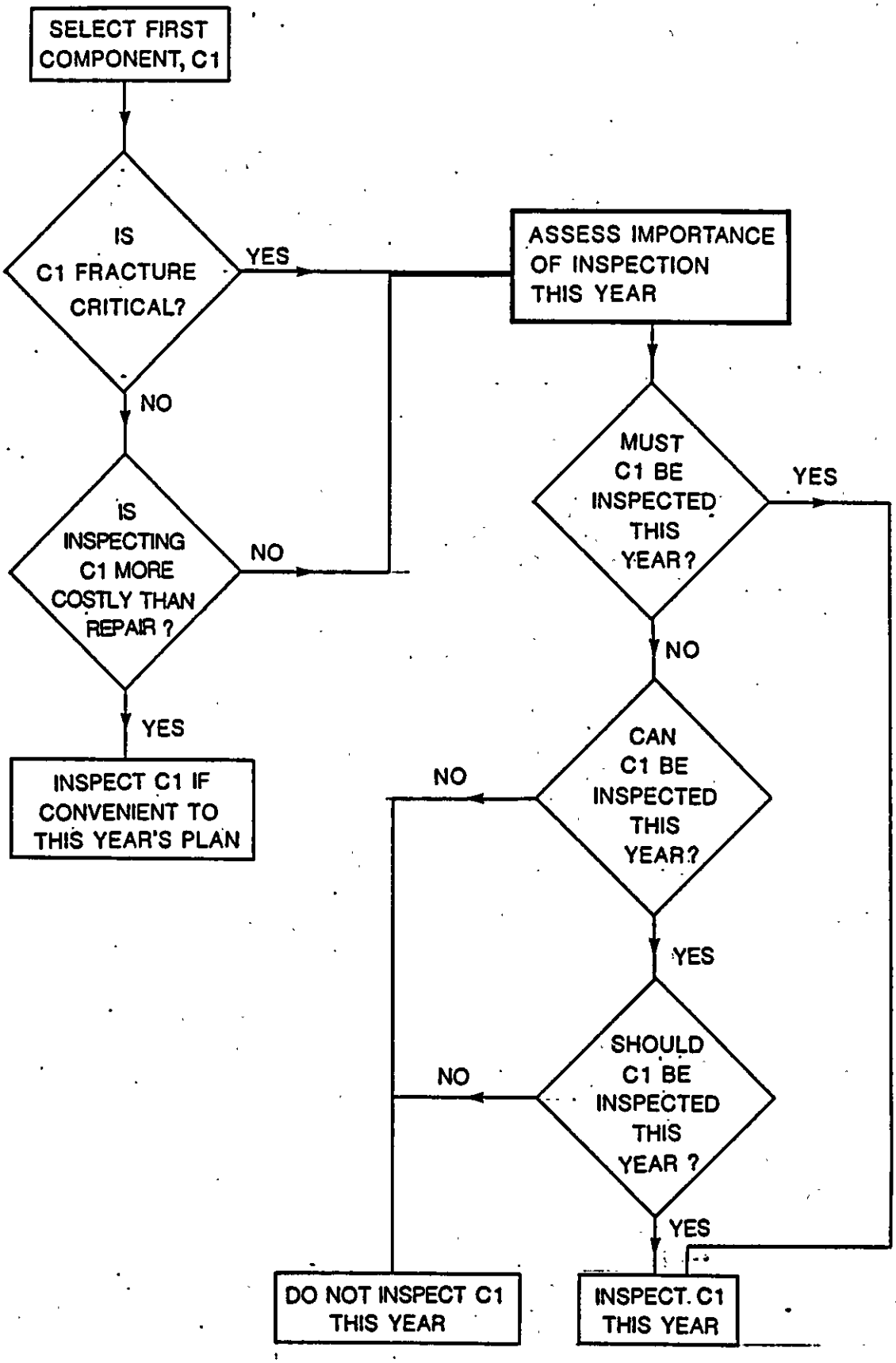

JACKET STRUCTURE TYPICAL(SIMPLIFIED) PHILOSOPHY FOR INSPECTION PLANNING YEAR 'n' "OPTIMISED STRATEGY"

PROJECT URP 72 : STUDY 4 INSPECTION PLANNING , THE ROLE OF DAMAGE ASSESSMENT	REPORT No. WOL109/86 FIG. 2·3

3. SCOPE OF THIS STUDY

3.1 Objectives

The objectives of this study are:

- To present an overview of the types of damage that can be sustained by offshore installations and their significance.
- To review methods that are currently available and under development for damage assessment.
- To present a report giving the options for the assessment of damage and how damage assessment can be integrated into an overall approach to underwater inspection.

Following the interim presentation to the Steering Group and discussions with UEG an additional aim was requested:

- To indicate the cost impact of adopting an optimised inspection strategy.

3.2 Approach

The aim has been to bound the scope of work in such a way that the bulk of the effort has addressed:

- The most promising damage assessment techniques.
- How the techniques are applied in practice.
- The impact on offshore inspection.

A certain amount of data collation was also carried out. It was not the intention that this should provide a comprehensive review of relevant available data. Operators were canvassed on their attitudes to and current utilisation of damage assessment techniques in their present and future inspection strategies.

It was apparent that the information received from interviews gave an incomplete picture of the types of damage experienced. Additional information has been provided from the first hand knowledge of the study contractor.

The data collection also aimed to collect from published sources real data, for use in the assessment method case studies presented in Section 6.6.

Recognising the amount of work necessary in applying each technique to all possible applications, the following strategy has been adopted:

- Identify types of damage to be assessed.
- Identify and review techniques which could be utilised on one or more damage type.
- Show application of promising techniques to a steel jacket structure, or components thereof.
- Comment on application of these techniques to other items subject to inspection.
- Discuss application of the methodology into an optimised inspection plan, taking due account of the findings from Studies 1 and 2 of the UEG project and the sampled opinion of industry.

4. INDUSTRY EXPERIENCE OF DAMAGE

4.1 Introduction

This Section reports on the experiences and attitudes of 6 Operators regarding damage and its assessment by theoretical techniques, reviews the published data pertaining to damage and presents a review of the types and locations of damage which are known to exist from direct experience of the study contractor. In this latter Section, Section 4.4, the second generation of damage types and locations are discussed. These defects are not yet adequately reported in published literature, but are in some respects of more interest than the first generation (conductor guide frame cracking, caisson support defects etc); defects arising early in the lives of first generation structures were designed out of second generation structures. 'Second generation defects' (including the effects of ineffective corrosion protection and problems with single sided butt welds) are only now coming to light on the first generation structures. It must be anticipated that defects in this category will be with us for many years as there is no reason to believe that they have been designed out of later generation structures.

It was not intended that the data capture exercise be exhaustive, but rather to confirm or otherwise the study contractor's perception of the types of damage being experienced and the way in which it is being assessed.

4.2 Information from Operators

A total of 6 visits to operators was undertaken both at operational locations (eg. Aberdeen) and at Head Office locations (in London). The basis for discussions with representatives of the operators was the following:

- Current inspection philosophy
- Attitude towards damage assessment
- Use of inspection data gained in modifying inspection philosophy
- Inspection techniques used and their reliability
- Nature of defects occurring
- Future developments and aims
- Cost of inspection.

The general views and subject points are given below:

4.2.1 Current inspection philosophy

All the operators canvassed used an S-N fatigue analysis to base their inspection requirements, with those areas showing low fatigue lives warranting most attention. One operator used the basis that joints should be inspected every 25% of their calculated fatigue life

although they admitted that in practice, the selection was more subjective than this with human factor, contingency inspections, budget and time of year all having a big influence. One operator had taken the step to incorporate redundancy analysis for setting part of their inspection programme with those joints having a short fatigue life and a major consequence should they fail having a high priority in the inspection list. The general impression was that most of the operators still used S-N fatigue analysis as the basis for their inspection but were beginning to turn to redundancy analysis as an aid to concentrate their efforts on those areas most critical. It should be pointed out that one operator who had new structures with a long design life was using the first 5 year recertification term to cover most of their structure by a detailed visual inspection so as to establish a base line for future inspection. The future inspection programme would then be based on fatigue, redundancy analysis and the findings from the 5 year base line.

4.2.2 Attitude towards damage assessment

The general attitude towards damage assessment amongst the operators is one of appreciating the theory but being apprehensive of the use on technical grounds. All of the operators use the techniques to assess the nature of defects discovered and to predict their course of failure and thus define what remedial action needs to be taken. However, two of the operators quite strongly recognised the deficiencies within the methods employed and felt that the large spread in results obtained due to lack of information either on input data or as support to proposed models left some quite large doubts. However those two operators did feel that the techniques were worth pursuing further.

One of these operators also suggested that where damage has been detected, they would carry out a large scale experimental test to verify the behaviour of the damaged component. It was clear that the operators consider that defect assessment techniques are useful tools in assessing known problem areas but have felt that the uncertainties in some areas needed further study and clarifications. None of the operators had yet considered defect assessment procedures in determining inspection plans for undamaged structures although most had considered redundancy analysis in one form or another. In some instances, this is done subjectively when damage is found and the effect of the damage on local and global integrity determined.

4.2.3 Use of inspection data obtained

All the operators canvassed emphasised that inspection programmes and attitudes and the response to inspection findings was a dynamic situation. Thus in the event of a defect being detected or an area of a structure being of particular concern, all the operators would place these as a high priority. Two of the operators indicated that they would increase their inspection efforts in these areas outside their normal inspection programme. One operator stated they would modify their programme so that sensitive areas would be examined every year. Another operator would base their inspection programme on "how much effort was required to be confident of the structure".

All but one of the operators stated that they would carry out detailed analysis of the damage found to aid them in their course of action. This analysis is not restricted to defect assessment in predicting the course to failure but is aimed at understanding the nature and cause of defect. This was particularly important to one operator who uses this information to update the computer models of his structures and to aid his future inspections by identifying similar areas to that in which defects have already occurred.

4.2.4 Inspection techniques used and their reliability

From the visits to the operators, it is evident that the reliability of inspection techniques is an area of disagreement between operators. This is clearly based on their own experiences of use of techniques whether they be good or bad. With the exception of one, all the operators are using flooded member detection as much as possible. Three of the operators visited relied solely on Magnetic Particle and Visual inspection in addition to the flooded member detectors.

One operator uses wet radiography and ultrasonics in addition to MPI and visual inspection.

With regards to reliability, there was a considerable degree of variation between the operators. Two felt that they would find

surface defects of 10mm length or less with a "reasonable degree of reliability". However, the same two operators (strongly) disagreed over the use of wet radiography with one claiming a successful use while the other believing it was a very ineffective tool. One of the other operators declined to comment too extensively on reliability as they thought it was very dependent on the human factor and varied between divers.

One notable difference in the visits was the attitude of the operator with new structures. They believed that for the best overall reliability in looking for cracks was to apply a "broad brush" approach of high reliability but low sensitivity. To this end, they were concentrating on flooded member detection. They believed that this allowed them to have coverage of all primary and secondary members (none of which is expected to be damaged) during the first 5 years for the equivalent cost and overall reliability of detailed NDT inspection of 5 welded joints per year.

They believed that the detailed inspection techniques, while offering a higher degree of sensitivity, had such a reduced reliability both in terms of operator capability and in the overall context of the amount of structure it was capable of covering, that during the first five years of their structures they were not cost effective. This same operator also believed that the detailed NDT techniques required a lot of experience and knowledge to enable reliable and sensitive readings to be maintained and therefore, they do not advocate the use of any techniques in the field until comprehensive, documented internal trials have been carried out.

4.2.5 Defects occurring

All the operators reported instances of fatigue cracking in their structures, this often occurring in places where the loading had been incorrectly assessed. Fatigue cracking in conductor guide frames was a case cited with this being a common problem amongst four of the operators. Additionally, fatigue cracks had been found in a number of welded joints with one operator reporting that these were occurring around the splash zone area.

Fabrication defects were an area of concern with at least two of the operators. They both noted that welding of a quality unacceptable by current standards had succeeded in entering service in some early jacket structures. A combination of poor design, poor quality control and poor welding procedures had lead to the fabrication defects. These defects were generally confined to single sided welds.

Boat impact damage had been one area of considerable concern to one operator. They have subsequently made alterations to operational procedures which has decreased the number of incidents. The degree of damage to members/components experiencing boat impact was not given. The same operator had also experienced other denting damage below the water line. Although scarce, this serious damage had occasionally happened and in all instances was dealt with, presumably by analysis and remedial repair.

Other operators had experienced installation damage in the form of gouges and dents but the extent of remedial action regarding this damage was unclear.

A further discussion of defects and damage is given in section 4.3.

4.2.6 Future developments

All the operators canvassed clearly had one single common aim in terms of future developments in offshore inspection. This was to move away from the diver based system. The directions for achieving this goal did vary between the operators but the objective was to increase the cost effectiveness and reliability of the current inspection programmes and to remove as far as possible the current subjectivity in inspection. One operator viewed this in the short term of employing existing techniques more effectively in order to establish a high probability of detecting a crack of a certain size. Their long term view was to replace divers by robotically operated machines. Similarly another operator envisaged having a permanently installed monitoring system operated from the surface. A third operator concurred with this view although they saw the emphasis on ROV's carrying out the majority of inspection with a centralised control located on the platform to monitor the findings. However, they felt

that the current emphasis for ROV's to carry out MPI was incorrect and they would like to see this changed to ROV's carrying out flooded member detection and cleaning, thus employing ROV's for 80% of the inspection time rather than 20%.

One operator, while recognising that efforts should be made to maintain the inspection as cost effective to drive it away from diver orientation, would like to see more time and money spent on analysis and inspection at the design stage. While desiring this, the operator recognised there were problems such as budget allocations which can be determined by other considerations and while it was good engineering practice to cover as much as possible in design, commercial and political factors have a large effect on this.

4.2.7 Inspection costs

Understandably, operators were reluctant to give a figure on the cost of their inspection programmes. They often felt that an exact figure was difficult to determine due to hidden costs often being involved. An example of this is the extensive use of research functions as back-up to understanding the various NDT techniques and equipment on offer. However it is believed[1] that inspection accounts for between 10-30% of operating costs. Some figures were given for costs of diving, these being £25,000 per day for a Diving Support Vessel. For this 24 hour period it was likely that only 1 node would be inspected and the majority of time would be spent cleaning. For air diving off the platform a cost of £8,000/day was estimated.

4.3 Information from Published Sources

4.3.1 Fixed structures

A review of the incidence of defects and analysis of their cause has been the subject of an earlier UEG study[2]. The study reported 61 cases of damage of which 41 involved primary structures, 18 secondary structures and 2 involved both. It is significant that of the 17 cases of fatigue failure, two affected primary structures, 13 secondary structures and two both. The high incidence of fatigue failure in secondary structures is believed to be due to the problem

of inadequately designed conductor guide framing; a problem common to many of the early platforms in the Northern North Sea. Of the 61 cases recorded, thirty were caused by accidental damage such as collision, installation damage or dropped objects. Twenty six defects were a result of design or construction defects which led to 17 cases of fatigue failure. Although the cause of one defect is listed in reference (2) as being due to a welding fault it is not clear how many of the fatigue failures resulted from construction defects. In all, 41 of the cases of damage had resulted in formation of a crack in the structure. The summary of damage from reference (2) is given in Table 4.1.

A recent study[3] was made of the structural damage of 21 steel platforms installed in the North Sea between 1971-78. The study was based on in-service records gathered from 1975 to 1984 comprising inspection findings and other occurrences reported from below water inspection. A summary of results reproduced from reference (3) is given in Table 4.2. Of significance is that cracks and dents were confirmed in 12 and 15 of the 21 platforms respectively which is in line with the findings of the earlier study.

Of the structural defects discovered, the most common causes were:

- direct design deficiencies eg. incorrect estimation of waveforce loading.
- indirect design deficiencies eg. access limitations for proper fabrication.
- construction deficiencies eg. faulty weldments which have been accepted due to poor quality control, undercuts, misalignments outside of tolerances.
- accidental damage eg. collisions, dropped objects resulting in gouges or dents. These dents often contain cracks in areas of reduced toughness (due to cold working) and one incidence of a propagating brittle crack emanating from a dent is reported.

From discussions with the operators and information reported in reference (3), three areas of damage are of major concern; fatigue cracks, dented members with or without cracking and, to an increasing extent over the past few years, construction defects now manifesting themselves as a consequence of poor design, poor welding and poor quality control. These welding defects often give rise to fatigue cracks.

One additional area of damage highlighted by reference (3) is the incidence of pitting corrosion. This was reported as occurring on 20 of the 21 jackets surveyed. Although none of the operators visited in this study reported it to be a major problem, it is known to be causing at least one operator concern.

In view of the increasing concern amongst Operators of the standard of welding of structures fabricated in the 1970's a paper by Rogerson and Wong[4] gives some information of the distribution of weld defects in offshore structures. The aim of the study was to have a good estimate of the flaw size and distribution so that a probabilistic analysis of failure by fracture due to weld defects could be made. For this, the authors collected data on defect height, length, location and type for 12 vertical node joints and 6 horizontal node joints in the splash zone region of one structure. A total of 1000m of welding was surveyed. The results showed that all defects were embedded and that 90% were in the horizontal nodes which were the most complicated connections. Most defects were located in the root region or at the fusion zone. The height distributions between non-planar and planar defects, reproduced in Figure 4.1 showed a marked difference, with planar defects showing greater defect height. The authors show that these defect heights can most appropriately be described by a Weibull function. From an analysis of their own and other published data, the authors present a table of the various parameters for the Weibull parameters as a function of defect types. The parameters are presented in Table 4.3. Hence an attempt at a reliability estimation can be made once the distribution of defects is known. However, because the factors affecting the critical size at which fracture will initiate (eg material toughness, yield stress, geometry and applied stress) are also distributed variables, determination of the probability of a failure from a given defect size becomes a complex calculation.

An additional area of information helpful in planning an inspection strategy is the depth of water in which defects are occurring. Reference (1) illustrated that the majority were between +10 and -20m of sea level although repairs down to the -140m level have been carried out.

To summarise, a database on defect damage for offshore structure would be a useful tool in analysing the type, location and cause of cracking and highlight those areas where inspection should be concentrated. For instance, it is clear that certain weld designs and procedures used in the mid - 1970's coupled with poor quality control has led to fabrication defects entering service and this highlights areas in which inspection should be concentrated particularly in the splash zone. Within the context of this project, the visits and information obtained from the operators was not of sufficient detail or from a wide enough scope to be able to present a full database of damage.

4.3.2 Pipelines

Damage to a pipeline represents a possibly more serious problem than damage for a single member of a well-designed structure. The obvious reason is because the pipeline has absolutely no redundancy and failure represents loss of production and possibly loss of public confidence due to environmental effects etc. Thus inspection of subsea pipelines represents an area of high effort in inspection. In service inspection of subsea pipelines normally entails the problem of line length as well as access limitations. Surveys made of the as-laid condition prior to burial, therefore, represent an important source of information. The study carried out by DnV[3] reported on the findings gathered from a review of North Sea pipeline records and the results are given in Tables 4.4 and 4.5. These indicated that more damage has occurred during laying of pipelines than during operation and the majority of this is in the form of buckles and gouges. The study also showed that external corrosion was more troublesome than internal corrosion and it is significant that the corrosion problems have all occurred near the platform, perhaps indicating inadequacy of the corrosion protection system when adjacent to another large mass of steel.

4.4 Overview of Locations and Modes of Structural Failure

As a preliminary to considering theoretical assessment techniques and before a rational inspection plan can be developed, it is necessary to have a knowledge of the likely modes of and locations at which structural failure may occur.

The principal types of failure pertinent to this study include: -

- Fatigue
- Fracture
- Member collapse
- Joint collapse
- Excessive corrosion

Although these failure modes are distinct, they are in many circumstances interrelated. For example, fracture is often merely the premature termination of a fatigue problem, and member collapse and joint collapse occur together when there has been gross local overloading on a structure.

The mode of failure is governed by a limited number of parameters, of which the most important are as follows:

- Loading type (eg. static or cyclic, tension or compression).
- Structural geometry (eg. slender or stocky; tension or compression).
- Structural detailing.

The internal member loads are obtained from the results of a structural analysis, which can provide valuable data for determining underwater inspection plans. The deficiencies of conventional analysis methods must however be clearly recognised. Firstly, because it is not possible to include fabrication and installation forces within the analysis, the predicted member forces may in fact be in error both in magnitude and direction. Additionally, whilst the predicted fatigue lives in a structure are of prime interest, these too are subject to error, and it would be unwise to base the inspection plan solely on the nominal fatigue lives.

Having derived the member loads, a number of simple rules may be applied to help determine likely failure modes. It may, for example, be assumed that fracture is only likely to occur in tension members, and member instability to occur in compression members. A number of considerations of this type are summarised in Table 4.6.

Of equal importance to the predicted behaviour is service experience gained from similar structures which have suffered problems. Listed below are a number of problem areas which have occurred previously on jacket structures, and which should receive special consideration when planning underwater inspections.

4.4.1 Fatigue cracking of conductor guide frames

It is generally recognised that the fatigue design of the conductor guide frames of early North Sea structures was deficient. As a result, many of these guide frames have experienced fatigue cracks at the saddle hot spot locations, which has necessitated repair or strengthening.

4.4.2 Rigidly attached appurtenances

A number of the earlier structures suffered from poorly detailed appurtenance supports. A common failing was that rigid welded supports were used which attracted framing loads from the primary structure. The resulting stresses have led to both failures in the appurtenance supports, on occasions leading to loss of the appurtenance, and also to the introduction of fatigue cracks in the support member.

4.4.3 Single sided butt welds

Single sided butt welds (SSBWs) occur mainly at brace/stub and chord/can joints, or less frequently at access windows. Several widely reported failures of members have occurred recently at SSBWs, which have drawn the attention of the offshore industry to this problem. Fatigue problems at these locations are particularly difficult to detect since the fatigue crack grows from the inside of the member outwards.

Conventionally, a rigorous fatigue analysis of these joints is not performed during design, or where performed uses the Class F2 S-N curve as recommended in the Department of Energy Guidance Notes; it is now generally accepted that the Class F2 curve is very optimistic for this detail, and that unrealistically long lives will be predicted.

The highest risk locations are those where there is a combination of large cyclic stresses and welding defects, particularly if the member also carries a large static tensile load. These locations may be identified by performing a fatigue analysis for all members to compute the comparative lives, and the locations with the highest risk of welding defects may be identified by examining the welding procedures and the post-weld NDE reports.

For circumferential butt welds where repairs to the weld root have been conducted through access windows, it may be assumed that the weld itself is sound, having been converted into a double sided butt weld, and that potential problems are confined to the window closure weld.

4.4.4 Ineffective cathodic protection systems

A number of cases has occurred of problems arising from incorrectly designed or malfunctioning cathodic protection systems. These included impressed current systems which have been inoperative for a period of time, sacrificial anode systems in which the location of anodes causes localised shadow areas at joints, and systems in which the presence of current drains (eg. pile guides and other non-structural steel) has not been allowed for in the design. Corrosion problems generally appear either as excessive pitting at weldments, or else as 'knife line' or crevice attack on the fusion zone of weldments.

4.4.5 Effect of welding variables and chemistry on corrosion

Experience has shown that high hardness microstructures are more susceptible to corrosion, and therefore that the welding varibles and chemistry have an important effect. Higher rates of corrosion will thus be prompted by the following conditions:

- Low preheat

- Low heat input welding
- Uncontrolled post weld cooling
- High carbon equivalent steels

Some operators have implemented a comprehensive database containing their fabrication records and procedures, and used this to identify the locations with a high risk of excessive corrosion.

Experience has shown that these conditions often occur in caissons and similar appurtenances, and corrosion failures have resulted.

4.4.6 Drilling cuttings

It has become apparent that on a number of structures insufficient attention was paid during design to the problem of the disposal of drilling cuttings, and that these accumulate around the base of the structure, applying additional loads to the members in this region. In some instances the deposits reach the next-to-bottom framing level, typically some 20m above the seabed. Detailed studies have shown that the pressures from the drilling cuttings can cause substantial overstressing of the members, and indeed one case of member collapse has already been reported.

4.4.7 Flooded members

Problems have been encountered on structures where insufficient attention has been paid to the member flooding. This includes both the case where members are designed incorrectly so that overstress occurs under normal hydrostatic loading, and also the case where the actual condition of flooding differs from the designer's original intentions, possibly resulting from poor detailing of the flooding holes. In one instance, diaphragm stiffeners in an X-joint were found to be severely overstressed because they were carrying the full hydrostatic loading on one side only, as a result of poor detailing which caused the space between the stiffeners to remain unflooded. By their nature, member flooding problems are confined to the base of structures installed in medium to deep water locations. The actual state of member flooding may be detected readily by use of a suitable meter.

Attention should also be drawn to the special corrosion problems of flooded members. To exclude oxygen and thus prevent corrosion is desirable to seal the flooding holes after platform installation. If this is done, the entrained water should be dosed to kill any sulphate reducing bacteria which would otherwise flourish in the anaerobic conditions.

4.4.8 Detailing

Although service experience assists in highlighting the areas in which structural problems are likely to occur, allowance should also be made for unexpected circumstances, such as departures from the 'as-built' drawings. Actual examples of this include unrecorded welded details on members subject to a high fatigue loading which have lead to failure (as on the Alexander Kielland), and ring stiffeners. Contingency inspections or monitoring should be planned to enable these problems to be detected in time for corrective action to be taken before failure occurs.

For each failure mode it is essential to have an appreciation of the visible evidence of damage or of impending failure, since the underwater inspection plan must be designed to detect this. For fatigue cracks, the visible evidence is generally a line indication on the surface, which may either be detected by MPI or by close visual examination, depending on the size. It is somewhat more difficult to detect cracks emanating from the inside of a member outwards, for which either underwater radiography or ultrasonics must be used, or alternatively a flooded member detector may be used to detect a crack in this location after it has grown through thickness. For an inspection plan based on the latter case, it would be essential to verify that there was an adequate residual life as a through-thickness crack, to ensure that this could be detected before final failure occurred.

For the case of ultimate load failure, there is generally little evidence of distress until a local failure has occurred, and this may be detected by general visual inspections or by structural monitoring. Failures of this type are usually caused by exceptional loadings, such as boat impact or from dropped objects; inspections should thus be carried out as soon as an incident is reported, or if other evidence is encountered, such as unexplained debris on the seabed.

The determination of potential failure modes and sites is summarised in Figure 4.2 and Table 4.6. The selection of appropriate inspection methods to detect different types of damage is reviewed extensively in URP72 Studies 1 and 2[5,6], and is not discussed here.

REFERENCES

1. Noroil February 1986 p.23

2. 'Repair to North Sea offshore structures - a review' CIRIA UEG Report No. UR21 1983.

3. E M Q Noren, T. Sollie and B Carlin. 'Case histories of structural damage - lessons learned' Behaviour of Offshore Structures 1985 p.1 - 6.

4. J W Rogerson and W K Wong. 'Weld defect distributions in Offshore Structures and their influence on Structural Reliability'. Paper OTC 4237 Offshore Technology Conference, Houston, Texas May 1982.

5. 'Guidance for Inspection of Offshore Structures'
CIRIA UEG Report No. URP 72/SG/10, November 1985.

6. 'Implications of Design to Inspection and Maintenance of Offshore Installation and Pipelines'.
CIRIA UEG Report No. URP72/SG/11, September 1985.

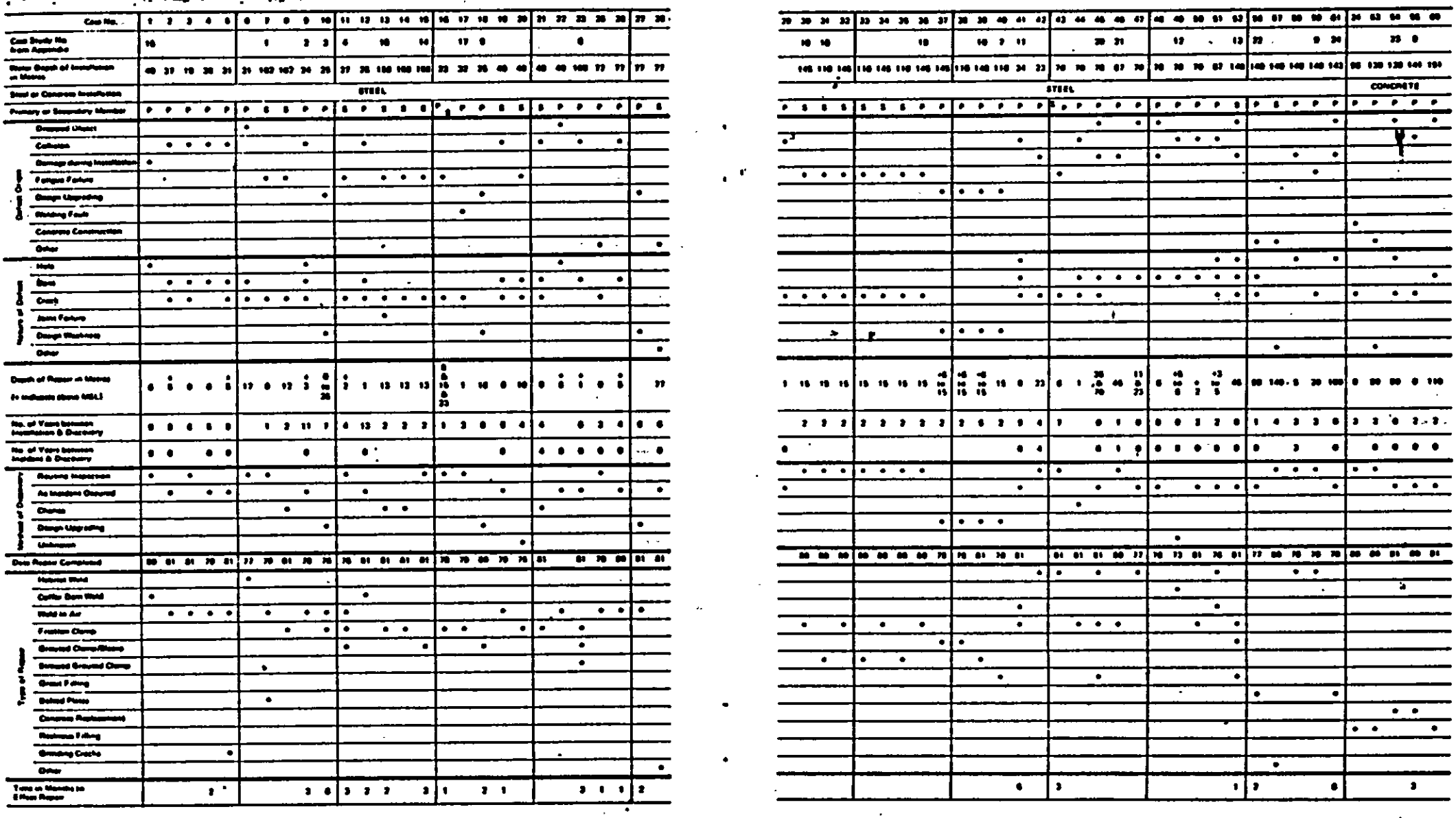

TABLE 4.1 SUMMARY OF DAMAGE AND REPAIRS - FROM REFERENCE 1

Plattform no.	1	2	3	4	5	6	7	8	9	10	11	12	13	14	15	16	17	18	19	20	21	Number of platforms with defect
Crack confirmed	X	X	X	X		X	X	X		X	X			X		X			X			12
Propagating crack							X			X	X											3
Dented member	X	X	X	X		X		X	X	X	X		X	X	X	X				X	X	15
Deflected member	X		X	X		X		X	X	X			X	X	X						X	11
Low potential value		X		X	X			X	X	X	X			X		X					X	10
Missing anode				X	X			X	X	X	X	X							X	X		9
Defected anode									X		X		X			X						4
Loose anode				X		X		X		X				X	X					X		7
Pitting corrosion	X	X	X	X	X	X	X	X	X	X	X	X		X	X	X	X	X	X	X	X	20
General corrosion				X						X												2
Burn mark					X				X	X	X											4
Heavy marine growth		X	X	X		X	X			X	X	X	X		X	X				X	X	13
Wire Chafe	X	X	X	X		X	X	X	X	X	X	X	X		X	X	X		X	X	X	18
Scour													X									1
Debris	X	X	X	X	X	X	X	X	X	X	X	X	X	X	X	X	X	X	X	X	X	21

TABLE 4.2 SUMMARY OF UNDERWATER INSPECTION FINDINGS FOR 21 STEEL JACKETS IN THE NORTH SEA (FROM REFERENCE 2)

Defect Type	β	γ	η
Offshore Structure Nodes Non-planar defects (height) As fabricated	0.70	0.1	0.83
Planar defects (height) As fabricated	1.4	0.1	5.0
All defects (height) As fabricated	0.95	0.1	3.20
All defects (height) After N.D.T. and Repair	0.80	0.1	1.12
Surface Breaking Cracks (height) Becher & Hansen	0.85	0.1	1.75
Slag inclusion (length) Becher & Hansen	0.45	2.0	5.50
Cracks (length) Kihara	0.85	1.0	18.5
Cracks (height) Kihara	1.10	0.1	2.62

$$n(x) = \frac{\beta}{\eta}\left[\frac{x-\gamma}{\eta}\right]^{\beta-1} \exp\left[-\left(\frac{x-\gamma}{\eta}\right)^{\beta}\right]$$

TABLE 4.3

WEIBULL PARAMETERS FOR DEFECT SIZE DISTRIBUTION

*	Buckles and Gouges[1]	15
*	Anchor wire	3
*	Floating	1
*	Pigs stuck	4
*	Pressure test	3
*	Others	1
TOTAL		24

1) Probably caused by anchor or trenching sledge.

TABLE 4.4

DISTRIBUTION OF PIPELINE FAILURES DISCOVERED AFTER LAYING BUT PRIOR TO START-UP (REFERENCE 3)

	Near Shore	Open Seas	Near Platform	Total
Anchor damage	1		3	4
Corrosion			4	4
Stability	3		1	4
Pinhole		1*		1*
Creep/Thermal			3	3
Cause unknown			1	1
TOTAL	4	1	12	17

* Detected during pressure testing

TABLE 4.5

NUMBER OF PIPELINE INCIDENTS DURING OPERATION CAUSING REMEDIAL ACTION, BY CAUSE AND LOCATION (REFERENCE 3)

Failure Mechanism	Promoting Agent	Inspect For	Location in Structure
Member buckling/ plastic collapse	Compressive loads. Geometry (slenderness ratio in imperfection sensitive range). Impact damage. Overload	Member dents. General evidence of abnormality.	Compressive members with high utilisations. Members suffering from impact/installation damage, or subject to exceptional loadings (eg. from drilling cuttings).
Joint failure (static load)	Impact damage. Overload. Fabrication errors.	General evidence of abnormality.	Joints with high utilisations. Joints to members subject to buckling/plastic collapse (see above).
Fatigue	Cyclic loads. Stress raisers Initial defects.	Fatigue cracks. Flooded members.	Low nominal fatigue life members and joints (esp. in splash zone). Poor fatigue details (eg. single sided butt welds and rigid appurtenance supports).
Fracture	Cracks (either fabrication or fatigue) Tensile stresses. Residual stresses. Low toughness materials.	Cracks. Flooded members.	Welds to tension members.
Hydrostatic collapse	Hydrostatic pressure. High diameter/thickess ratio. Dents.	Dents. General evidence of abnormality.	Thin walled members at base of structure.
Corrosion	Ineffective cathodic protection. High hardness microstructures.	Pitting and 'knife line' attack. Loss of wall thickness.	Welded Joints. Flooded members. Structure adjacent to current drains (eg. pile guides).

TABLE 4.6

CHECKLIST TO IDENTIFY POTENTIAL FAILURE MODELS

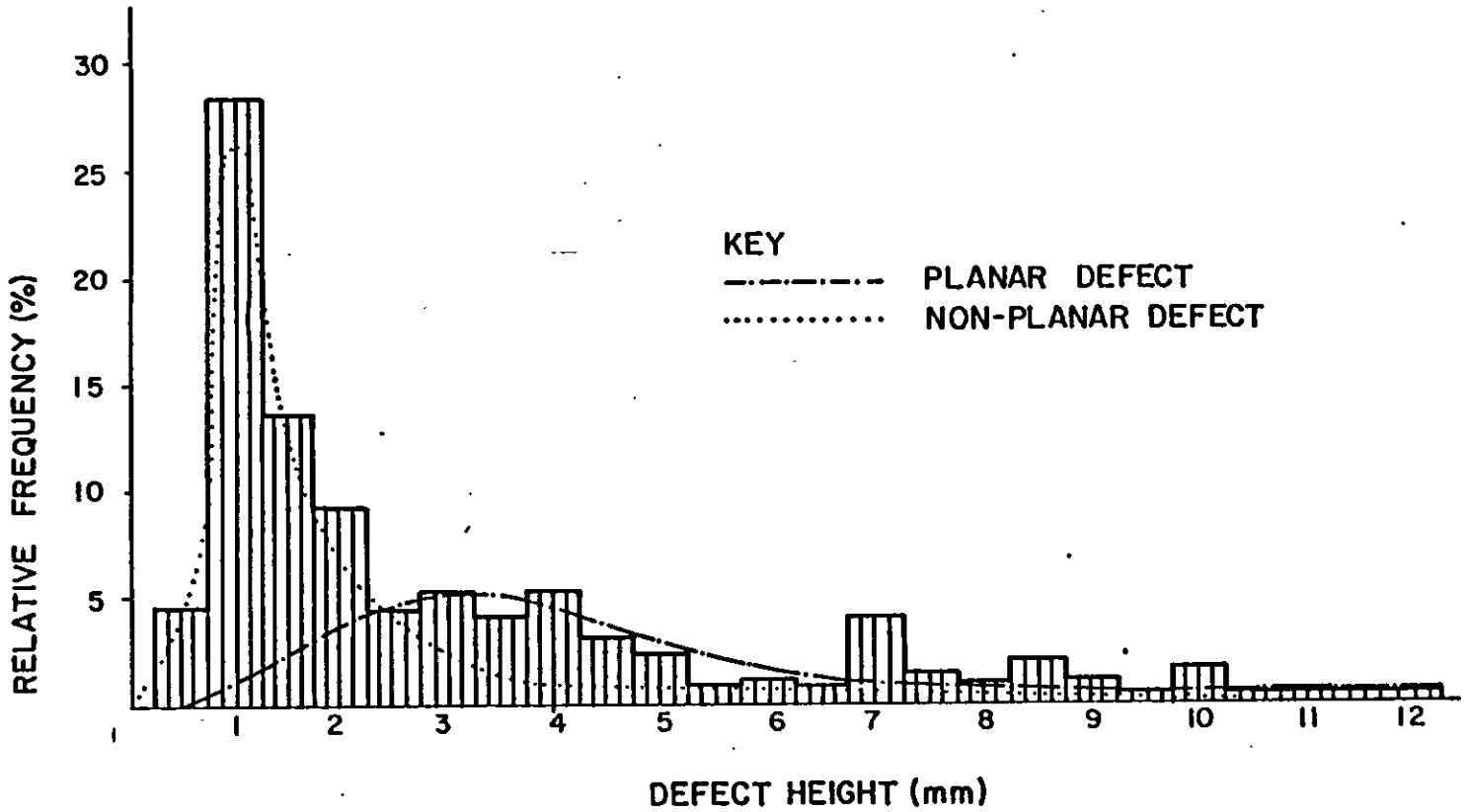

WELD DEFECT HEIGHT DISTRIBUTION FOR WELDED NODES (Ref. 4)

PROJECT URP 72 : STUDY 4

INSPECTION PLANNING , THE ROLE OF DAMAGE ASSESSMENT

WIMPEY OFFSHORE REPORT No. WOL109/86

FIG. 4.1

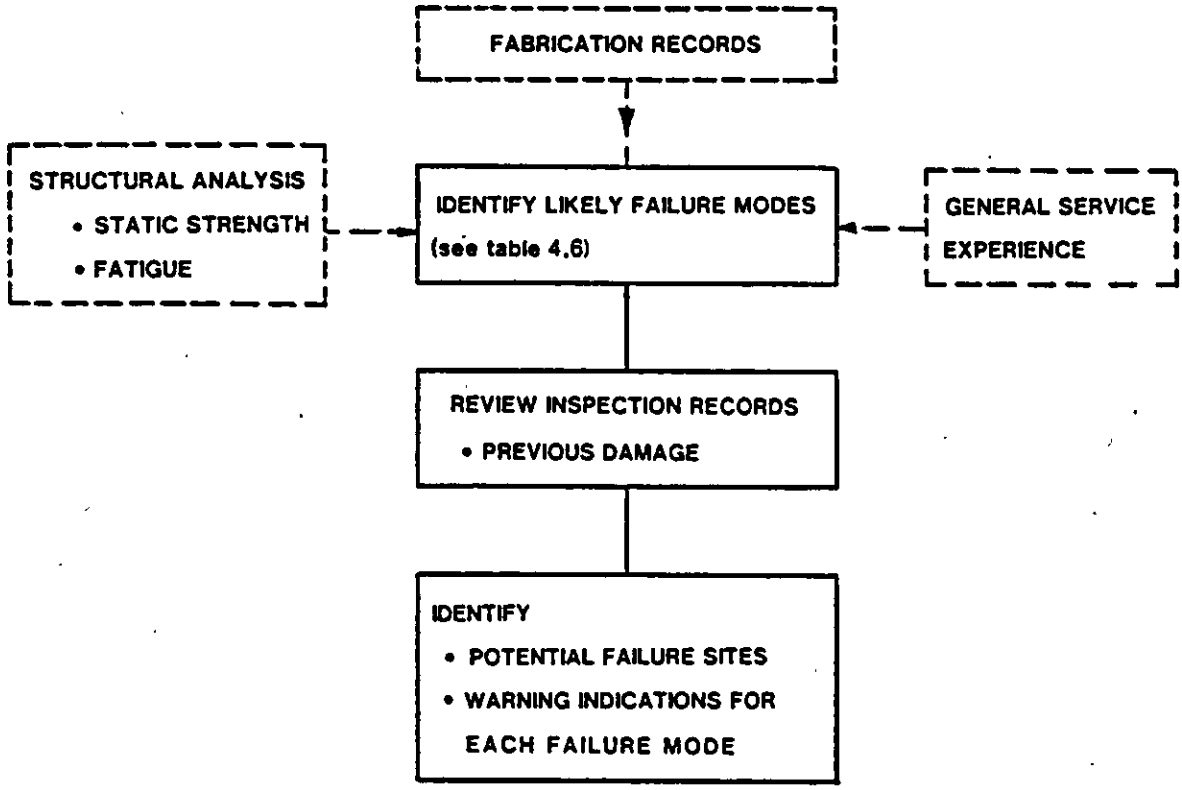

IDENTIFICATON OF FAILURE MODES

PROJECT URP 72 : STUDY 4 INSPECTION PLANNING THE ROLE OF DAMAGE ASSESSMENT	REPORT No. WOL 109/86 FIG. 4.2

5. ENGINEERING DATABASES/INFORMATION REQUIRED

The objective of this section is to highlight additional information that is required or useful in applying the damage assessment techniques discussed in Section 6. This information take two forms:

- a compilation of experimental results which illustrates the behaviour of damaged components.
- a compilation of relevant technical information into databases necessary for the assessment techniques. A typical database required is that of material properties obtained form mill sheets/test certificates of the steel plate used in the structure.

5.1 Experimental results

This section highlights information on the behaviour of damaged components. Knowledge of this behaviour enables analytical models to be modified and benchmarked for accuracy. It also enables understanding of development of damage to final failure for different types of component. This is particularly important in recognising that the way a crack penetrates through a tubular member may vary with joint type. In addition, predictions of fatigue crack growth (see section 6.3) rely entirely on growth constants derived from experimental tests under various conditions.

The section concentrates on experimental fatigue cracking, the behaviour of dented members is dealt with in section 6.1. Within a defect assessment or optimised inspection analysis, in addition to the fatigue crack growth constants, two areas of crack development are of particular interest;

i. the development of cracks through the thickness with respect to type of joint tested and

ii. the aspect ratio of the crack, defined here as the ratio of crack depth 'a' to the half crack length c.

In the absence of totally reliable subsea inspection methods for accurately determining crack depths, knowledge of the aspect ratio becomes an important factor in that a surface crack length measured by MPI can be related to a certain depth of crack via reliable experimental results for the joint type

in question. Furthermore it is likely that the aspect ratio will change as cracking progresses. This is an important consideration for fatigue crack growth in tubular joints and the fatigue crack growth model should include provisions for such changes.

It is not intended that the information supplied in this section should be a totally comprehensive database and bibliography of all experimental data but should highlight with examples some of the differences and difficulties to be encountered and give details of key sources of information.

5.1.1 Tubular joints - Crack development

Early studies on the fatigue lives of tubular joints concentrated mainly on the derivation of design life S-N curves for ultimate joint life and ignored, to a certain extent, the study of crack formation and growth. However, development of a reliable system for measuring crack depth during the UKOSRP I programme[1] has led to greater observations of crack development being made. Summaries of some of these observations have been made in references[1] and[2].

In many cases the development of cracks in a tubular joint can be complex with initiation occurring as several cracks at the weld toe of a connection which coalesce to produce larger cracks. These are usually visible within about 10% of the total fatigue life[3]. Initiation usually occurs in the chord due to the higher notch stress at the weld toe even though the 'hot-spot' stress may be higher in the brace. It is also found that initiation sites are more widely spaced in axial loading than in bending. Following initiation and coalescence, crack branching may occur with cracking proceeding along both the weld toe and the chord. In this situation, the criterion is to assess the growth of the dominant crack which will eventually be the first to break through the thickness and will also have the greatest length where branching has occurred.

Early observations of both T and K joints[3,4] indicate that after an initial delay (probably due to the coalescing of initiation cracks), the crack depth increases approximately linearly with the number of cycles until the chord wall is penetrated. However, it should be noted that crack growth characteristics vary between simple (non-overlapping) and complex (overlapping) joints. Figure 5.1 illustrates the normalised crack growth through the thickness (a/t) as a function of the normalised number of cycles to failure, N_f, for a number of different joints. N_f is defined here as the occurrence of through thickness cracking.

Figure 5.1 gives the crack growth characteristics of two T-joints, one tested in air and one in seawater[9], a simple K joint[3] and an overlapping K Joint[6] half. As previously reported by Dover[4], crack initiation in a T-joint subjected to axial loading occurs at the saddle sites in chord material and occupies approximately 10% of total life. Other work, being generated as part of the UKOSRP II programme, does show a variation in both the initiation life and time to through thickness cracking. The data in this programme will greatly increase the database on crack growth behaviour and will be published in the open literature in 1987[7]. After initiation, through the thickness cracking occurs steadily such that half thickness cracking occurs around 70-80% of total life. It is evident from figure 5.1 that simple K joints and T joints both in air and seawater appear to behave very similarly with regards to crack initiation and crack growth through the thickness. Included in Figure 5.1 is an example of crack development in an overlapping K-joint. This shows that initiation takes approximately 30% or more of total life and through thickness cracking develops quite late as illustrated by the crack depth being less than 25% of the thickness for 75% of total life. This variation in crack growth is also reflected in the aspect ratio as illustrated below. It should be noted that in this case cracking occurred in the brace member and not in the chord. With overlapping K joints, the position of cracking can vary from either chord or brace dependent on stress level, stiffness of chord member and degree of overlap. Figure 5.1 serves to illustrate the possible differences in crack growth characteristics between different joints. Of particular importance is the fact that for simple joints cracking appears to occur steadily throughout the life of a joint but for more complex joints, initiation occupies a much larger portion of total life but once a

crack is established cracking proceeds rapidly to failure. This illustrates the fact that more attention to a complex joint should be made once cracking is established as the time to failure is much less than for a T-joint. Obviously, the actual number of cycles to failure is dependent upon stress range and size of joint. It should be noted that none of the studies[3,4,5,6] suggest that crack development through the thickness in terms of the normalised endurance is affected by applied stress levels.

5.1.2 Crack development through the thickness

As suggested in section 5.1.1, the development of the crack aspect ratio is an important parameter when assessing fatigue lives of tubular joints. If a reliable database on crack development in tubular joints can be established, it then becomes possible to estimate the level of crack penetration through the thickness from the length of observed surface cracking. This is particularly attractive in the offshore world where reliable detection of surface cracks can be achieved through MPI.

With respect to surface crack length, Gibstein[3] suggests that it increases linearly while Dover[4] believes that a sigmoidal growth occurs. Clayton's analysis of the UKOSRP I data suggests that something between the two occurs dependent on whether a shallow or deep crack is initially formed.

Clayton[1] also analysed the aspect ratio of the crack. The analysis showed that after an initially low aspect ratio at short crack lengths, a mean ratio of 0.15 corresponding to a total surface crack to crack of 13:1, develops throughout most of the fatigue life. However, due to the development of the monitoring system, most of the data is believed to be unreliable and subject to considerable scatter as shown in Figure 5.2. The findings should thus be treated with caution.

However, since the publication of references (1) and (2) more reliable information on crack development has become available. Dover[5] has recently published some interesting data for both Y

joint air tests and some seawater T-joint tests. Figure 5.3 reproduced from reference[5] shows the aspect ratio for the Y-joint tests verses the normalised crack depth. The results show a fair degree of scatter at shallow crack depth but much greater consistency once the crack has penetrated 40% of the wall thickness. The scatter at shallow crack depths is a consequence of multiple crack initiation early in the test such that relatively short cracks appear which subsequently coalesence to produce long shallow cracks. The greatest inaccuracy of the monitoring system will also occur at short crack depths.

Once crack coalesence has occurred, it can be seen that the cracks develop at an aspect ratio between 0.07 and 0.10 tending towards a figure of around 0.10 as through thickness cracking is reached. This is equivalent to a minimum surface crack length to depth of 20:1.

Dover also includes in the same reference some data on aspect ratios for stress relieved T-joints tested in seawater with cathodic protection. These results are given in Figure 5.4 and apart from one test result at shallow crack depth, indicate a maximum aspect ratio of 0.2, equivalent to a minimum total surface crack length to crack depth of 10:1. These results indicate that the way a crack develops is dependent either on the geometry or on the mode of loading the Y-joints having been subject to in-plane bending. At present, the database for aspect ratios is limited but the publication of results from at least four large test programmes on tubular joints in 1987 will increase the amount of data available and hopefully give details of crack development for each type of joint geometry. It should also highlight whether the aspect ratio is dependent on the type of loading the joint experiences.

Table 5.1 gives an indication of the type of information that is required in this type of analysis and which will become available as the details of the test programmes become available. Given in the table are the crack lengths and depths and the derived aspect ratio of two joints, one an axial loaded T-joint tested in air and the other an overlapping K-joint subjected to balanced axial loading. The data is also presented graphically in Figure 5.5. A similarity to the data given by Dover is evident in that a high scatter in

aspect ratio is seen early on followed by a much more consistent value once the crack has penetrated 40% of the wall thickness. The T-joint in air gives a maximum aspect ratio of 0.16 and keeps to this shape for the second half of its life to through thickness. This high degree of consistency is encouraging for developing a database on aspect ratio values for different joint types. The 0.16 aspect ratio represents a minimum surface crack length to depth ratio of 13:1, which is in close agreement with Dovers value of 10:1 for a T-joint in seawater. The results from the overlapping K-joints show a clear difference in aspects ratio with a maximum of 0.057 being recorded, equivalent to surface crack length of 35:1. The crack generally appears to proceed at a ratio of around 35-40:1 to through thickness. Thus a clear difference in behaviour is seen for overlapping K-joints in that initiation apparently occupies a longer period of total life and that through thickness cracking occurs rapidly after this. However the cracks develop at a far smaller aspect ratio equivalent to surface crack length to depth ratio of approximately 35:1 thus aiding detection once cracking is established.

5.1.3 Fatigue crack growth data

The concept of fatigue crack growth via fracture mechanics assessments is comprehensively dealt with in section 6.3. Fundamental to the assessment is the crack growth law and associated constants which are empirically determined. The purpose of this section is to give a limited review and key bibliography of these constants and to update the model for fatigue crack growth in seawater with cathodic protection as this is the most appropriate environmental condition for subsea components.

A great deal of data on crack growth rates under various environmental conditions was generated by the UKOSPP I programme and a summary of the results are given in references (2) and (8). Tests were carried out on through thickness cracks using Compact Tension or Single Edge Notch type specimens with axial loading. Material tested was to BS4360 50D steel. The UEG design guide[2] gives a good summary of this and other published data and figure 5.6 representing crack growth data in air is reproduced from this publication. All the data has been assessed using Paris' Law,

$$da/_{dN} = C\ (\Delta K)^{m} \qquad (5.1)$$

where C and m, the materials constants are the intercept and gradient of the presented line respectively.

There is quite a variation within the value of C and m quoted although a mean line for air has generally been accepted as

$$da/_{dN} = 1.00 \times 10^{-11}\ (\Delta K)^{3.0} \qquad (5.2)$$

A recent study at the University of Glasgow[9] on three point bend specimens gives an upper bound very similar to this;

$$da/_{dN} = 1.12 \times 10^{-11}\ (\Delta K)^{2.92} \qquad (5.3)$$

Testing in seawater, with and without cathodic protection complicates the picture and a higher degree of scatter ensues. This is illustrated by Figure 5.7 showing the crack growth for 50D steel in seawater at a potential of - 0.850V. As indicated in Section 6.3, the problem is confused further by the possibilities of interaction between the various parameters. The conclusions from these studies show that the crack growth of freely corroding structural steel in seawater is described by an upper bound six times the growth rate in air. High R ratios were found to increase the crack growth rate. Cathodic protection had a variable effect on crack growth rate dependent on level applied. At - 0.850V with respect to the Ag/AgCl cell, a small decrease in growth rate relative to seawater was observed but over protection resulted in higher crack growth rates than for unprotected air.

One of the major disadvantages of the Paris Law is that it is only valid at intermediate crack growth rates (see below). Near the threshold (low ΔK values) there are many cycles where predictions may be over-conservative. In addition the Paris Law should also not be used where crack growth is predominantly at high rates (high ΔK values), as predictions will be non-conservative. Alternatively, injudicial selection of a ΔK threshold value could lead to non-conservative predictions of crack growth[10] in the region I area of crack propagation.

An advance on the Paris crack growth model has come from a major study into the fatigue of steel structures at Southwest Research Institute[11]. They propose a basic crack growth law of three terms which is illustrated in Figure 5.8. The individual terms of the equation account for the growth rate in the principal regimes,

I - near threshold
II - intermediate growth rate
and III - low cycle fatigue regime

and has the form

$$da/dn = \frac{1}{A\Delta K^{n}} + \frac{1}{C\Delta K^{m}} - \frac{1}{C[1-R)K_{IC}]^{m}} \qquad (5.4)$$

I II III

SWRI in their review of available data derived crack growth constants for offshore steels under 6 sets of conditions. These were;

1. Air environment, low R

2. Air environment, high R

3. Seawater environment, free corrosion potential, low-R

4. Seawater environment, free corrosion potential, high-R

5. Seawater environment, cathodic polarisation, low-R

6. Seawater environment, cathodic polarisation, high-R

The constants, reproduced in Table 6.2, have varying degrees of confidence. Growth in air is well researched and can be predicted with a reasonable degree of assurance, whereas growth in seawater with cathodic protection is less well understood. The constants have been selected in most cases to give a near upper bound to the test data. In all conditions, the three component model yields improved estimates of fatigue life. Furthermore, it illustrates that correct selection of crack growth constants for the conditions pertaining at the area of interest is necessary to improve the accuracy of any defect assessment. For instance, if potential levels at the joint of interest have been reliably measured, it is important that the correct constants are chosen as different rates occur for under, optimum and over protection.

A recent publication[12] compares the fatigue crack growth data of both the UEG guide and SWRI. This draws the conclusion that generally different data has been examined and that SWRI have 'weighted' certain data as more significant, correctly in some instances with respect to frequency of loading but have ignored without justification apparently authentic data generated by UKOSRP I. This is particularly true for seawater data at low R with cathodic protection. As these are very pertinent conditions for the North Sea, the data for this condition has been reviewed.

For the above condition ie. seawater with cathodic protection at low R ratio, the SWRI law/data shows an unusual plateau at high stress intensity factor ranges, Figure 5.9. The existence of this plateau has not been confirmed in all laboratory tests and its validity is open to question. Of prime concern is that the data of Vosikovsky[13] which shows this plateau effect, has been weighted as being of more sigificance. This has resulted in the introduction of a fourth constant term to the crack growth law. This constant is simply the reciprocal of the plateau crack velocity ie. $1/_{10^{-6}}$.

In introducing this constant, SWRI have ignored data not only from UKOSRP I but also from Vosikovsky at a rate > 10^{-6}m/cycle. This point was recognised by SWRI who suggested that an additional term, similar to the first two terms but with different constants would be required. A review of the SWRI and UEG data has been carried out and updated the crack growth law for steels in seawater with cathodic protection at low R ratios.

This new crack growth law, plotted in Figure 6.23 has the form:

$$\frac{1}{da/dN} = \frac{1}{A_1\Delta K^{n_1}} + \frac{1}{C\Delta K^{m}} - \frac{1}{C[(1-R)K_{IC}]^{m}} + \frac{1}{A_2\Delta K^{n_2}} - \frac{1}{A_2[(1-R)K_{Ic}]^{n_2}} \quad (5.5)$$

The values of the constants are given in Section 6.3.3. This new law is still similar to those originally derived by SWRI but has introduced an upper intermediate cracking regime. This takes account of both the tendency to form a plateau crack velocity and the additional data at ΔK's between 8 and 80 MPa/m occuring above the plateau. Hence it prevents the non-conservatism introduced by the large constant value and the over conservatism that would have occurred for this condition if the original SWRI single region II term had been used for crack propagation.

Although this new crack growth law (Equation 5.5) appears somewhat more complicated that the Paris Law, in essence it is the same and is simple to use. The crack growth rate is computed at the levels of ΔK of interest by simply substituting this into the various parts of the equation with the appropriate constants. In using Equation 5.5, four additional simple calculations are made which greatly enhance the confidence of the fatigue crack growth assessment and prevent the non-conservatism and over conservatism discussed above and give a safer interpretation of the life of a joint.

The approach to updating the information on crack growth was to digitise the existing data for UEG and SWRI together with some additional information[14] and re-plot in a single figure. Some SWRI data was excluded for the following reasons:

i. Data generated in region I by Bardal et al[15] at low stress intensity factors. No additional data in this region is, to our knowledge, available and the constants produced by SWRI remain valid.

ii. Any experimental data derived at frequencies outside the range 0.1 - 0.2 Hz. Frequency of testing has an important effect on fatigue in seawater, therefore only data generated at the frequency relevant to offshore structures has been assessed.

One important aspect of the updating is that crack growth rates at cathodic protection levels of -0.850V and -1.1V have been included. The former represents the level at which corrosion protection is normally achieved, the latter a degree of overprotection. Whilst there is almost certainly a difference of crack propagation rate between the two levels of protection, use of an upper bound approach will give a conservative but realistic crack growth law for a seawater environment with cathodic protection. This results in the crack growth rate of the new law being, over a small range of ΔK's, greater than the rate in freely corroding seawater. This is explained in terms of the applied potential enhancing fatigue crack growth at potential more negative than -0.7V due to the corrosion mechanism being moved towards hydrogen embrittlement.

Of the new fatigue crack growth law, region I cracking remains originally as proposed but the validity is extended slightly to encompass some of Vosikovsky's data at stress intensity factors less then 10MPa$\sqrt{m}$. This results in a slight adjustment of the constants in the lower intermediate (region II) regime followed by the extra term for the upper intermediate region as discussed above. The fourth and fifth terms of the law, which take the form of $\frac{1}{A_i[(1-R)K_{IC}]^{n_i}}$, account for crack growth in the upper (region III) regime where rapid crack growth takes place as

instability approaches. These terms are in fact of the same format used for region III crack growth under air and freely corroding conditions but the addition of an extra term in region II necessitates an extra growth term in region III. The choice of R = 0.2 and Kc =250 MPa/m results in the region III crack growth extending exponentially as ΔK approaches 200 MPa$\sqrt{m}$. This part can be adjusted if more appropriate or accurate data is produced i.e. all crack propagation data at R=0.1 is available and the final value of material toughness at the onset of instability can be satisfactorily determined.

In a brief review of other fatigue crack growth data[16, 17], it is clear that the tendency to form a plateau or at least produce a change in slope of the da/dN versus ΔK curve, highlighted by SWRI, is not an isolated occurrence in seawater testing. It is evident in the data from UKOSRP I[2] for seawater tests with cathodic protection and is very marked in some recent work by Cowling and Appleton[17] for tests in 3% NaCl solution containing various poisons that prevent the hydrogen evolution reaction and promote adsorption of nascent hydrogen into the metal and increases hydrogen embrittlement. The evidence available suggests that the phenomenon does not occur or is not as marked in freely corroding seawater but is most in evidence for cathodic protection. The change in gradient always appears to occur at around 7.10^{-6}m/cycle for frequencies of 0.1 - 0.2 Hz but is shifted by changes in frequency outside of this range.

The reason for the change in slope is difficult to understand but obviously reflects a change in crack growth mechanism at this propagation rate. The fact that it appears to only occur in seawater, possibly only under cathodic protection, suggests that it also involves a change in the corrosion mechanism but why it should also be affected by the frequency is difficult to reconcile. It is recommended that this potentially interesting observation be examined further.

Additionally it is recommended that the five part growth law should be used for accurate but conservative assessment of fatigue crack growth in seawater with cathodic protection and a low R ratio. An additional refinement to the law could be achieved by separating the two levels of cathodic protection potential and determining whether any significant differences occur. Additionally similar reviews of air, freely corroding and cathodically protected conditions at high R ratio could be performed to update the constants and continually improve the laws originally proposed by SWRI. Hence, if an accurate measure of the cathodic protection potential can be made, the appropriate database on the six sets of conditions that closely approximates those experienced offshore can be used to calculate the fatigue propagation rate of any defect discovered or postulated.

For pipelines, fatigue loading arises from pressure variations in operation, surges leading to a damped mode of oscillation, low frequency cycles associated with start up and shut down and thermal loadings associated with changes in temperature. It is thought that the latter within the North Sea will be very minor. For pipelines, an internal defect subjected to fluctuating stress experiences a different environment than for steel structure ie. a crude oil or gaseous environment. For these conditions, a different set of information is required ie. the crack growth constants within crude oil or gas. The data generated by Vosikovsky[18] and by Vosikovsky and Rivard[19] is useful for this purpose. They carried out fatigue crack propagation studies in X65 line pipe in crude oil subjected to various concentrations of H_2S approximating from 1ppm to saturation level of 4700ppm. It is reported that the maximum acceleration of growth rate relative to air was 3 times at the low H_2S content and 20 times at saturation level when compared to air propagation rates on similar material[20]. The results are shown in figures 5.10 and 5.11. For testing in crude oil with the low level of H_2S, Figure 5.10, the growth data in the low ΔK range fall on a common curve for all frequencies,

with a slope higher than that in air (m = 4.67 versus m = 2.82). Below ΔK =18 MPa√m the growth rate in crude oil is lower than that in air and the data indicates that the threshold limit could be significantly higher. At higher ΔK, the cracks in oil grow faster than in air with a maximum acceleration of 3 times compared to air.

With a higher concentration of H_2S a much higher increase in crack growth rate occurs compared with air, Figure 5.11. The slope for this crack growth curve below ΔK = 20MPa√m is 6.3 indicating a very high dependence of the crack growth rate on ΔK. Above 20MPa√m, the curve runs approximately parallel to the air date. It is interesting to note that the change in slope again occurs around a crack growth rate of 10^{-6}m/cycle as was observed for testing in seawater. In a later study,[19], the fatigue crack growth in varying concentrations of H_2S were further determined. It was found that with H_2S concentrations greater than 350ppm a change of slope again occured at 1.4×10^{-6}m/cycle and that the two segments of the line could be described by the Paris equation. For the lower segment of the curves, the constant m averaged 6.4 and the constant A was found to be linearly dependent on H_2S concentration,

$$A = 7.12 \times 10^{-19} \times (H_2S \text{ concentration in ppm}) + 3.4 + 10^{-16}.$$

The upper parts of the curves ($\frac{da}{dN} > 1.4 \times 10^{-6}$ m/cycle) are are linear at H_2S > 350ppm and the slope n = 2.7.

For comparison, the constants for air and plain crude oil at 0.1 Hz are given in Table 5.3. Note that an adjustment in the air slope is given at ΔK = 20MPa√m.

The conclusion from this work is that the environmental enhancement of fatigue crack growth rates in sour crude oil depends primarily on the hydrogen-sulphide content of the oil.

At high H_2S concentrations (>350ppm) substantial crack growth enhancement occurs at intermediate and high stress intensity ranges.

At low H_2S concentrations (<350ppm) a substantial growth enhancement occurs in the intermediate ΔK range.

At low ΔK, close to the crack-growth threshold, oil appears to be less aggressive than air and with low H_2S concentrations produces lower growth rates than air.

5.2 Miscellaneous Databases

This section covers those additional areas of information required in the form of databases, to carry out a defect assessment/inspection rationalisation. Two typical areas of supplementary data necessary are material toughness information and levels of residual stresses to be found in as-welded and post weld heat treated tubular joints.

5.2.1 Material Toughness

1. Parent plate

In assessing the stability of cracks in steel structures in addition to determining the crack driving force as illustrated in Section 6.4, it is also necessary to have a measure of the materials resistance to fracture. In an idealised situation, this toughness would be the initiation toughness for fracture measured by a suitable test such as the crack tip opening displacement (CTOD) test for each steel plate supplied together with its exact location in the structure. However, with respect to North Sea structures, this information is rarely available due to;

(i) CTOD testing not being a common place requirement in specifications at the time of steel production. This is particularly true of pre-1979 structures.

(ii) Documentation of earlier structures is also unlikely to be complete such that neither all the material certificates nor all the exact locations for steel plates in the structure can be traced.

Hence, the data available is in the form of Charpy V impact tests at a test temperature less than that of application. For the base material ie. parent plate, the toughness is usually available as three individual results on the mill certificates. The best approach here is to tabulate the data available from each individual mill sheet for each tubular joint and joint locations eg. stub or chord together with additional useful information such as plate thickness, yield and ultimate strength and steel supplier, as usually more than one supplier is involved. An example of the type of tabulation required is given in Table 5.3.

In addition it is recommended that each individual Charpy test for thickness and steel supplier is tabulated and a summary of the mean and standard deviation recorded as shown in Table 5.4. In some instances, this information may already be available from the supplier as part of his production histograms. An example for Charpy impact results of BS 4360 50E steel currently supplied by NKK is given in Figure 5.12. This approach allows the question of material toughness to be considered in a number of ways dependent on the amount of data available.

- As an average for material thickness and steel manufacturer.
- As minimum/maximum values for the above categories
- As a mean value ± x standard deviations where a probabilistic approach could be taken
- As individual precise values for joints and locations of interest.

Alternatively, the approach can be a combination of the above such as use of the individual precise values at points of interest but where the required data is absent, use of the database allows a probabilistic approach to be taken to give, say, a 95% confidence limit for determined toughness values.

In addition to the mill sheet data, further information on the material toughness can be sought from a number of different areas such as the steel manufacturers, a search of the literature for steel of the relevant era and a review of the original material specifications. This has two purposes, (a) to increase background information on the nature of the steel so that any approximation to the level of toughness to be expected can be based on firm knowledge and (b) a requirement to relate the toughness data given on the mill sheets to the temperature of interest, usually -10 or 0°C. To achieve the latter, it is necessary to either obtain CTOD values of similar steel or Charpy transition curves of similar steel.

The problem arises in that parent plate material toughness data for steels of, say, the mid-1970's is difficult to obtain due to the toughness generally being greater than that of weld metal and HAZ and, therefore, being of little concern in comparison. It is possible that the steel manufacturers concerned may have records of material properties carried out in production trials which would contain Charpy transition curves but it is known that some manufacturers destroy records after 5 years. Some CTOD data measured on parent plate for the UKOSRP I programme[21] is available but differences in calculation procedures prior to the issue of BS 5762 in 1979 lead to overestimates of toughness and the data has to be disregarded.

Information supplied after that time will be relevant. However, it should be emphasised that improvement in steel manufacture over the past 15 years has led to significant improvements in steel toughness. Thus when obtaining additional information for an assessment, it should have a similar composition, yield strength and Charpy toughness at the same temperature as for the steel in the structure of interest. For example Figures 5.13 and 5.14 illustrate Charpy transition curves for two steels, both to BS 4360 50D steel.

Figure 5.13[22] is for 63.5mm thick normalised BS 4360 50D steel supplied to BP for the Forties Field and gives the mean Charpy impact energy at various temperatures. Figure 5.14 is for 50mm steel currently available from NKK where a great improvement in toughness is evident particularly in the transverse direction. Table 5.5 gives the chemical composition of the two steels and shows that the reduction in C and S levels in modern steel practice has brought large benefits in terms of toughness without a reduction in strength.

Having obtained either the actual material's Charpy transition curve or an appropriate curve from the literature, it then becomes necessary to convert the Charpy values recorded for each joint from their test temperature to the temperature of interest.

To use the examples of Table 5.3, these were recorded at -40°C and Figure 5.13, an appropriate Charpy transition curve for this steel shows that a shift in temperature from -40 to 0°C improves the impact value from 58J to 92J, a factor of 1.59. Hence, all the impact values of the joints of interest can, on average, have an increase in toughness from that recorded to that in service by a factor of 1.59.

This approach should however be used with caution. For the older, mid - 1970's steels it is appropriate as most steels used would have been in the lower to mid transition range at the temperature of test. However, some of the later supplied steels have much improved properties and exhibit upper transition or even upper shelf behaviour at -40°C. In these instances use of a transition curve to correlate results at -40°C to 0°C by use of a transition curve conversion factor could well lead to overestimates of the level of toughness at 0°C because a large increase in toughness cannot be expected. In these instances, the best approach is to use the original Charpy impact values given in the mill certificates. This will introduce an element of conservatism into the calculations as a small increase in toughness will result with an increase in temperature. The instances where this approach will need to be taken will be few as the general increase in material toughness was accompanied by an increase in specifying CTOD toughness data such that many of steels supplied since 1980 will have CTOD values, determined usually at -10°C, and these can be directly used in any crack stability assessment.

2. Orientation

The toughness data recorded in the mill certificates is usually for Charpy specimens located in the transverse orientation ie. it represents cracks located parallel to the direction of rolling. In some instances cracks in the structures will be located in the direction transverse to the rolling direction (the longitudinal Charpy direction). However, for the assessment of crack stability, it is recommended that the transverse toughness data should be exclusively used for two reasons;

a) Longitudinal toughness data has not usually been measured on the steels supplied and limited additional data is available.

b) Transverse data is conservative in comparison to longitudinal data.

3. Heat Affected Zone Data

A further database of toughness information is required for the heat affected zone. One source of toughness information is to examine the welding procedure qualification test results for the components under interest and tabulate the toughness results. Examination of the welding production tests for the same procedures will increase the database of the HAZ and allow a mean value to be determined for each level of appropriate thickness. If these results are not CTOD values, which is very unlikely, there are two alternatives to dealing with the Charpy impact results. The first approach is similar to the parent plate approach and converts the toughness recorded at, say, -40°C to 0°C via Charpy transition curves. These curves are unlikely to be available within the documentation of the structure but a considerable amount of data for HAZ toughness relating to BS 4360 50D/E and 40D/E steels exists within the literature[23,24]. These give impact transition curves for different structures, heat inputs and consumables. Examples are given in Figures 5.15 and 5.16 where lower bound transition curves have been added irrespective of the heat input. Wong and Rogerson[25] in a study of the probabilistic factors involved in fracture of offshore structures produce mean and standard deviations of toughness measured by Charpy impact and CTOD test data for a variety of welding methods at various temperatures. This is reproduced in Table 5.6.

The alternative approach is to examine the level of toughness obtained in the HAZ in comparison to the parent plate material. It is nearly always found that the HAZ toughness is significantly lower than the parent plate. If a consistent degree of reduction in HAZ toughness compared to the parent plate is evident, a reduction factor can be determined for each level of plate thickness and the toughness at each structure component/joint reduced accordingly to give the HAZ toughness. This obviates the use of Charpy transition curves.

Once the toughness has been obtained at the temperature of interest, a crack stability assessment is carried out as outlined in Section 6.4. This derives a crack driving force curve for a number of crack depths in terms of δ_{app} and the material toughness δ_c is compared to this. Obviously, if the toughness available is in the form of Charpy impact values, a further correlation is required to convert this into the material's critical CTOD toughness. The procedure for this is outlined in Section 6.4.3.

5.2.2 Residual stresses

Residual stresses in welded components arise directly from the localised shrinkage associated with the cooling down of hot weld metal which is restrained either internally or externally by the cold sections of the fabrication surrounding the weldment. The residual stresses are the result of plastic deformation due to severe thermal stresses arising because the temperature distribution in the body ie. fabrication will be far from uniform. While the body is hot a compatible system will exist between the plastic and thermal deformations, but in the course of cooling the thermal strains disappear and the plastic deformation remains. By themselves, however, these plastic deformations will not satisfy the compatibility conditions so that a residual stress system is formed. More detailed descriptions of what is in fact a highly transient and complex process that leads to the formation of residual stress fields can be found in references 26 to 30.

The size and consequently the effect of the residual stress field is affected by a number of variables. These include material properties, material thickness, degree of restraint, weld preparation, welding process and welding parameters. The level of yield stress restricts the level of residual stress formed whereas

the welding process and parameters together with the material thickness and weld preparation also influence the level of stress by affecting the degree of restraint. A high degree of restraint limits distortion and gives rise to high residual stress. This in turn greatly increases the risk of failure as high tensile residual stresses can greatly increase the crack driving force on a defect such that this exceeds the material fracture resistance and crack instability occurs. There is also some suggestion[29] that the formation of residual stresses can have a deleterious effect on material properties and a reduction in the resistance to fracture.

Thus in making an assessment of the significance of defects in welded joints, whether in weld metal or HAZ, it is necessary to make allowances for the residual stresses caused by the weld. In a review of the origin and nature of residual stresses, Parlane[26] gives the typical 'traditional' residual stress distributions for longitudinal and transverse surface directions and the through thickness transverse direction. These are given in Figure 5.17. Figure 5.18 illustrates the location of defects/fatigue cracks at a weld toe similar to the situation of concern within the current study. This shows that the transverse through thickness residual stresses are those which will act on the crack tip and hence it is this residual stress field which is of concern. Figure 5.19 gives the generally accepted through thickness residual stress patterns for single sided and double sided 'V' butt welds[30]. However, despite these 'traditional' and generally accepted residual stress patterns, experimental verification is not apparent and a review of the literature does not confirm these patterns. The main reason for this is that the measurements of residual stresses within welds is not a particularly easy task and a large experimental effort has gone into the measuring techniques rather than determination of residual stress patterns.

In measuring residual stresses, a number of techniques exist all of which have advantages and disadvantages. Although carried out in 1977, the work of Parlane[31] gives a useful summary of the

techniques available and later work by Leggatt of the Welding Institute (32, 33) gives further information on the techniques available. It is clear from the literature that measurement of through thickness residual stresses is of particular difficulty due to the time consuming and expensive nature of the techniques available, the destructive nature of the procedure and the difficulty of removing specimens without releasing the residual stress field. This has resulted in very few attempts at measuring through thickness residual stress patterns.

This is disappointing as frequently welding defects or crack like defects of partial wall thickness depth need to be assessed in terms of stability when subjected both to membrane stresses and some level of residual stress. Hence it has been customary to assume that the residual stresses in a weld which has not been post weld heat treated to be tensile and of yield magnitude. This clearly cannot be true as an essential feature of the residual stress field is that it is self-equilibrating. Thus, if the residual stress distribution is known the accuracy of any fracture assessment can be improved[34].

Unfortunately, within the literature, very few examples of measuring the through thickness residual stress can be found although there is some recent work on measuring the through thickness residual stresses remaining after post weld heat treatment[32]. In the as-welded conditions some very early work[35] using hole drilling and cutting and slicing techniques gave an almost random distribution in the transverse direction with both tension and compression peaks of $\approx$ 350N/mm^2 ocurring. In a study of fatigue crack propagation, Truchon et al[36] took the trouble to actually measure the residual stress patterns in their welded specimens using the X-ray technique. Their results, reproduced in Figure 5.20 show that in the region of the HAZ, high tensile surface stresses occur but that through the thickness high compressive stresses (230N mm^2) exist, balancing the tensile residual stresses measured on the surface of the specimen.

These results are in agreement with some very recent work carried out by Leggatt[32] on the effectiveness of post weld treatment in alleviating residual stresses. This work also shows that in the transverse direction compressive stresses exist through the thickness

balanced by tensile stresses at the surface. An example of the results from reference 32 is given in Figure 5.21. Note that the stress levels in Figure 5.21 are much lower than in Figure 5.20, indicating the effectiveness of post weld heat treatment.

The level of residual stress found by Leggatt after PWHT at around $50N/mm^2$ is also in agreement with the X-ray technique work where an additional study showed that PWHT at 580°C resulted in very low stress ($\approx 30N/mm^2$).

A very recent study[37] attempts to experimentally measure residual stress distributions in welded tubular T-joints by the block sectioning and layering techniques. Three T-joint specimens were examined and the through thickness residual stress determined at three points around the weld toe at both crown and saddle points for each specimen. This is illustrated in Figure 5.22. The authors report that a study of the detailed results reveal no consistent trend across the weld toe in any trio of distributions taken at a given location. Therefore, the mean distribution obtained from each trio has been presented to give through-thickness distributions of transverse stress (normal to weld) and longitudinal stress (parallel to the weld), representative of conditions at the weld toe. The results from this exercise are reproduced in Figure 5.23. Values of residual stress on the chord inner surface, determined by centre hole drilling at the weld toe section are also shown, marked by a dense spot. It should be noted that the authors claim a standard deviation of 80 N/mm^2 for the mean residual stress distributions hence, the results shown in Figure 5.23 do not have a high degree of accuracy. However the stress distributions obtained do follow the patterns generally accepted for through thickness residual stresses and the authors should be commended on attempting such a difficult and time consuming task.

The experimental results for the different studies above would seem to confirm that taking a fully tensile stress at yield level for a welded joint is a very conservative estimation of the residual stress contribution in any defect assessment/crack stability calculations. They also show that assuming a tensile level of 25% of yield to be remaining after PWHT[34] is also conservative. Thus it can be argued

that the residual stress goes to zero and then becomes compressive at some point through the thickness. There is some evidence to suggest that a tensile force also exists on the inner surface so that a pattern similar to that in Figure 5.19(a) exists. However, without more detailed study it is difficult to put firm values on the peak stress levels and a mathematical description to this residual stress pattern. On the other hand it is also clear that to use a constant tensile stress level equal to the yield stress is very conservative and a sensible compromise would seem to be to assume a residual stress pattern that is of tensile magnitude at the surface of cracking and reduces to zero at the opposite surface as shown in Figure 5.24. This would increase the accuracy of the crack stability calculations while maintaining a degree of conservatism. The literature would also seem to suggest that taking a similar stress pattern to that in Figure 5.24 but with the peak stress reduced to 25% of yield for post weld heat treated joints will maintain a degree of conservatism in crack stability assessments.

REFERENCES

1. R M Clayton. "Assessment of UKOSRP Crack Growth data to investigate the remaining life of offshore structures following inspection' UKAEA report No. ND-R-852(R) November 1982.

2. "Design of tubular joints for offshore structures". CIRIA Underwater Engineering Group, London 1985.

3. M B Gibstein "Fatigue strength of welded tubular joints tested at Det Norske Veritas Laboratories" Paper 8.5 of Conf. Steel in Marine Structures, Paris, 1981.

4. W D Dover, S J Holbrook and R D Hibberd "Fatigue life estimates for tubular welded T joints using fracture mechanics" Welding Institute Select Seminar on European Offshore Steels Research, Cambridge, 1978.

5. W D Dover, T J Wilson "Corrosion fatigue of tubular welded' T joints International Conference on Fatigue and Crack Growth in Offshore Structures 7-8 April 1986 p.135-153.

6. United Kingdom Offshore Steels Research Project Phase II. Testing of tubular joints Task 5.2.

7. International Offshore Conference on Steel in Marine Structure to be held at Delft, The Netherlands 15-18 June 1987.

8. H G Morgan et al. "An investigation of the corrosion fatigue crack growth behaviour of structural steels in seawater". Paper 5.1 of conf. Steel in Marine Structure, Paris, 1981.

9. J W Hancock, D S Gall and X. Huang. "Fatigue Crack Growth due to random loading in air and seawater with applications to the growth of semi-elliptical cracks in the tubular welded joints of offshore structures". International Conference on Fatigue and Crack Growth in Offshore Structures 7-8 April 1986 p.49-58.

10. A Saxena, S J Hudak Jr and G M Jouris "A three component model for representing wide-range fatigue crack growth rate behaviour" Engineering Fracture Mechanics, 12 1979, p.103-115.

11. O H Burnside et al "Long term corrosion fatigue of welded marine steel". Report No. 06-6292 South West Research Institute, San Antonio, 1984.

12. Tubular Joints Group Newsletter Supplement Number One CIRIA Underwater Engineering Group, London. October 1985.

13. O Vosikovsky. "Fatigue crack growth in an X-65 line-pipe steel at low cyclic frequences in aqueous environments" Internal report PM-M-74-11 Canada. Department of Energy, Mines and Resources, Ottawa, July 1978.

14. United Kingdom Offshore Steels Research Project Phase II.

15. E B Bardal, P J Haagensen and O Solli "Corrosion Fatigue - Offshore" SINTEF/DnV Final Report, NTNF project B.0601.5185. October 1978.

16. H G Scholte and H Wildschut "Fatigue crack propagation tests on welded specimens in air and sea water". Paper 5.2 and Conf. Steel in Marine Structures, Paris 1981,

REFERENCES

17. M J Cowling and R J Appleton "Corrosion Fatigue of a C-Mn Steel in Seawater Solution" International Conference in Fatigue and Crack Growth in Offshore Structures 7-8 April 1986 p.77-92.

18. O Vosikovsky "Fatigue Crack Growth in an X65 Line-Pipe Steel in Sour Crude Oil". Corrosion-Nace Vol 32, NO12, December 1976 p.472-475.

19. O Vosikovsky and A Rivard "The effect of hydrogen sulphide on fatigue crack growth in a pipe line steel". Canada Centre for Mineral and Energy Technology. Report MRP/PMRL 80-53J. July 1980.

20. O Vosikovsky "Fatigue Crack Growth in a X65 line pipe steel at low cycle frequencies in Aqueous environments". J.Eng, Mat. Tech. ASME, Vol 97, No. 4. P298. 1975.

21. G O Johnston "CTOD values calculated to BS 5762 Welding Institute Research Bulletin. July 1981.

22. J D Harrison. "The Effect of Post Weld Heat Treatment on the Toughness of Welds for an Offshore Platform". Performance of Offshore structures p.75.

23. H G Pisarski "Preliminary Structure Toughness Results from the UKOSRP Fracture Programme" Interim Technical Report UKOSRP 5/01 3509/11/78.

24. H G Pisarski "Fracture Toughness of Some Materials used in Fabricating Fixed Offshore Structures. OTC 4034. Offshore Technology Conference, Houston, Texas 1981.

25. W K Wong and J H Rogerson. "A probabilistic estimate of the relative value of factors which control the failure by fracture of offshore structures". Paper 9. 2nd International Conference on Offshore Welded Structures. London. November 1982.

26. A J A Parlane "Origin and nature of residual stresses in welded joints' Residual Stresses and their Effect, The Welding Institute, 1981.

27. T R Gurney 'Residual stresses' BWRA Bulletin Vol. 9, No. 3 March 1968.

28. K Masubuchi 'Models of stresses and deformation due to welding - A review', Journal of Metals December 1981. p19-23.

29. C E Turner 'Post Yield Fracture Mechanics', ed. Latzko, Applied Science, Ch. 2, 1979.

30. H Pisarski, Private Communication

31. A J A Parlane 'The determination of residual stresses : a review of contemporary measurement techniques'. Paper 8 - Residual stresses in welded construction and their effects. London, November 1977.

32. R H Leggatt 'Relaxation of Residual Stresses During Postweld Heat Treatment of Submerged Arc Welds in a C-Mn-Nb-Al Steel', Welding Institute Research Project 288/1985.

33. P L Threadgill and R H Leggatt, 'Effects of Postweld Heat Treatment on Mechanical Properties and Residual Stress Levels of Submerged Arc Welds in a C-Mn-Nb-Al Steel 'Welding Institute Research Report 253/1984.

34. R H Leggatt, 'Residual Stresses at Circumferential Welds in Pipes', Welding Institute Research Bulletin Vol 23, No. 6 June 1982 p.181-188.

35. H T Gencsoy and J P O'Learly, 'Residual Stresses in a Butt-Welded Flat Plate', Welding Research Supplement February 1965 p.56-63.

36. M Truchon, H P Lieurade and C Putot, 'A study of fatigue crack propagation in E36 steel welded joints', paper 9.1 Steel in Marine Structures October 1981.

37. J G Payne and R F D Porter-Goff "Experimental residual stress distributions in welded tubular T-nodes". International Conference in Fatigue and Crack Growth in Offshore Structures. The Institution of Mechanical Engineers 7-8 April 1986.

N(x 10^5)	2c	a	a/t	a/c	2c : a
9	37	3	.09	.16	12:1
9.5	44	3	.09	.14	15:1
10	90	4	.125	.09	23:1
10.5	101	6	.19	.12	17:1
11	152	9	.28	.12	17:1
11.5	188	13	.41	.14	14:1
12	211	16	.5	.15	13:1
12.5	243	20	.63	.16	12:1
13	281	21	.66	.15	13:1
13.5	321	25	.78	.16	13:1
14	354	28	.88	.16	13:1
14.5	398	31	.97	.16	13:1
15	419	32	1.09	.15	13:1

T-Joint Axially Loaded in Air

Chord Diameter = 914mm
Chord Thickness = 32mm
Brace Diameter = 457mm
Brace Thickness = 16mm

f_{nom} = 46.19

SCF = 6.5
Hot Spot = 300 N/mm^2

N(x 10^5)	2c	a	a/t	a/c	2c : a
4.85	180	.75	.09	.008	240:1
8.28	180	3.00	.38	.033	60:1
9.23	190	4.8	.60	.051	39:1
11.43	210	6.0	.75	.057	35:1
13.00	236	6.5	.81	.055	36:1
14.32	260	6.8	.85	.052	38:1
15.48	320	7.4	.93	.046	43:1

Overlapping K balanced axial loading.

Chord diameter = 457mm
Chord thickness = 16mm
Brace diameter = 244mm
Brace thickness = 8mm

from = 102 N/m^2

Failure in brace

TABLE 5.1

ASPECT RATIOS OF TWO TUBULAR JOINTS TESTED (REFERENCE 6)

Air	Lower n = 3.5 $C = 1.3 \times 10^{-12}$	Upper ($\Delta K > 20$ MPa$\sqrt{m}$) n = 2.5 $C = 5.2 \times 10^{-11}$
Oil (R = 0.05)	Lower n = 4.8 $C = 2.7 \times 10^{-14}$	Upper ($\Delta K > 34$) n = 1.9 $C = 7.3 \times 10^{-10}$
Oil With H_2S	n = 6.4 $C = 7.12 \times 10^{-19}$ (H_2S conc (ppm)) $+ 3.4 \times 10^{-16}$	Upper ($\Delta K > 20$) n = 2.7 $C = 6 \times 10^{-8}$ (H_2S >350 ppm)

TABLE 5.2

FATIGUE CRACK GROWTH CONSTANTS FOR X-65 LINE PIPE STEEL SUBJECTED TO DIFFERENT ENVIRONMENTS: (REFERENCE 19)

JOINT NUMBER	CHORD/ STUB	THICKNESS	STEEL SUPPLIER	CV% @ -40°C	CV%	f_y (1) N/mm^2	f_u (1) N/mm^2	f_f N/mm^2	PLATE NUMBER	PWHT	f_{res} N/mm^2
1	S	50.8	Company A	85, 87,88 112, 109, 107	96.3	351.5	493.25	422	83416/1	No	351.5
2	S	50.8	Company A	100, 123, 124 91, 70, 77	97.5	366.75	515.25	441	83424/1	No	366.75
3	S	50.8	Company A	87, 93, 90 78, 93, 73	85.67	375	506	440	83432/1	No	375
4	C	63.5	Company B	54, 50, 53	52.33	314	482	398	430201	Yes	78.5
5	C	63.5	Company B	51, 58, 68	59.00	317	494	406	101101	Yes	77.25
6	C	63.5	Company B	41, 40, 42	41	307	489	398	430401	Yes	76.75
7	S	38.1	Company B	42, 131, 65	79.3	367	539	453	960701	No	367
8	S	38.1	Company B	135, 175, 103	137.67	369	529	449	210101	No	369
9	S		Company B	56, 87, 48	63.67	358	525	442	210401	No	358
10	C	44.5	Company A	96, 98, 89 70, 68, 73	82.3	367	511.75	440	83419/1	No	367
11	C		Company A	94, 83, 87 78, 87, 85	85.67	371.25	512.25	442	83431/1	No	371.25
12	C		Company A	103, 94, 106 99,103, 91	99.3	346.75	494.75	421	83427/1	No	346.75

(1) For Company A, average of 4 values, for Company B single value recorded.

TABLE 5.3 TYPICAL DATABASE FROM MILL CERTIFICATES FOR 12 JOINTS IN STRUCTURE

	t mm	Cv J range	Cv J AV	s.d.	f y	f u
Company A	50.08	70-124	93.7	15.9	364	505
	44.5	68-106	89.1	11.4	362	506
Company B	63.5	40-68	50.8	9.0	313	488
	38.1	42-175	93.6	45.9	365	531

TABLE 5.4

SUMMARY OF MATERIAL PROPERTY DATA FROM DATABASE IN TABLE 5.3 SHOWING MEAN AND STANDARD DEVIATION OF TOUGHNESS PER THICKNESS PER STEEL MANUFACTURER

	C	S	P	Si	Mn	Cr	Cu	Nb	Al
BP	0.18	0.009	0.009	0.48	1.30	0.16	0.15	0.049	0.04
N KK	0.15	0.004	0.015	0.39	1.40	-	0.18	0.03	-

TABLE 5.5

CHEMICAL COMPOSITION OF STEEL WHOSE TRANSITION CURVES ARE GIVEN IN FIGURES 5.13 AND 5.14

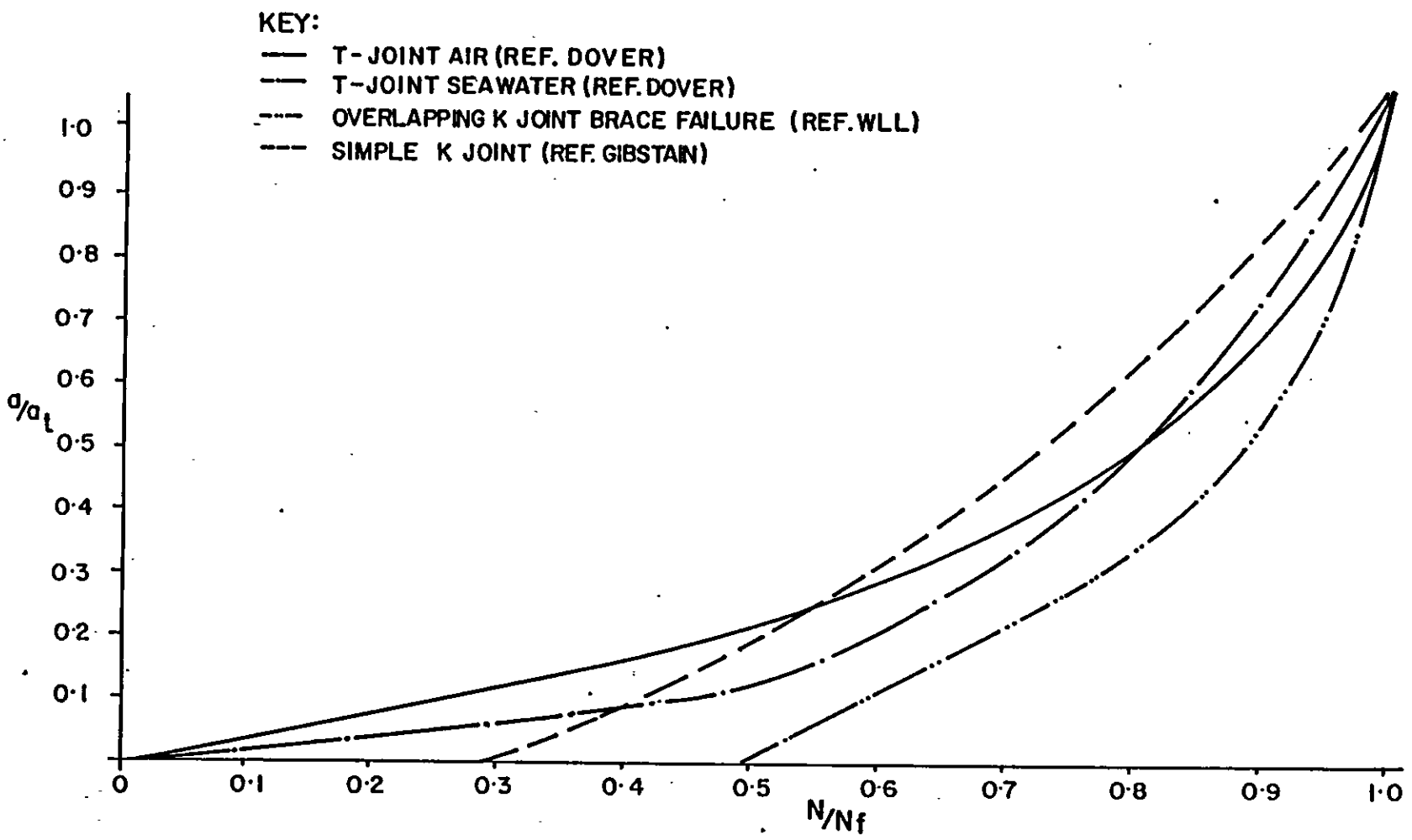

CRACK DEVELOPMENT FOR FOUR DIFFERENT JOINTS.

PROJECT URP 72 : STUDY 4

INSPECTION PLANNING , THE ROLE OF DAMAGE ASSESSMENT

WIMPEY OFFSHORE REPORT No. WOLI09/86

FIG. 5.1

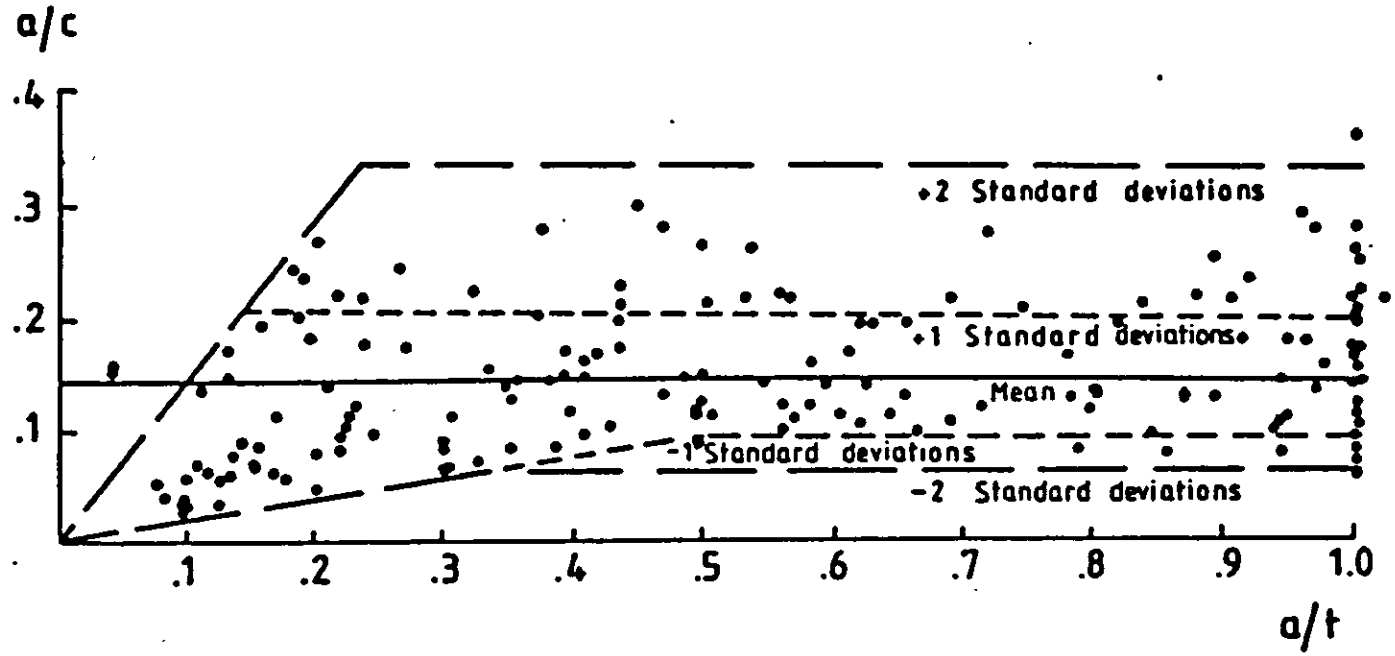

CRACK ASPECT RATIO Vs CRACK DEPTH FOR TUBULAR T-CONNECTIONS (Ref.1)

PROJECT URP 72 : STUDY 4

INSPECTION PLANNING , THE ROLE OF DAMAGE ASSESSMENT

WIMPEY OFFSHORE REPORT No. WOLI09/86

FIG. 5.2

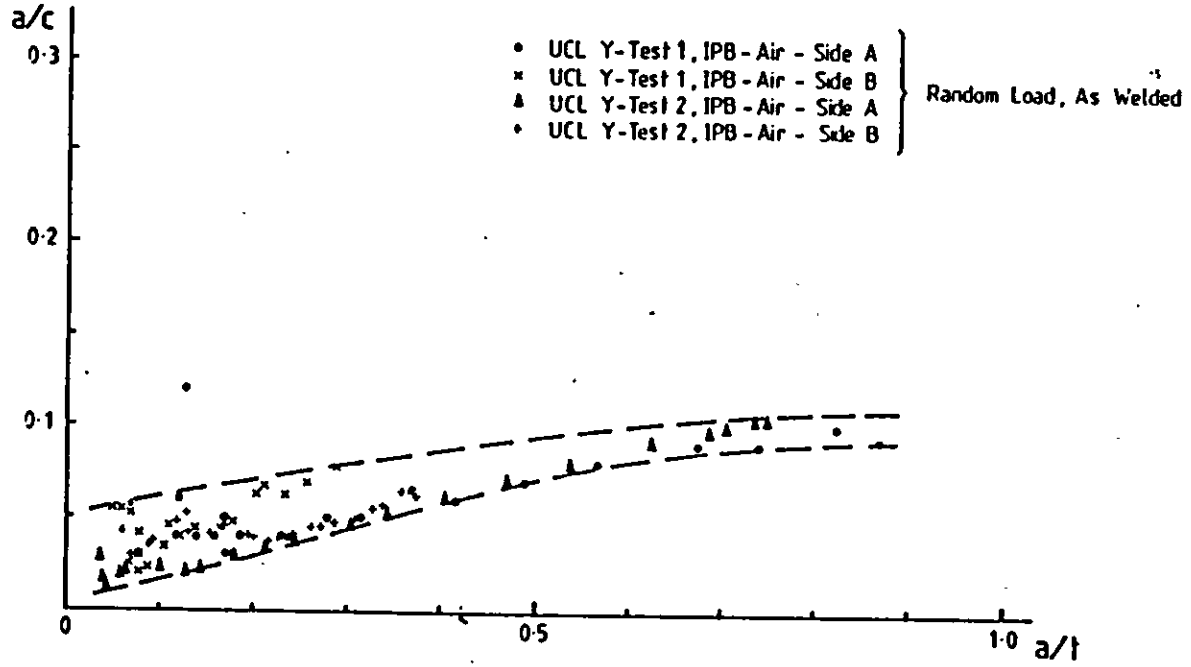

ASPECT RATIO Vs. CRACK DEPTH FOR TWO Y-JOINT TESTS IN AIR (Ref. 5)

PROJECT URP 72 : STUDY 4

INSPECTION PLANNING , THE ROLE OF DAMAGE ASSESSMENT

WIMPEY OFFSHORE REPORT No. WOL109/86

FIG. 5.3

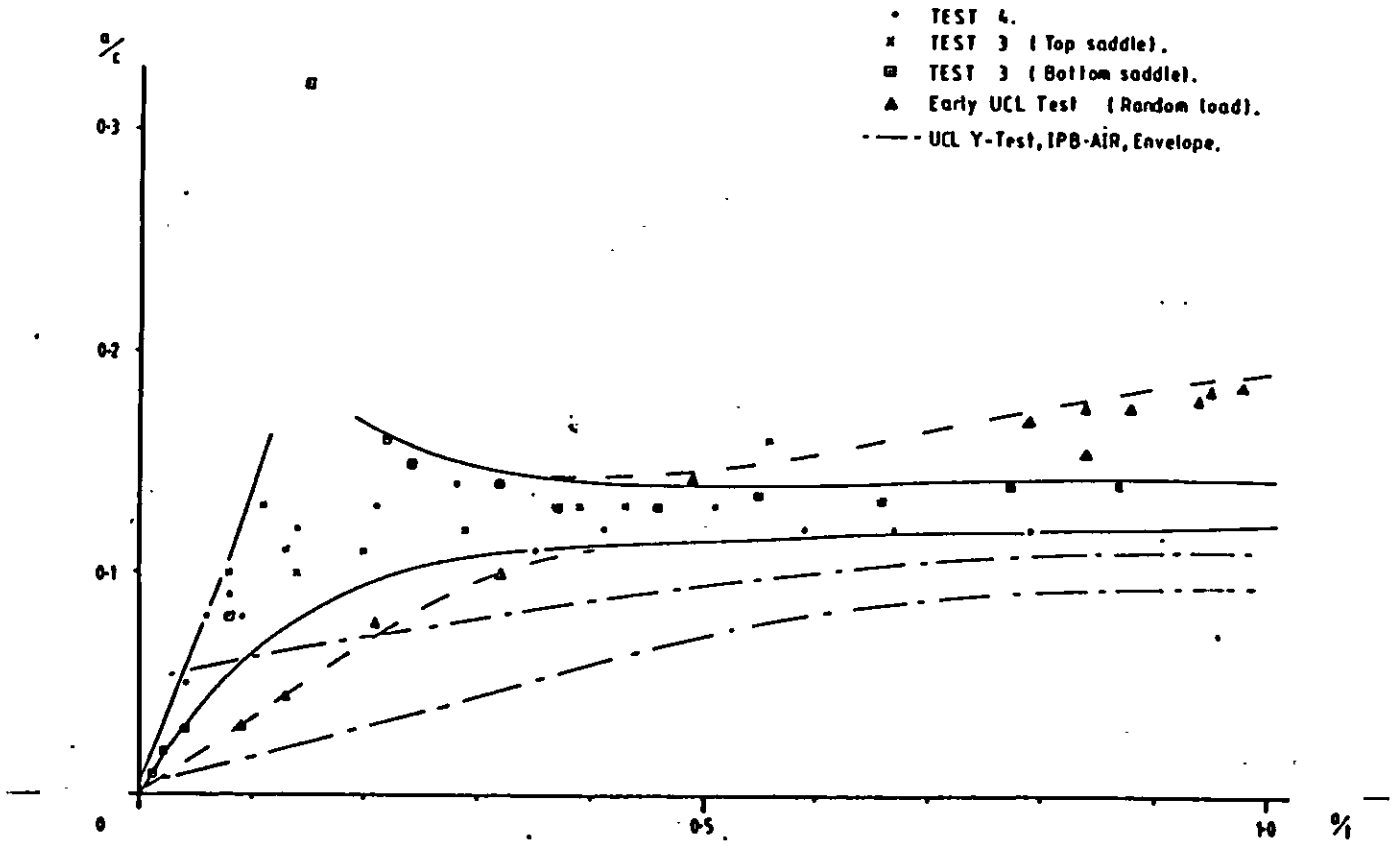

ASPECT RATIO Vs. CRACK DEPTH FOR TWO T-JOINTS TESTED IN SEAWATER (Ref. 5)

PROJECT URP 72 : STUDY 4 **INSPECTION PLANNING , THE ROLE OF DAMAGE ASSESSMENT**	**WIMPEY OFFSHORE REPORT No. WOL109/86**	
		FIG. 5.4

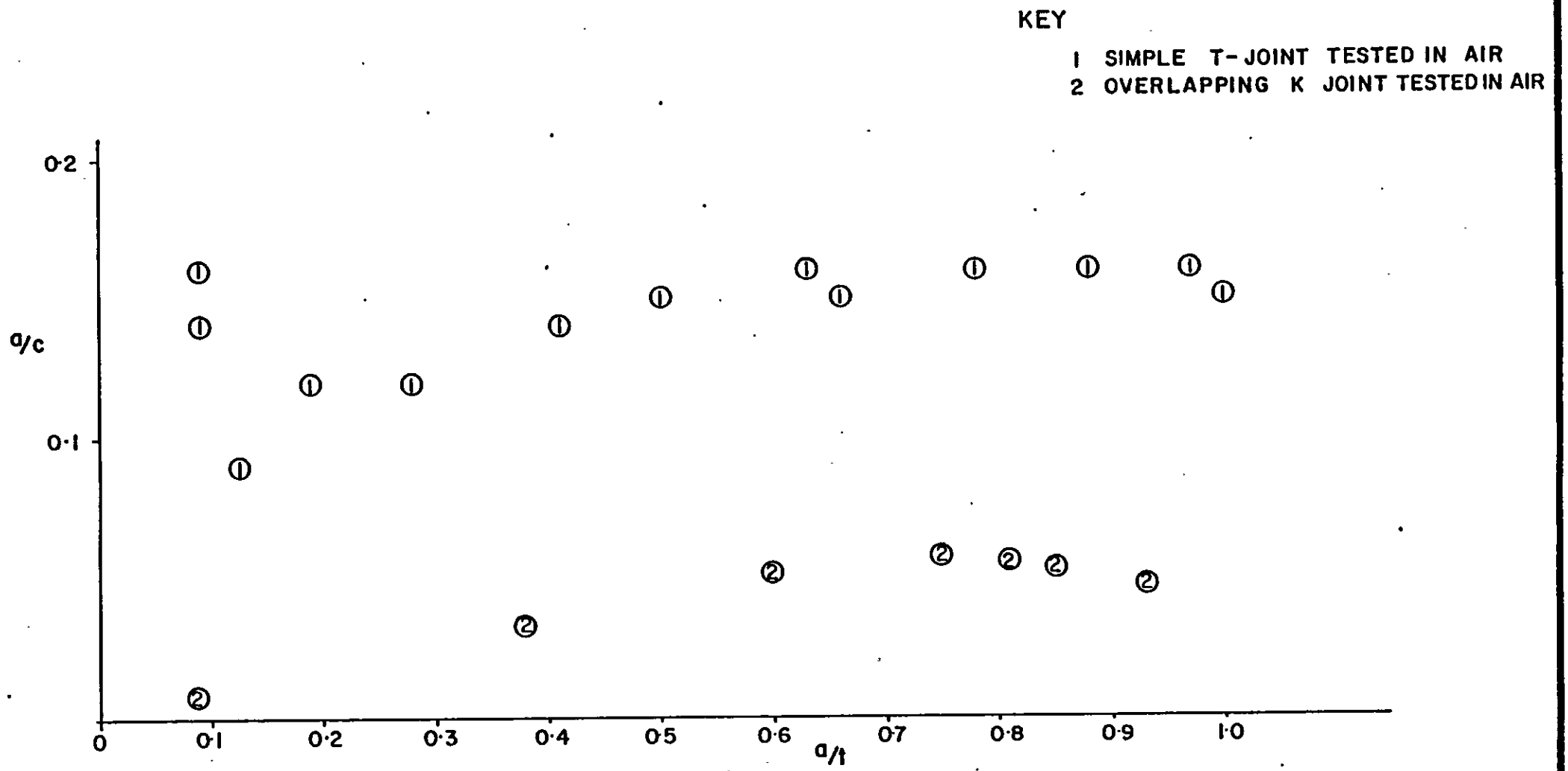

ASPECT RATIO Vs CRACK DEPTH FOR TUBULAR JOINT (Ref. 6)

PROJECT URP 72 : STUDY 4

INSPECTION PLANNING , THE ROLE OF DAMAGE ASSESSMENT

WIMPEY OFFSHORE REPORT No. WOLI09/86

FIG. 5.5

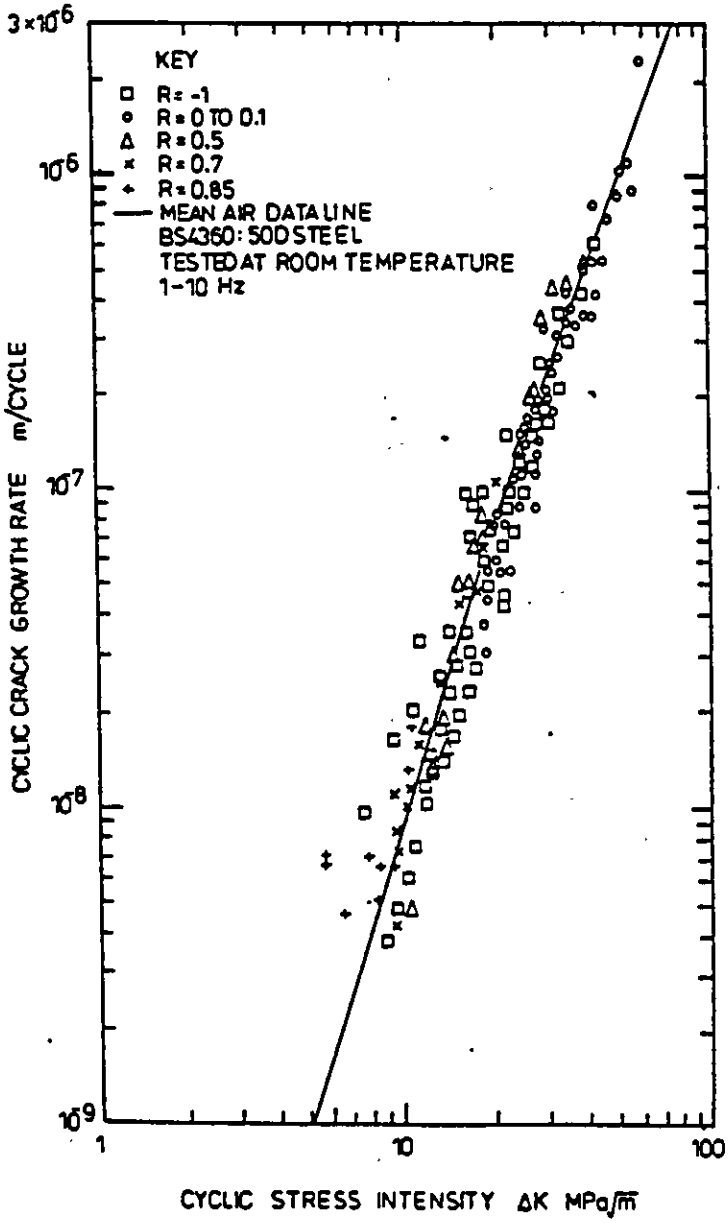

CRACK GROWTH FOR BS4360 GRADE 50D STEEL IN AIR (Ref.2)

PROJECT URP 72 : STUDY 4 **INSPECTION PLANNING ,** **THE ROLE OF DAMAGE ASSESSMENT**	**REPORT No. WOL109/86**	
		FIG. 5.6

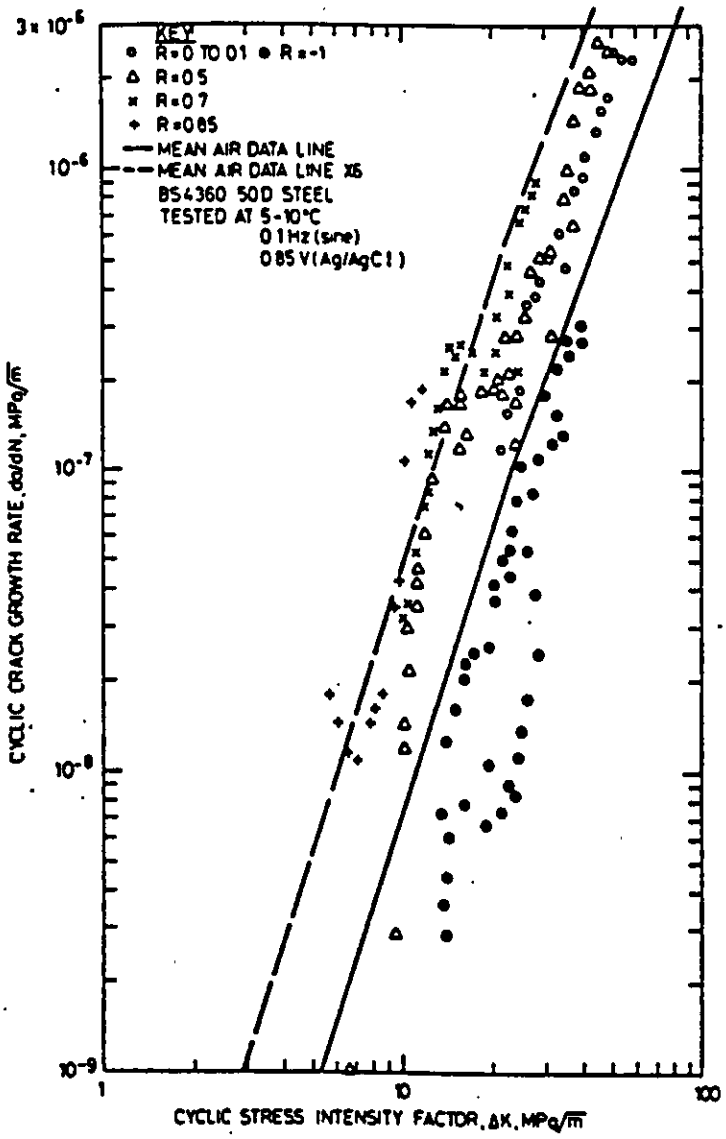

CRACK GROWTH DATA FOR BS4360 GRADE 50D STEEL AT POTENTIAL OF -0.85V (Ag/AgCl) (Ref. 2)

PROJECT URP 72 : STUDY 4 **INSPECTION PLANNING ,** **THE ROLE OF DAMAGE ASSESSMENT**	**REPORT No. WOL109/86**	
		FIG. 5.7

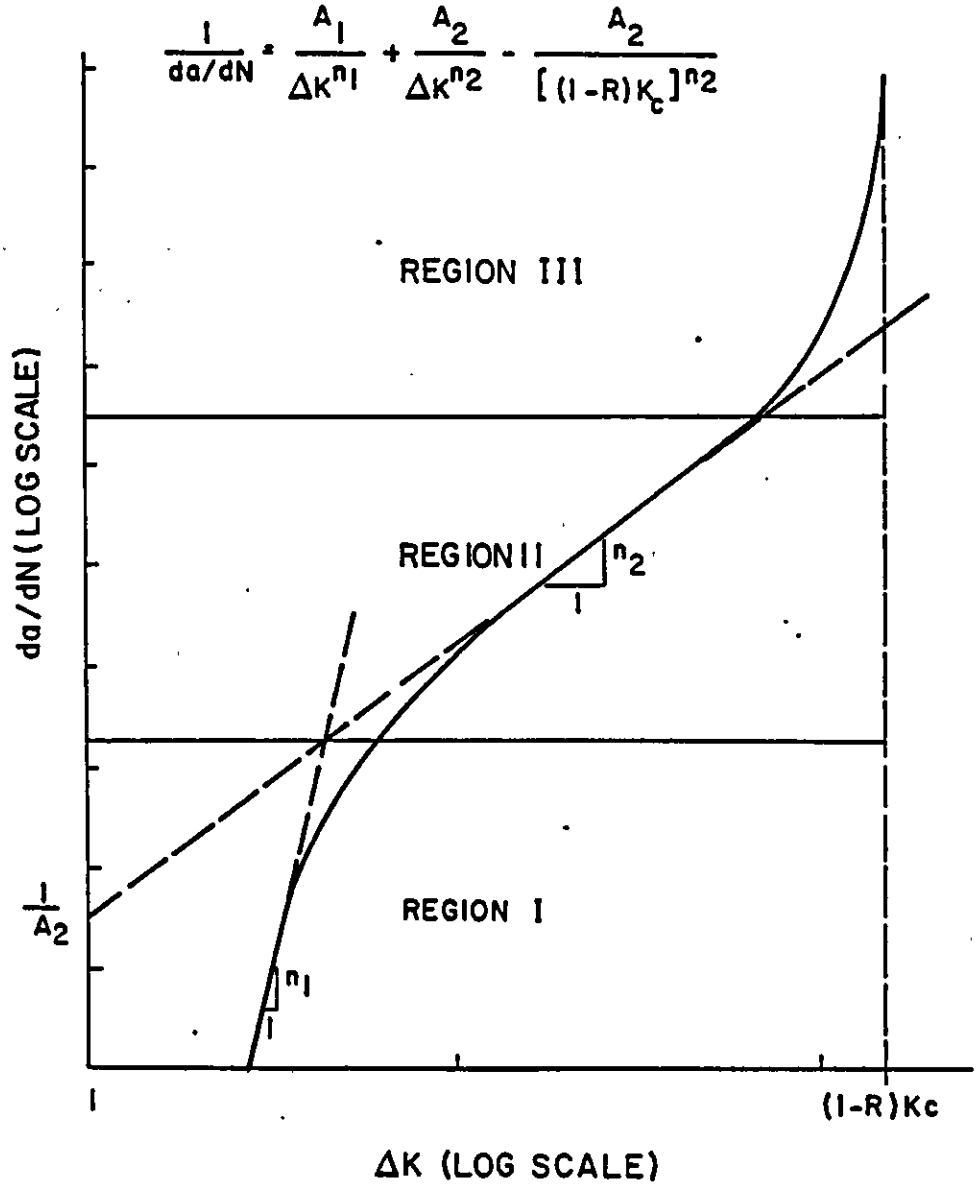

SCHEMATIC REPRESENTATION OF THREE COMPONENT CRACK GROWTH RATE EQUATION

PROJECT URP 72 : STUDY 4 **INSPECTION PLANNING ,** **THE ROLE OF DAMAGE ASSESSMENT**	**WIMPEY OFFSHORE REPORT No. WOL109/86**	
		FIG. 5.8

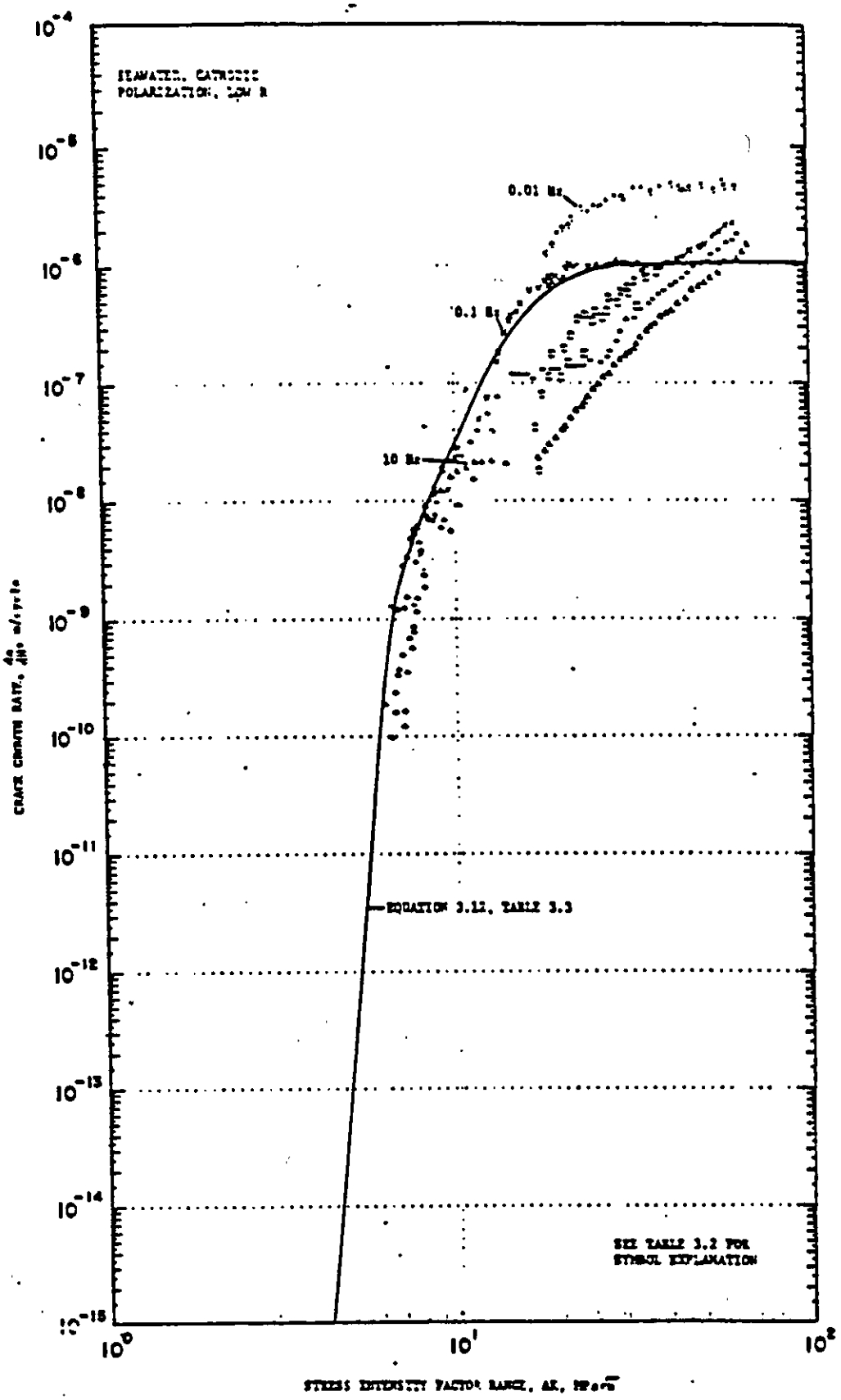

CRACK GROWTH DATA, SEAWATER, CATHODIC POLARIZATION, LOW R (Ref.11).

PROJECT URP 72 : STUDY 4 **INSPECTION PLANNING ,** **THE ROLE OF DAMAGE ASSESSMENT**	**REPORT No. WOL109/86**	**FIG. 5.9.**

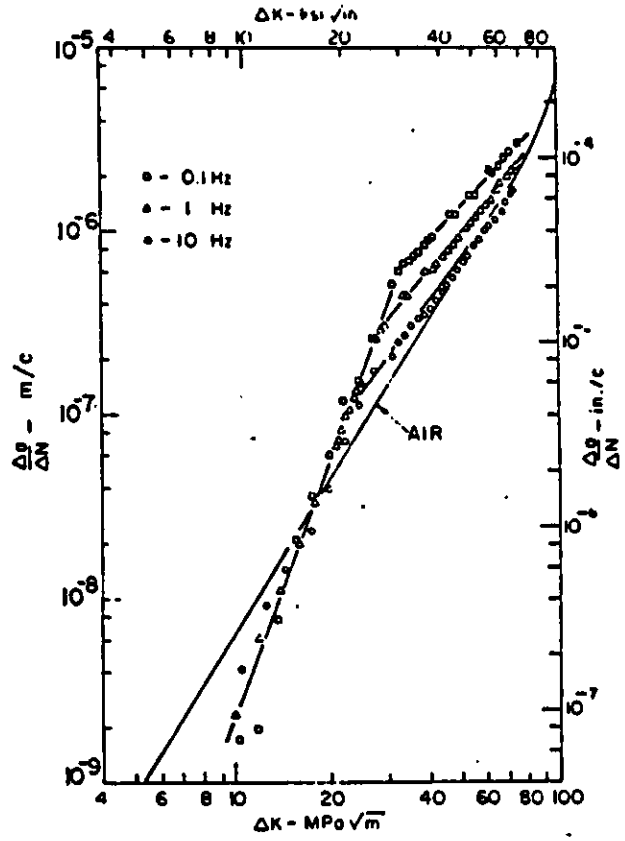

FATIGUE CRACK GROWTH RATES IN CRUDE OIL CONTAINING 1ppm H_2S AT THREE FREQUENCIES. R=0.2 (Ref. 18)

PROJECT URP 72 : STUDY 4 INSPECTION PLANNING , THE ROLE OF DAMAGE ASSESSMENT	REPORT No. WOL109/86 FIG. 5.10

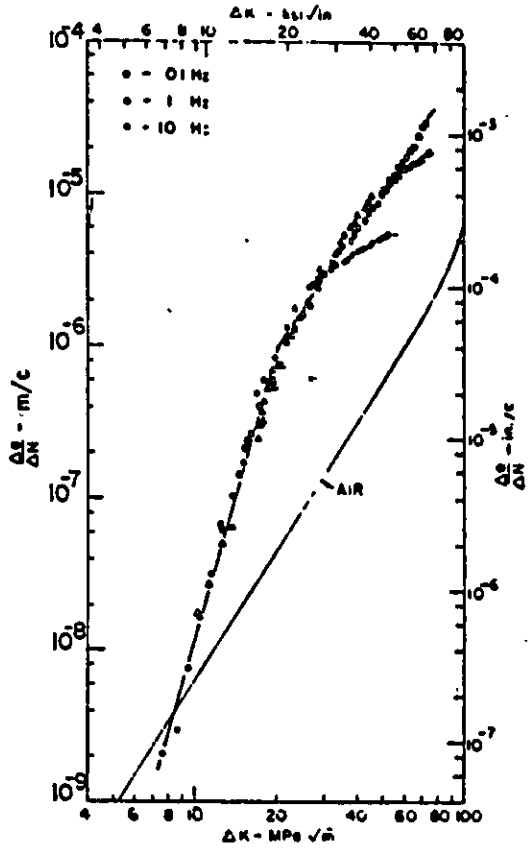

FATIGUE CRACK GROWTH RATES IN CRUDE OIL SATURATED WITH H_2S (4700ppm) AT THREE FREQUENCIES. R-0.2 (Ref. 18)

PROJECT URP 72 : STUDY 4 INSPECTION PLANNING , THE ROLE OF DAMAGE ASSESSMENT	REPORT No. WOL109/86 FIG. 5.11

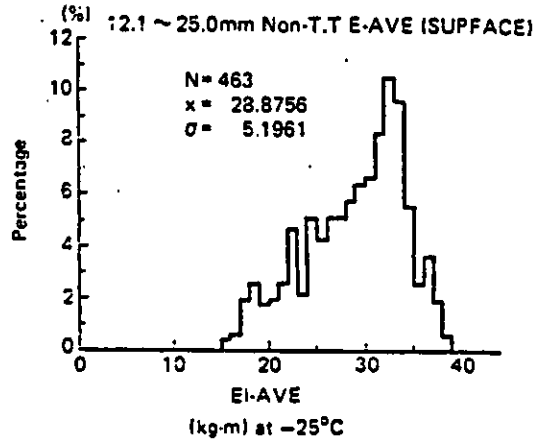

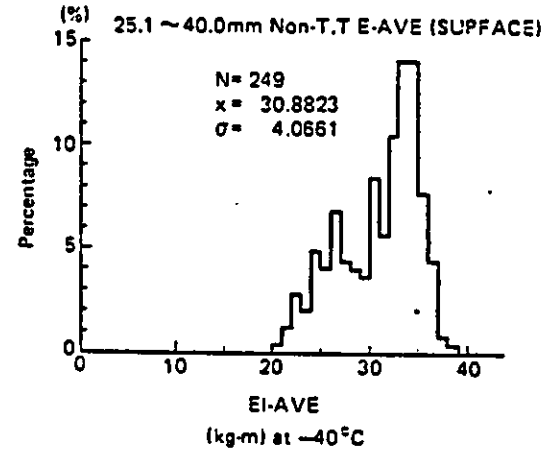

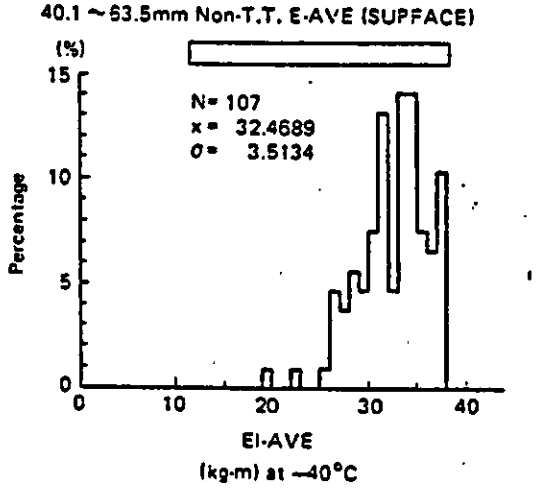

PRODUCTION HISTOGRAMS FOR CHARPY IMPACT DATA OF BS4360 50E STEEL FOR THREE THICKNESS RANGES (FROM NKK)

PROJECT URP 72 : STUDY 4 **INSPECTION PLANNING ,** **THE ROLE OF DAMAGE ASSESSMENT**	**REPORT No. WOL109/86** **FIG. 5.12**

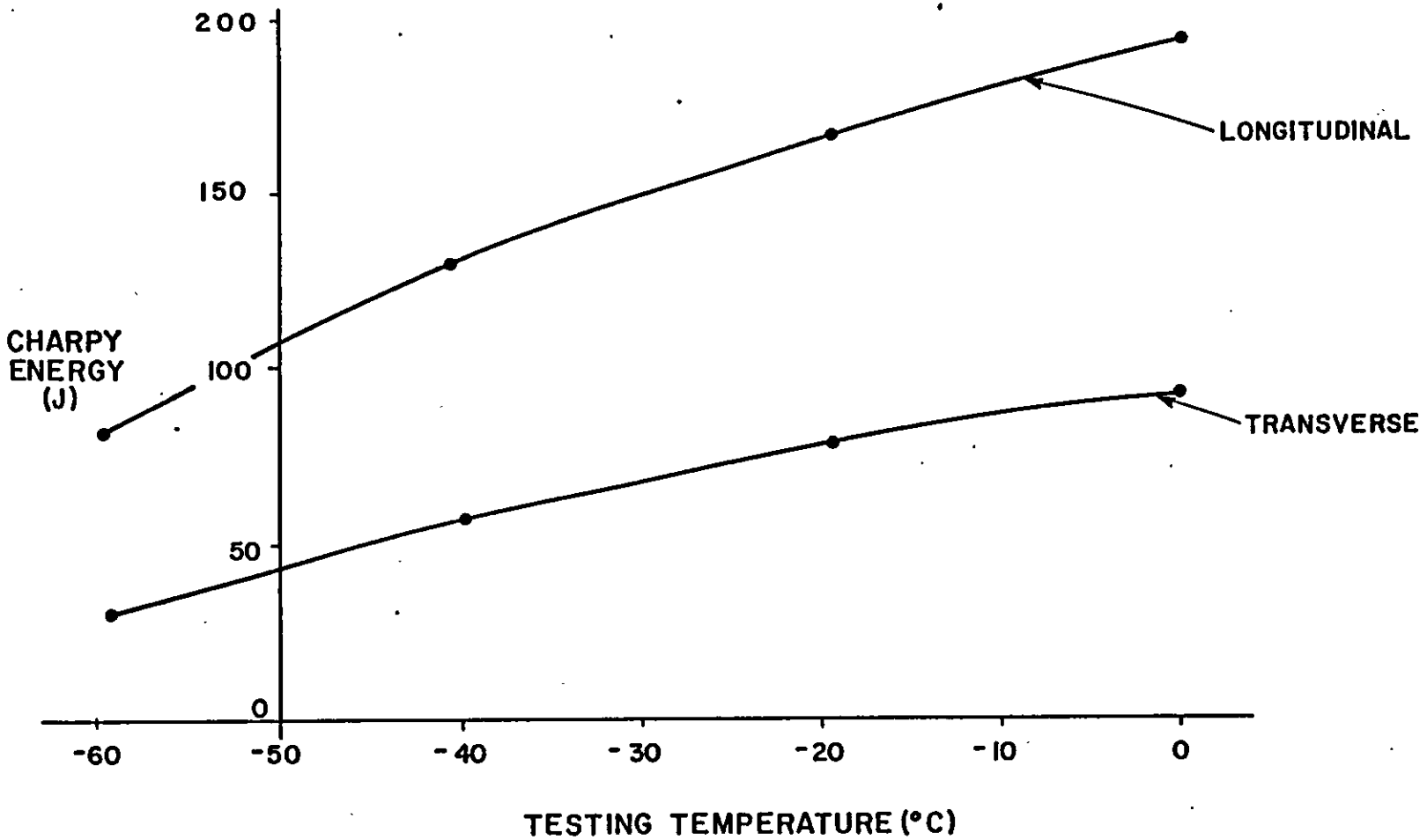

CHARPY TRANSITION CURVES FOR STEEL SUPPLIED TO BP FOR FORTIES FIELD

PROJECT URP 72 : STUDY 4

INSPECTION PLANNING , THE ROLE OF DAMAGE ASSESSMENT

WIMPEY OFFSHORE REPORT No. WOL109/86

FIG. 5.13

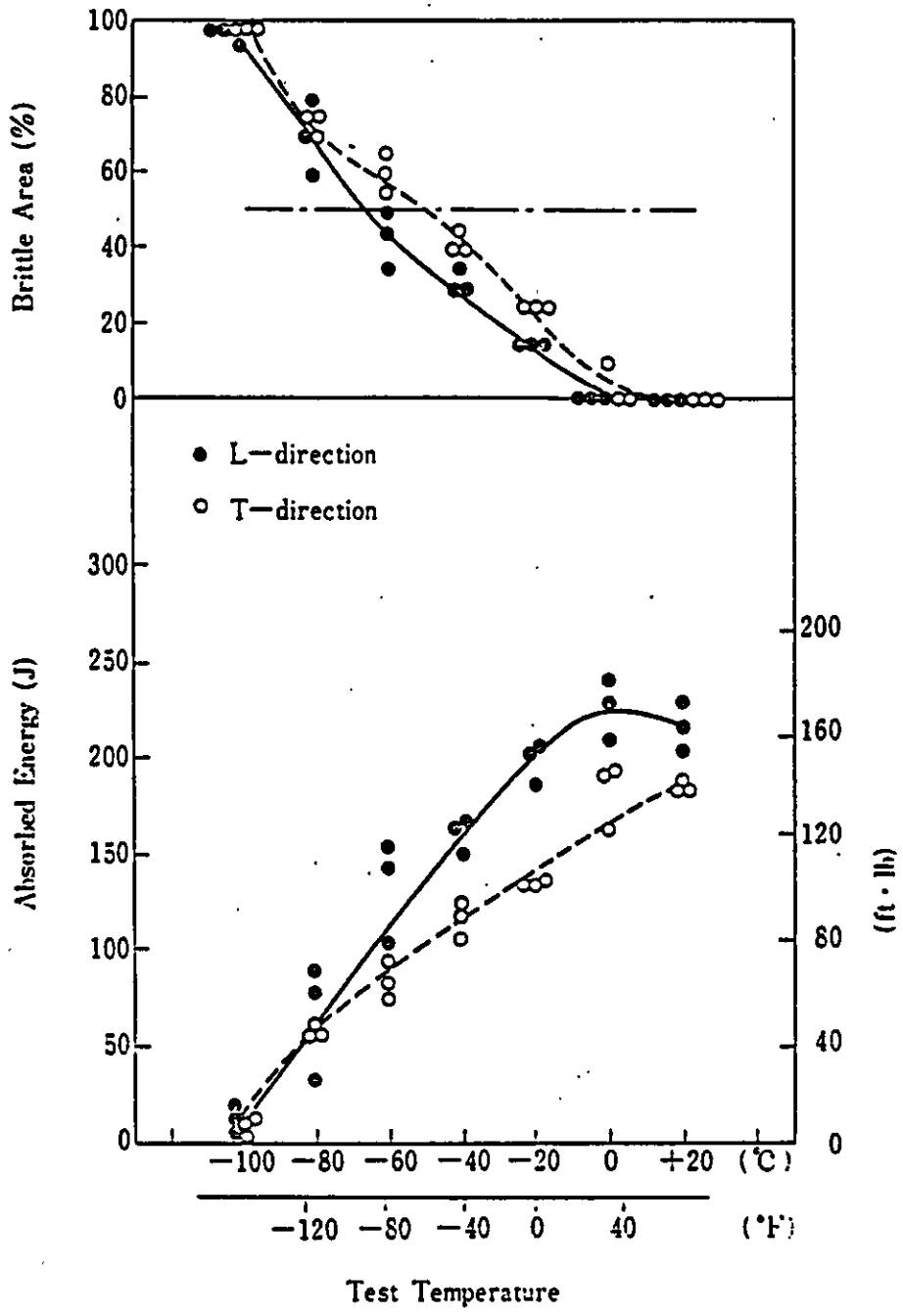

CHARPY IMPACT TEST FOR BS4360 50D, 50 mm THICKNESS.

NKK DATA

PROJECT URP 72 : STUDY 4 **INSPECTION PLANNING ,** **THE ROLE OF DAMAGE ASSESSMENT**	**REPORT No. WOLI09/86**	
		FIG. 5.14

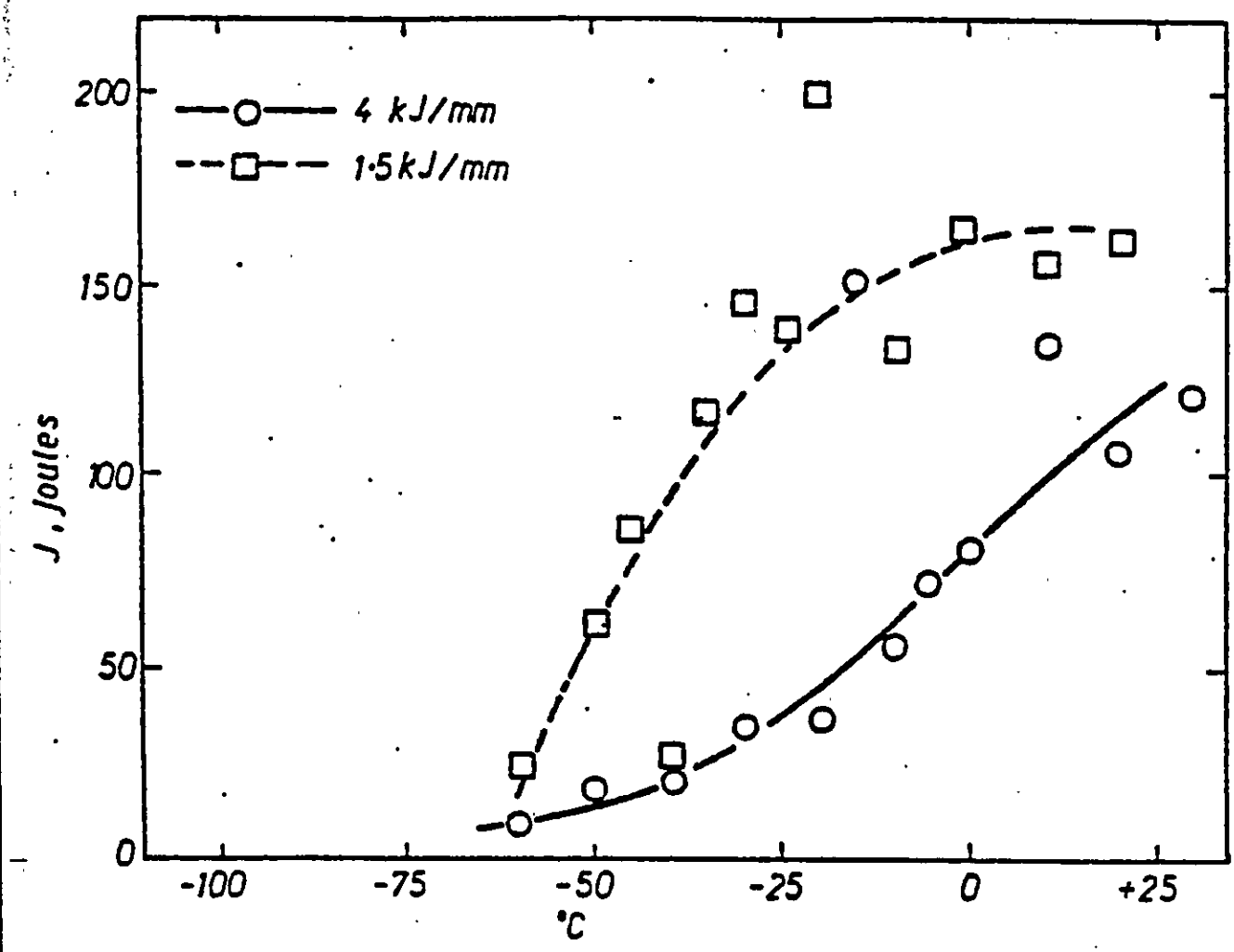

HAZ transition curve for 50mm thick BS 4360 50D.

PROJECT URP 72 : STUDY 4 **INSPECTION PLANNING ,** **THE ROLE OF DAMAGE ASSESSMENT**	**REPORT No. WOL109/86** **FIG. 5:15**

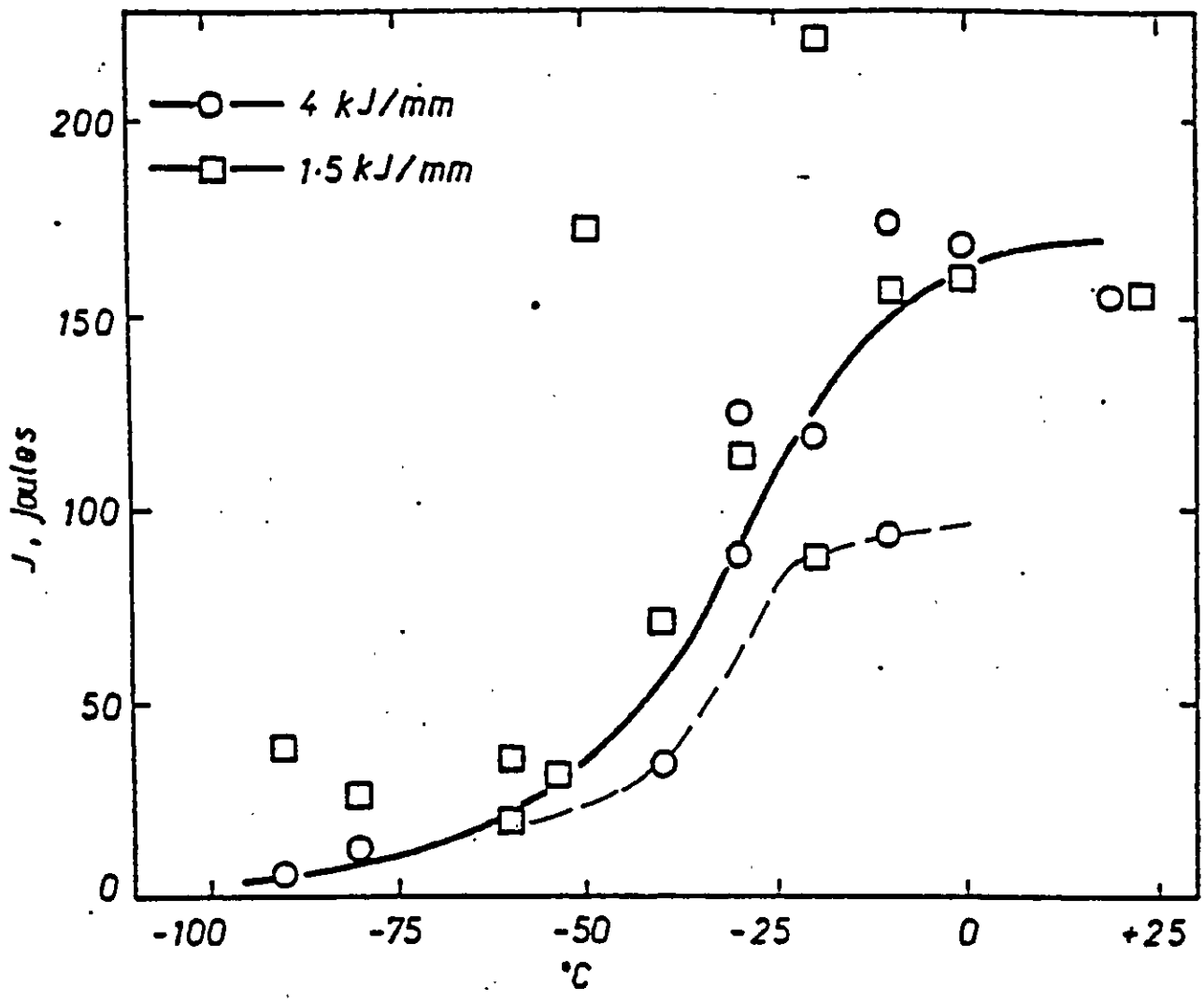

HAZ transition curve for 75mm thick BS 4360 40E.

PROJECT URP 72 : STUDY 4 **INSPECTION PLANNING ,** **THE ROLE OF DAMAGE ASSESSMENT**	**REPORT No. WOL109/86** **FIG. 5:16**

AARQUE 7865/84

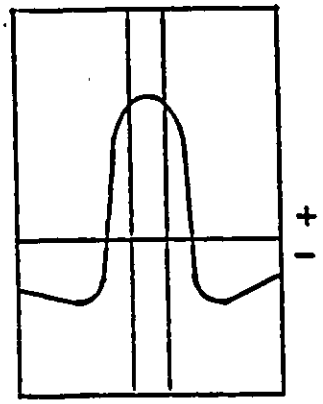

(a) LONGITUDINAL

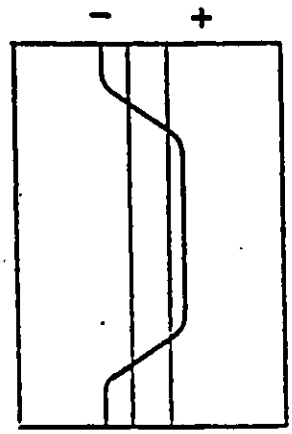

(b) TRANSVERSE

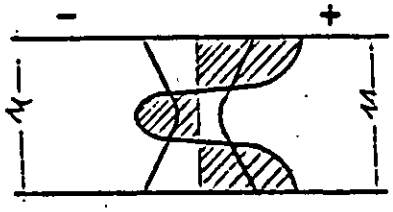

(c) THROUGH THICKNESS

TYPICAL TRADITIONAL RESIDUAL STRESS PATTERNS

FROM REFERENCE 26

PROJECT URP 72 : STUDY 4 INSPECTION PLANNING , THE ROLE OF DAMAGE ASSESSMENT	REPORT No. WOL109/86 FIG. 5.17

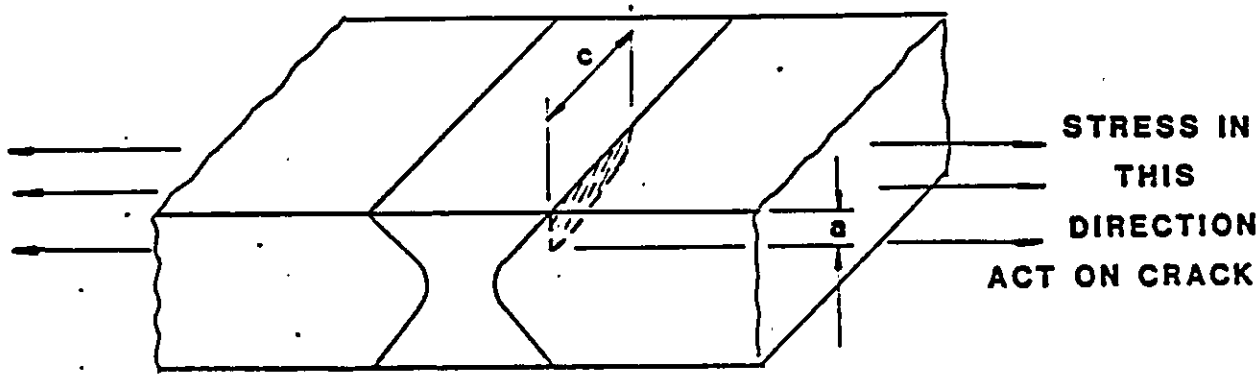

LOCATION OF DEFECTS/CRACKS OF CONCERN
WITH RESPECT TO RESIDUAL STRESS DIRECTION

PROJECT URP 72 : STUDY 4 INSPECTION PLANNING , THE ROLE OF DAMAGE ASSESSMENT	REPORT No. WOL109/86 FIG. 5.18

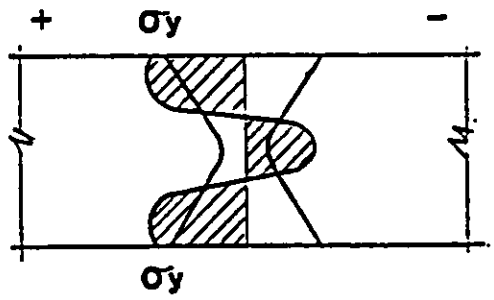

(a) DOUBLE SIDED

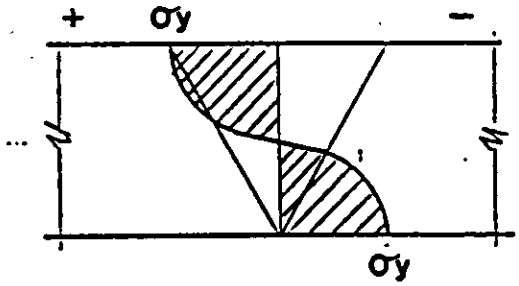

(b) SINGLE SIDED

GENERALLY ACCEPTED THROUGH THICKNESS

RESIDUAL STRESS PATTERNS

PROJECT URP 72 : STUDY 4 INSPECTION PLANNING , THE ROLE OF DAMAGE ASSESSMENT	REPORT No. WOL109/86 FIG. 5.19

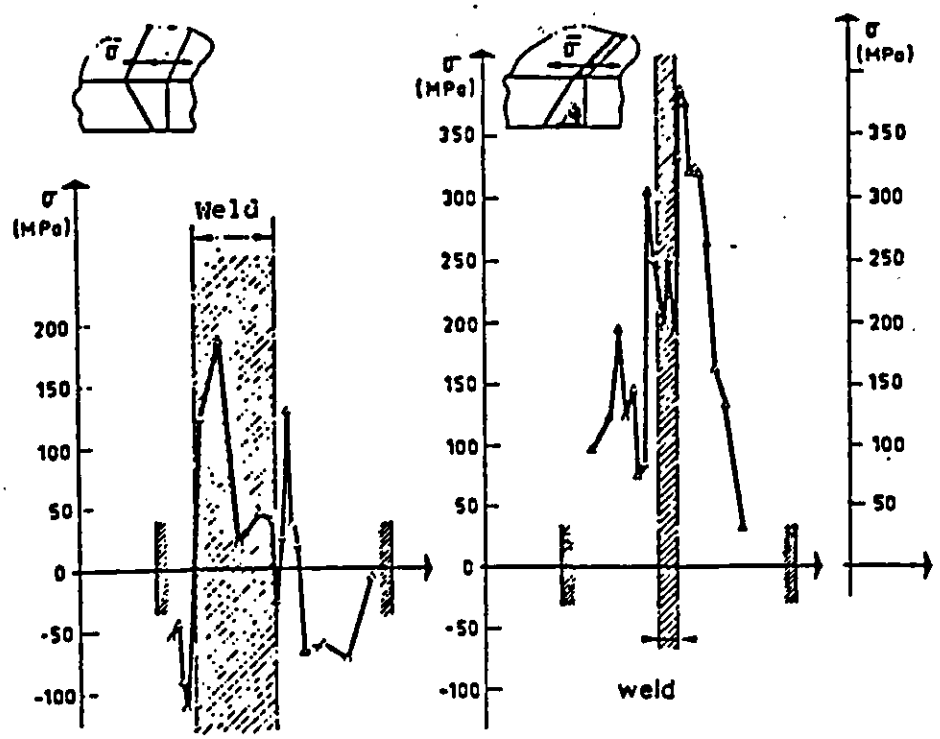

Figure 1 : Residual stresses normal to the weld . As-welded condition. 40 mm thickness.

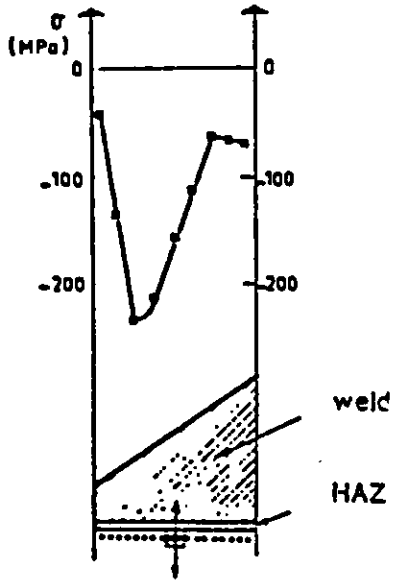

Figure 2 : Through thickness residual stresses. As-welded condition. 40 mm thickness.

MEASURED RESIDUAL STRESS PATTERNS FROM REFERENCE 36

PROJECT URP 72 : STUDY 4 **INSPECTION PLANNING ,** **THE ROLE OF DAMAGE ASSESSMENT**	**REPORT No. WOLI09/86** **FIG. 5.20**

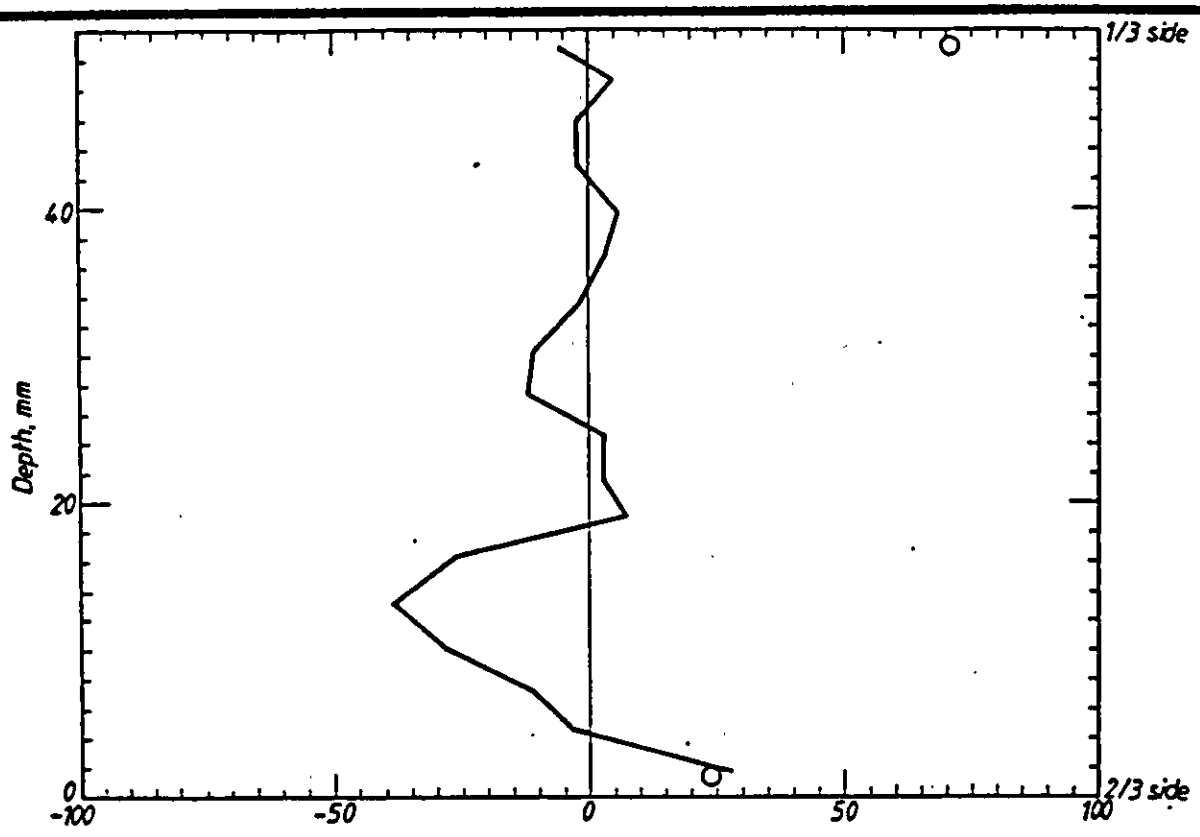

Surface and internal residual stresses in W1 after 1 cycle of 2hr at 600°C.

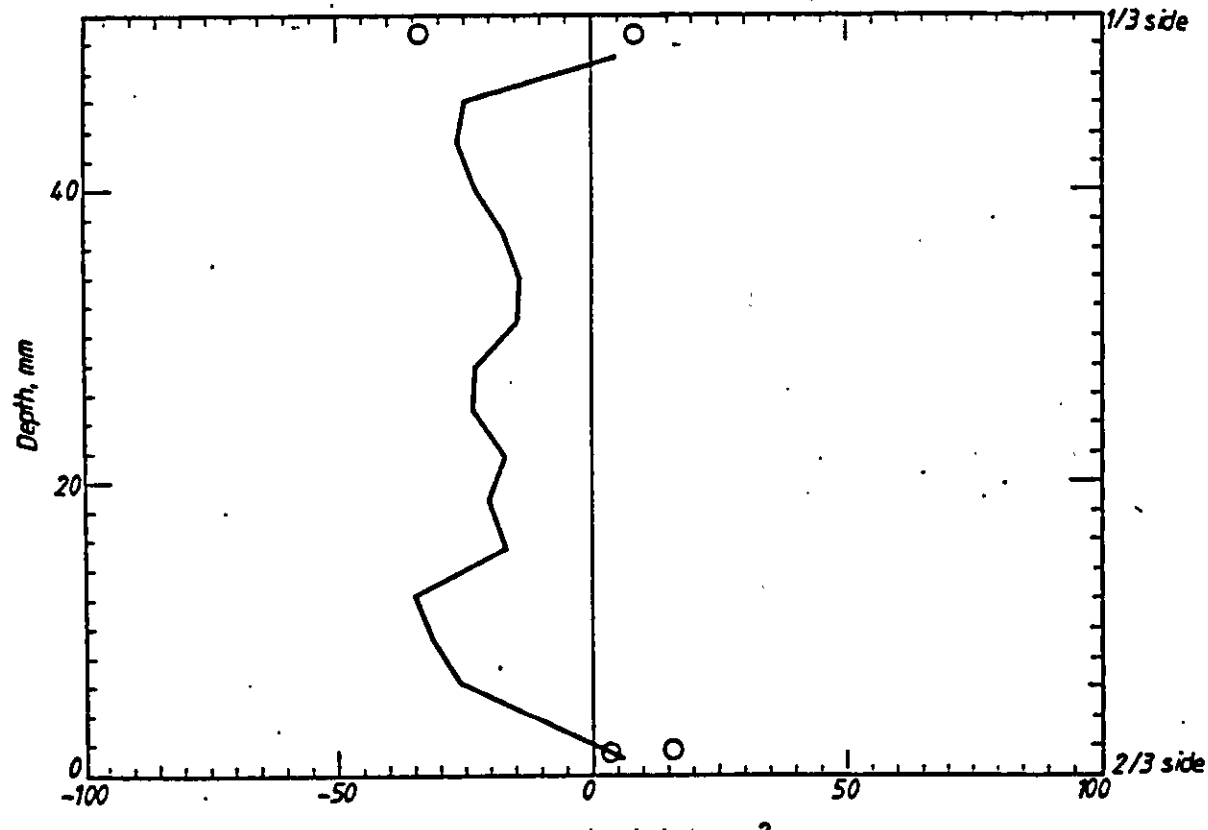

Surface and internal residual stresses in W3 after 3 cycles of 2hr at 600°C.

EXAMPLES OF MEASURED RESIDUAL STRESS PATERNS AFTER POST WELD HEAT TREATMENT FROM REFERENCE 32

PROJECT URP 72 : STUDY 4 **INSPECTION PLANNING ,** **THE ROLE OF DAMAGE ASSESSMENT**	**REPORT No. WOLI09/86** **FIG. 5:21**

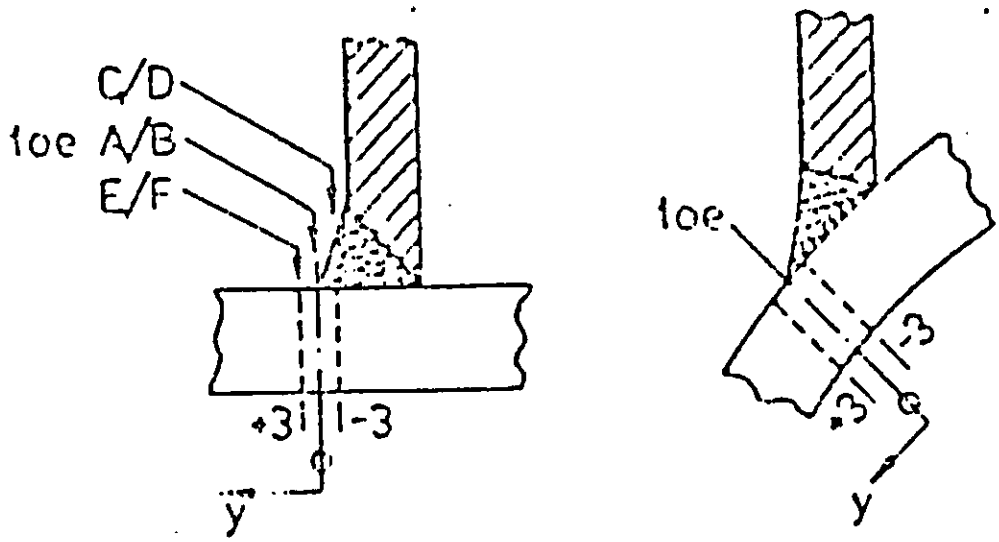

POSITIONS OF RESIDUAL STRESS MEASUREMENTS FOR T-JOINTS (Ref. 37)

PROJECT URP 72 : STUDY 4 **INSPECTION PLANNING ,** **THE ROLE OF DAMAGE ASSESSMENT**	**REPORT No. WOL109/86** **FIG. 5.22**

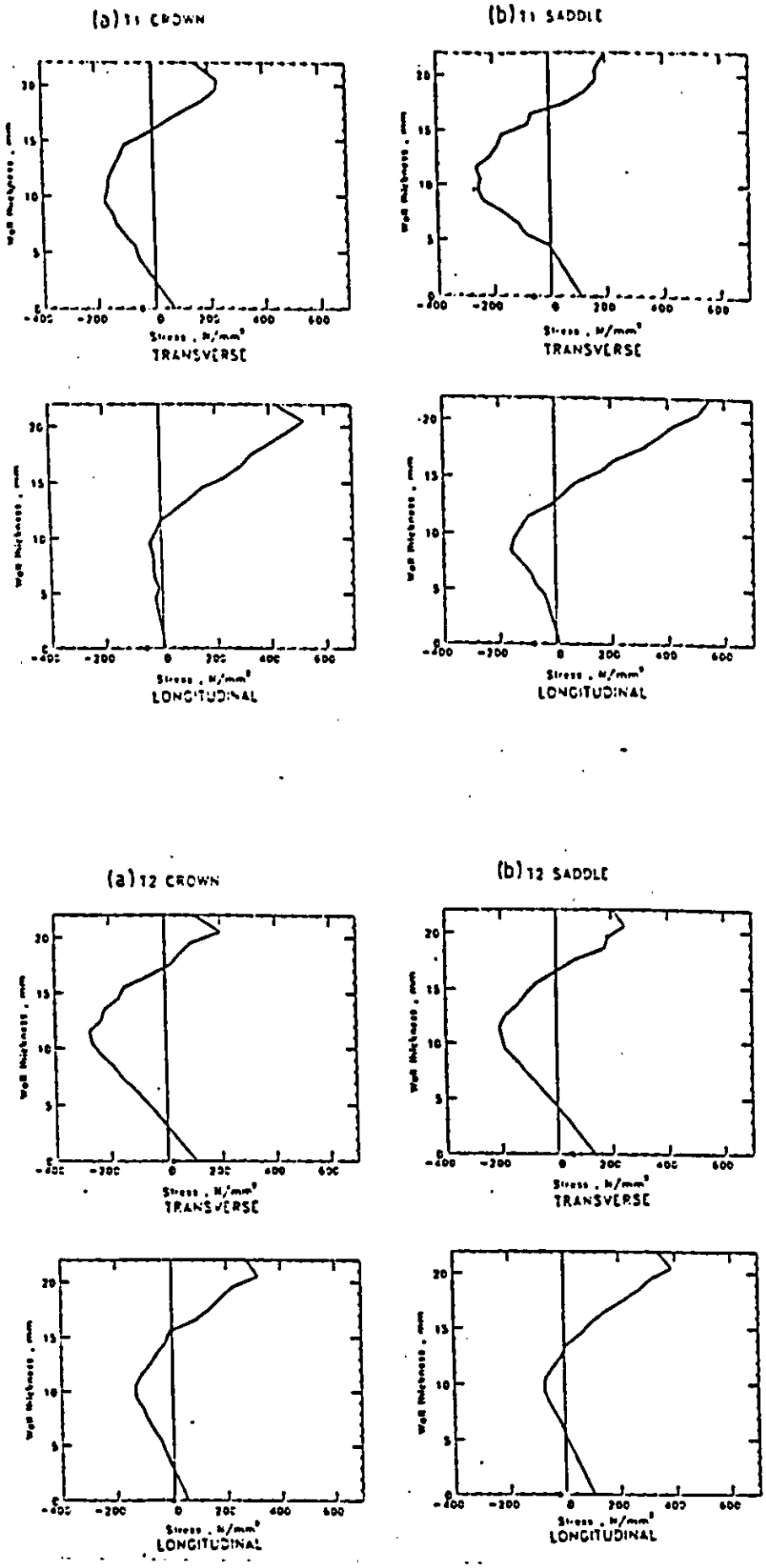

MEASURED RESIDUAL STRESS PATTENS (Ref. 37)

PROJECT URP 72 : STUDY 4 **INSPECTION PLANNING ,** **THE ROLE OF DAMAGE ASSESSMENT**	**REPORT No. WOL109/86** **FIG. 5.23**

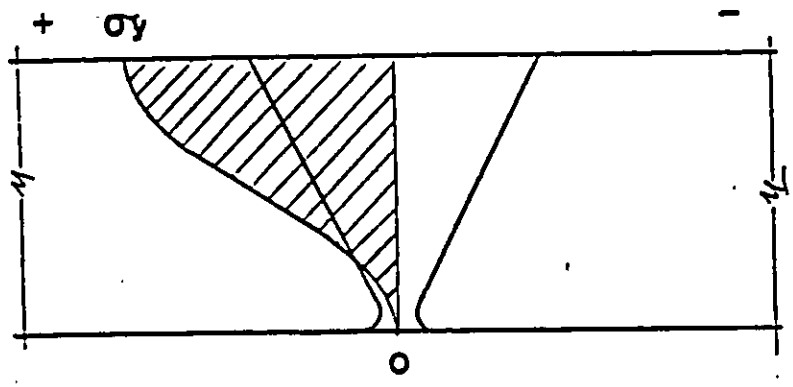

ASSUMED RESIDUAL STRESS PATERN

INCORPORATING A DEGREE OF CONSERVATISM

PROJECT URP 72 : STUDY 4
INSPECTION PLANNING ,
THE ROLE OF DAMAGE ASSESSMENT

REPORT No. WOL109/86

FIG. 5.24.

6. ASSESSMENT OF DAMAGE

6.1 The Role of Damage Assessment

The overall strategy of the determination of an underwater inspection programme is detailed in Section 7. As part of this strategy, it is required to perform an assessment of structural damage. There are two contexts in which this is required.

1. Damage assessment before performing an inspection

   In this case, the assessment is performed for postulated damage, with the aim of determining the type of damage which must be detected and, the required frequency of inspection. This type of study is particularly suited to fatigue cracks, for example.

2. Assessment of damage after performing an inspection

   The objective of this type of assessment is to determine the significance of actual damage which has been detected in an underwater inspection. The findings would be used to make a repair/no repair decision, or to determine a programme of future inspections for the damaged area.

In this Section, assessment methods are given for the most commonly occurring types of damage, namely dents and fatigue cracks, and a brief review is given of methods of redundancy analysis. By definition, damage assessment is not covered by design codes, and so non-codified methods are presented. It is not possible within the scope of this document to perform a comprehensive review of assessment methods, and so the methods presented have been carefully selected as being the most suitable for use in practical situations.

6.2 Damaged Members

6.2.1 Damage to members of offshore steel structures is frequently caused as a result of collisions with supply boats or by falling objects. The form of such damage has been found, from experimental tests and in-service experience, to have the following forms:

- Local denting of the brace wall without any overall bending of the member. This situation occurs mainly in short members with large diameter: thickness D/t ratios or at the ends of brace members.

- Overall bending of the brace without any local denting. This situation occurs mainly in long members with small D/t ratios due to impacts near mid-span.

- A combination of local denting and overall bending of the brace. This situation is most commonly encountered in practice.

- Fracture of the member due to the ultimate axial tensile capacity being exceeded as a consequence of gross deformation and subsequent membrane yielding tension.

- In addition to damage to the impacted member the adjacent joints may be damaged if the ultimate capacity of the member exceeds the ultimate capacity of the tubular joint.

- Adjacent members may be damaged if they are not sufficiently strong to absorb the end forces from the impacted member.

The members in a jacket structure which are most likely to be affected by boat impact are vertical and diagonal members located in the splash zone. These members are loaded in compression due to the topside dead weight and therefore fail through lateral buckling.

Damage to tubular members can be classified as minor if the ultimate load capacity of the member has not been reduced (as a consequence of the damage) to a value less than the maximum applied load. Similarly, severe damage can be considered to have occurred when the reduced

ultimate load capacity of the damaged member has been exceeded by the applied load. In this situation the damaged member can only sustain its post-collapse load and the balance of the applied load must be re-distributed to adjacent members.

6.2.2 Review of published literature

A large amount of theoretical and experimental research has been undertaken since 1979 into the following two related areas of damaged members;

1. Investigation into the mechanisms for a tubular member to absorb energy from a lateral collision with a supply boat or dropped object.

2. Investigation into the residual strength and stiffness of a tubular member which has suffered from a lateral collision.

The findings from item 1. above are of primary interest during the design of a jacket as it is possible to quantify the damage incurred for a given impact energy. This information can subsequently be used to ensure that the global structural integrity is not compromised by local damage.

Some of the most recent developments in this area are due to Richards and Andronica[1], Ellinas and Walker[2] and Pettersen and Johnson[3]. The method proposed by Richards allows the impact energy to be absorbed, in the correct proportions, by the following mechanisms in a tubular member with various end conditions:

- energy absorbed by elastic deformation
- energy absorbed by local denting
- energy absorbed by formation of plastic hinges
- energy absorbed by membrane tension yielding

Figures 6.1 and 6.2 show the results produced by the mathematical model of Reference (1) for two simply supported tubular members. These models are based on data from members on offshore structures which have been damaged. The relevant details of the members are given in Table 6.1. Several points of general interest can be seen

from inspection of these two figures:

- Impact energy is absorbed firstly by elastic bending and dent formation until a mechanism develops due to the onset of plastic hinges.

- The dent depth and total resisting force remain virtually constant after the formation of a mechanism. The magnitude of the resisting force is maintained at large lateral deflections due to a significant contribution from the membrane tension yielding effect.

The majority of the recent research in item 2 above has been conducted by Smith[4, 5, 6, 7, 8], Taby and Moan[9], and Ellinas[10]. This work has been directed towards computing the residual strength and stiffness of damaged tubular braces with simply supported end conditions and, to a lesser extent, with general rotational stiffness at the member ends.

A detailed description of the findings of the above work and methods of using this information to aid defect assessment is presented in Sections 6.2.4 to 6.2.6.

6.2.3 Buckling behaviour

The buckling behaviour of tubular members can take either, or a proportion of both, of the following forms:

- Column buckling
- Local buckling

It is important to establish if local buckling is liable to have a controlling influence in the buckling behaviour of a tubular brace since the post-collapse behaviour of damaged (and undamaged) tubular members is catastrophic in such circumstances.

6.2.3.1 Column buckling

Column buckling is an overall effect which takes the following forms:

- Long, slender tubular columns ($\lambda > 1.5$) fail by elastic buckling at the Euler stress.
- As λ reduces from 1.5 to 0.0 the column failure becomes increasingly controlled by inelastic buckling and by the compressive strength of the material.

In the above λ is the reduced slenderness ratio, defined by:

$$\lambda = (F_y/E)^{\frac{1}{2}}(L/r.)\ K/\pi \qquad \ldots.(6.1)$$

where F_y = material yield stress
(L/r) = the actual slenderness ratio of the column
K = effective length factor

The two regimes of column buckling described above can be clearly seen in Figure 6.3.

6.2.3.2 Local buckling

Local buckling occurs when a local 'bulge' or 'lobe', forms on the surface of the tubular. This form of buckling becomes increasingly dominant as the D/t ratio exceeds 60. The classical failure stress for local buckling of perfect, thin cylinders in a periodic mode with 'diamond' shaped lobes is

$$F_u = 1.21\ Et/D \qquad \ldots.(6.2)$$

However, for the typical bracing members used in offshore structures, which are fabricated from a series of rolled plates ('cans'), the local buckling mode takes the form of an axisymmetric bulge rather than the classical diamond lobes. This bulge can occur at the member ends or, as shown in Figure 6.4, at circumferential butt welds between adjacent cans. In this situation it has been

found that the local buckling stress has the form:

$$F_u = F_y - 0.0012\ F_y\ D/t \qquad \ldots.(6.3);$$

A more conservative estimate of the local buckling strength of typical offshore tubular members is given in Reference[10] as:

$$F_u/F_y = 1 - 0.0024\ (D/t) + 0.000003\ (D/t)^2 \qquad \ldots.(6.4)$$

The effect of local buckling failure on the ultimate axial capacity of an undamaged tubular member has been illustrated in Reference (10) and reproduced in Figure 6.5. Tubular members which are susceptible to local buckling and have in addition suffered bending or denting damage, will exhibit a further loss of strength from that shown in Figure 6.5. This aspect is discussed further in Section 6.2.4.2.

6.2.4 Residual strength and stiffness

The analytical method which is developed in this section to assess the residual strength of bent and dented members is based on incremental elasto-plastic, large displacement beam-column analysis. The pertinent features of this type of analysis are summarised as follows:

- The tubular brace is idealised as a series (typically 20) of straight beam elements. The lengths of individual elements usually vary to allow small element lengths to be used in areas where plasticity is expected.

- The tubular cross section is divided into element 'fibres' as shown in Figure 6.6 thus allowing the progressive development of plasticity over the member cross section.

- Loads are applied incrementally with a linear solution being obtained at each increment from the following equation (see Reference (4)):

$$(K_t + K_g)\ u = P \qquad \ldots.(6.5)$$

where u = nodal deflections

P = applied load

K_t = incremental stiffness matrix based on the tangent stiffness matrix

K_g = geometric stiffness matrix

- Damage to a member resulting in permanent bending is modelled by specifying initial lateral deflections at the element nodes.

- Following the methods proposed by Smith[7], damage to a member resulting in the formation of a dent is modelled by reducing the values of Young's modulus, and the yield stress for the 'fibres' in the dent zone (see Figure 6.7). The resulting bi-linear stress/strain curve is shown in Figure 6.7 where, for a dent of depth d, k is given by:

$$k = 0.59 - 0.0096\ D/t + 0.0003\ E/F_y - 0.57\ d/D \quad \ldots.(6.6)$$

The expression for k has been established by correlating the analysis procedure described above with experimental tests on damaged tubular members and using a least-squares method to fit the equation to the data points.

Upper and lower bounds on the collapse strength of a damaged tubular can be obtained by setting k = 1 and 0 respectively. Typical experimental values for k lie in the range 0.2 to 0.4.

- Dent damage is modelled by Taby and Moan[9] by an analytical method as shown in Figures 6.8 and 6.9. In this model the undamaged section of the tubular is modelled by an offset beam and the load carried by the dented region is applied as an offset point force Q. For a compression member Q, is given by the following semi- empirical equation.

$$Q = 80t\ F_y \cos^{-1}(1-2d/D)C \quad \ldots.(6.7)$$

where $C = (4n^2 + t^2)^{\frac{1}{2}} - 2n$

and n is defined in Figure 6.9.

The development of the above computer models has enabled a wide range of damaged tubulars to be studied with the results being verified against experimental results where possible. Using the results of these studies, the effects of various parameters on the residual stiffness and strength will now be discussed.

6.2.4.1 Bending damage

- The effect of varying the slenderness of the damaged member (expressed in terms of λ the reduced slenderness ratio) is shown on Figures 6.10 and 6.11 for simply supported and clamped tubulars[4]. In these examples D/t and E/F_y are held constant at 35 and 638 respectively. It can be seen from these figures that by choosing K = 0.6 for the clamped tubes the residual strength characteristics are almost identical for an equivalent value of λ. The damage effects are most marked in the post-collapse range of tubulars with a λ value lying in the imperfection-sensitive range $0.7 < \lambda < 1.1$.

- The shape of the initial bending damage has been found to have a negligible effect on the residual strength compared to the maximum magnitude of the initial lateral deformation. The forms of bending damage that have been considered consist of sinusoidal, parabolic and bilinear (ie. 'dog leg').

- The effect of varying the initial bending damage can be seen from Figures 6.10 and 6.11 to dominate post-collapse behaviour for low λ tubulars and pre-collapse behaviour for high λ tubulars.

- The effect of residual weld stress from a seam weld on the strength of compressed, undamaged tubulars is shown in Figure 6.12 for varying values of η. The form of the residual stress

field for this situation, together with the definition of η, are shown in Figure 6.13(a). Typical values of η for offshore tubulars are about 4 which will normally affect the member strength by less than 10%.

- The effect of a residual stress distribution of the form shown in Figure 6.13(b) (which occurs in bracing members with bending damage) has been found to have a negligible effect on the residual strength of a damaged tubular. Figure 6.14 shows the effects of the residual stress distribution on residual strength for a tubular member with three levels of bending damage.

6.2.4.2 Dent damage

- Experimental results show that residual strength of a dented tubular is a function of the depth of the dent and does not depend on the shape of the dent. This conclusion was reached after testing tubulars with 'knife edge', 'round' and 'square' dents.

- The effect of the location of the dent on the length of the tubular has a negligible effect on the residual strength as shown in Figure 6.15. Also shown on Figure 6.15 is the negligible effect that the length of the dent (measured along the tube axis) has on the residual strength for a given dent depth.

- Typical load deflection characteristics for a tubular susceptible to a local buckling failure are shown in Figure 6.16. These characteristics were obtained experimentally[5] for tubes with $D/t = 87$, $L/r = 48$, $E/F_y = 470$ and three levels of dent damage. The sudden and drastic loss of strength following ultimate load is characteristic of a local buckling failure and shows that such tubes should not be used for bracing members which may suffer collision damage.

- After occurrence of dent damage the subsequent increase in axial compression load will not increase the dent depth until

the residual ultimate strength is achieved. However, the post-collapse strength is reduced due to an increase in dent depth as shown on Figure 6.17. If the post-collapse strength of a dented tubular requires to be established numerically it is important that the computer program has the ability to model the growth in dent depth - this would require an advanced non-linear program and powerful computing facilities.

6.2.4.3 Combined bending and dent damage

- The value of D/t has an influence on the ultimate residual strength of a tubular member suffering from dent damage as shown in Figure 6.18.

  As the level of dent damage increases, the residual strength becomes independent of the level of bending damage. This trend is clearly seen in the curve on Figure 6.19 for tubes with $\lambda = 0.5$ and varying D/t.

- The ultimate residual strength of a damaged tubular will be further decreased if lateral loading is present (eg. wave load or buoyancy load). The curves in Figure 6.20 show that a linear interaction formula is conservative for stocky tubes and slightly non-conservative for slender tubes.

6.2.5 Fatigue behaviour of damaged tubulars

The fatigue behaviour of tubular braces which have suffered denting and bending is the subject of a current study being sponsored by the Department of Energy. Although the study has only recently commenced, initial findings show a substantial reduction in fatigue life occurs when a tubular is dented and bent. Thus, although the static behaviour of damaged tubulars is now well defined their fatigue behaviour could provide the limiting condition in assessing the resulting integrity of the jacket.

6.2.6 Defect assessment after collision damage

The information presented in this section can be used to establish the integrity of a steel jacket which has a damaged (but not severed) compression member as the result of a collision.

The methods described have been concerned with establishing the residual strength of an isolated member having pinned or clamped ends. In order to perform a jacket defect assessment it is necessary to incorporate the behaviour of the damaged tubular into the computer model of the complete jacket structure. Ideally, the special techniques which have been developed[4,9] to perform mathematical modelling of damaged tubulars could be incorporated in jacket analysis computer programs. However, until such developments take place the following is proposed:

Assume that the damaged brace acts primarily as a compression member with local wave or buoyancy load providing lateral force. This assumption is generally true for bracing members in a triangulated jacket structure.

Based on this assumption the proposed method can be described in stages as follows:

1. Perform a linear static jacket analysis, with the damaged member completely removed, for the following loadcases:

   (a) Storm environmental and topside dead loads.

   (b) Self-equilibrating unit forces acting on the end nodes of the missing damaged member. These forces model the effect of a unit value of compression from the missing member on the remainder of the jacket.

2. If the member and punching shear utilisations are less than unity for loadcase (a) then the jacket's structural integrity is not compromised by assuming the damaged member has no residual strength. If this is the case then no repair or further inspection of the member is necessary. However, as the loads in the jacket members may be redistributed due to a reduction in the damaged members stiffness, an analysis should be conducted to re-appraise the fatigue performance of the jacket.

3. If the member or joint utilisations exceed unity then the actual residual strength and stiffness of the damaged member should be established. This can be achieved by an elasto-plastic, large-displacement analysis of the isolated member as described in references[4,9]. In order to obtain the depth of the dent and/or the maximum deflection due to bending, a detailed survey of the damaged member would be required. The bending deflection could be measured by using a taut wire for reference while the dent depth could be measured with the aid of a template.

4. Having found the axial load/deflection characteristics of the damaged member a non-linear compatibility equation can be solved to obtain the value of axial compression. The equation has the form:

$$e(P) = d_1 - Pd_2 \qquad \ldots.(6.8)$$

where $e(P)$ is the non-linear relationship between the axial compression, P, and the axial shortening, e, of the damaged member

d_1 is the shortening of the line connecting the nodes of the removed member due to loadcase (a).

d_2 is the extension of the line connecting the nodes of the removed member due to loadcase (b).

5. The axial compression carried by the damaged member can then be included in the jacket model by linearly combining the displacement from loadcase (a) with P times the displacements from loadcase (b). The jacket member and joint utilisations are then computed for this new load combination. If the utilisations are greater than unity then an immediate repair will be required to ensure the integrity of the jacket. If the utilisations are less than unity then the immediate integrity of the jacket is assured. However, due to the poor fatigue behaviour of damaged members this situation may be temporary.

The above procedure is illustrated by a case study in Section 6.6 of this report.

6.3 Fatigue Crack Growth Calculation

6.3.1 Introduction

This section reviews methods for assessing the significance of fatigue cracks in offshore structures with particular reference to tubular joints. The analysis methods presented are for the calculation of the residual fatigue life, where the 'end of life' is defined as the attainment of a pre-defined crack size (for tubular joints this is taken to be the formation of a through-thickness crack). Premature failure may arise from unstable crack extension, which is discussed in Section 6.4.

The standard method for calculating fatigue lives is by the S-N method, which is inappropriate for damage assessment since it is based on fatigue data obtained from initially undamaged specimens. The calculation of residual fatigue lives must therefore be performed by the alternative approach of fracture mechanics (FM). When comparing the two approaches for the calculation of fatigue life, it is useful to note that they are consistent (within certain limitations) in two key areas[11].

1. The variation of fatigue life against stress range, for constant amplitude cycling, is a power law relationship. This plots as a straight line on a logarithmic scale, which is the usual form of presentation for S-N curves.

2. For variable amplitude stress ranges, the FM calculation is equivalent to the Miner's law which is generally used with the S-N method.

It may thus be seen that provided that the same assumptions are made, similar overall fatigue lives will be predicted by both the S-N and FM methods.

The starting point for a fatigue crack growth analysis is the "crack growth model", which has three main components:

1. The crack growth law. The simplest and most widely used law is Paris' equation.

2. The crack growth constants. These are controlled by environmental conditions and other factors, and are particular to the crack growth law for which they were derived.

3. The stress intensity factor solution.

A number of advanced crack growth models are available which can give accurate results under laboratory conditions. For crack growth in tubular joints in seawater the situation is more complex, and there are a number of factors which are imperfectly understood. These include:

- Crack initiation - governed by the size of welding defects and the surface profile.

- Effect of seawater properties.

- Effect of electrochemical variables.

- Effect of material variables (mechanical properties, welding processes, etc).

- Loading variables (frequency, R-ratio etc).

The picture is further confused since the effects of the various parameters is often inter-related, which makes it extremely difficult to isolate the effect of any one parameter. As a result, observed crack growth behaviour exhibits some randomness, with very different results being obtained from nominally identical specimens. Because of the inherent randomness of fatigue processes, caution must be exercised when interpreting the results of analytical studies.

Notwithstanding these problems, it is still possible to obtain crack growth predictions which are sufficiently reliable to use as a basis for engineering decisions affecting inspection and repair.

6.3.2 General background and recent advance in the assessment of fatigue crack growth

Fatigue crack growth in steel structures is an area which has received considerable attention from the offshore industry. Initial research was undertaken in the UKOSRP I programme, and this has more recently been supplemented by the UKOSRP II and the SERC Cohesive Fatigue Programmes. Additional data on the service performance of offshore structures in a fatigue environment has become available, and a number of high quality studies have been undertaken on specific fatigue problems by specialist consulting organisations. The net result is that the offshore industry has a fuller understanding of the behaviour of fatigue cracks in offshore structures, and is therefore better able to plan underwater inspections.

A number of introductory texts are available on fatigue fracture mechanics and it is therefore not considered appropriate to include this material in the current document. A review was published in the CIRIA UEG Design Handbook on Tubular Joints[11] (hereafter referred to as the 'Design Guide'), which included data available at the time of writing (1983). It is an indication of the speed of progress in this field that much of the earlier work has since been superseded by recent developments. A brief overview of some of the most significant recent developments in fatigue research is given hereunder. It is likely that the items described would be considered in a present day assessment of fatigue damage, and will be demonstrated in the case studies later in this section.

1. Stress intensity factor solutions

The calculation methods for stress intensity factors (SIFs) reviewed in the Design Guide followed two basic approaches, namely the experimental approach, in which the stress intensity factor for a particular case is inferred from the results of a fatigue test, and the analytical approach.

The leading experimentally based model is that developed at the London Centre for Marine Technology[12] (LCMT), which is based on the results of fatigue tests for T and Y joints. For the model to achieve widespread usage in the design office, it would be necessary for a large number of additional tests to be performed to enable parametric formulae for SIFs to be developed. It is significant that the most recent application of the model[13] was as a benchmark for analytical models, and it is likely that this is where the future of this approach lies.

Early analytical models were based on highly idealised geometries which were not truly representative of tubular joints. These models have generally been superseded by models based on surface cracks in flat plates, such as the widely used Newman and Raju solution[14]. Whilst offering considerably improved accuracy, models of this type suffer from the disadvantages of not being able to account for shell curvature effects, and only being able to accommodate simple stress fields (tension and bending). More powerful techniques, such as the influence function and the line spring methods, are able to overcome these deficiencies, and one such model will be developed in this section. It is significant that the more advanced models are able to utilise laboratory data on stress distributions and residual stress fields, which should act as an incentive for additional research in this area.

A more detailed review of current analytical approaches may be found in Reference (15).

2. Stress distributions

All stress intensity factor solutions rely to a varying degree on the stress distribution acting on the crack. Some models are dependent on the distribution through the wall thickness, others on the distribution around the joint intersection, and

more advanced models depend on both. There are three main stress fields which govern fatigue crack growth (deformation stresses, notch stresses and residual stresses), as defined in Reference (11).

Research on deformation stresses has been governed by the requirements of S-N methods of analysis, and hence has focussed on the computation of hot spot stresses. Useful progress has been made in this field, including extending the ranges of applicability of the parametric formulae[16], developing formulae for overlapping joints[17] and accounting for the effect of chord end loads on the hot spot stress[18]. However, little work has been published on stress distributions, particularly through the wall thickness, and this continues to act as a restraint on the development of fracture mechanics models.

A considerable amount of work has been performed on stress fields at weld toes in simple plate geometries by Lawrence and co-workers[19] for the purpose of developing analytical models for crack initiation. More recently, data has become available on notch stresses for multiplanar K-joints using photoelastic techniques[20] and for Y and K-joints using strain gauged steel specimens[13]. Whilst notch stresses have a major influence on the growth of small cracks, the effect on cracks of significant size, which could be detected in an underwater inspection, is less important.

The detrimental effect of welding residual stresses on fatigue life was demonstrated in UKOSRP I using fillet welded plate specimens, and this trend has recently been confirmed for welded tubular joint specimens in seawater[21]. To date it has not been possible to incorporate residual stress effects meaningfully into fracture mechanics models because of a lack of published data on residual stress levels and distributions (see Section 5.4). However, measurements on residual stresses have recently been made on three T joints[22], and this will be supplemented by additional data in the next phase of the SERC Cohesive Fatigue Programme.

3. Environmental and related effects

The conventional method of presentation of crack growth data is the form of a plot of crack growth rate, (da/dN), versus stress intensity factor range, ΔK. The classical form for this curve is sigmoidal, with the central portion described by a power law relationship, such as Paris' law (see Figure 6.21). This presentation permits a ready comparison of environmental effects to be made.

Conventional fatigue design practice is based on S-N curves, such as the UK Department of Energy T curve[23], which were originally derived for tubular joints fatiguing in air. The application of these methods to joints in seawater implicitly assumes that the correct application of cathodic protection removes the problem of corrosion fatigue. Recent work undertaken in the SERC Cohesive Fatigue Programme indicates that this assumption is not valid[21].

It is beyond the scope of this document to perform a detailed review of this complex and still developing subject. However, data for the important case of crack growth in seawater with cathodic protection has been collated and is presented in Section 5.3. Inspection of this data leads to the important conclusion that simple crack growth laws of the Paris type are insufficient to reproduce the observed behaviour. More general multi-term laws are necessary[24], for which constants may be derived to suit the prevailing conditions.

4. Fatigue crack development

A major advance in the understanding of fatigue crack growth in tubular joints was marked by the development of the ACPD method for measurement of crack depths[25]. Early data obtained with this method in the UKOSRP I programme proved unreliable although recent data has permitted a more consistent picture of crack development to emerge. A screened database on crack shape development and growth characteristics is given in Section 5.3. Realistic crack growth models should

be able to reproduce this behaviour if confidence is to be placed in the computed results.

A very important regime which is frequently not addressed in tubular joint fatigue tests is crack development after the formation of through-thickness cracking. This is because the conventional definition of fatigue life (N_2) is taken to be the appearance of a through-thickness crack, on the basis that subsequent crack growth under constant amplitude loading is likely to be very rapid. However, it is known that a major change in compliance usually accompanies the development of a through-thickness crack in a tubular joint, which in a redundant structure will lead to load shedding, and possibly to significant retardation of the growth rate[26]. Since the detection of though-thickness cracks is much easier and less costly than for part-through cracks, it is likely that this regime will receive greater attention in the future.

6.3.3 Analysis methods for part-through cracks

There are a number of alternative approaches which may be used to model crack growth. In this report, one of the leading crack growth models, originally developed by the Southwest Research Institute[27] (SWRI), has been selected as an example of a state-of-the-art model and its features are presented in some detail. Where deficiencies in the model are noted, in the light of recently available research, these are highlighted and improvements introduced. The improved model is implemented in the crack growth program KTUBE[28], which has been used for case studies in Section 6.6.

The model contains procedures both for the calculation of crack initiation lives, and for the calculation of subsequent crack growth. In the context of the assessment of fatigue damage, it is the crack growth regime which is of primary interest since the crack initiation period has already passed. The calculation of crack initiation lives will not be considered further in this document.

1. Crack growth law

A multi-term crack growth law was proposed by SWRI which is able to account for the differing growth rates in the various regimes. The law is expressed as the inverse of the crack growth rate, and has the following form:

$$\frac{1}{da/dN} = \frac{1}{A_1 \Delta K^{n_1}} + \frac{1}{C\Delta K^m} - \frac{1}{C[(1-R)K_{IC}]^m} + \frac{1}{(da/dN)_p} \qquad (6.9)$$

where R is the load ratio and is calculated from

$$R = \frac{K_{min}}{K_{max}} \text{ if } K_{min} > 0 \qquad (6.10a)$$

$$= 0 \text{ if } K_{min} < 0 \qquad (6.10b)$$

C,m are material properties and will usually have the same values as the constants used in the simpler Paris law. These constants govern crack growth in the lower intermediate range.

A_1, n_1 are additional material properties which define crack growth at low growth rates.

K_{IC} is the plane strain fracture toughness. This property governs high crack growth rates, resulting from the intervention of static failure processes.

$(da/dN)_p$ is the plateau crack growth rate, exhibited by some material/environment systems.

Values of the material properties suggested in Reference (27) are presented in Table 6.2. The crack growth characteristics derived by substituting these constants into Equation (6.9) are shown in Figure 6.22.

Data on fatigue crack growth in seawater with cathodic protection was presented in Section 5.3, and it is apparent that the plateau behaviour predicted in the SWRI model has not been observed generally in laboratory tests. A modified crack growth law is proposed which has the form:

$$\frac{1}{da/dN} = \frac{1}{A_1 \Delta K^{n_1}} + \frac{1}{C \Delta K^{m}} - \frac{1}{C[(1-R)K_{IC}]^{m}} + \frac{1}{A_2 \Delta K^{n_2}} - \frac{1}{A_2[(1-R)K_{IC}]^{n_2}} \qquad (6.11)$$

In Equation (6.11), the first 3 terms on the right hand side are identical with the corresponding terms in Equation (6.9), and the last two terms have been introduced to govern growth in the upper intermediate regime. The following values for the constants are proposed in MN,m units:

$A_1 = 0.125 \times 10^{-34}$
$n_1 = 32.2$
$C = 0.35 \times 10^{-13}$
$m = 5.96$
$A_2 = 0.16 \times 10^{-7}$
$n_2 = 1.395$

The crack growth law given by Equation (6.11) has been plotted in Figure 6.23.

2. Stress Intensity Factor Solution

The SIF solution proposed for use with the SWRI model is for a surface crack in a flat plate acting under tension and bending, originally proposed by Newman and Raju[14] see Figure 6.24. The solution is of the form:

$$K_I = (f_t Y_t + f_b Y_b) \sqrt{\pi a/Q} \qquad (6.12)$$

where $Y_t, Y_b = F(a/T, a/c, c/W, \phi)$

$Q = Q\ (a/C)$

Although this solution takes account of both the crack length and depth, it is not a true two dimensional solution since the stress field must be constant in the length direction. Other limitations are that shell curvature effects are ignored, and that only a linear variation of stress is permitted in the thickness direction.

An alternative approach, which overcomes the latter objection, is to use an influence function to calculate the SIF for a crack under arbitrary loading (see Figure 6.25).

$$K_I = \int_o^a f(\eta)\ g(\eta, a, \text{etc})\ d\eta \qquad (6.13)$$

where $f(\eta)$ is the stress field on the crack face
$g(\eta, a)$ is the influence function

There are a limited number of influence function solutions available, but the Tada[29] solution for a finite width strip is suitable. To account for shell curvature effects, the forces and displacements on the crack zone must be matched to those in the surrounding material; this may be achieved by the line spring method[30], as demonstrated in Reference (31).

The major disadvantage of the combined influence function/line spring approach is that it is strictly a one dimensional solution, taking no account of the flaw shape. However, as an approximation the Newman and Raju solution may be used to provide an aspect ratio correction factor, Y_a, as outlined in Reference (15). The aspect ratio factors for tension and bending, Y_{ta} and Y_{ba}, are plotted in Figure 6.26.

To summarise, the features of the SIF model are as follows;

- The basic SIF is calculated by an influence function method, using Tada's solution.
- The effect of shell curvature is allowed for using the line spring approach.

- An approximate allowance for the flaw shape is made by use of the Newman and Raju solution.

This calculation procedure is probably the most comprehensive which may be adopted, short of a full two dimensional crack solution, and has been used for the case studies.

3. Stress Fields

The accuracy with which the stress fields acting on the crack face may be determined is often the limiting factor in the accuracy of the total analysis. It is normal to expend considerably more effort in developing the stress field for a fatigue crack growth analysis than for an S-N fatigue analysis.

Considering firstly the deformation stresses, procedures for calculating stresses on the outside surface of the chord and brace are comparatively well developed. These may be estimated by use of standard parametric SCF formulae, with assumed distribution functions[32] to give the variation around the joint intersection. It is, however, preferable to take account of the effect of the loading from all incoming braces and from the chord, by the influence coefficient technique. The details of this approach are given, in the case of K and Y joints, by Buitrago[18].

Having determined the outer fibre stress f_o, it is necessary to estimate the variation through the wall thickness by splitting the stress into tensile and bending stresses (f_t and f_b). This may be expressed in terms of the distribution parameter, λ_s, as

$$f_t = \lambda_s f_o \qquad (6.14a)$$

$$f_b = (1-\lambda_s)\, f_o \qquad (6.14b)$$

It is still not common practice in the technical literature for the value of λ_s to be reported with stress analysis results or laboratory test data, and this represents a serious omission. For the case studies it will be necessary to use values of λ_s obtained by Wimpey Offshore from finite element studies of similar joints.

Superimposed on the deformation stresses are the notch stresses at the weld toes. The results of the finite element work of Lawrence[19] will be used to estimate the notch stresses.

The notch stress, f_n, is given in terms of the outer surface stress, f_o, by

$$f_n = (K_t - 1)\, f_o \qquad (6.15)$$

where K_t is the notch stress concentration factor.

The value of K_t is dependent on the ratio of the plate thickness, T, to the local weld toe radius, r, and is of the following form:

$$K_t = 1 + \alpha\, (T/r)^{\frac{1}{2}} \qquad (6.16)$$

where α has been determined by finite element studies.

$\alpha = 0.35$ for $\lambda_s = 1$
$\alpha = 0.19$ for $\lambda_s = 0$

It is argued that an infinite range of radii may be found in as-welded weld profiles, and that for conservatism the value of r should be selected to give the minimum crack initiation life. The procedure for calculation r is given in Reference (19).

4. Numerical Aspects of the Computation Procedure

The crack growth law, Equation (6.11), is of the form

$$\frac{da}{dN} = h(\Delta K) \qquad (6.17)$$

which may be integrated to give

$$N_p = N(a_f) - N(a_i) = \int_{ai}^{af} \frac{1}{h(\Delta K)}\, da \qquad (6.18)$$

where a_i is the initial crack depth
a_f is the final crack depth

The solution method proposed by SWRI is to apply a given number of cycles, say corresponding to a one year loading period, and to compute the final crack depth, a_f, and length c_f. This procedure is somewhat complex since an iterative solution must be performed of Equation (6.18) to determine a_f.

The alternative procedure is to specify the increment in crack size, and to perform a direct integration of Equation (6.18) to determine the number of loading cycles. The integration must be performed numerically, and significant errors can be introduced if the integration step is too large. In the program KTUBE an adaptive integration procedure is used, whereby the specified crack growth increment is successively sub-divided until convergence is achieved.

For a given increment in crack depth, the change in crack length may also be computed if it is assumed that the same law and crack growth constants govern crack growth in both the length and depth directions. However, with stress corrosion there may be substantial differences in crack growth conditions along the crack front, and hence the validity of this assumption is doubtful. The preferred method is therefore for the user to specify the corresponding increments in both length and depth, based on experimental data for crack shape development.

To commence the calculation, it is necessary to specify the initial crack depth. It is normal to take this as the nominal depth at crack initiation to enable the complete crack growth characteristic to be generated - this characteristic may then be entered at any crack depth to determine the residual life. Following the procedure of Chen[33] which was developed to join crack initiation and fatigue crack growth models, the initial crack size may be calculated as

$$a_i = \frac{0.0954\ \sqrt{T}}{\alpha\ F_u^{0.9}} \text{ in MN,m units} \qquad (6.19)$$

where F_u is the ultimate tensile strength of the material

α is as defined for Equation (6.16).

The crack growth procedure outlined above is for constant amplitude stress cycling. If variable amplitude cycling is experienced, as in offshore structures under hydrodynamic loading, it is necessary to weight the contribution to crack growth from each stress range by the relative frequency of each range. The resulting equation is

$$\frac{da}{dN} = \int_o^\infty \left[\frac{da}{dN}(\Delta K)\right] f(\Delta K)\ d(\Delta K) \qquad (6.20)$$

where $f(\Delta K)$ is the probability density function for the SIF range.

Equation (6.20) implicitly assumes that load interaction effects do not occur.

A flowchart for the crack growth computation is given in Figure 6.27.

6.3.4 Analysis methods for through-thickness cracks

Increased interest is currently being expressed by the offshore industry in the behaviour of through-thickness cracks, since these may be detected more economically and reliably than for part-through cracks. Analysis methods for these cracks are thus required to enable the behaviour to be predicted reliably.

For through-thickness cracks located at tubular joints, the situation is very complex, because of the geometry and the nature of the stress fields at the intersection. The only feasible analysis technique is to use a numerical method, such as finite element analysis, in which the crack is represented in the model. Such analyses are expensive because of the number of elements required to model the cracked joint, and because a separate analysis is required for each crack length under considerations.

There are several cases of interest in which through-thickness cracks may occur in a tubular member, remote from any tubular joints. These include:

1. Through-thickness cracks which have developed from single sided butt welds, for example at brace to stub joints, or at access windows.

2. Cracks which have developed at appurtenance supports. On early North Sea platforms these were frequently rigidly welded to the structure and have proven troublesome in fatigue, sometimes leading to a local failure.

Examples of both types of crack geometries are illustrated in Figure 6.29. For the simple circumferential crack, analytical solutions are available[34] which give the SIF for axial load of bending acting on the member. The SIF may be expressed in the form

$$K_I = (f_t Y_t + f_b Y_b) \sqrt{\pi a} \qquad (6.21)$$

where f_t and f_b are the tensile and bending stresses acting in the member

Y_t and Y_b are plotted in Figure 6.29.

It should be noted that the SIF for the tubular member rises steeply with increasing crack size. It is very unconservative to apply an SIF solution derived for an infinite plate to this geometry.

The case of cracks emanating from a circular hole has been extensively studied for flat plates[35]. It should be noted that it is generally non-conversative to idealise the hole and the adjacent edge cracks as a single crack of the same overall length, since this ignores the stress concentration caused by the presence of the hole. It is thus necessary to determine the stress field surrounding the hole in order to estimate the SIF for the edge cracks.

6.3.5 Benchmark Studies

To establish confidence in the use of the crack growth model, and to gain an understanding of the sensitivity of the results to the governing parameters, a number of benchmark studies have been performed.

A system of reference numbers has been applied to the benchmark analyses. Details of each analysis are given in Table 6.3. Certain parameters remained constant, and are as follows:

1. R-ratio. All studies were performed at R-ratio of 0, using the low R-ratio crack growth constants for each environment.

2. Residual stress. A uniform tensile residual stress of 250 MN/m^2 was assumed.

3. Crack shape. The aspect ratio (ratio of crack depth to total length) was assumed to be 1/15.

4. Weld toe stress concentrations. The weld toe stress fields recommended by Lawrence[19] were used. The constants are reported in Table 6.4.

5. Initial crack sizes. The procedure for calculating the initial crack size, proposed by Chen and Lawrence[33], was used. These crack sizes for various plate thicknesses are given in Table 6.5.

The results of the individual benchmark studies are reported in the following:

Crack Growth in Air

Analysis number 2 was used to verify the calculation procedure against an experimentally derived design SN curve for joints with the same wall thickness (16mm). The results are shown in Figure 6.30. Generally very good agreement is noted. The computed break point in the curve occurs at close to 10^7 cycles, which is in agreement with the design SN curve. At lives beyond 10^7 cycles the FM analysis predicts a smaller negative slope for the SN curve than the widely used design value (-1/5). This value is, however, known to be a conservative approximation to the actual behaviour in the threshold regime.

Effect of Stress Distribution Factor, λ_s

A comparison between analyses numbers 2 and 3, for which λ_s = 0.15 and 1.0 respectively, is shown in the form of SN curves in Figure 6.30, and as crack growth characteristics in Figure 6.31. It may be noted that for a given hot spot stress range, increasing λ_s causes a substantial reduction in the fatigue life. Significantly, a high value of λ_s makes the crack much more difficult to detect since the crack is at an inspectable size for a much lower proportion of its total life.

Effect of Wall Thickness

The effect of wall thickness is demonstrated by comparison of the results of analyses 1 and 2 in Figure 6.32. The expected reduction in fatigue life is noted, and close agreement obtained with the appropriate SN curves.

Effect on Environment

The effect of environment on the fatigue life is shown in Figure 6.33 by comparison between analyses 2, 4 and 5. The comparison between the air environment and freely corroding seawater conditions is as expected, with a reduction in the fatigue life in seawater.

The SN curve for seawater with cathodic protection is unusual, with a reduction in life at higher stress ranges and a very significant increase at lower stress ranges. These comparisons, reported in terms of the total life, are disproportionately affected by the life spent as a small crack. Plotting out the crack growth characteristic against the residual life (Figure 6.34) shows that the behaviour for cracks of finite size is less sensitive to the surrounding environment. This is an important conclusion since underwater inspections are aimed to detect cracks of this size.

6.4 Crack Stability

6.4.1 Introduction

This section reviews methods of assessing the stability of cracks in steel structures. The objective of a crack stability assessment is to determine, for a given crack size, the load which will cause unstable crack extension (ie. fracture). Stability assessments are frequently conducted in conjunction with fatigue crack growth studies.

Calculations on crack stability, in common with fatigue crack growth analyses, rely on fracture mechanics techniques. In several respects, the emphasis of the two analysis procedures is rather different. Firstly, unstable crack extension is generally preceded by yielding in the crack zone, and this should be accounted for in the analysis. Secondly, the number of loadcases to be considered in a stability assessment is generally much reduced, so it may be possible to devote greater effort into the analysis of each crack size/loadcase combination.

There are a number of areas of difficulty associated with the assessment of crack stability, including the following:

- The complexity of the analysis problem which either necessitates the use of very powerful analysis techniques, or the introduction of simplifying assumptions.
- The development and interpretation of toughness data for the steel, both in the welded and unwelded conditions.
- Lack of data on residual stresses.
- The diversity of approach of the commonly used assessment procedures.

An additional problem is that, unlike fatigue crack growth, test results obtained from large scale specimens of representative geometries are not available. There is thus no effective benchmarking of stability analyses for cracks located in complex

geometries, such as tubular joints, and it is therefore prudent to utilise conservative assessment procedures. If good quality steels have been used in the construction, and if the structure is well-designed so that the stress levels are moderate, it may be possible to demonstrate conclusively that adequate defect tolerance exists. In other cases the results will be more marginal, even if the actual risk of crack instability is low, because of the inherent conservatism of the assessment procedures. In these cases engineering judgement must be exercised in the interpretation of the results, and consideration should also be given to the consequences of failure.

6.4.2 General background

6.4.2.1 Overview

The failure of flawed structures acting under tension is governed by two separate, though interrelated, processes:

1. Crack extension (fracture)
2. Plastic collapse

A fundamental aspect of any assessment procedure is the manner in which the two failure mechanisms are handled. The simplest approach is to treat each mechanism separately for the purposes of the analysis, and to link the two mechanisms by a failure interaction equation. This approach may be typified by the CEGB R6 method[36]. The alternative strategy is to perform a rigorous analysis of crack stability, making full allowance for plasticity as appropriate. In such an analysis, the calculated crack driving force will automatically tend to infinity as plastic collapse approaches, and hence failure will be correctly predicted.

It is generally accepted that there are three basic regimes which govern crack extension:

1. Linear elastic behaviour, which governs brittle failure.

2. Elastic-plastic behaviour, associated with ductile failure.

3. Tearing behaviour.

In the linear elastic and elastic-plastic regimes failure is generally defined as the point at which crack 'initiation' occurs, where in this context initiation means the onset of crack growth under static loading. The tearing regime is concerned with the behaviour of the crack after initiation. Although widely used in the nuclear industry, the types of steels and the service temperatures severely limit the applicability of tearing stability methods in the offshore industry, and they will not be considered further in this report.

For both the linear elastic and the elastic-plastic regimes the criterion for failure is of the following form:

Crack driving force parameter > material resistance parameter (6.22)

In the linear elastic case the crack driving force is characterised by the stress intensity factor (K_I), and the material resistance by the plane strain fracture toughness (K_{IC}). However, steels with good low temperature properties, commonly used in the offshore industry, generally preclude true brittle failure, and linear elastic methods are therefore of secondary interest.

In the elastic-plastic regime the crack driving force and the material resistance may be characterised by the crack tip opening displacement (CTOD) or the J-integral; the two quantities are somewhat interchangeable although the CTOD is much more widely used in the offshore industry because of the availability of material property data. An important difference compared to the linear elastic regime is that the crack driving force is not proportional to the load, typically varying with the square of the load.

6.4.2.2 Basic analytical approaches

The most widely used analytical methods are linear elastic techniques which have been derived to compute stress intensity factors. A number of compendia of solutions and analytical techniques are available which enable SIFs to be computed for a wide range of geometries and loading conditions - a review of these may be found in Reference (11).

The SIF is of limited use in crack stability calculations because for the high toughness/low yield stress steels commonly encountered in the offshore industry, fracture is generally preceded by significant yielding. The role of plasticity in the behaviour of cracks has been investigated in a number of detailed analytical studies performed using nonlinear finite element analysis[37]. An important conclusion of this work was the fundamental difference in behaviour between 'contained' and 'uncontained' plasticity.

Contained plasticity typically occurs around short cracks, with the plastic zone not extending to any of the free surfaces of the body, except possibly breaking back to the faces of the crack. This typically occurs with cracks in localised stress concentrations, such as at fillet welds. Provided that the crack is small, the plastic zone may remain contained even for applied stress levels approaching general yield. For uncontained plasticity the plastic zone extends across the full width of the body at the cracked section, and marks the onset of plastic collapse. An example of each, for an internally pressurised cylinder, is shown in Figure 6.35. It may be noted that a greatly increased crack diving force accompanies the onset of uncontained plasticity.

Provided that the plasticity is contained, the stress fields surrounding the crack are not greatly affected by the presence of the plasticity, and linear elastic methods of analysis remain valid, with some modifications. The most usual modification is simply to increase the affective crack size by means of a plastic zone correction[38]; this procedure has been found to be effective for

applied stresses up to approximately 80% of yield, although this is dependant on the geometry and the material properties.

An alternative approach for performing an approximate analysis of crack tip plasticity is the Dugdale strip yield model[39]. In theory this model is only applicable to cases where limited yielding occurs, but it has been found that the solution can perform well at load levels approaching plastic collapse.

A major advantage of analysis methods which depend on modifications of linear elastic techniques is that the wide range of available elastic crack tip solutions may be used. These analysis methods are generally both easy to use, and are sufficiently powerful to handle complexities such as non-uniform stress fields and arbitary crack geometries.

When uncontained plasticity occurs, true elastic-plastic analysis methods should be used. It is of course possible to undertake a nonlinear finite element analysis for the geometry under consideration, although this is likely to be prohibitively expensive, particularly since a separate analysis must generally be performed for each loadcase. However, for certain simple geometries parametric studies have been performed which enable the crack driving force to be read from tables of results[40]. The geometries studied include cracks in tubular members and pipelines, and in plated structures (deck girders, etc), but do not include more complex configurations like tubular joints. Whilst the range of geometries studied to date is somewhat restrictive, it is anticipated that this range will be extended in due course.

By far the most widely used analysis method for use in practical situations is design curves. The most important of these is the CTOD design curve[41], reproduced in Figure 6.36, which computes the applied CTOD from the strain acting in the crack location, calculated for the uncracked body.

This curve is closely paralleled by the less widely used J-design curve[43]. The major advantage of design curves is their inherent simplicity and ease of use. However, by virtue of their simplicity they are unable to cater adequately for the full range of problems encountered and the resultant factor of safety is variable. A number of criticisms have been levelled against the CTOD design curve, of which perhaps the most serious are that plastic collapse is inadequately treated, and that little guidance is offered on computing the strains for use in the design curve equations. Several proposals[44, 45] have recently been made to overcome these major failings, and it is likely that these proposed modifications will achieve official status in due course.

An alternative design curve approach is the CEGB R6 method[36], which takes the form of an interaction diagram for failure arising from either fracture or plastic collapse (see Figure 6.37). Whilst this method overcomes most of the critisisms afflicting other design curves, its applicability in the offshore industry is undermined because the fracture criterion is expressed in terms of the plane strain fracture toughness, for which there is comparatively little test data available. An equivalent curve, utilising CTOD as the parameter to characterise fracture, has been proposed by Anderson and co-workers[45].

A number of studies[46, 47] have been performed to compare the relative performance of the most widely used design curves. One recently performed study[47] which made a careful comparison between the CTOD design curve and the CEGB R6 methods arrived at the following conclusions:

1. The R6 method developed well-behaving solutions with narrow scatter bands. The solutions were conservative in all cases.

2. The CTOD design curve developed solutions with a wide scatter. A number of these solutions were unconservative, particularly at high applied stress levels.

3. The performance of the CTOD design curve could be improved very significantly by making use of the actual stress-strain curve of the material, and by taking proper account of the geometry and the actual loading on the crack.

Design curve assessment procedures will continue to be used for the foreseeable future because of the practical advantages in their application. Although methods of improving the accuracy of design curve methods have been identified, it nonetheless remains essential to include an adequate factor of safety within the procedure to cover all possible applications of the method. This may be unsatisfactory for certain situations where a large factor of safety is not required. It is therefore likely that multi-level assessment procedures will find greater usage; in these a design curve would be used initially to give a simple, conservative assessment of defects but more advanced methods would be used for critical applications, or where greater accuracy was required.

6.4.3 Material Property Behaviour

In an assessment of crack stability in steel structures a knowledge of the materials properties for the components under examination is required. The type of data needed is dependent in the analysis being carried out.

For the CTOD based approach, both the CTOD value, δ, and the yield strength F_y are required. When determining the toughness, the material can exhibit different behaviour with the following toughness classification;

δ_c, crack tip opening displacement at either unstable fracture or at the onset of an arrested brittle crack when there is no evidence to suggest that slow crack growth has occurred.

δ_i, crack tip opening displacement at which slow crack growth commences.

δ_m, crack tip opening displacement at first attainment of maximum load plateau.

δ_u, crack opening displacement at either unstable fracture or onset of arrested brittle crack or pop-in where there is evidence to suggest that slow crack growth has occurred.

These types of behaviour are illustrated in Figure 6.38 and can be thought of in terms of a measure of the degree of ductility of the material. The behaviour is dependent on the inherent nature of the material (which is a factor of chemical composition, heat treatment, steel making practice etc) and also on the temperature of testing. Generally for offshore steels at the temperature of interest (-10°C), δ_c and, to a limited extent, δ_u values occur.

As discussed in the previous section, the CTOD approach is only applicable to cases where limited yielding occurs. Where a material exhibits a high degree of stable, ductile crack extension, use of the δ_u or δ_m value can lead to unconservative assessments. To maintain the conservatism in the analysis the selection of the critical CTOD should be limited to that at the crack initiation ie. δ_c or δ_i rather than that at the maximum load for highly ductile materials which can develop extensive stable tearing before crack instability. This suggests that a limitation of applicability of the CTOD design curve method can be directly related to the capability of a material for ductile tearing before crack instability. For most of the steels used in the North Sea the amount of stable cracking before instability will be limited and on the whole the CTOD concept will remain applicable at the temperature of interest (-10 to + 4°C) provided that the value of crack initiation is used and the appropriate steps are taken to maintain conservatism as outlined in the previous section. It should be emphasised, however, that although a method for determining the

initiation value δ_i is outlined in BS5762[48], in reality it is often difficult to determine this on the load trace and the specimen. An alternative method for predicting this stage is to construct the materials resistance curve, R[49]. In essence, the R-curve is a graphical representation of the variation in crack growth resistance during the process of stable crack extension but also provides information at the point of crack initiation. It is directly compatible with tearing stability analyses and is likely to become more important as offshore steels improve in quality in the future.

For an R6 analysis, the crack initiation stress intensity factor, K_{IC} and the flow stress are required. The latter is usually taken as the average of yield and tensile strength for work hardening materials. For other analyses such as J-integral or the WI Level 2 method (see Section 6.4.4) the material's resistance can be measured either as a J-integral or again the CTOD toughness. However it should be noted that the material's stress-strain curve is required for satisfactory assignment of correct Ramberg-Osgood parameters although it is believed that a good assessment of these is possible from knowledge of the yield strength, tensile strength and elongation to fracture.

As discussed in Section 5.2, the most generally available fracture data available is in the form of Charpy impact data and rarely as CTOD or K_{IC} toughness. In the absence of the most suitable toughness data for crack stability assessment, the Charpy impact values have to be transformed into suitable toughness data at the temperature of interest via transition curves and suitable correlations. The first stage of transformation, ie. obtaining Charpy values at the temperature of interest has already been discussed in Section 5.2. The following section provides a means of correlating the impact data to fracture toughness and illustrates the conservation of the correlations with two examples.

6.4.3.1 Correlation of Charpy Impact Data to Fracture Toughness Data

To obtain the appropriate material fracture resistance, δ_c, used for the crack stability calculations, a correlation relating Charpy

impact energy to CTOD toughness is essentially required. However, correlations of parent plate and HAZ toughness have not been attempted because Charpy impact requirements for steels have generally been derived from large scale wide plate fracture initiation tests and correlations of the smaller initiation test (CTOD), to Charpy impact values have not been required. Hence CTOD toughness has been measured for welding procedure qualification, comparison of effect of varying welding procedure techniques on toughness and for engineering critical assessments where CTOD toughness is the most suitable material property input parameter.

For weld metals, the situation is slightly different in that few wide plate tests have been carried out and attempts at CTOD/Charpy correlations have been carried out[51].

Although direct comparisons do not exist for HAZ and parent plate, empirical correlations of impact toughness to the plane strain fracture toughness K_{IC} do exist[52] and have been subject to review[53]. Of the correlations in existence, a number are shown to be conservative with respect to measured K_{IC} values of BS 4360 50D steel having a Charpy transition curve similar to many of the steels used in the North Sea. (See Fig 6.39). Those correlations marked (5) and (9) in Figure 6.39 and due to Rolfe and Novak[54] and Sailors and Corten[55] are most appropriate for consideration here due to having been derived from impact data in the transition range and having the larger data base. Of the two, the Sailors and Corten relationship gives the more conservative approach except at impact energies less than 19J but as the Rolfe and Novak correlation has been derived from a greater number of steels including those of similar strength levels to steels used in the North Sea it was decided that this is the most appropriate correlation to use.

Having converted the toughness data from an impact value to a linear elastic fracture mechanics value, it is then necessary to replace this by the elastic-plastic fracture resistance, CTOD, as appropriate to the crack stability assessment being carried out. For this, the analysis of Ingham and Harrison[56] proves particularly useful. In a study of the various methods of determining defect acceptance, an attempt was made to correlate, on

the basis of experimental relationships, between K_{JC} (upper shelf initiation toughness) and CTOD at temperatures corresponding to upper shelf and upper transition conditions and between K_{IC} and CTOD for lower shelf and lower transition conditions.

The results gave the following relationships;

UPPER SHELF TEMPERATURES (T > 10°C)

$$\delta = \frac{K_{JC}^2 (1 - \nu^2)}{1.5 E F_f} \text{ where } F_f = \frac{F_y + F_u}{2} \qquad (6.23)$$

UPPER TRANSITION REGION (-4°C < T < + 24°C)

$$\delta = \frac{n (K_{JC})^2 (1 - \nu^2)}{m E F_y} \qquad (6.24)$$

LOWER TRANSITION REGION (-73° < T < -4°C)

$$\delta = \frac{n (K_{IC})^2 (1 - \nu^2)}{m E F_y} \qquad (6.25)$$

LOWER SHELF TEMPERATURES (T < - 73°C)

$$\delta = \frac{K_{IC}^2 (1 - \nu^2)}{2 F_y E} \qquad (6.26)$$

(m,n are experimentally derived constants)

Equations (6.24) and (6.25), applicable to the transition range are essentially the same, the only difference being the measured value of fracture toughness, either K_{JC} the elastic/plastic fracture toughness, or K_{IC} the plane strain fracture toughness and the value of M (where M = m/n) applicable for the temperature range in question. As the correlation of Charpy toughness to fracture toughness is based on linear elastic determinations, it is appropriate to use equation (6.25) where the measured values of m and n give a value of M between 1.73 and 1.87 depending on temperature.

The lower figure is applicable to the upper end of the temperature range ie. towards -4°C therefore it is considered appropriate to use a value of 1.75 in determining the CTOD levels of the steels in common use in the North Sea and maintain a continuing level of conservatism.

Thus the following procedure is recommended in arriving at a CTOD toughness level for each area of component/joint of interest.

1) Determine the average Charpy impact toughness for the component/joint in question from the mill sheets available.

2) By use of Charpy transition curves, relate this to impact toughness at 0°C or -10°C, whichever is appropriate.

3) Convert Charpy impact toughness to linear elastic fracture toughness using the Rolfe and Novak correlation:

$$(K_{IC})^2/E = 0.22\ (CV)^{1.5} \qquad (6.27)$$

4) Convert K_{IC} value to elastic plastic fracture toughness, δ, using the following relationship;

$$\delta = \frac{K_{IC}\ (1 - \nu^2)}{MF_y\ E}$$ Where F_y is the appropriate value of yield stress

6.4.3.2 Examples of Correlations

(i) Table 6M 6 gives some data on BS 4360 50D steel provided by the Welding Institute[57] both for Charpy testing and CTOD testing. However by taking the minimum recorded Charpy value at -50°C of 21J, a CTOD toughness of 0.027mm is obtained for that temperature via the above correlations. The minimum toughness recorded in CTOD tests at -78°C for the same material was 0.049. Thus a safety factor of 1.81 was introduced by the correlation irrespective of the extra conservatism introduced by the difference in test temperature.

(ii) Heat Affected Zone and Weld Metal

Table 6.7 gives data for Charpy and CTOD toughness of HAZ's and weld metal from two sources [58, 59]. For the heat affected zone, a measured Charpy impact value of 41J correlates to a CTOD toughness of 0.071mm compared to the actual measured value of 0.13mm, indicating a safety factor of 1.84,. Likewise for the weld metal data taken from Wong and Rogerson[59] the CTOD figure derived from a Charpy value of 76.3 is 0.19 compared to the actual measured value of 0.37. Note that as these are upper shelf values, equation (6.23) has also been used assuming a low value of flow stress of 475 N/mm^2 for the weld metal. This slightly reduces the toughness value to 0.18mm. These examples indicate that the conservatism introduced by this approach to deriving an appropriate CTOD toughness is quite high with a safety factor of just under 2 being common. However, due to uncertainties in data and areas of applicability for the correlations, it is felt that this degree of conservatism is appropriate.

6.4.4 Benchmark Studies

A simple benchmark study on crack stability has been performed to demonstrate the use of some of the stability assessment methods outlined in this section. The methods selected have been chosen because of their ease of use or accuracy. The CTOD design curve has not been selected because of its inherent limitations, and because it is, in its present form, likely to be superseded in the near future.

The problem selected, which has also been analysed in Reference (47), is a tubular member with an internal circumferential crack loaded in tension. This geometry would be representative of a tubular member or a pipeline with a crack developing from a circumferential butt weld. Details of the problem are shown in Figure 6.40, and the material properties are presented in Table 6.8. The stress-strain characteristics, which have been idealised as a Ramberg-Osgood material, are plotted in Figure 6.41.

In this benchmark problem, the definition of failure is based on the initiation of crack extension, which may be expressed as:

$$\delta_{app} = \delta_c$$

where δ_{app} is the applied CTOD

δ_c is the CTOD at the onset of crack extension

(6.28)

The results of the analysis are presented in the form of a stability diagram, Figure 6.43, in which the failure load is given by the intersection point between the crack driving force curve and the toughness line. For design purposes, it would be necessary to apply a factor of safety to the load to prevent fracture from occurring. The selected value would depend on a number of considerations, including the consequences of failure, and the forewarning of imminent failure, but it would not normally be less than 1.5.

(1) Plastic Zone Corrected Elastic Solution

The stress intensity factor for an internally cracked cylinder under axial tensile stress f_t is:

$$K_I = f_t \sqrt{\pi a}\, Y_t(R_i/R_o,\ a/t) \qquad (6.29)$$

where the function $Y_t(R_i/Ro,\ a/t)$ is given in graphical format in Figure 6.42.

The plane strain plastic zone correction is calculated as follows. The crack tip plastic zone size is approximately:

$$r_y = K_I^2/6\pi F_y^2 \qquad (6.30)$$

When a plastic zone has formed, the effective crack size becomes

$$a_{eff} = a + r_y \qquad (6.31)$$

The effective crack size a_{eff} is substituted for in Equation (6.29) and K_I is recomputed. It may be seen that the new value of K_I will affect the size of the plastic zone, and it is thus necessary to iterate Equations (6.29) to (6.31) - convergence is normally achieved in 2-5 iterations. Finally, the CTOD may be calculated from the stress intensity factor, as:

$$\delta_{app} = \frac{4}{\pi} \frac{K_I^2}{E' F_y} \qquad (6.32)$$

where E' is the effective modulus
(= E for plane stress, $E/(1-\nu^2)$ for plane strain)

The applied CTOD is plotted against load in Figure 6.43. Although the computed CTOD is accurate at stress levels up to 250 N/mm^2, which is approximately 80% of general yield, beyond this level the predicted CTOD is underpredicted as expected from the known behaviour of this analytical model. A separate calculation should be performed to check for plastic collapse at the cracked section, which in this case governs failure.

2. Elastic - Plastic Finite Element Solution

Parametric studies on various cracked geometries have been performed by the EPRI[39]. In this work, the crack driving force, expressed in terms of the J-integral, is computed from the equation

$$J = g(a_{eff}, R_i/R_o) \frac{f^2}{E'} + \alpha (F_y^2/E) (T-a) h(a/T, n, R_i/R_o) (f/F_y)^{n+1} \qquad (6.33)$$

$$= J_{ep} + J_p \qquad (6.34)$$

where g and h are functions computed in Reference (39).
a_{eff} is as defined in Equation (6.31)
α, n are constants in the Ramberg-Osgood material model.

The equation has two terms, which correspond to the elastic-plastic and the fully plastic regimes. At low load levels the first term is the more important, whereas at high load levels the second term becomes dominant. It should be noted that the second term scales with the applied load level, raised to a power dependant on the work hardening properties of the material. This feature, which leads to a great simplification of the form of the solution, is a result of the use of the Ramberg-Osgood material model. To convert Equation (6.33) to the more familiar CTOD, the following should be used:

$$\delta_{app} = \frac{4}{\pi} \frac{J_{ep}}{F_y} + d_n \frac{J_p}{F_y} \qquad (6.35)$$

where d_n is a conversion factor dependent on the material properties (= 0.55 in the present case).

The applied CTOD for this model is plotted in Figure 6.42. Because the analysis technique takes full account of the plastic response, the computed CTOD becomes large as plastic collapse is approached. At lower load levels, the results are close to those predicted by the simpler modified elastic solution.

3. The WI Level 2 Method

As part of a comprehensive review of methods to overcome the inherent weaknesses of the CTOD design curve, as presented in PD6493, the Welding Institute have recently proposed a 3 level assessment procedure[44]. The level of the procedure to be used in a given case would depend on importance of and the stress levels in the structure under examination. The 2nd level procedure, which is intended to combine accuracy with simplicity of use, calculates the applied CTOD from the following equation:

$$\delta_{app} = \frac{\pi F_y a}{E} \left[\frac{f_p}{f_n}\left[\frac{8}{\pi} \ln \sec\left(\frac{\pi}{2}\frac{f_n}{F_y}\right)\right]^{\frac{1}{2}} + \frac{f_s}{F_y}\right]^2 \qquad (6.36)$$

where f_p, and f_s are the effective primary and secondary stresses, as defined in Reference (44).

f_n is the net section stress, defined for this geometry as:

$$f_n = \frac{f_t}{1 - a/T} \qquad (6.37)$$

Equation (6.36) is derived from the expression for the CTOD in a centre cracked panel under tension. The value of the equation becomes very large as the quotient f_n/F_y tends to unity, which represents onset of plastic collapse. This test for plastic collapse is conservative, since the actual collapse load is generally higher owing to constraint and work hardening. It is also known that under conditions of high bending stress, as at the hot spot of a tubular joint, the collapse of the remaining ligament at a cracked section will be restricted by the general continuity of the structure[46].

Although derived originally for a very simple geometry and loading condition, Equation (6.36) is extended to other more complex cases by means of the calculation procedure for the effective primary and secondary stresses, f_p and f_s.

The calculated CTOD is shown, together with the results of the other two analysis methods, in Figure 6.43. Generally good agreement is noted with the other models at stress levels up to 250 N/mm^2, but at the nominal collapse stress (320 N/mm^2) the crack driving force tends to infinity.

The results of the study graphically illustrate the interaction between crack stability and plastic collapse; because of the high toughness level in the steel (δc = 0.93mm), the latter mechanism governs failure. Methods which do not specifically address plastic collapse do not perform well in this regime, but may be more satisfactory when applied to the lower toughness materials commonly found in weldments.

The Welding Institute level 2 model is conservative in its treatment of plastic collapse - a simple improvement in this respect would be to substitute the flow stress for the yield stress in Equation (6.36) to give a better estimate of the collapse load. The handling of plastic collapse is likely to be excessively conservative for bending loads where restraint is provided by the remainder of the structure. A summary of the applicability of the three methods investigated is given in Table 6.9.

6.5 Assessment of Structural Redundancy

Structural redundancy plays a major role in determining an optimised inspection plan. The classification of a member or joint as fracture critical or non-fracture critical is largely dependent on the redundancy of the structure.

It is potentially very costly and time consuming to investigate redundancy in a jacket type structure, and therefore the method for achieving this should be carefully considered.

The basic method for establishing structural redundancy is to sever the member being investigated, and to re-run a linear elastic static strength analysis for the jacket. A more rigorous method would involve analysing the jacket, with the severed member, by an elastoplastic static strength analysis. The elastoplastic analysis is more rigorous since members adjacent to the severed member may become plastic and, in turn, cause a secondary distribution of loads in the jacket. In the limit, this secondary distribution could lead to progressive collapse of the jacket due to formation of a mechanism.

The complexity and the cost of a large nonlinear analysis should not be underestimated. One operator who was performing ultimate load studies on a southern North Sea gas platform quoted computer run times in excess of 100 x those for an elastic analysis. From the technical standpoint, whilst elastic-plastic beam theory is reasonably well established and can give good answers for simple geometries, the nonlinear behaviour of tubular joints is considerably more complex. At the present time a full nonlinear analysis cannot be considered a realistic alternative, except for small structures where the degree of nonlinearity is low.

Example 2 shows the procedure required to compute fatigue crack growth characteristics for a longitudinal crack at the chordside weld toe in a simple tubular joint. The example is cross referenced in Section 8.1.

Example 3 shows the assessment procedure for a crack stability study of a longitudinal part-through crack in a simple tubular joint.

Example 4 shows the assessment procedure for the effect of a damaged member on the utilisation of adjacent members. This procedure is illustrated by investigating the consequences of a damaged member on a small jacket structure.

REFERENCES

13. Dover W D and Connolly M P
'Fatigue fracture mechanics assessment of tubular welded Y and K joints'.
International Conference on Fatigue and Crack Growth in Offshore Structures, London, April 1986.

14. Newman J C and Raju I S
'An empirical stress intensity factor equation for the surface crack'.
Engineering Fracture Mechanics, Vol 15, No. 1-2, pp 185-192, 1981.

15. Nicholson R W
'A review of the analysis of cracks in tubular joints in steel jacket structures'.
Conference on Offshore and Arctic Frontiers, New Orleans, February 1986.

16. Tebbett I E and Lalani M
'A new approach to stress concentration factors for tubular joint design'.
Paper OTC 4825, of Offshore Technology Conference, Houston, 1984.

17. Dharmavasan S and Seneviratne L D
'Stress analysis of overlapped K-joints'.
International Conference on Fatigue and Crack Growth in Offshore Structures, London, April 1986.

18. Buitrago J et al
'Combined hot-spot stress procedures for tubular joints'.
Paper OTC 4775 of Offshore Technology Conference, Houston, 1984.

19. Lawrence F V et al
Predicting the Fatigue Resistance of Welds.
Annual Review of Materials Science, 1981.

20. Elliott K S and Fessler H
'Stresses at Weld Toes on Non-Overlapped Tubular Joints'.
International Conference on Fatigue and Crack Growth in Offshore Structures, London, April 1986.

21. Dover W D and Wilson T J
'Corrosion Fatigue of Tubular Welded T-joints'.
International Conference on Fatigue and Crack Growth in Offshore Structures, London, April 1986.

22. Payne J G and Porter-Goff R F D
'Experimental Residual Stress Distributions in Welded Tubular T-Nodes'.
International Conference on Fatigue and Crack Growth in Offshore Structures, London, April 1986.

23. Department of Energy
'Offshore Installations: Guidance on Design and Construction'.
HMSO, London, April 1984.

REFERENCES

24. Saxena A et al
'A Three Component Model for Representing Wide-range Fatigue Crack Growth Rate Behaviour'.
Engineering Fracture Mechanicas, Volume 12, 1979.

25. Connolly, M P
'A fracture mechanics approach to the fatigue assessment of tubular welded Y and K joints' Ph.D Thesis University of London, 1985.

26. Brown D K et al.
3rd International Conference on Numerical Methods in Fracture Mechanics, Swansea 1984.

27. Hudak S J et al
'Analysis of corrosion fatigue crack growth in welded tubular joints'.
Paper OTC 4771 of Offshore Technology Conference, Houston 1984.

28. Wimpey Offshore Engineers & Constructors
'KTUBE. A program for the frature mechanics analysis of cracked tubular members'.
Report WOL 8/85, London, January 1985.

29. Tada H et al
'The stress analysis of cracks handbook'.
Del Research Corporation, St Louis, 1983.

30. Rice J R
'The line-spring model for surface flaws, in the Surface Crack': Physical Problems and Computational Solutions (ed J L Swedlow), ASME, New York 1982.

31. Parks D M
'The inelastic line-spring: estimates of elastic-plastic fracture mechanics parameters for surface cracked plates and shells'.
Journal of Pressure Vessel Technology, Vol 103, pp 246-254, August 1981.

32. Gulati K C et al
'Analytical study of stress concentration effects in multibrace joints under combined loading'.
Paper OTC 4407 of Offshore Technology Conference, Houston 1982.

33. Chen W C and Lawrence F V
'A model for joining the fatigue crack initiation and propagation analyses'.
FCP Report No. 32, College of Engineering, University of Illinois, Urbana, November.

REFERENCES

34. Sanders J L
'Circumferential through-crack in a cylindrical shell under combined bending and tension'.
Trans. ASME, Journal of Applied Mechanics,
Brief Note, Vol. 50, p.221, 1983.

35. Bowie O L
'Analysis of an infinite plate containing radial cracks originating at the boundaries of an internal circular hole'.
Journal of Mathematics and Physics, Vol. 35, p60, 1956.

36. Harrison R P et al
'Assessment of the integrity of structures containing defects'.
Document R/H/R6, Central Electricity Generating Board, 1976.

37. Sumpter J D G and Turner C E
'Design using elastic-plastic fracture mechanics'.
International Journal of Fracture, Vol. 12, No. 6, pp 861-871, December 1976.

38. Irwin G R
'Plastic zone near a crack and fracture toughness'.
Proceedings of the 7th Sagamore Ordinance Material Research Conference, Report No. MeTE 661-611/F, Syracuse University Research Institute, August 1960.

39. Dugdale D S
'Yielding of steel sheets containing slits'.
Journal of the Mechanics and Physics of Solids, Vol. 8, pp 100-104, 1960.

40. Kumar V et al
'An engineering approach for elastic-plastic fracture analysis'.
Report EPRI NP-1931, Electric Power Research Institute, Palo Alto, July 1981.

41. Harrison J D et al
'The COD approach and its application to welded structures'.
ASTM STP 668, American Society for Testing and Materials, pp 660-631, Philadelphia 1979.

42. British Standards Institution
'Guidance on some methods for the derivation of acceptance levels for defects in fusion welded joints'.
PD6493

43. Turner C E
'A J design curve based on estimates for some two dimensional shallow notch configurations'.
OECD/NEA Specialists Meeting on Elastic-Plastic Fracture Mechanics, Daresbury, 1978.

44. Dawes M G
'The CTOD design curve approach: limitations, finite size and application'.
Report 278/1985, the Welding Institute, Abington, June 1985.

REFERENCES

45. Anderson T L et al
'The use of CTOD methods in fitness for purpose analysis'.
GKSS workshop on CTOD Methodology, Geesthacht, West Germany, April 1985.

46. Burdekin F M et al
'Comparison of COD, R6 and J-contour integral methods of defect assessment, modified to give critical flaw sizes'.
Paper 41 of Fitness for Purpose Validation of Welded Constructions, London, November 1981.

47. Rhee H C and Salama M M
'Applications of fracture mechanics method to offshore structural crack instability analysis'.
Paper OTC 5023 of Offshore Technology Conference, Houston, 1985.

48. 'Methods for Crack Opening Displacement (COD) Testing'. BSI BS5762: 1979.

49. Gordon J R
'The Welding Institute Procedure for the Determination of the Fracture Resistance of Fully Ductile Metals'.
Welding Institute Report No. 275/ 1985 June 1985.

50. Pisarski H G
'Basis for the Charpy V requirements for Parent Plate, HAZ and Weld Metal in the Proposed Revisions to the 1977 Edition of the Department of Energy Guidance Notes'.
The Welding Institute Report No. 3866/2.

51. Dolby R E
'Some Correlations between Charpy V and COD test data for ferritic weld metal'.
Metal Construction, 13,1 (1981) 43-51.

52. Roberts R and Newton C
'Interpretive report on small scale test correlations with K_{IC} data'.
Welding Research Council, Bulletin 265, February 1981.

53. Pisarski H G
'A review of correlations relating Charpy energy to K_{IC}.
The Welding Institute Research Bulletin, December 1978.

54. Rolfe S T and Novak S T
'Slow bend K_{IC} testing of medium strength high toughness steels 'ASTM STP 463 1970 p.124 - 159.

55. Sailors R H and Corten H T
'Relationship between material fracture toughness using fracture mechanics and transition temperature tests' ASTM STP 514 1973 164-191.

REFERENCES

56. Ingham T and Harrison R P
'A comparison of published methods of calculation of defect significance'.
Paper 46: Fitness for Purpose Validation of Welded Constructions London, November 1981.

57. Hayes B
'Test Data on BS4560 50D Steel' Welding Institute.
Private Communication.

58. 'BS4560 50D, Weldable Structures Steel Plate'.
NKK Technical Bulletin.

59. Wong W K and Rogerson J H
'A probabilistic estimate of the relative value of factors which control the failure by fracture of offshore structures'.
Paper 9 Second International Conference on Offshore Welded Structures, London 1982.

EXAMPLE	A	B
D (mm)	356	406
t (mm)	12.7	12.7
L (mm)	13904	12450
f_y (N/mm^2)	355	235
d (mm)	40.3	78
x (mm)	9635	7644
u (mm)	127	110
U (N.mm)	6.6×10^7	5.6×10^7

d = dent depth

x = location of dent from member end

u = displacement at dent location

U = estimate of energy involved in the collision

TABLE 6.1 - DAMAGED MEMBER PROPERTIES

CONDITION	A_1	C	n_1	m	KIC	R	$(\frac{da}{dN})_p$
Air, Low R	0.53×10^{-29}	0.4×10^{-11}	32.0	3.15	250	0.2	(0.0)
Air, High R	1.0×10^{-14}	1.1×10^{-11}	13.3	3.15	250	0.5	(0.0)
Seawater, Free Corrosion Potential, Low R	0.53×10^{-20}	0.303×10^{-11}	17.5	3.65	250	0.2	(0.0)
Seawater, Free Corrosion Potential, High R	1.1×10^{-14}	0.59×10^{-11}	13.3	3.65	250	0.5	(0.0)
Seawater, Cathodic Polarisation, Low R	0.125×10^{-34}	0.34×10^{-13}	32.0	5.93	250	0.2	1.0×10^{-6}
Seawater, Cathodic Polarisation, High R	Insufficient experimental data to determine constants						

Units are MN and m

$$\frac{1}{da/dN} = \frac{1}{A_1 \Delta K^{n_1}} + \frac{1}{C \Delta K^m} - \frac{1}{C[(1-R)K_{IC}]^m} + \frac{1}{(da/dN)_p}$$

TABLE 6.2 - CONSTANTS IN SwRI CRACK GROWTH LAW

ANALYSIS REFERENCE	CHORD SIZE (mm)	λ	ENVIRONMENT
1	914 x 32	0.15	Air
2	457 x 16	0.15	Air
3	457 x 16	1.0	Air
4	457 x 16	0.15	Seawater, freely corroding
5	457 x 16	0.15	Seawater, cathodic polarisation

Note: This table to be read in conjunction with Section 6.3.5

TABLE 6.3 - SCHEDULE OF BENCHMARK ANALYSES

THICKNESS (mm)	MEMBRANE TENSION (= 1.0)	BENDING (= 0.0)
16	3.65	2.44
25.4	4.33	2.81
32	4.74	3.03
38.1	5.08	3.22
50.8	5.71	3.56
63.5	6.27	3.86
82.55	7.01	4.26
101.6	7.67	4.62
107.95	7.67	4.73

Note: Weld toe stress field is of the form[24]

$$f_n = f_o (K_t - 1) \exp [-35 (K_t - 1) a/T]$$

TABLE 6.4 - VALUES OF K_t FOR WELD TOE STRESS CONCENTRATIONS FOR GRADE 50D STEEL

THICKNESS (mm)	MEMBRANE TENSION (= 1.0)	BENDING (= 0.0)
16	0.12	0.22
25.4	0.15	0.28
32	0.17	0.31
38.1	0.18	0.34
50.8	0.21	0.39
63.5	0.24	0.44
82.55	0.27	0.50
101.60	0.30	0.56
107.95	0.31	0.57

TABLE 6.5 - INITIAL CRACK DEPTHS FOR FATIGUE CRACK STUDIES FOR GRADE 50D STEEL (units : mm) (after Chen & Lawrence[32])

BS 4360 50D (Reference 57)

Material Property	Temperature °C
CTOD toughness, δ_c, mm 0.099, 0.049, 0.147 0.127, 0.057, 0.221	-78
Charpy Impact, CV, J 71, 21	-50
Yield Strength, f_y, N/mm^2 410	-70

Correlation 21J at - 50°C

$$\frac{(K_{IC})^2}{E} = 0.22\ (CV)^{1.5}$$
$$= 0.22\ (21)^{1.5}$$
$$= 21.17$$

$$\delta_c = \left(\frac{K_{IC}}{E}\right)^2 \left(\frac{1-\nu^2}{m, f_y}\right) \qquad \text{where } m = 1.75$$

$$= \frac{21.17,\ 0.91}{1.75,\ 410} = 0.027\text{mm}$$

Minimum measured CTOD = 0.049mm

Safety factor = 1.81

TABLE 6.6 - CHARPY V NOTCH TO CTOD TOUGHNESS CORRELATION FOR BS4360 50D STEEL

NKK (Reference 58)

Submerged Arc welding

Heat Input = 3.5 kJ/mm
HAZ CV at - 40°C = 41J
CTOD at - 40°C = 0.130mm
F_y at - 40°C = 425 N/mm^{2*}

CV correlation gives CTOD at - 40°C = 0.071
= 1.84 safety factor

*Estimated from data; F_y = 399 N/mm^2 at 0°C
= 428 N/mm^2 at -60°C

Wong and Rogerson (Reference 59)

MMA on BS 4360 50D

CV Upper Shelf = 76.3J F_y = 400 N/mm^2
CTOD Upper Shelf = 0.37mm F_y = 550 N/mm^2

Using equation (6.25) lower transition region
76.3J correlates to CTOD of 0.19mm
Safety factor = 1.95

Using equation (6.23), appropriate to upper shelf

76.3J correlates to CTOD of 0.18mn
Safety factor = 2.06

TABLE 6.7 - CHARPY V NOTCH TO CTOD TOUGHNESS CORRELATIONS FOR HAZ AND WELD METAL

	Low (δ_c/F_y) steel		High (δ_c/F_y) steel	
	Bending	Tension	Bending	Tension
Modified elastic solution	Y	Y	N(1)	N
WI level 2 model	Y	Y	Y(2)	Y
Full elastic-plastic solution	Y	Y	Y	Y

Notes: 1. May give acceptable answers if adequate restraint provided by continuity with the remainder of the structure.

2. Excessively conservative if restraint provided by continuity with the remainder of the structure.

TABLE 6.9 - APPLICABILITY OF THE ASSESSMENT METHODS TO VARIOUS PROBLEM TYPES

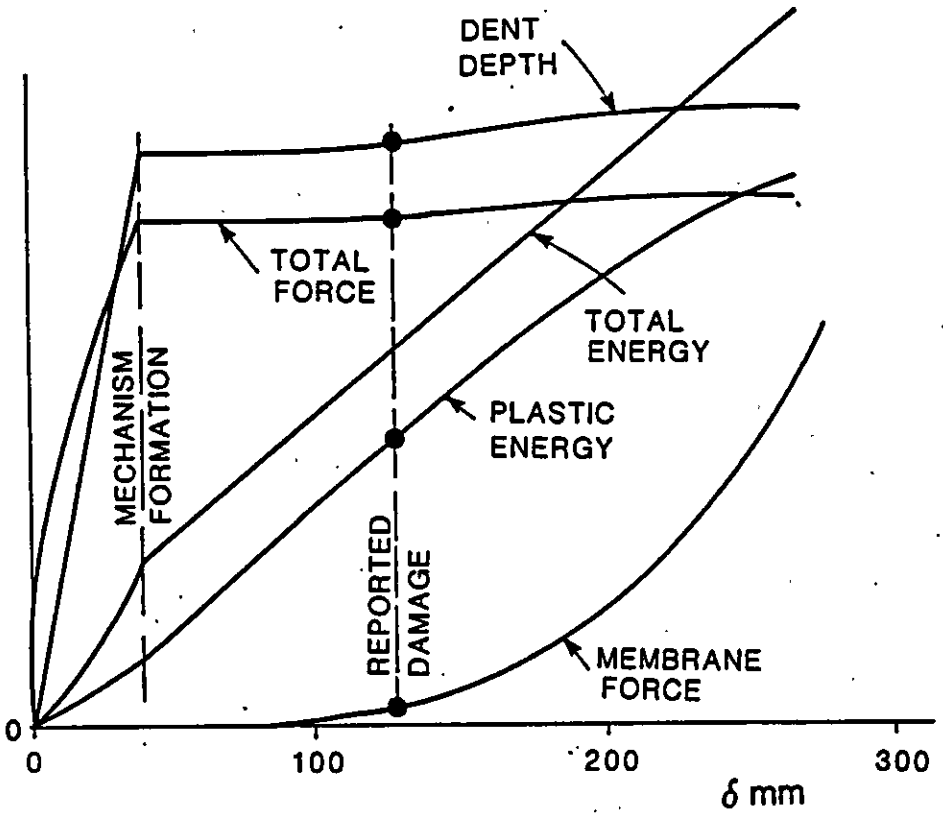

DAMAGE HISTORY: EXAMPLE A (ref. 1)

PROJECT URP 72 : STUDY 4 INSPECTION PLANNING , THE ROLE OF DAMAGE ASSESSMENT	REPORT No. WOLI09/86 FIG. 6·11

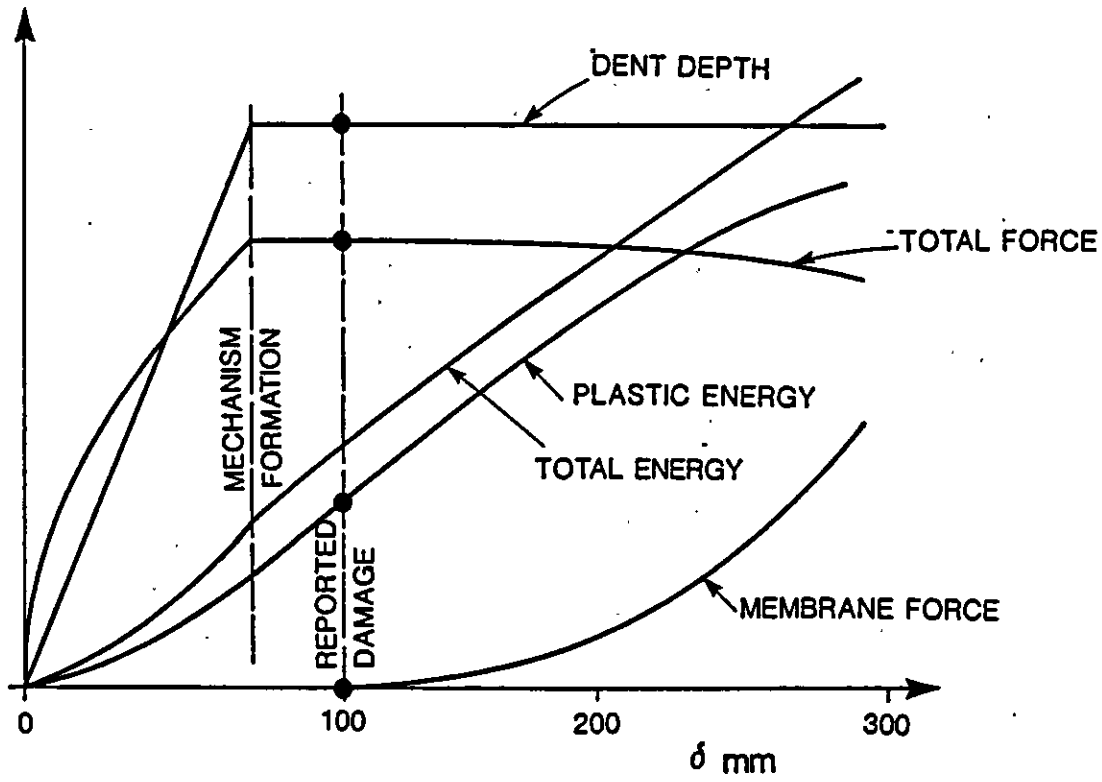

DAMAGE HISTORY: EXAMPLE B (ref. 1)

PROJECT URP 72 : STUDY 4 INSPECTION PLANNING , THE ROLE OF DAMAGE ASSESSMENT	REPORT No. WOLI09/86 FIG. 6·2

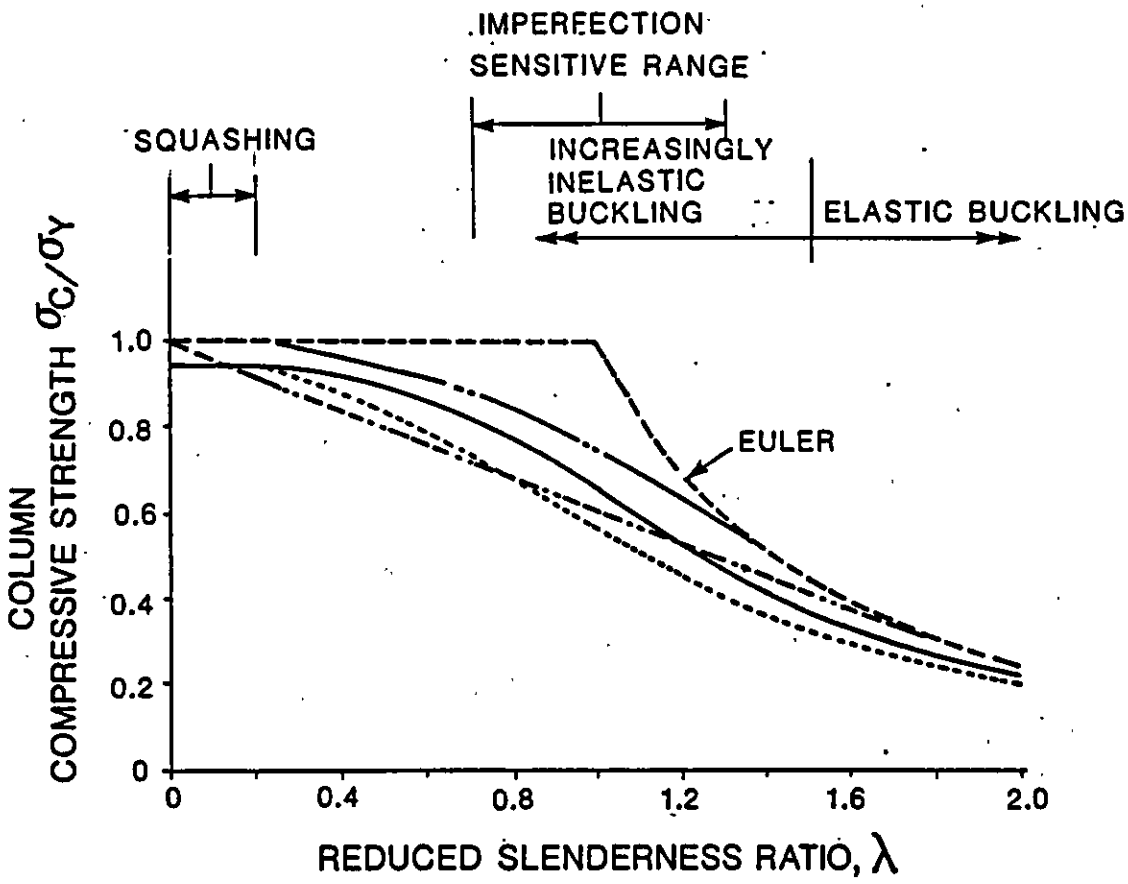

NOTES:-

KEY: DESIGN CODES

- ECCS/DnV-OS STRENGTH CURVE 'a'
- ECCS/DnV-OS STRENGTH CURVE 'b'
- API/BS6235/AISC/SSRC
- WOLFORD AND REBHOLZ-LINEAR
- EULER-PERFECT COLUMN

COLUMN BUCKLING CHARACTERISTIC (Ref.10)

PROJECT URP 72 : STUDY 4 INSPECTION PLANNING , THE ROLE OF DAMAGE ASSESSMENT	REPORT No. WOLI09/86 FIG. 6·3

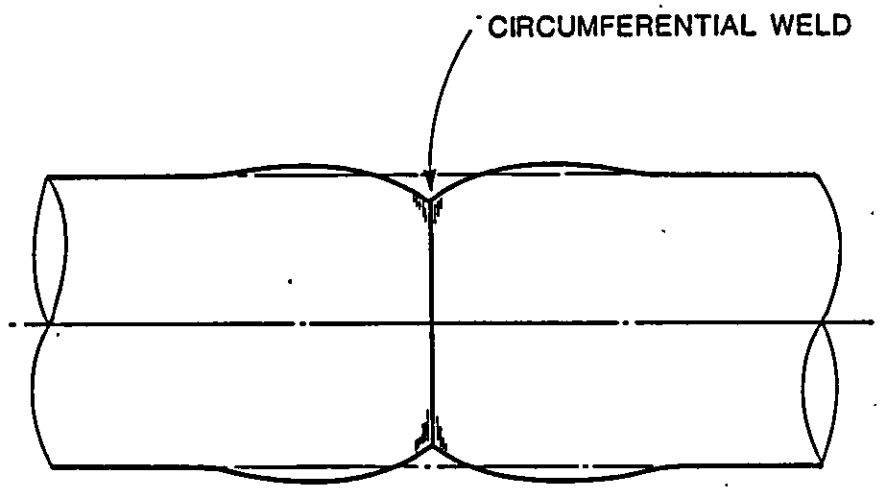

BULGE-TYPE IMPERFECTIONS INTRODUCED BY CIRCUMFERENTIAL WELDS. (ref. 10)

TYPICAL AXISYMMETRIC 'BULGE-LIKE' BUCKLING OF TUBES D/t·200 (ref. 10)

PROJECT URP 72 : STUDY 4 INSPECTION PLANNING , THE ROLE OF DAMAGE ASSESSMENT	REPORT No. WOLI09/86 FIG. 6·4

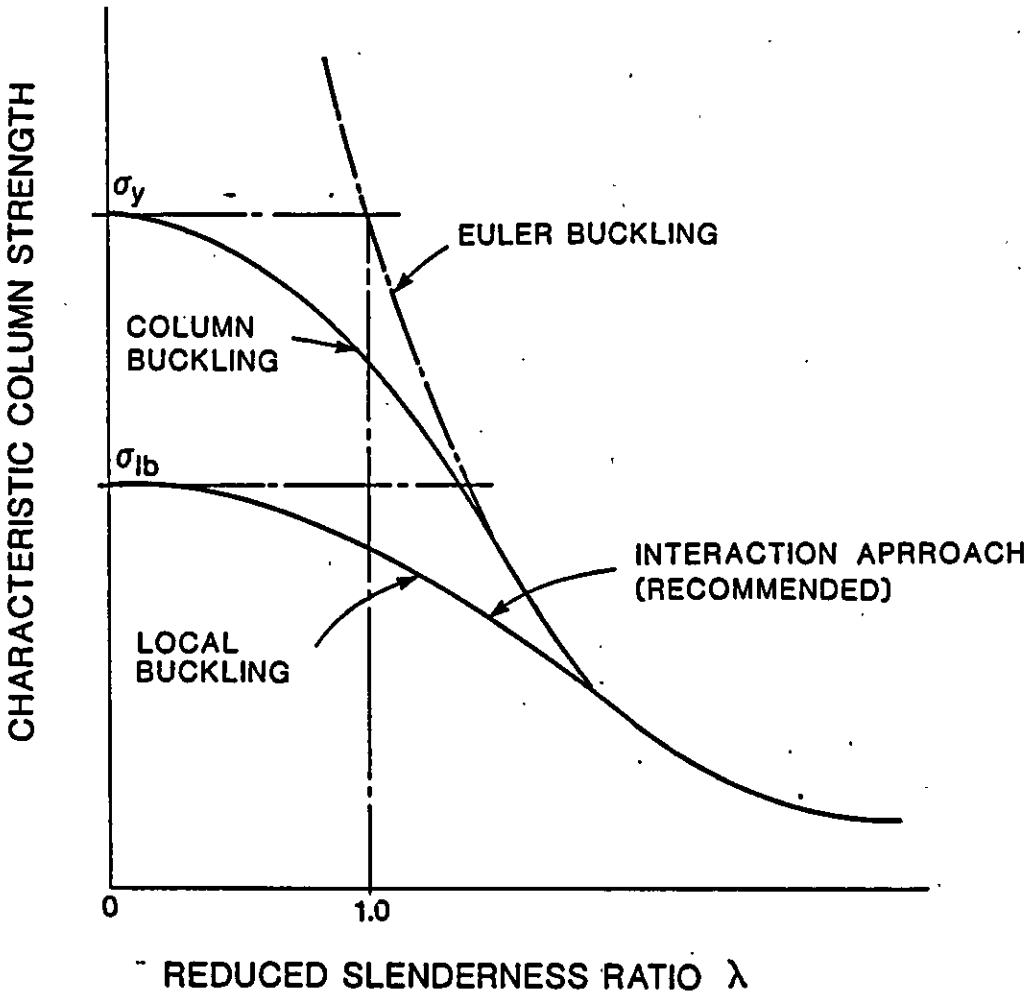

ILLUSTRATION OF INTERRACTION BETWEEN COLUMN AND LOCAL BUCKLING. (ref. 10)

PROJECT URP 72 : STUDY 4 INSPECTION PLANNING , THE ROLE OF DAMAGE ASSESSMENT	REPORT No. WOLI09/86 FIG. 6·5

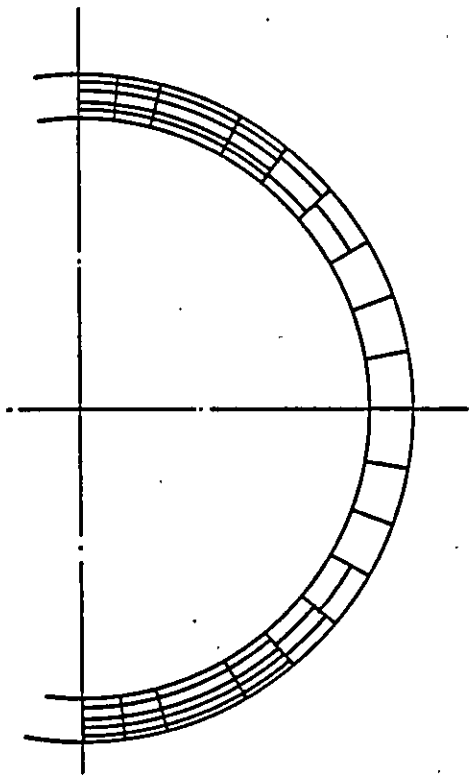

SUBDIVISION OF CROSS-SECTION INTO "FIBRES" (Ref.4)

PROJECT URP 72 : STUDY 4 INSPECTION PLANNING , THE ROLE OF DAMAGE ASSESSMENT	REPORT No. WOL109/86 FIG. 6·6

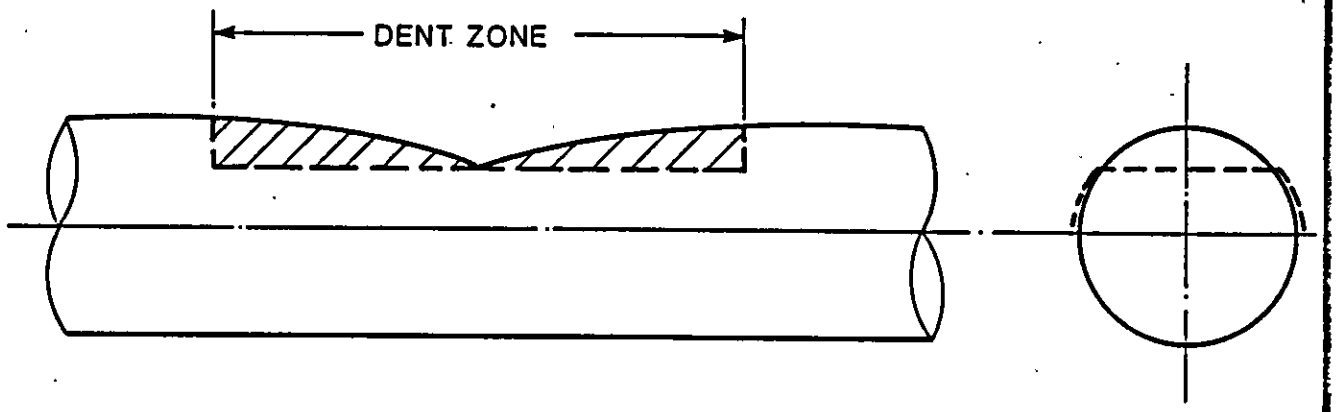

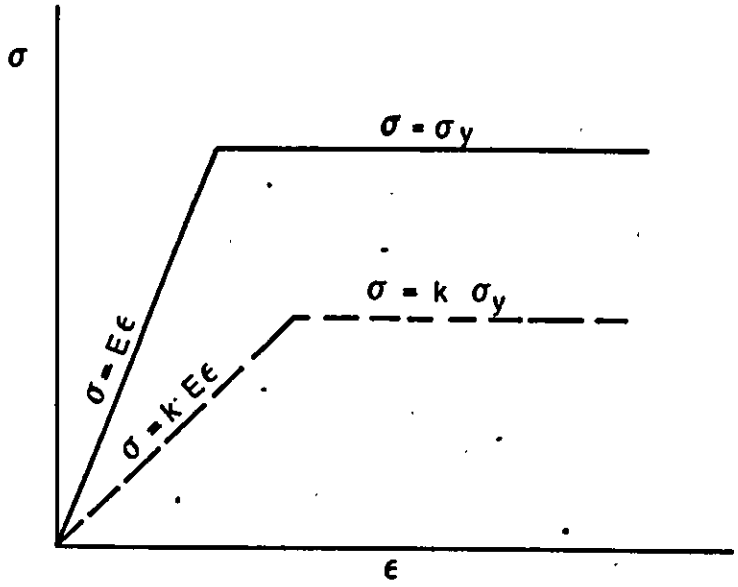

NUMERICAL CHARACTERIZATION OF DENTS (Ref.7)

PROJECT URP 72 : STUDY 4 INSPECTION PLANNING , THE ROLE OF DAMAGE ASSESSMENT	REPORT No. WOL109/86 FIG. 6·7

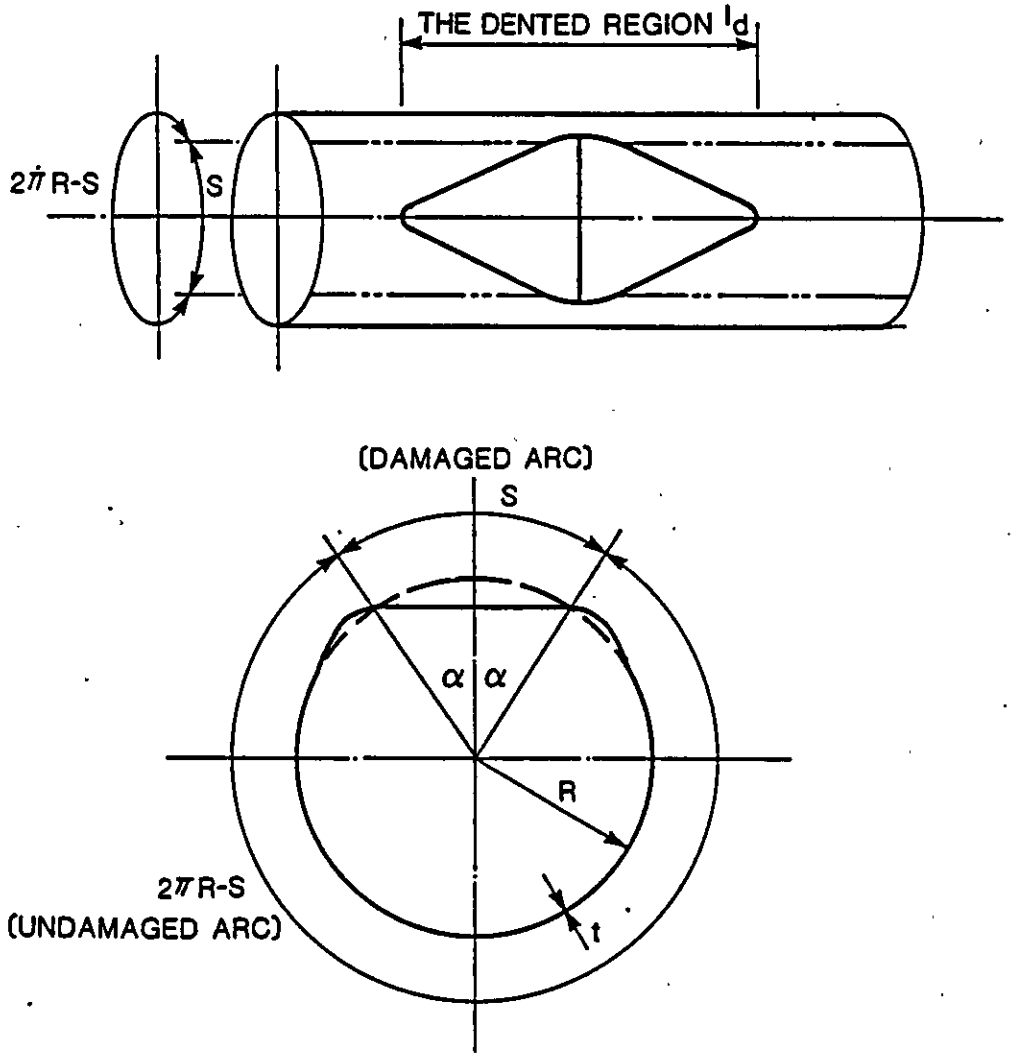

IDEALIZATION OF SHARP DENT. (Ref.9)

PROJECT URP 72 : STUDY 4 INSPECTION PLANNING , THE ROLE OF DAMAGE ASSESSMENT	REPORT No. WOL109/86	
		FIG. 6·8

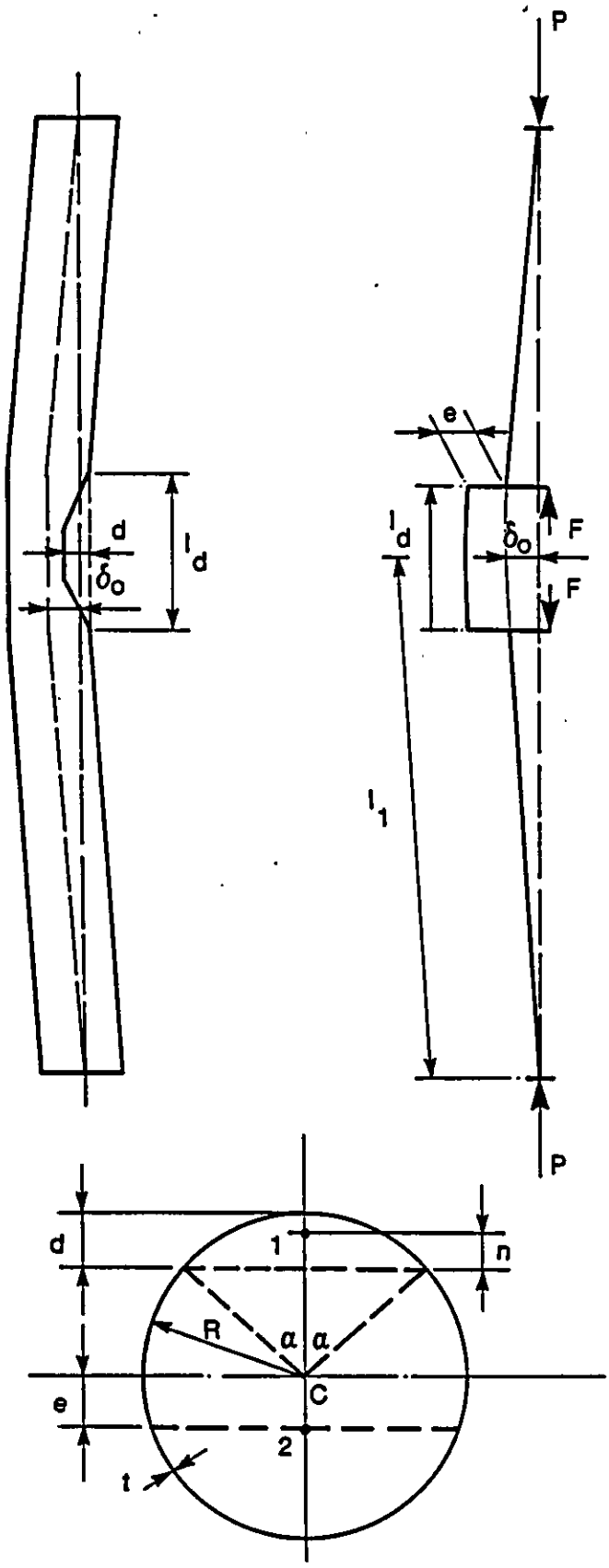

THEORETICAL MODEL (Ref.9)

F ACTS THROUGH POINT 1 , P-F ACTS THROUGH POINT 2

PROJECT URP 72 : STUDY 4 INSPECTION PLANNING , THE ROLE OF DAMAGE ASSESSMENT	REPORT No. WOL109/86 FIG. 6·9

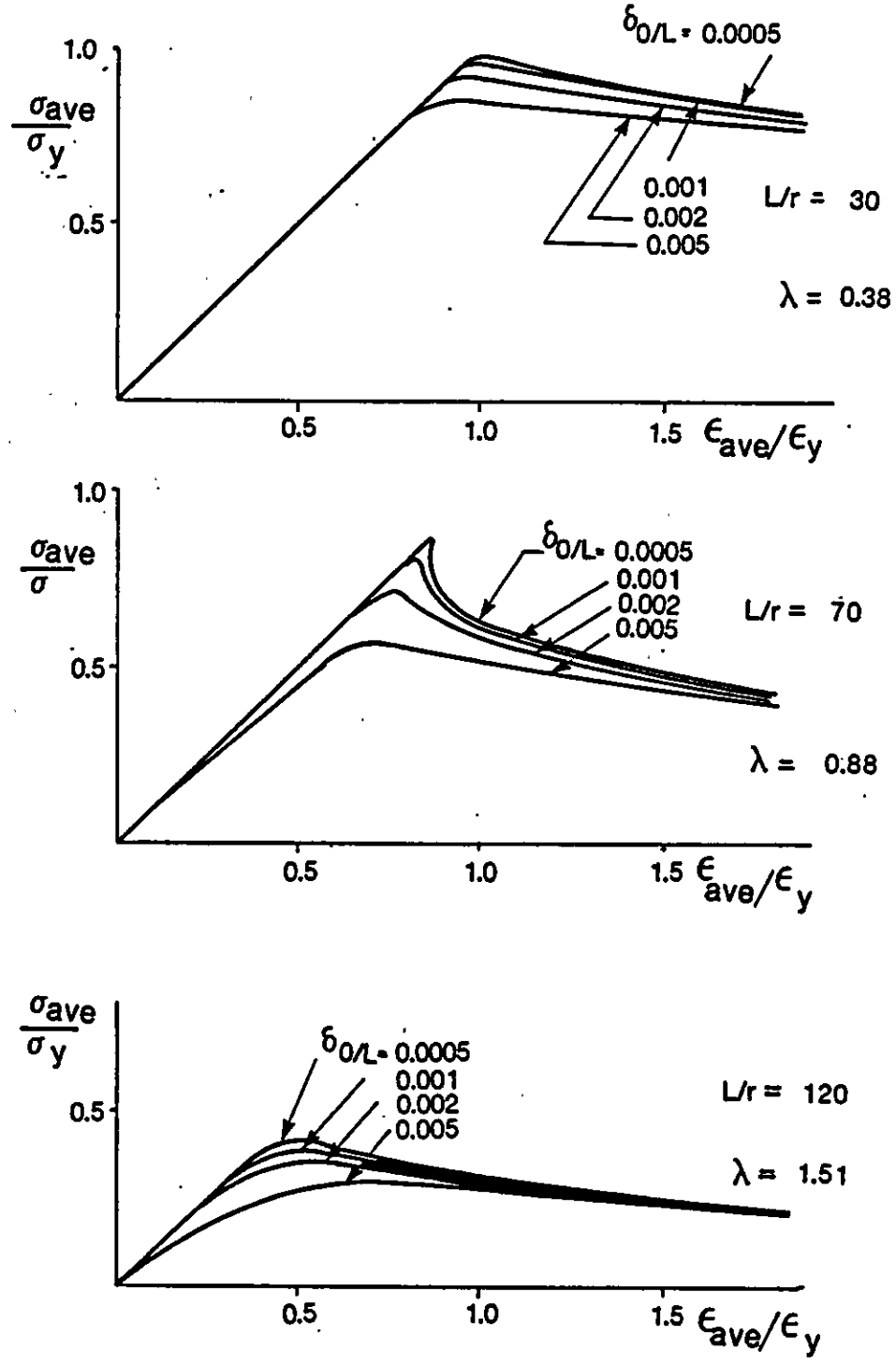

(a) SIMPLY-SUPPORTED TUBES (Ref.4)

PROJECT URP 72 : STUDY 4 INSPECTION PLANNING , THE ROLE OF DAMAGE ASSESSMENT	REPORT No. WOL109/86 FIG. 6·10

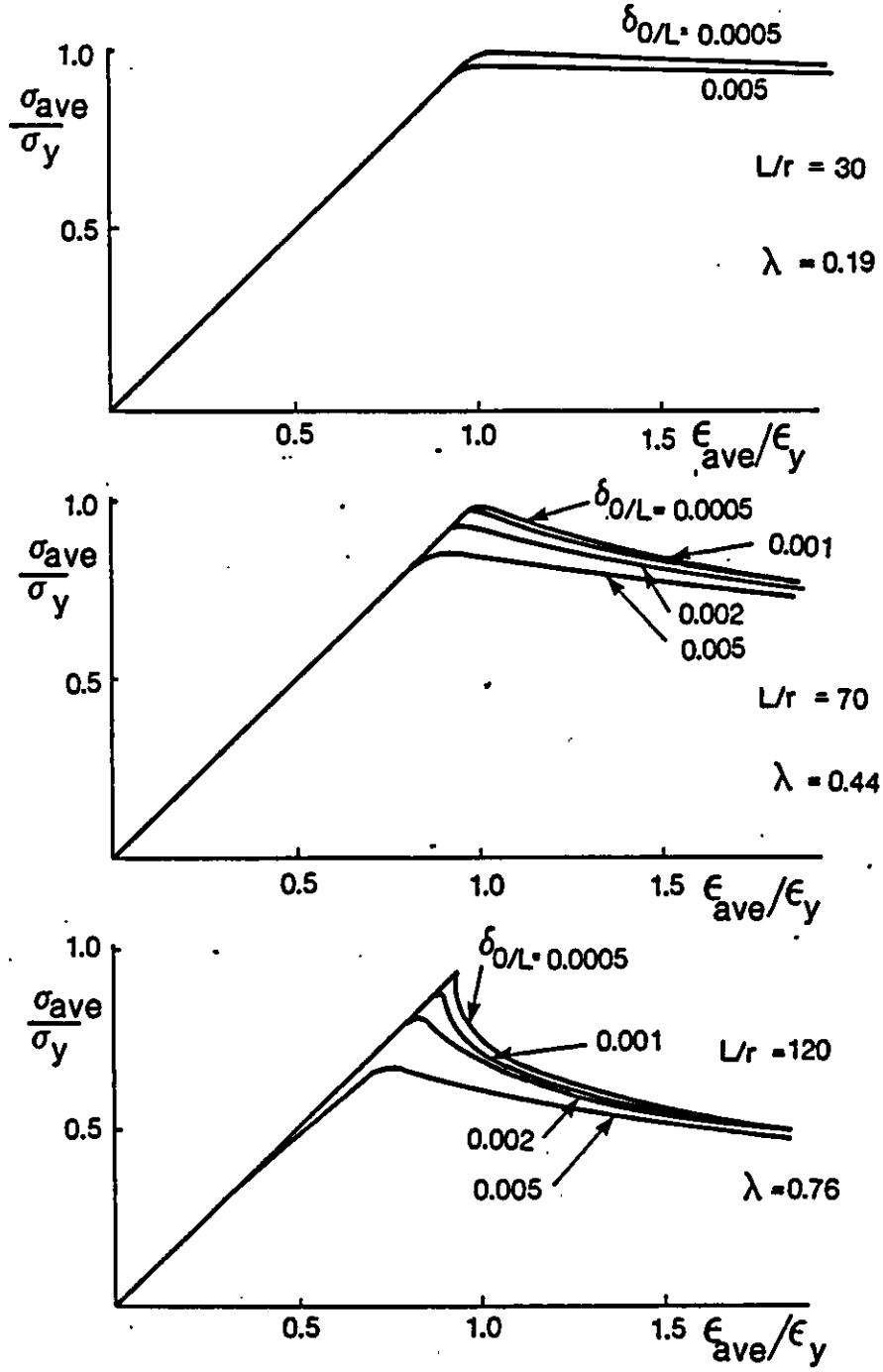

(b) CLAMPED TUBES (Ref.4)

PROJECT URP 72 : STUDY 4 INSPECTION PLANNING , THE ROLE OF DAMAGE ASSESSMENT	REPORT No. WOL109/86 FIG. 6·11

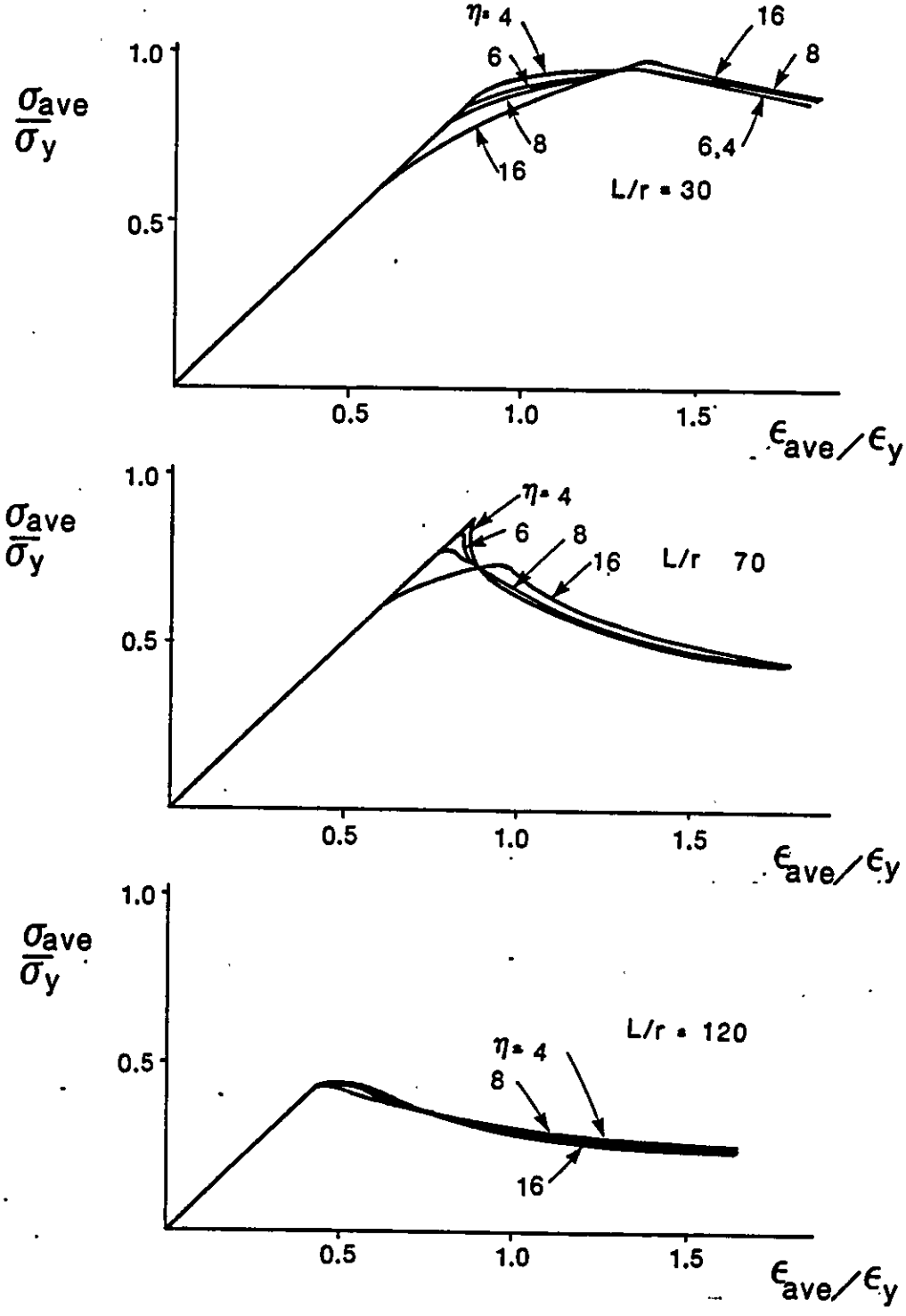

EFFECT OF WELD-INDUCED RESIDUAL STRESS ON LOAD-SHORTENING CURVES FOR SIMPLY-SUPPORTED TUBES (Ref.4)

PROJECT URP 72 : STUDY 4 INSPECTION PLANNING , THE ROLE OF DAMAGE ASSESSMENT	REPORT No. WOL109/86 FIG. 6·12

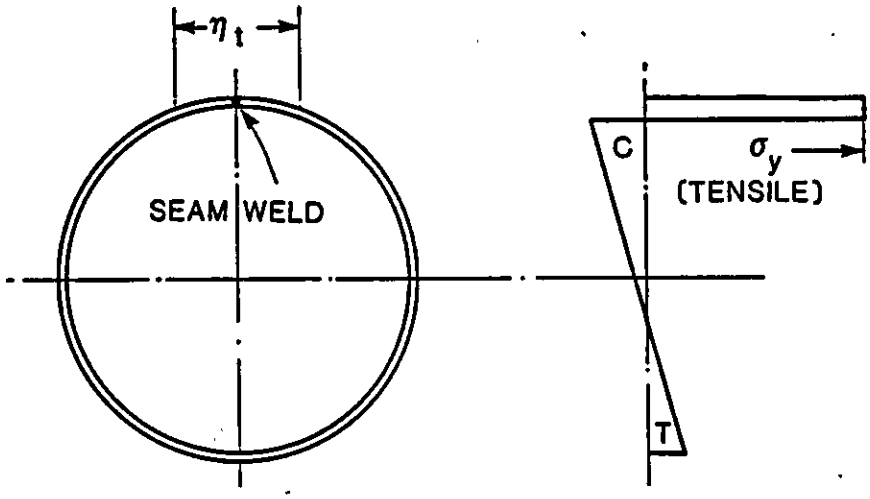

(a) WELD-INDUCED RESIDUAL STRESS

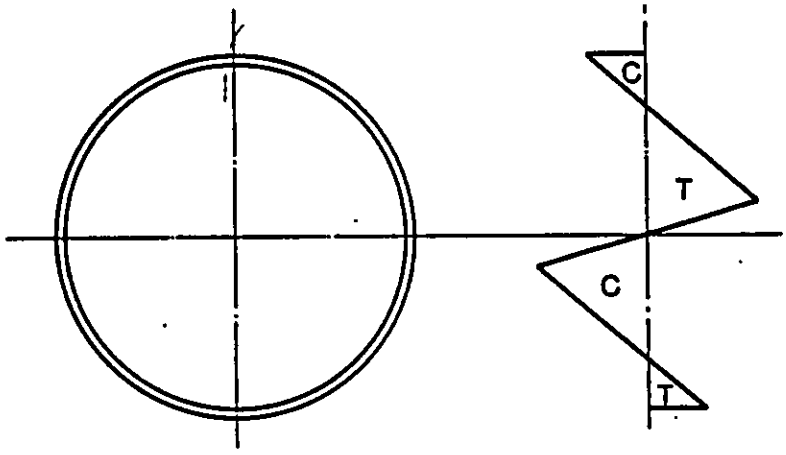

(b) RESIDUAL STRESS CAUSED BY ELASTO-PLASTIC BENDING OF TUBE.

RESIDUAL STRESS DISTRIBUTIONS (Ref.4)

PROJECT URP 72 : STUDY 4
INSPECTION PLANNING ,
THE ROLE OF DAMAGE ASSESSMENT

REPORT No. WOL109/86

FIG. 6·13

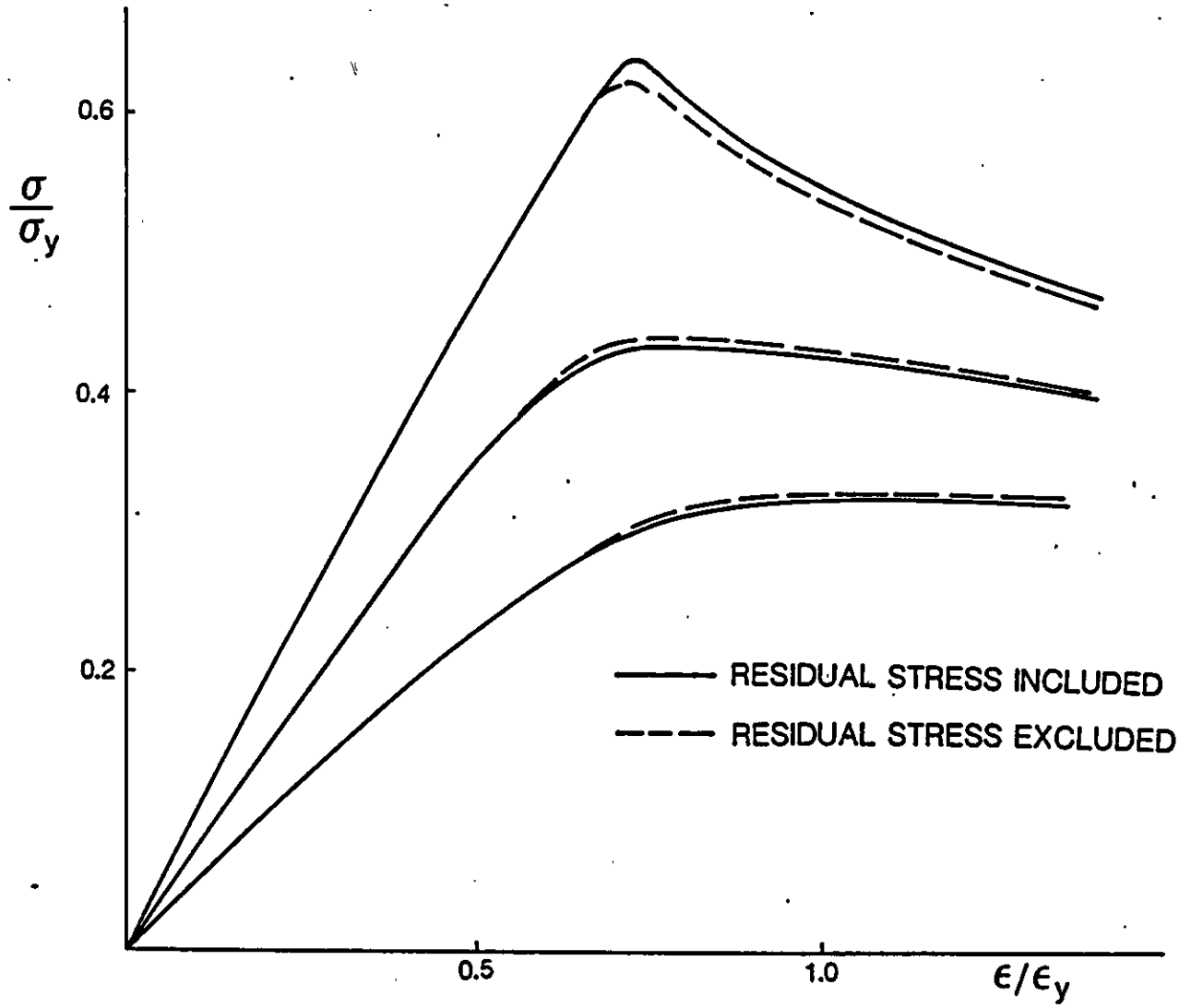

CONTRIBUTION OF RESIDUAL STRESS TO DAMAGE EFFECT (SIMPLY SUPPORTED TUBES, L/r-7C)(Ref.5)

PROJECT URP 72 : STUDY 4 INSPECTION PLANNING , THE ROLE OF DAMAGE ASSESSMENT	REPORT No. WOLI09/86 FIG. 6·14

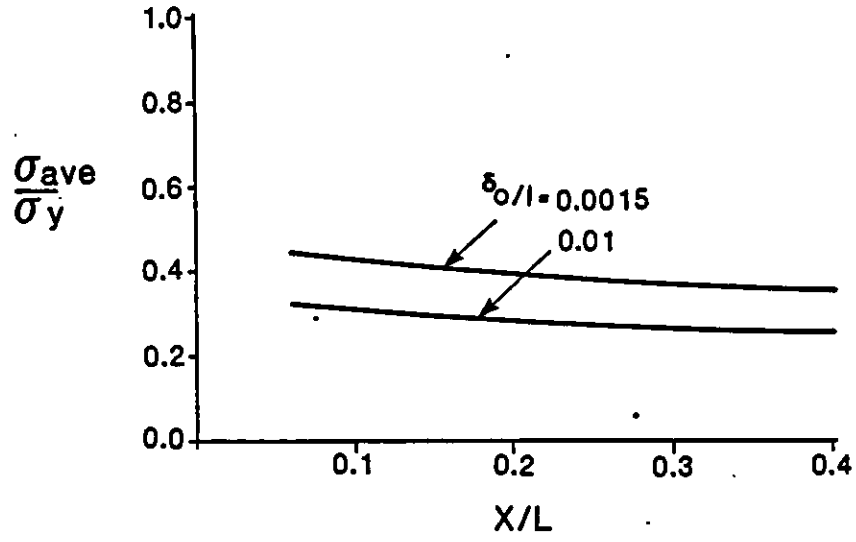

ULTIMATE LOAD VERSUS LENGTH OF DENT. λ = 0.7, D = 100mm, t = 2.0mm, σ_y = 360 N/mm^2, E = 210 000N/mm^2, d/D = 0.15, DENT AT MIDSPAN. (Ref.9)

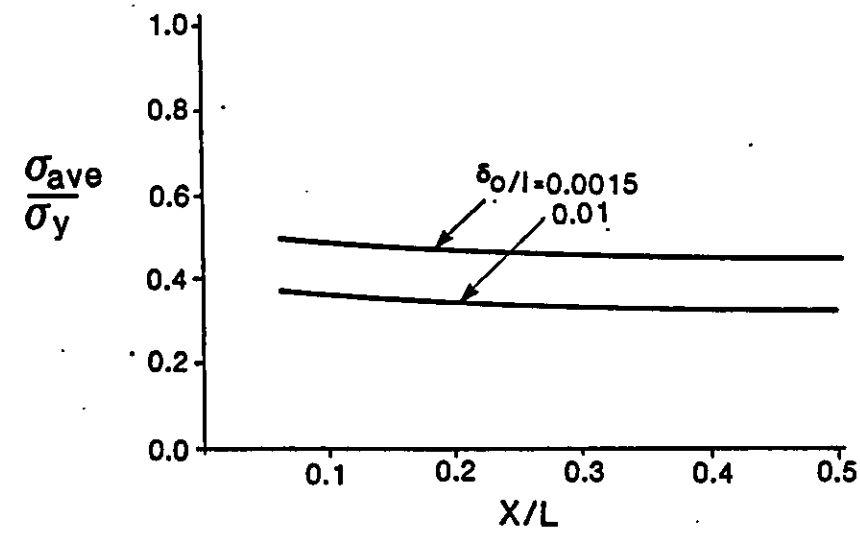

ULTIMATE LOAD VERSUS LOCATION OF DENT. λ = 0.7, D = 100mm, t = 2.0mm, σ_y = 360 N/mm^2, E = 210 000N/mm^2, d/D = 0.15, SHARP DENT. (Ref.9)

PROJECT URP 72 : STUDY 4 INSPECTION PLANNING , THE ROLE OF DAMAGE ASSESSMENT	REPORT No. WOL109/86 FIG. 6·15

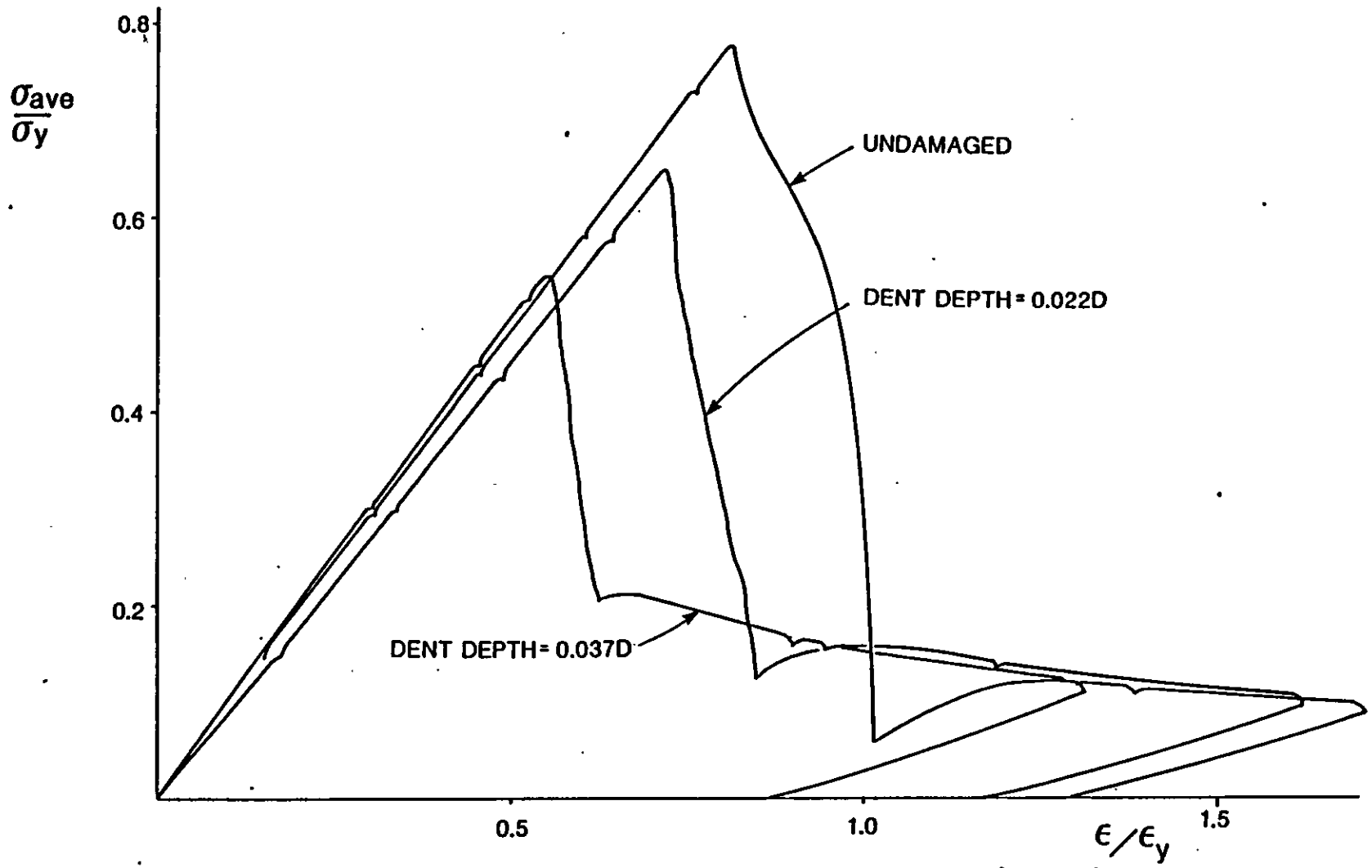

COLLAPSE OF THIN-WALLED TUBULAR COLUMNS (Ref.5)

PROJECT UPR 72 : STUDY 4

INSPECTION PLANNING ; THE ROLE OF DAMAGE ASSESSMENT

REPORT No. WOL109/86

FIG. 6·16

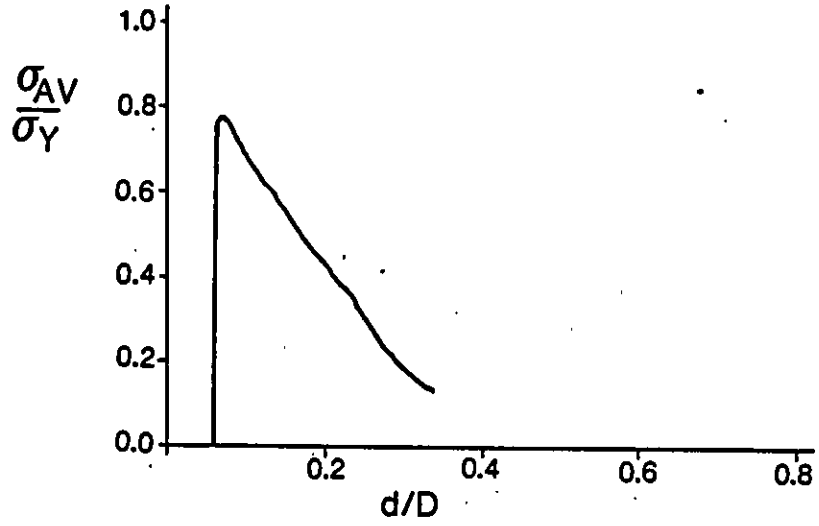

GROWTH OF DENT DEPTH AS A FUNCTION OF AXIAL LOAD DETERMINED EXPERIMENTALLY (Ref.9)

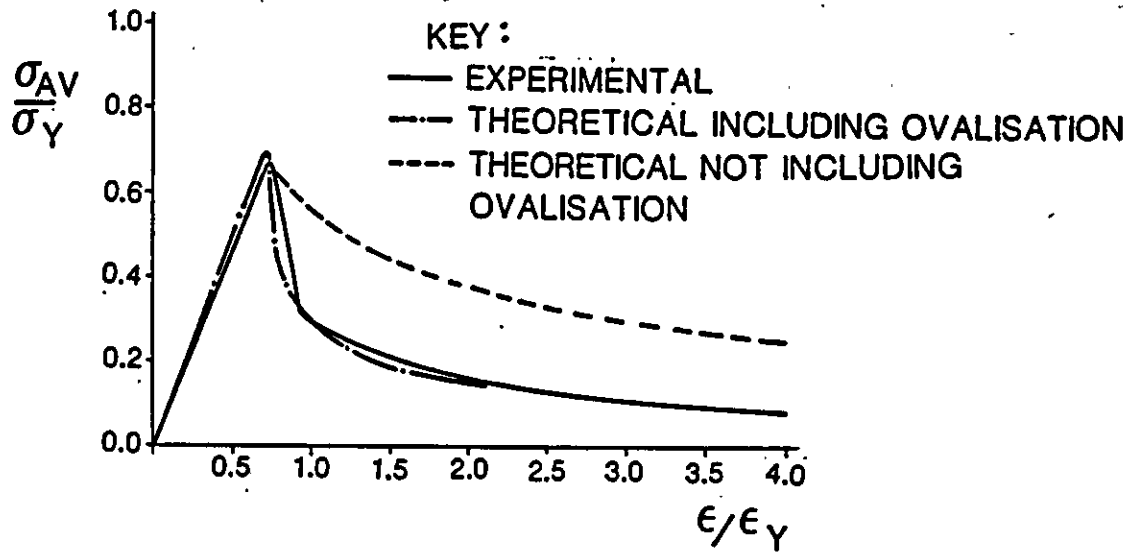

AXIAL LOAD VERSUS AXIAL SHORTENING (Ref.9)

PROJECT URP 72 : STUDY 4 INSPECTION PLANNING , THE ROLE OF DAMAGE ASSESSMENT	REPORT No. WOL109/86 FIG. 6·17

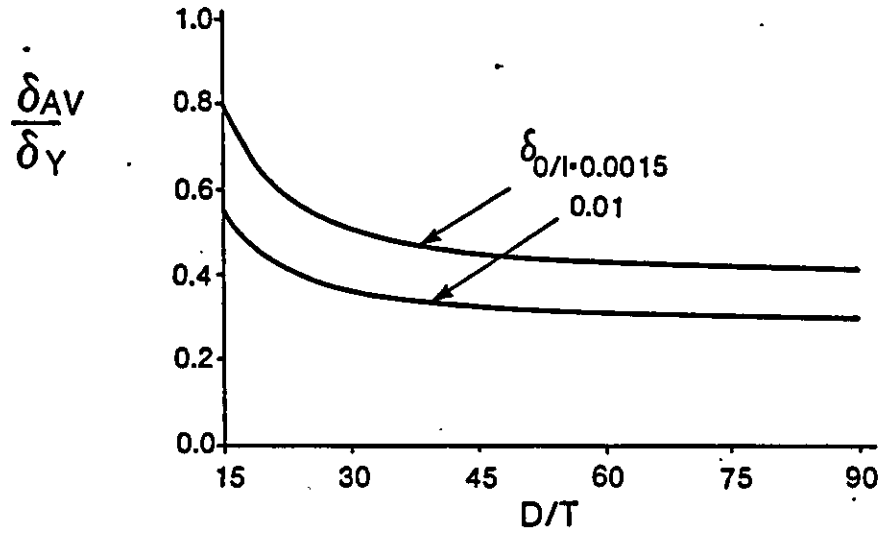

ULTIMATE LOAD AS FUNCTION OF D/t RATIO; λ = 0.7, D = 100mm, σ_y = 360N/mm^2, E = 210 000 N/mm^2, d/D = 0.15, DENT AT MIDSPAN

(Ref.9)

PROJECT URP 72 : STUDY 4 INSPECTION PLANNING , THE ROLE OF DAMAGE ASSESSMENT	REPORT No. WOL109/86 FIG. 6-18

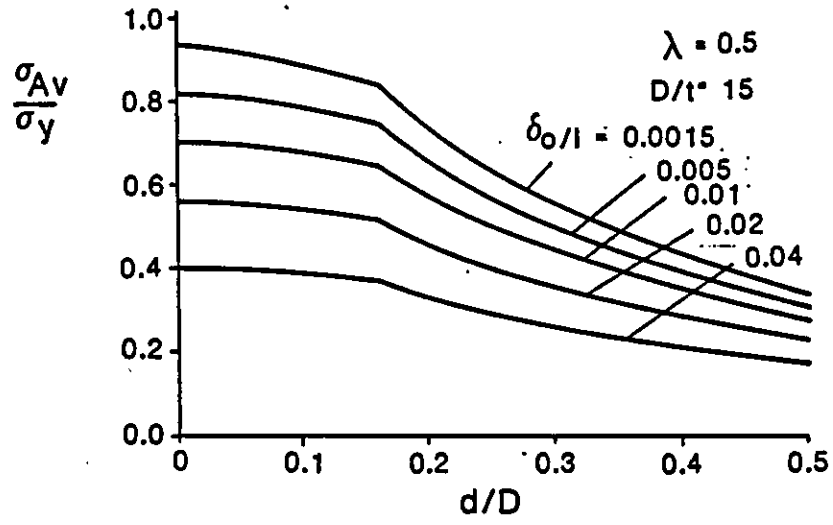

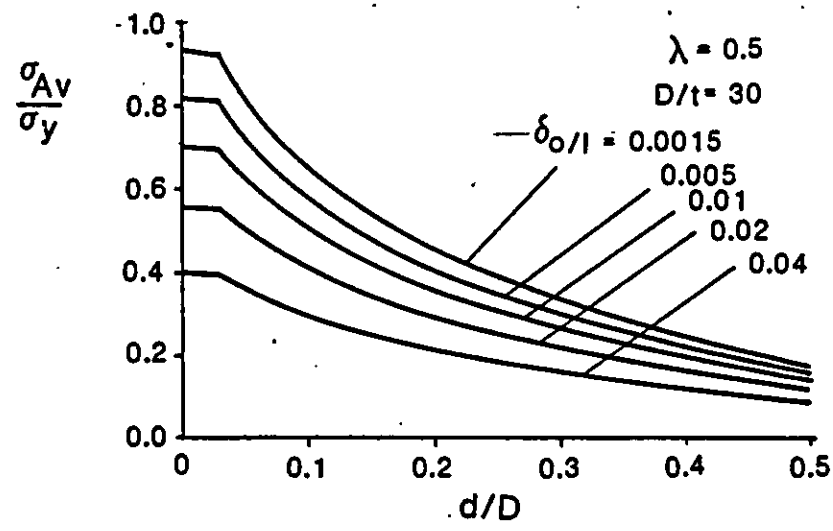

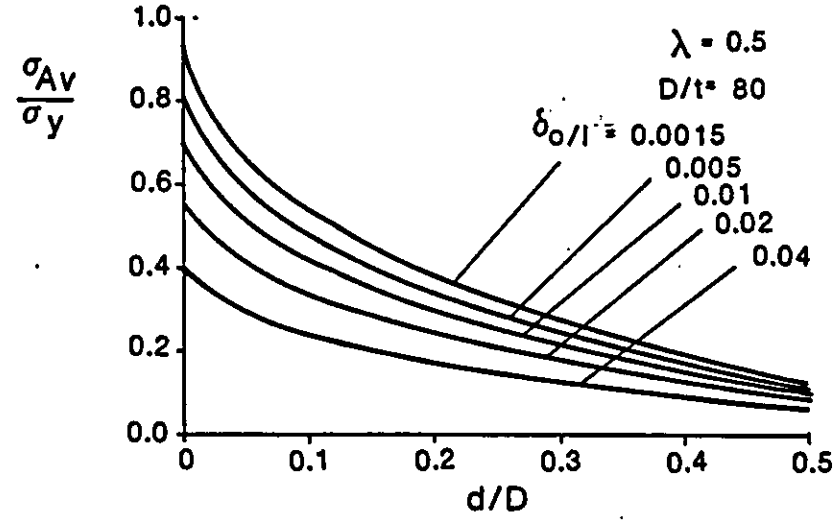

ULTIMATE LOAD/DEPTH OF DENT (Ref.9)

PROJECT URP 72 : STUDY 4 INSPECTION PLANNING , THE ROLE OF DAMAGE ASSESSMENT	REPORT No. WOL109/86 FIG. 6·19

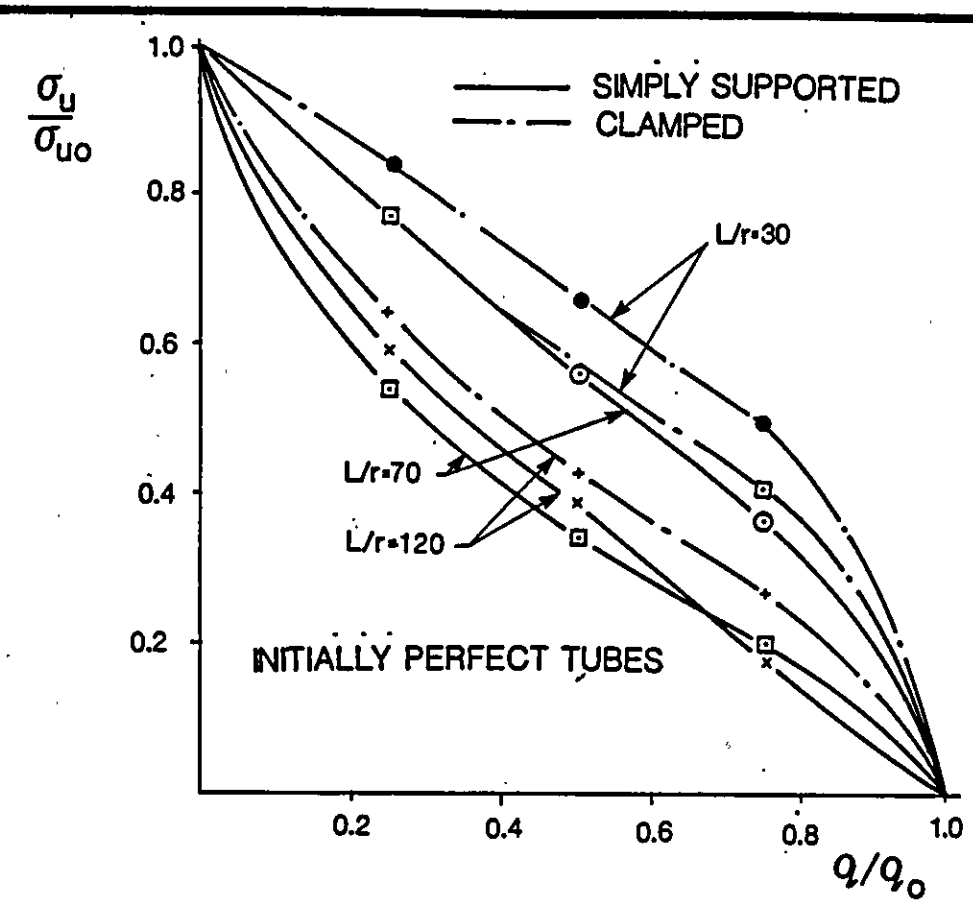

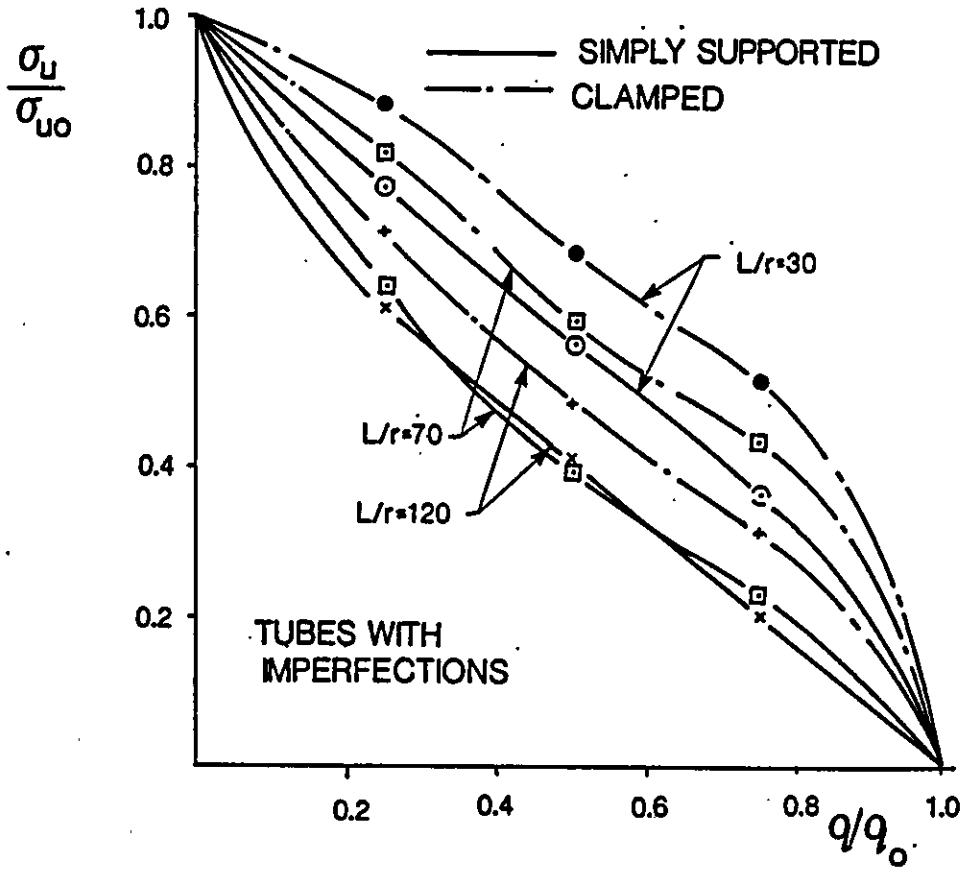

EFFECT OF UNIFORM LATERAL LOAD-INTERACTION CURVES (Ref.5)

PROJECT URP 72 : STUDY 4 INSPECTION PLANNING , THE ROLE OF DAMAGE ASSESSMENT	REPORT No. WOLI09/86 FIG. 6·20

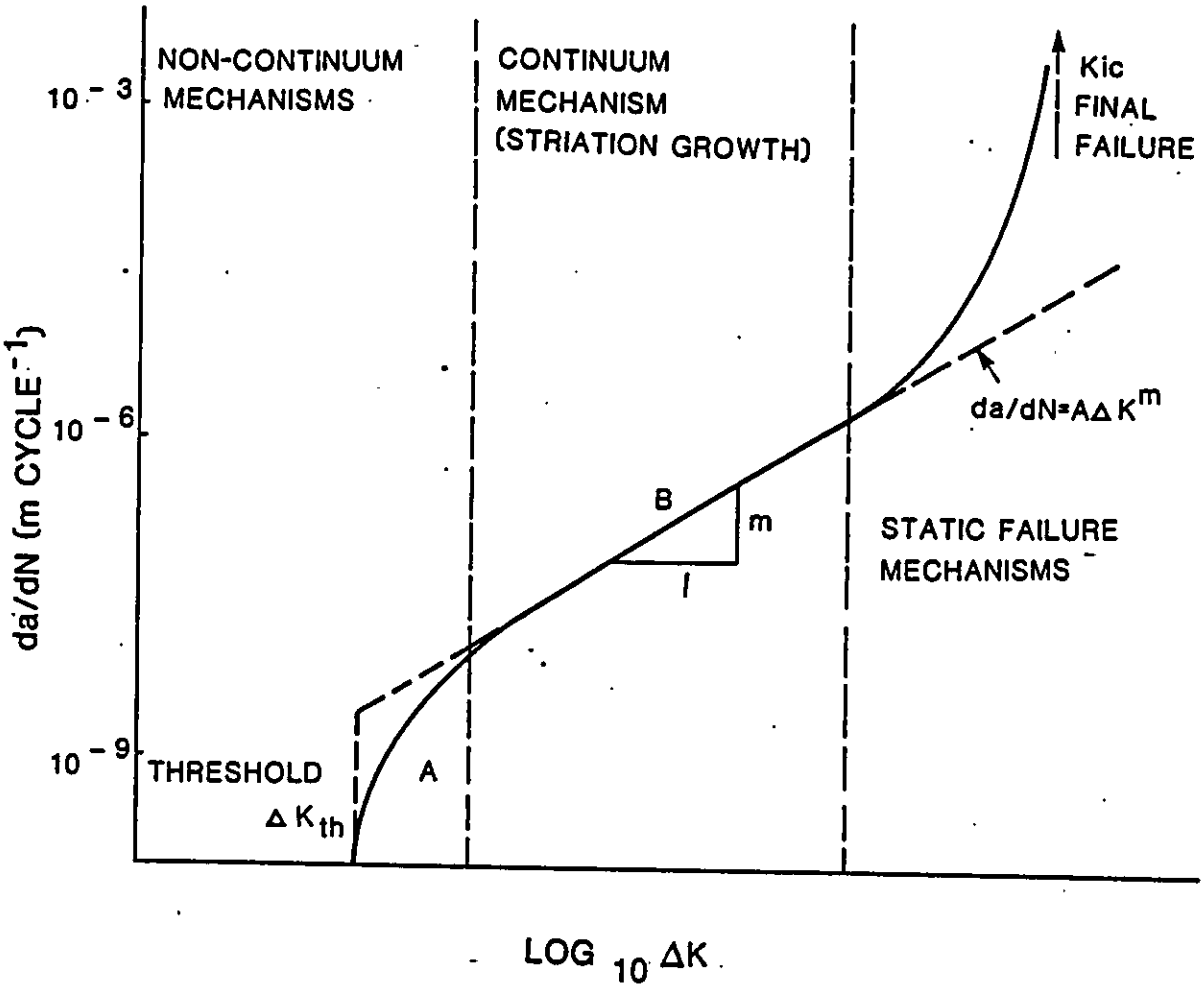

SCHEMATIC da/dN VERSUSΔK PLOT

PROJECT URP 72 : STUDY 4 INSPECTION PLANNING , THE ROLE OF DAMAGE ASSESSMENT	REPORT No. WOL109/86 FIG. 6.21

AARQUE 7865/84

NOTE : DATA VALID FOR LOW R-RATIO CRACK GROWTH

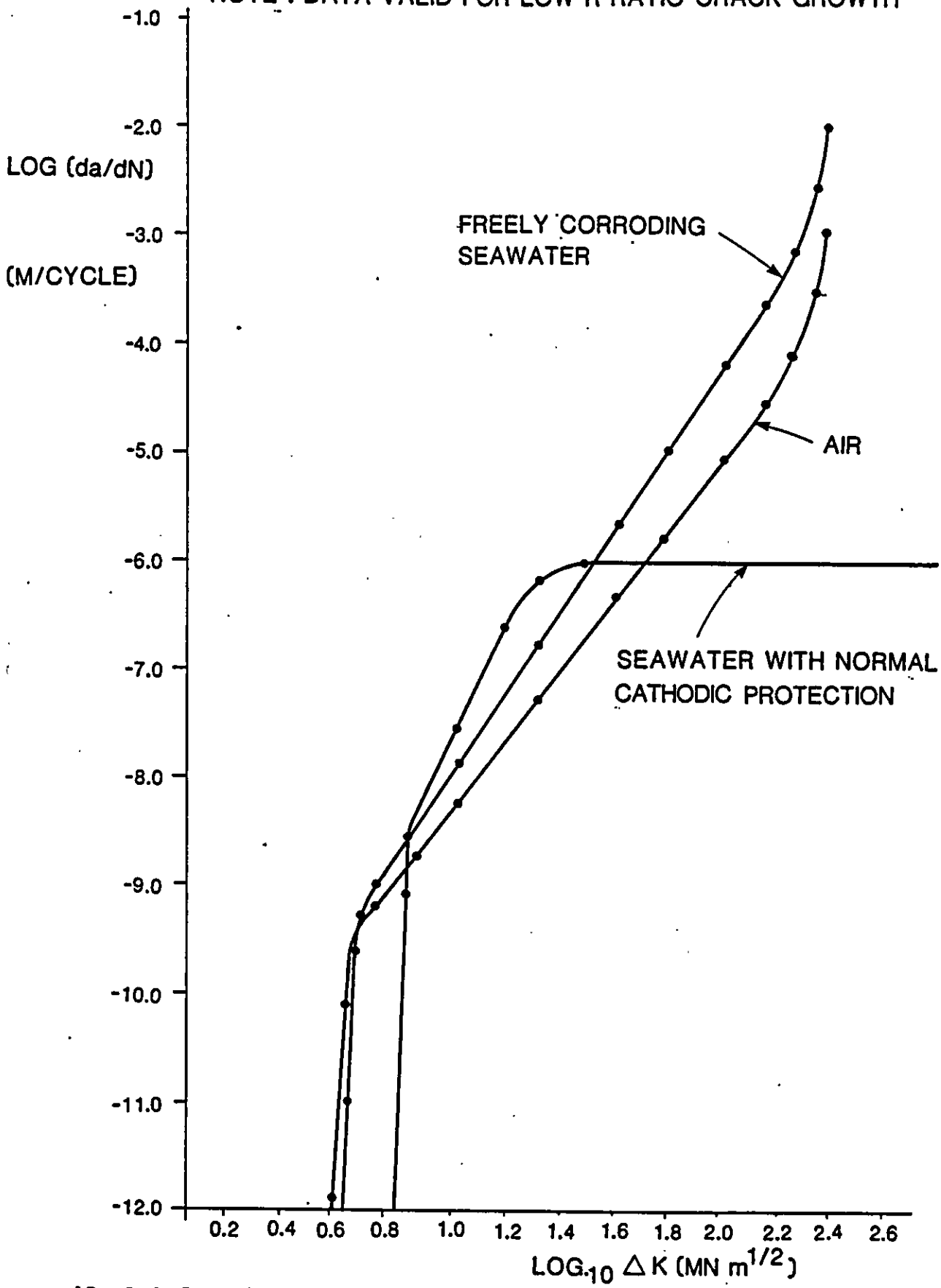

SwR1 CRACK GROWTH LAW FOR VARIOUS ENVIRONMENTS

PROJECT URP 72 : STUDY 4 **INSPECTION PLANNING ,** **THE ROLE OF DAMAGE ASSESSMENT**	**REPORT No. WOLI09/86** **FIG. 6.22**

AARQUE 7865/84

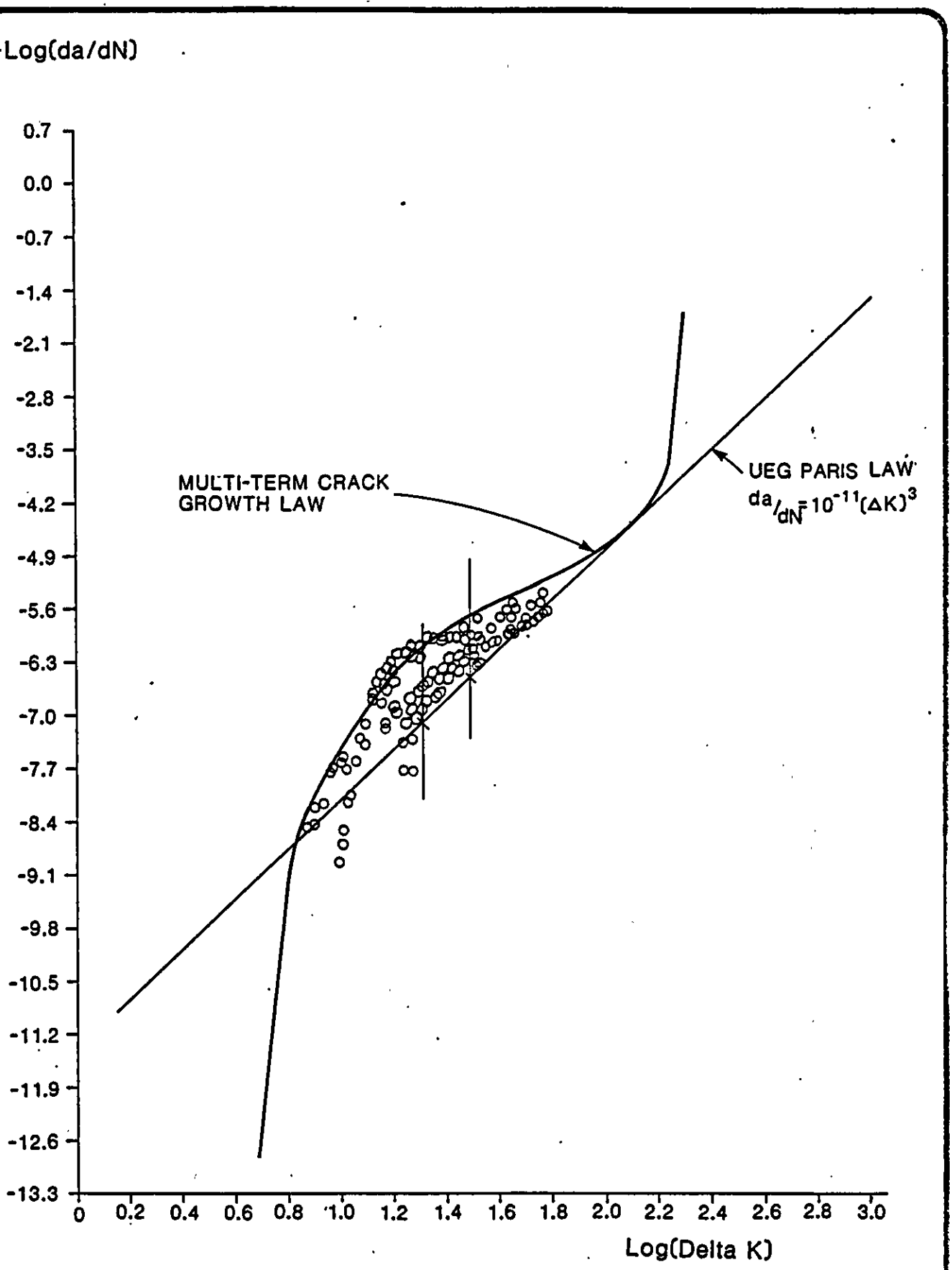

CRACK GROWTH IN SEAWATER WITH C. P.

PROJECT URP 72 : STUDY 4 INSPECTION PLANNING , THE ROLE OF DAMAGE ASSESSMENT	REPORT No. WOLI09/86 FIG.6.23

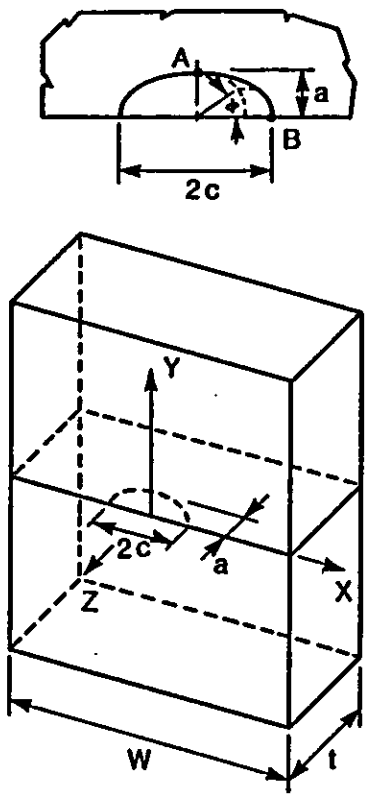

GEOMETRY

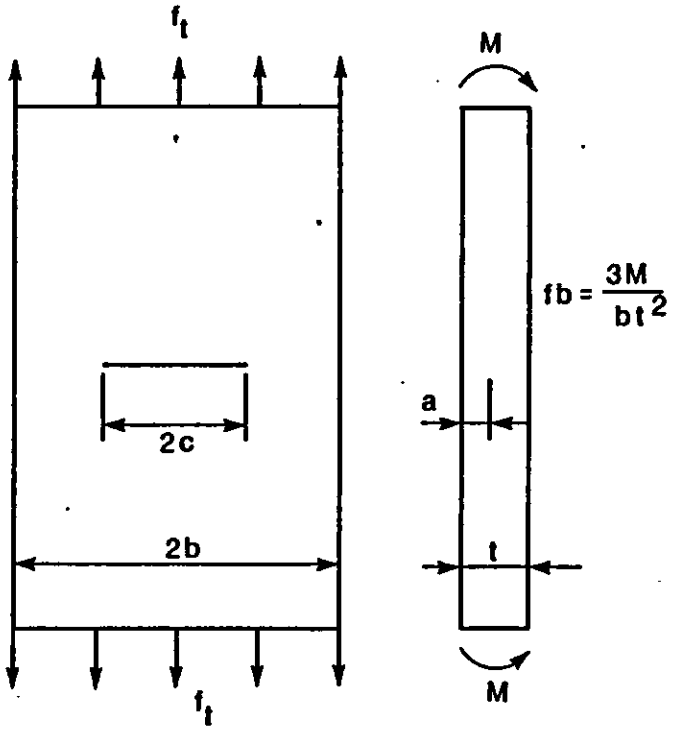

(a) TENSION (b) BENDING

LOADING

SURFACE CRACK IN FLAT PLATE

PROJECT UPR 72 : STUDY 4

INSPECTION PLANNING ; THE ROLE OF DAMAGE ASSESSMENT

WIMPEY OFFSHORE
REPORT No. WOL109/86

FIG. 6.24

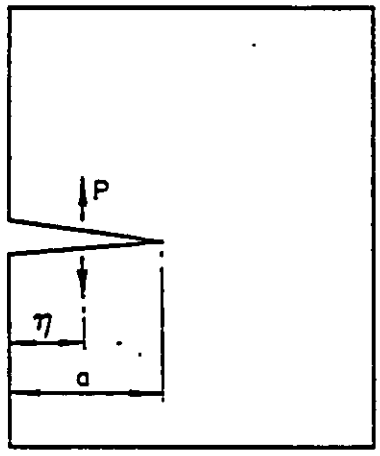

$K_I = Pg(\eta, a, \text{etc.})$

(a) ORIGINAL SOLUTION FOR WEDGE FORCES P

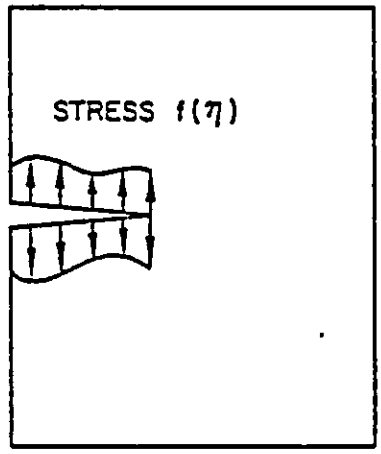

$K_I = \int_0^a f(\eta) g(\eta, a, \text{etc.})\, d\eta$

(b) DERIVED SOLUTION FOR CRACK FACE LOADING $f(\eta)$

DEVELOPMENT OF STRESS INTENSITY SOLUTION FROM THE CASE OF WEDGE OPENING FORCES

PROJECT URP 72 : STUDY 4 **INSPECTION PLANNING ,** **THE ROLE OF DAMAGE ASSESSMENT**	**REPORT No. WOL109/86**
	FIG.6.25

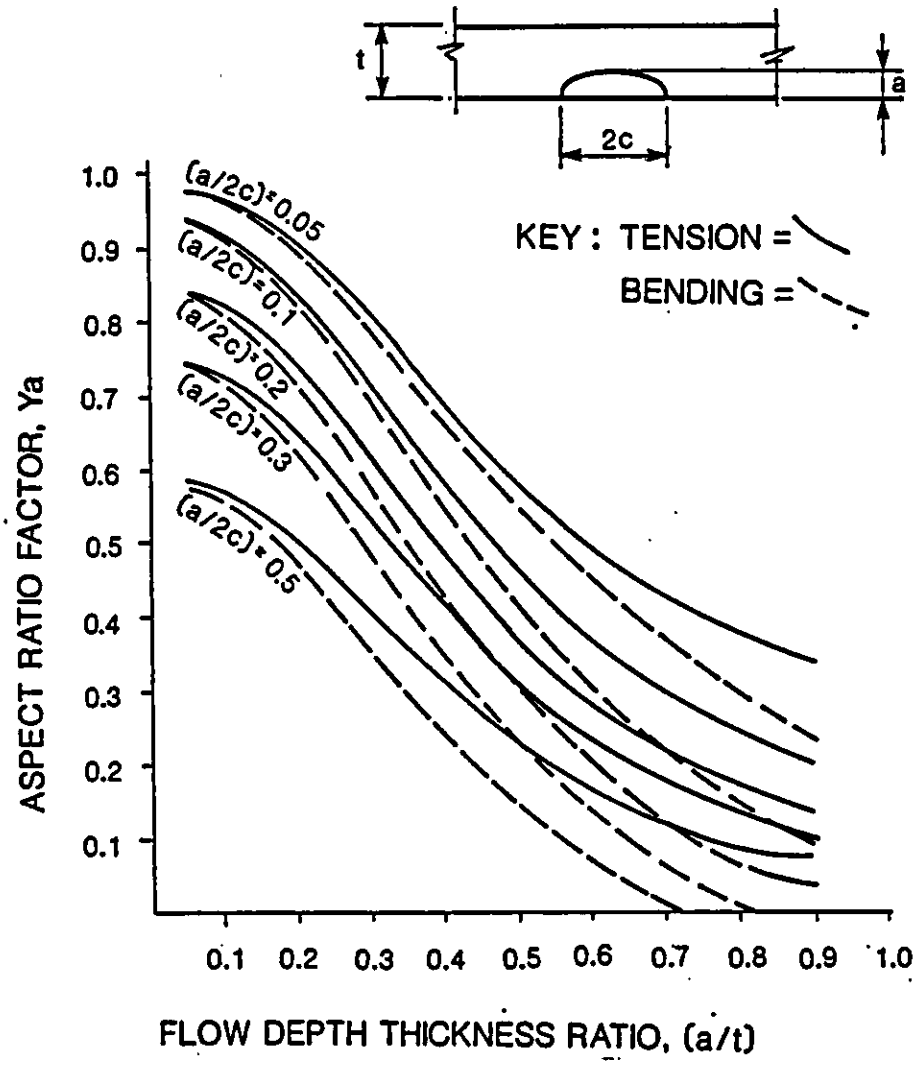

ASPECT RATIO CORRECTION FACTOR ,Ya

PROJECT URP 72 : STUDY 4 INSPECTION PLANNING , THE ROLE OF DAMAGE ASSESSMENT	REPORT No. WOL109/86 FIG. 6.26

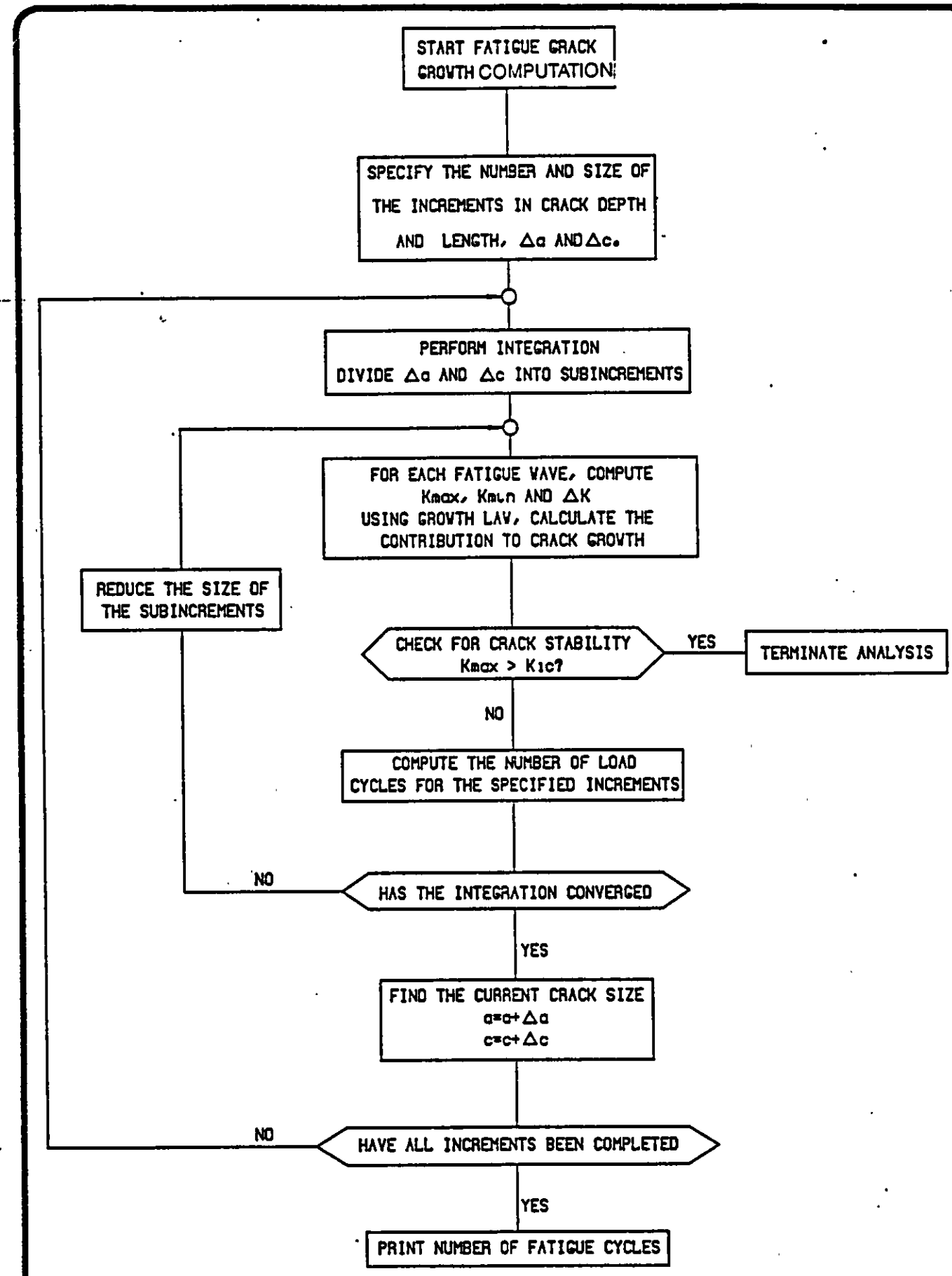

FLOWCHART FOR FATIGUE CRACK GROWTH COMPUTATION

PROJECT URP 72 : STUDY 4 **INSPECTION PLANNING ,** **THE ROLE OF DAMAGE ASSESSMENT**	**REPORT No. WOL109/86**	
		FIG. 6.27

AARQUE 7865/84

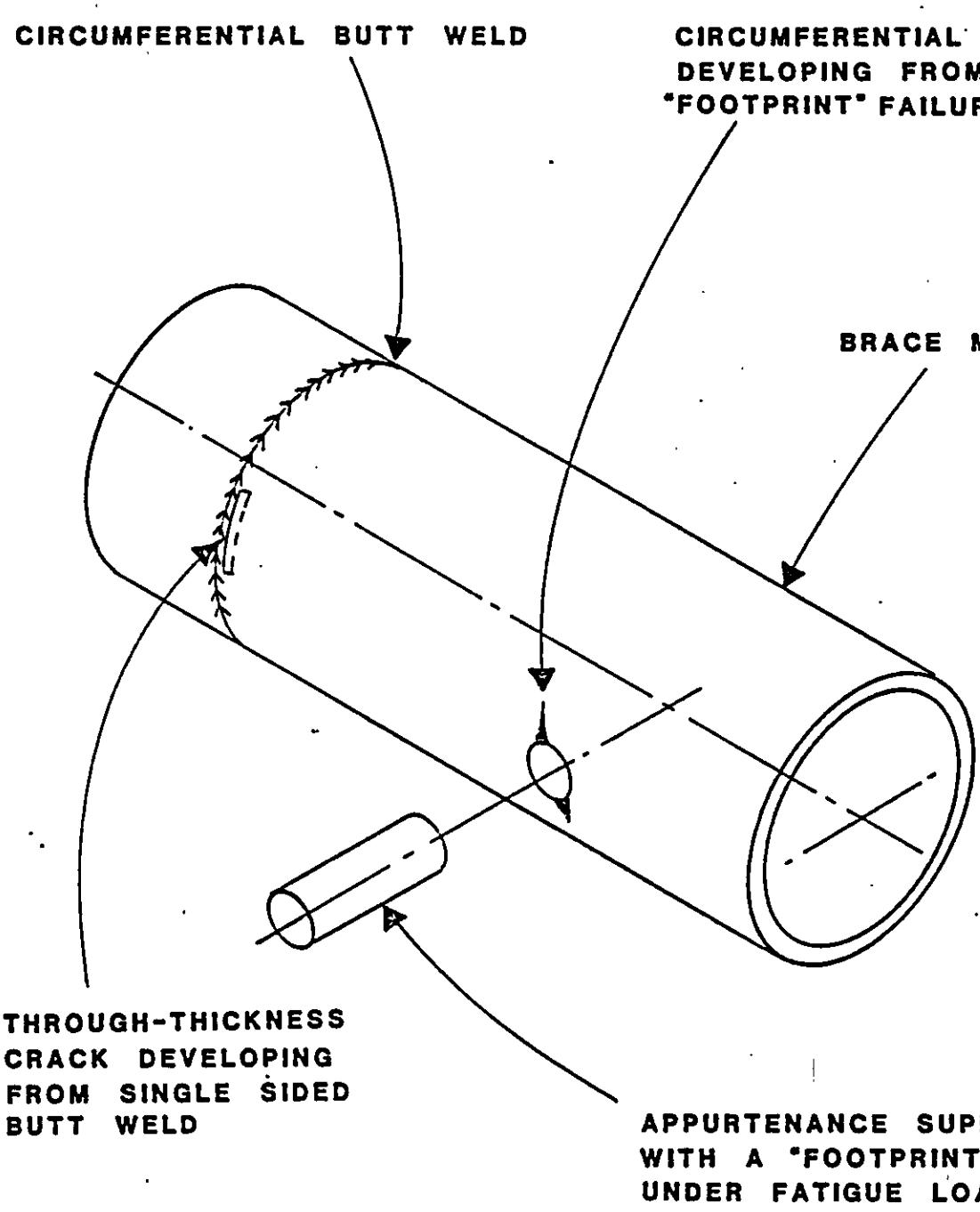

TYPICAL THROUGH - THICKNESS CRACK GEOMETRIES IN A TUBULAR MEMBER

PROJECT URP 72 : STUDY 4 INSPECTION PLANNING , THE ROLE OF DAMAGE ASSESSMENT	REPORT No. WOL109/86	FIG.6.28

AARQUE 7865/84

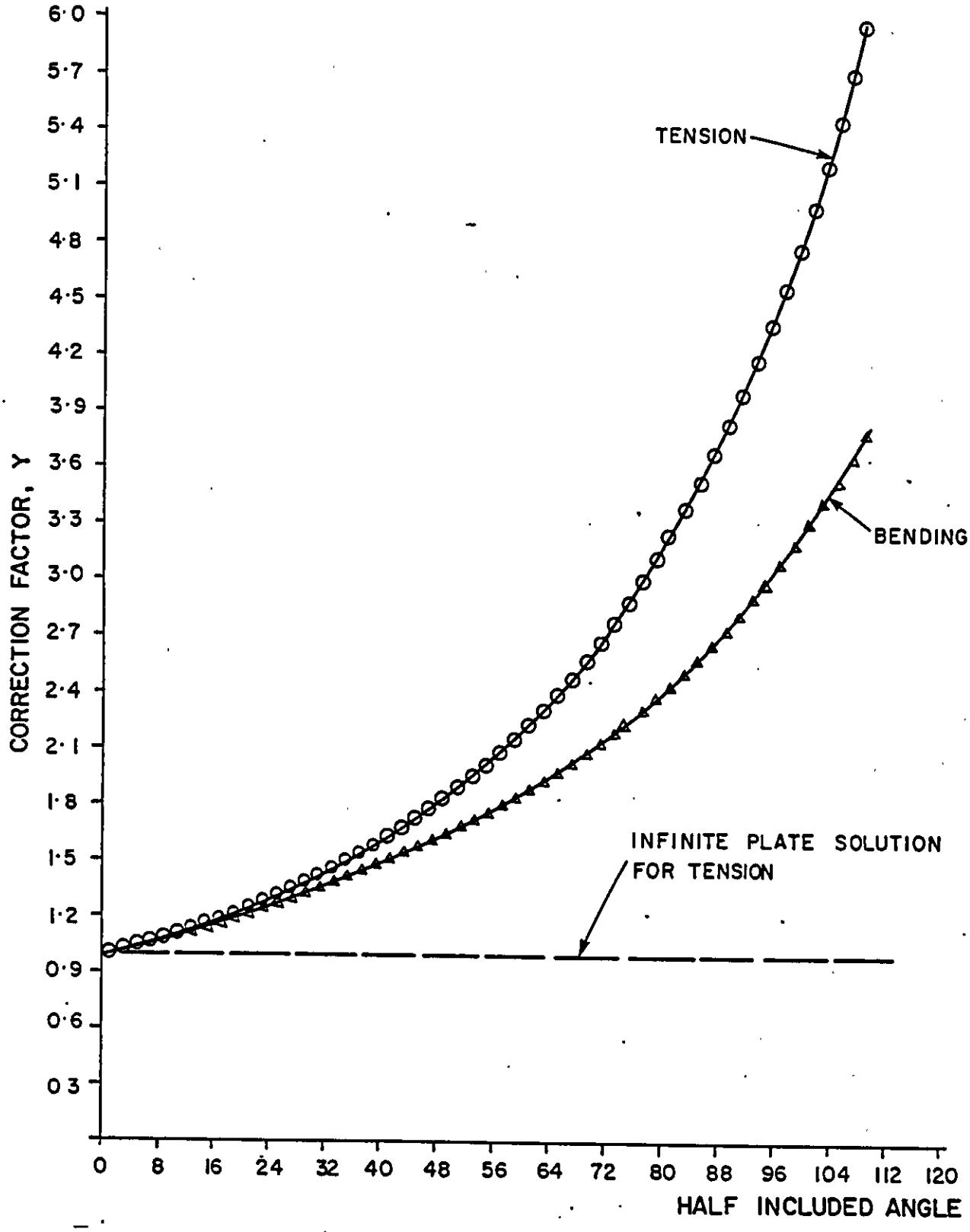

STRESS INTENSITY SOLUTION FOR THRO. THIC. CIRCUM. CRACK IN CYLINDER.

PROJECT URP 72 : STUDY 4 INSPECTION PLANNING , THE ROLE OF DAMAGE ASSESSMENT	REPORT No. WOL109/86 FIG. 6.29

AARQUE 7866/84

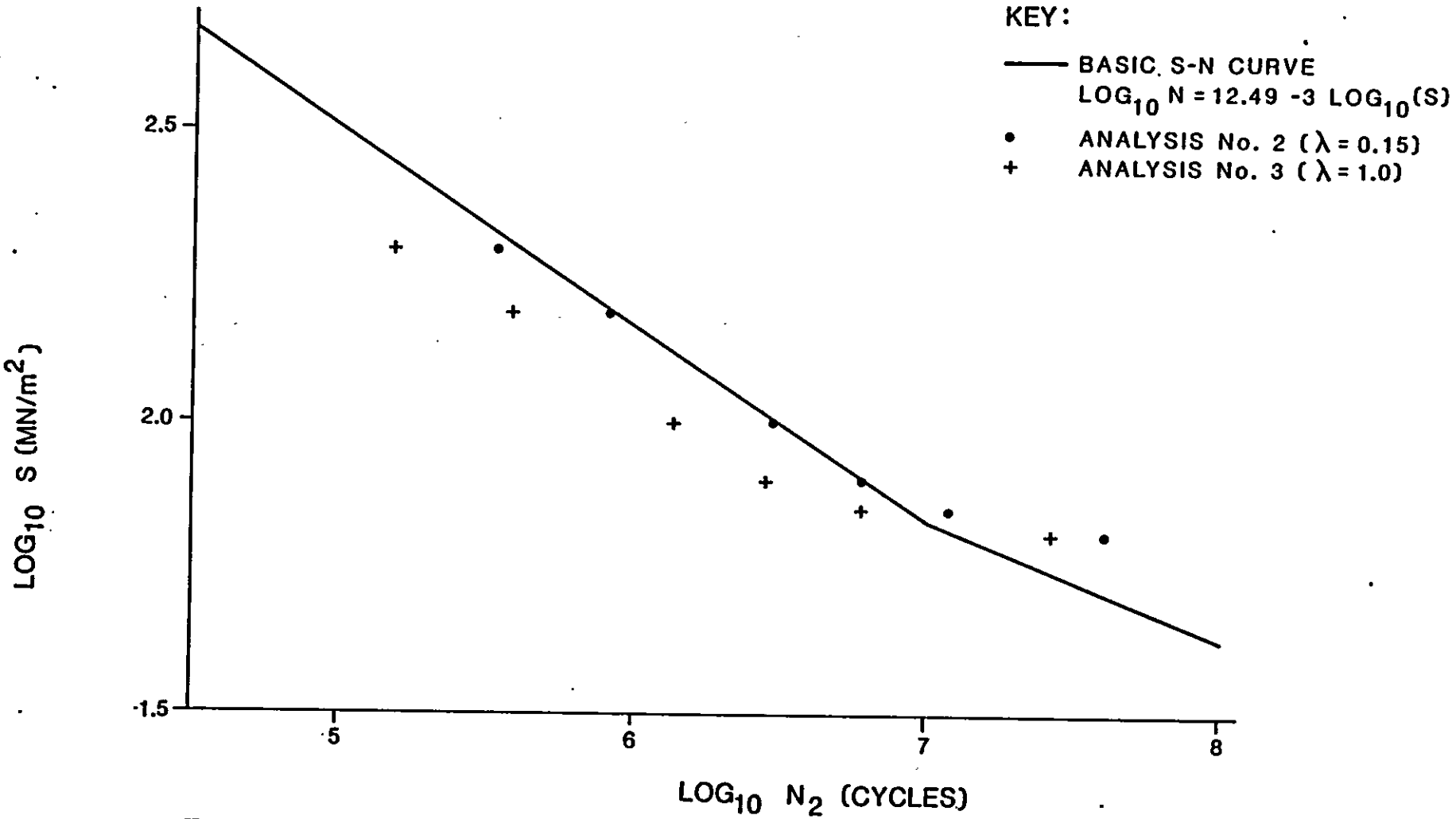

EFFECT OF STRESS DISTRIBUTION FACTOR ,λ, ON FATIGUE LIFE

PROJECT UPR 72 : STUDY 4

INSPECTION PLANNING ; THE ROLE OF DAMAGE ASSESSMENT

WIMPEY OFFSHORE REPORT No. WOL109/86

FIG. 6.30

KEY:- • ANALYSIS No2 (λ= 0·15)
+ ANALYSIS No3 (λ= 1·0)

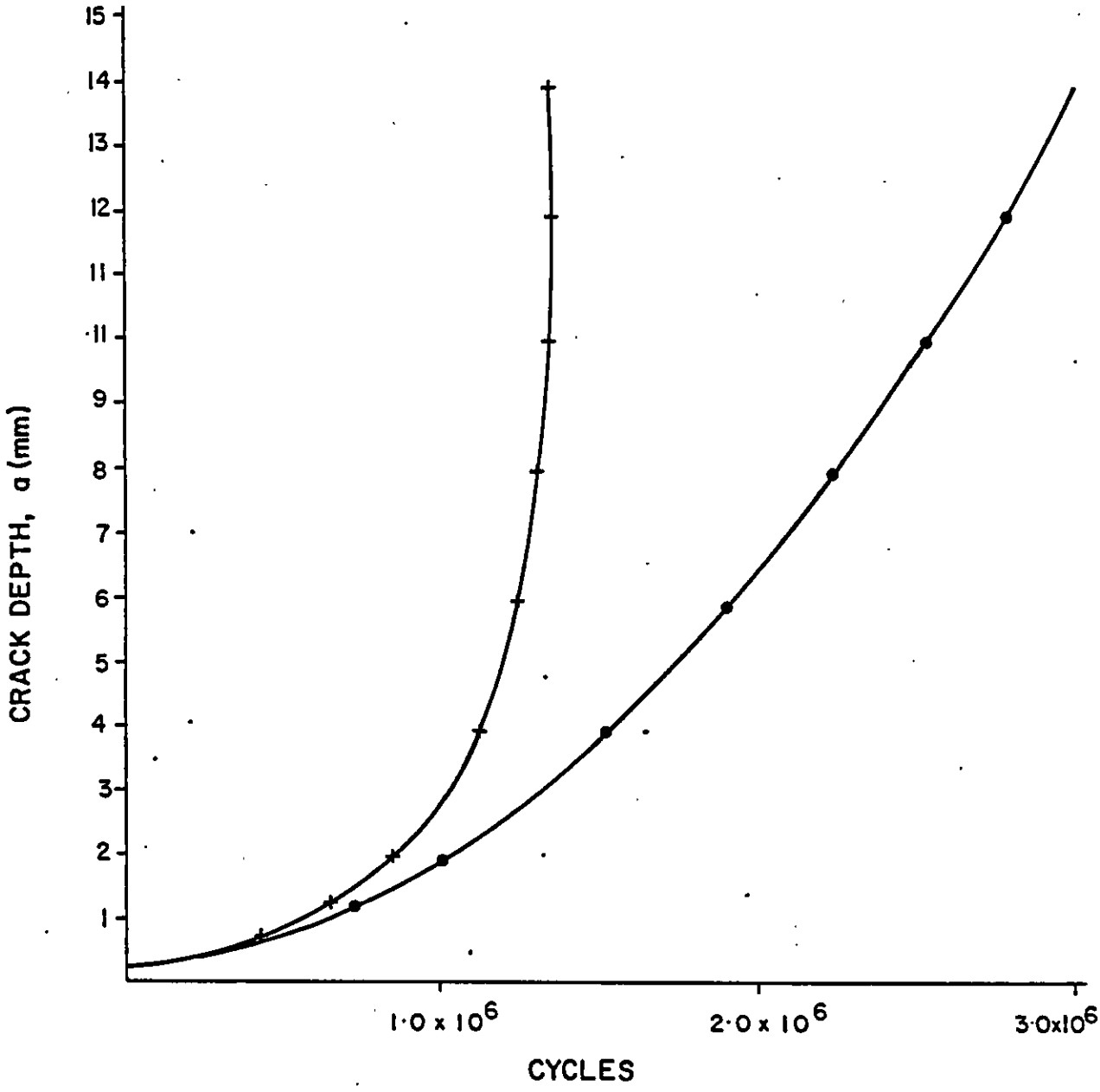

EFFECT OF STRESS DISTRIBUTION FACTOR ,λ, ON CRACK GROWTH CHARACTERISTICS

PROJECT URP 72 : STUDY 4 INSPECTION PLANNING , THE ROLE OF DAMAGE ASSESSMENT	REPORT No. WOLI09/86 FIG. 6.31

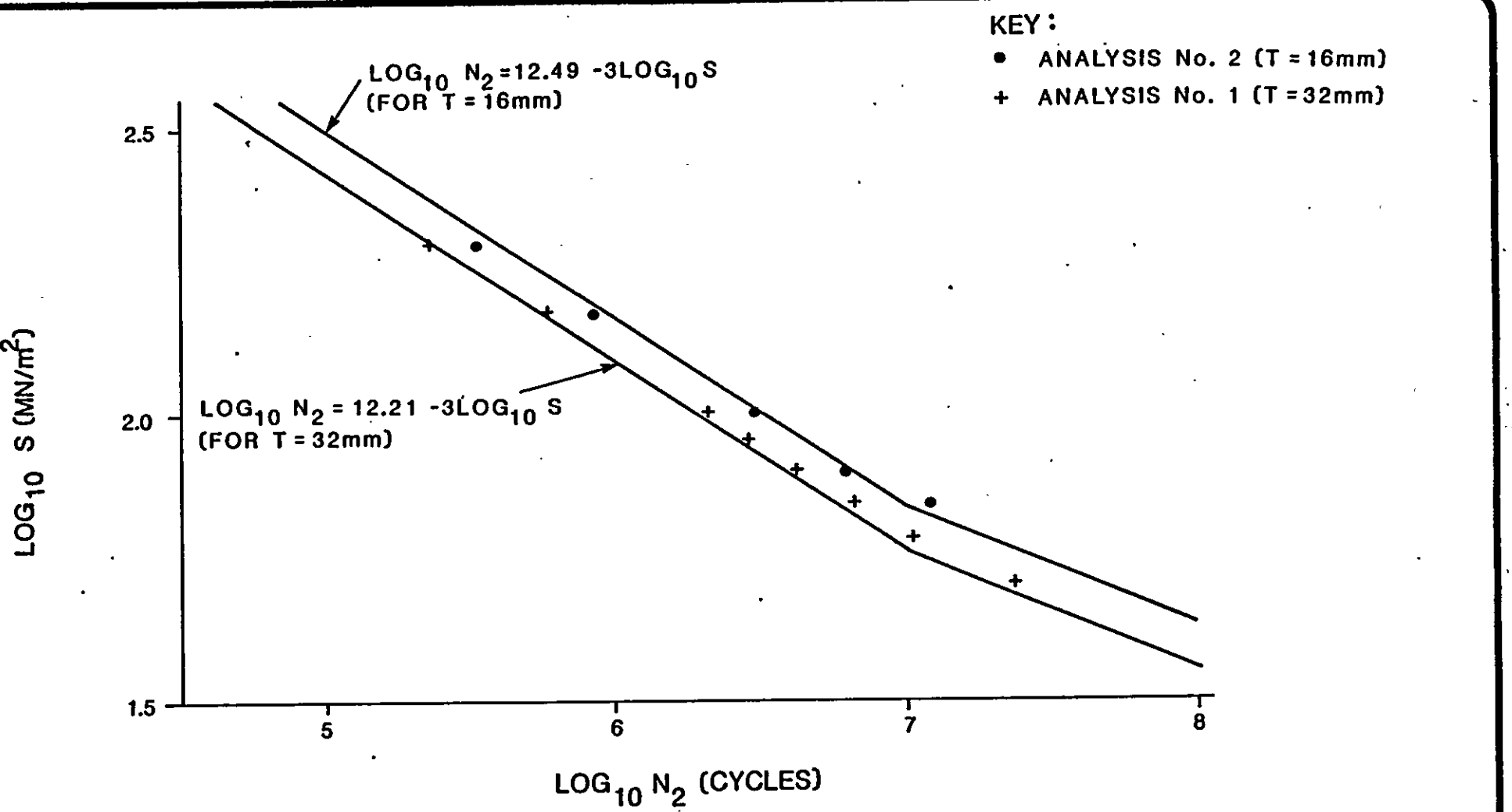

EFFECT OF WALL THICKNESS ON FATIGUE LIFE

PROJECT UPR 72 : STUDY 4

INSPECTION PLANNING ; THE ROLE OF DAMAGE ASSESSMENT

WIMPEY OFFSHORE REPORT No. WOL109/86

FIG. 6.32

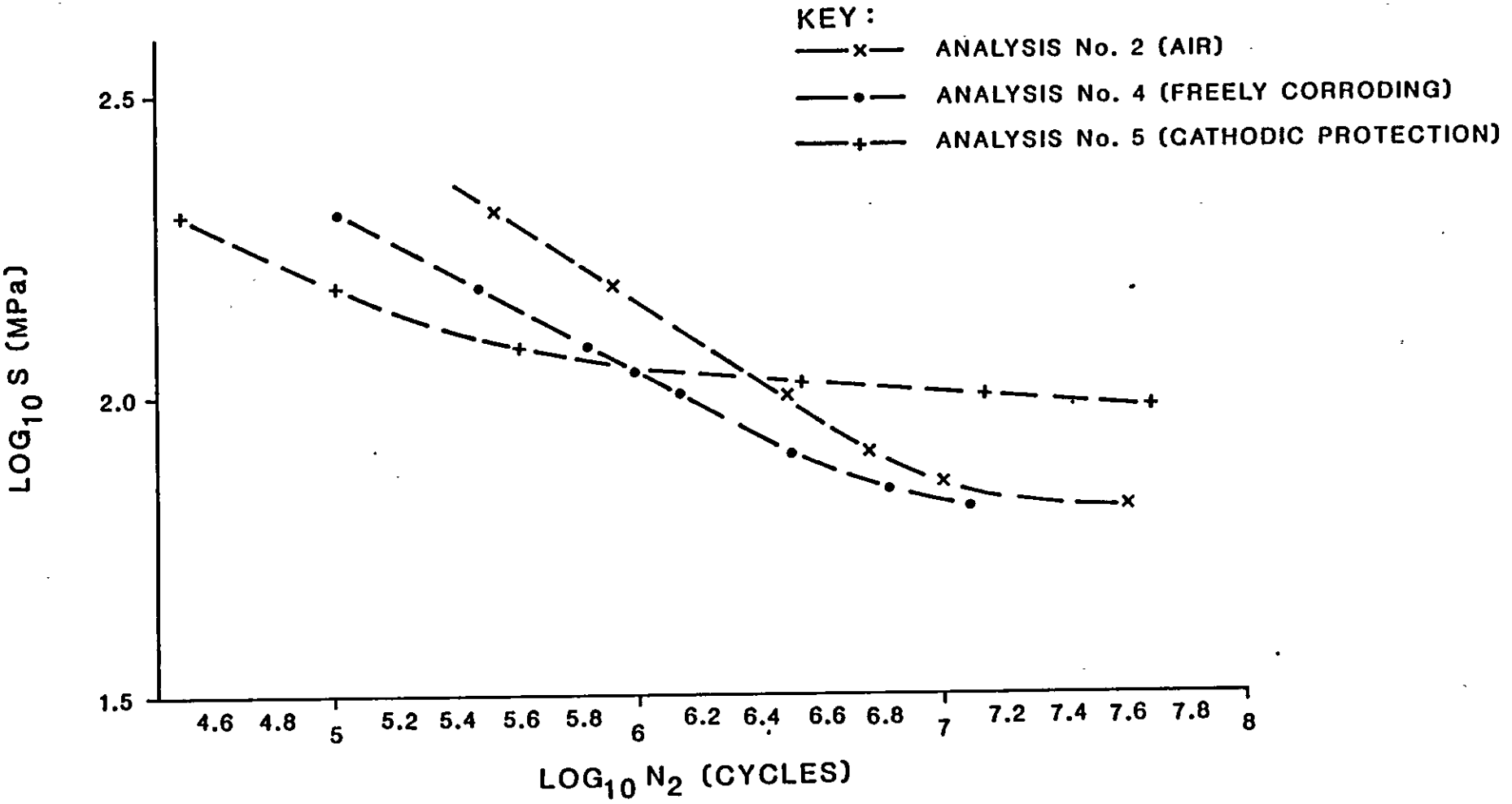

EFFECT OF ENVIRONMENT ON FATIGUE LIFE

PROJECT UPR 72 : STUDY 4

INSPECTION PLANNING , THE ROLE OF DAMAGE ASSESSMENT

WIMPEY OFFSHORE REPORT No. WOL109/86

FIG. 6.33

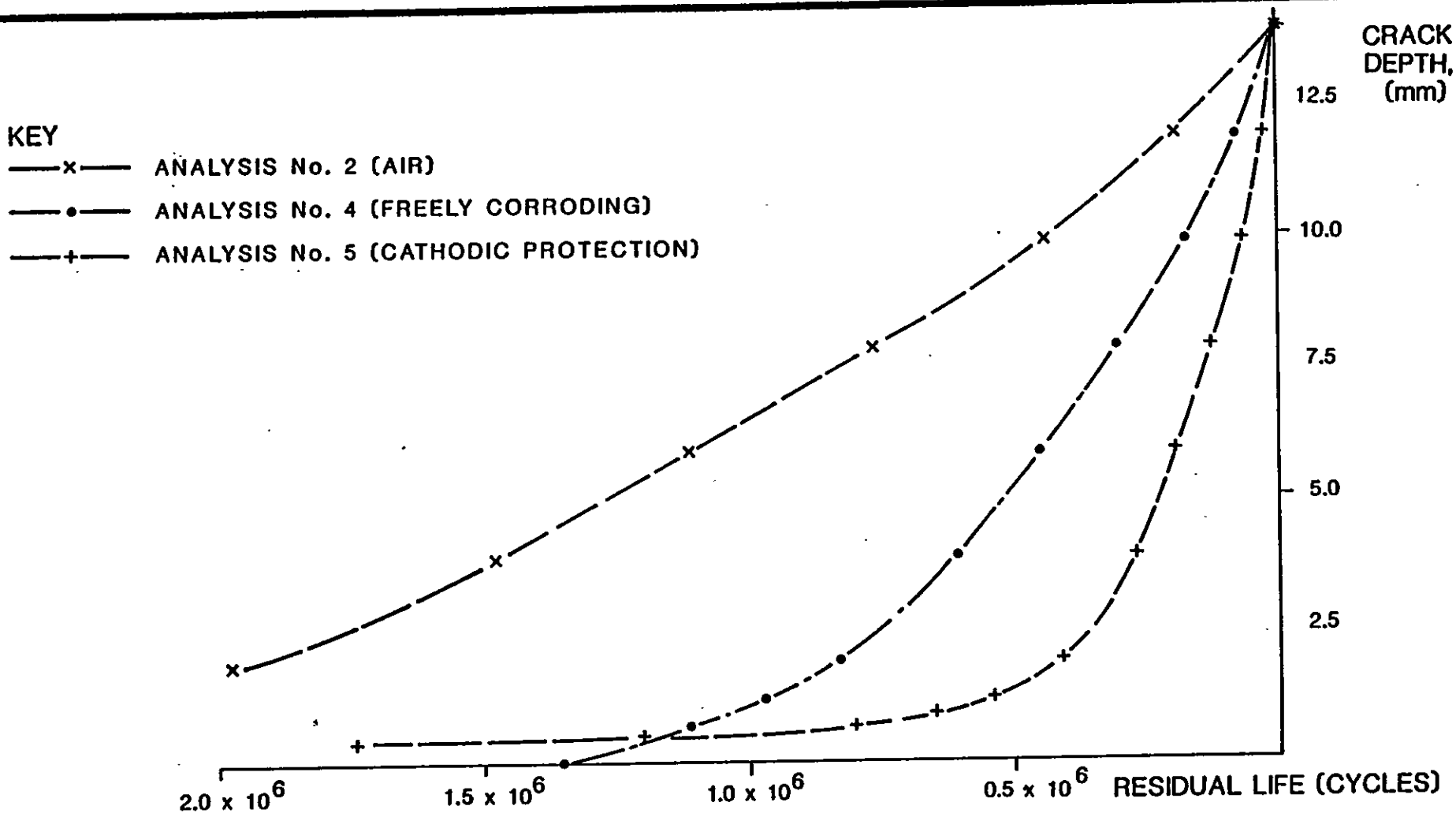

CRACK DEPTH VERSUS RESIDUAL LIFE FOR VARIOUS ENVIRONMENTS

PROJECT UPR 72 : STUDY 4

INSPECTION PLANNING ; THE ROLE OF DAMAGE ASSESSMENT

REPORT No. WOLI09/86

FIG. 6.34

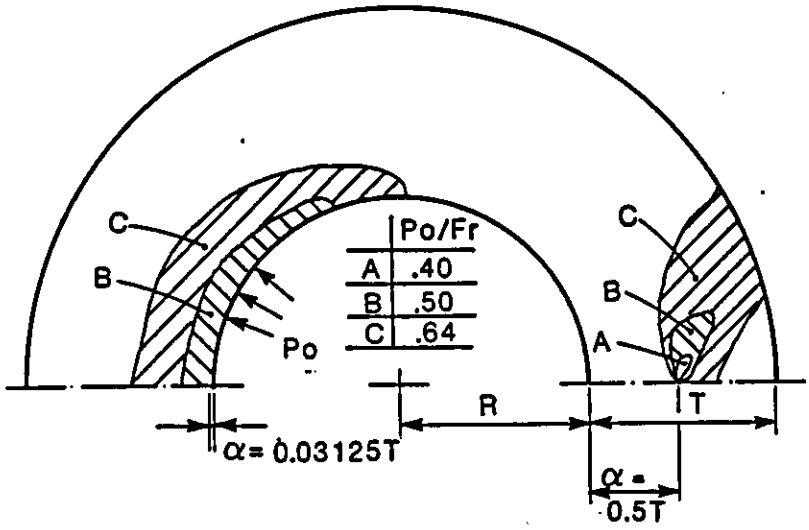

PRESSURISED CYLINDER WITH INTERNAL CRACKS

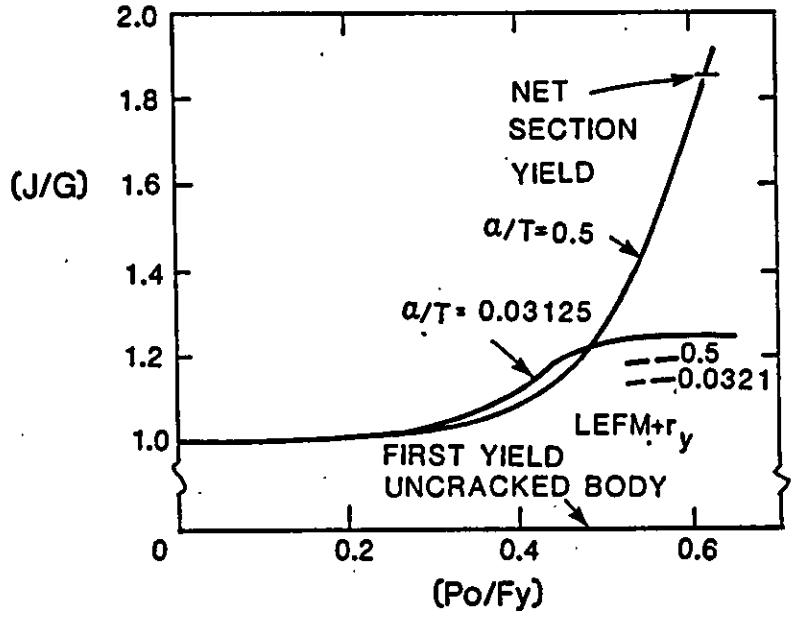

CRACK DRIVING FORCE VERSUS LOAD

EFFECT OF PLASTICITY ON CRACK BEHAVIOUR[37]

PROJECT URP 72 : STUDY 4 INSPECTION PLANNING , THE ROLE OF DAMAGE ASSESSMENT	REPORT No. WOL109/86 FIG. 6.35

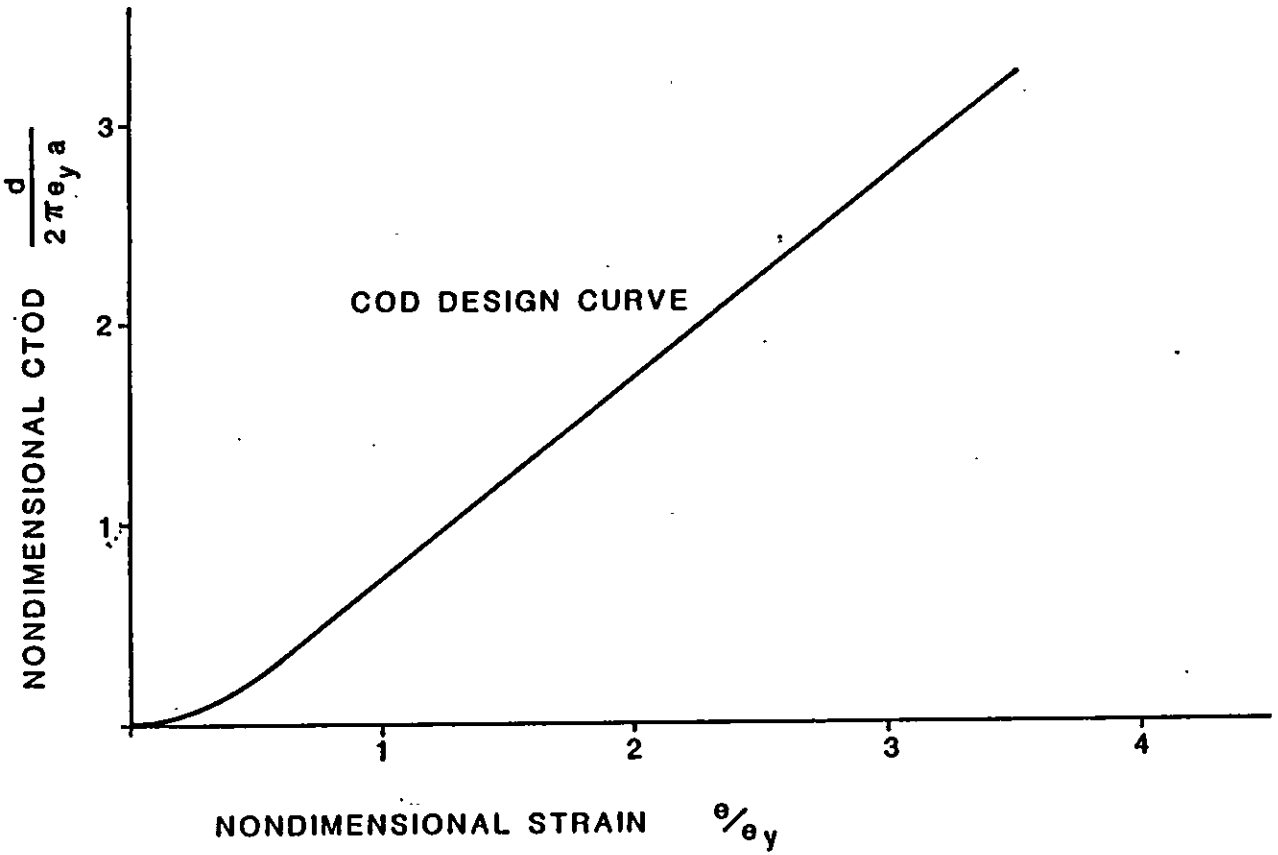

CTOD DESIGN CURVE[41]

PROJECT UPR 72 : STUDY 4

INSPECTION PLANNING ; THE ROLE OF DAMAGE ASSESSMENT

WIMPEY OFFSHORE REPORT No. WOL109/86

FIG. 6.36

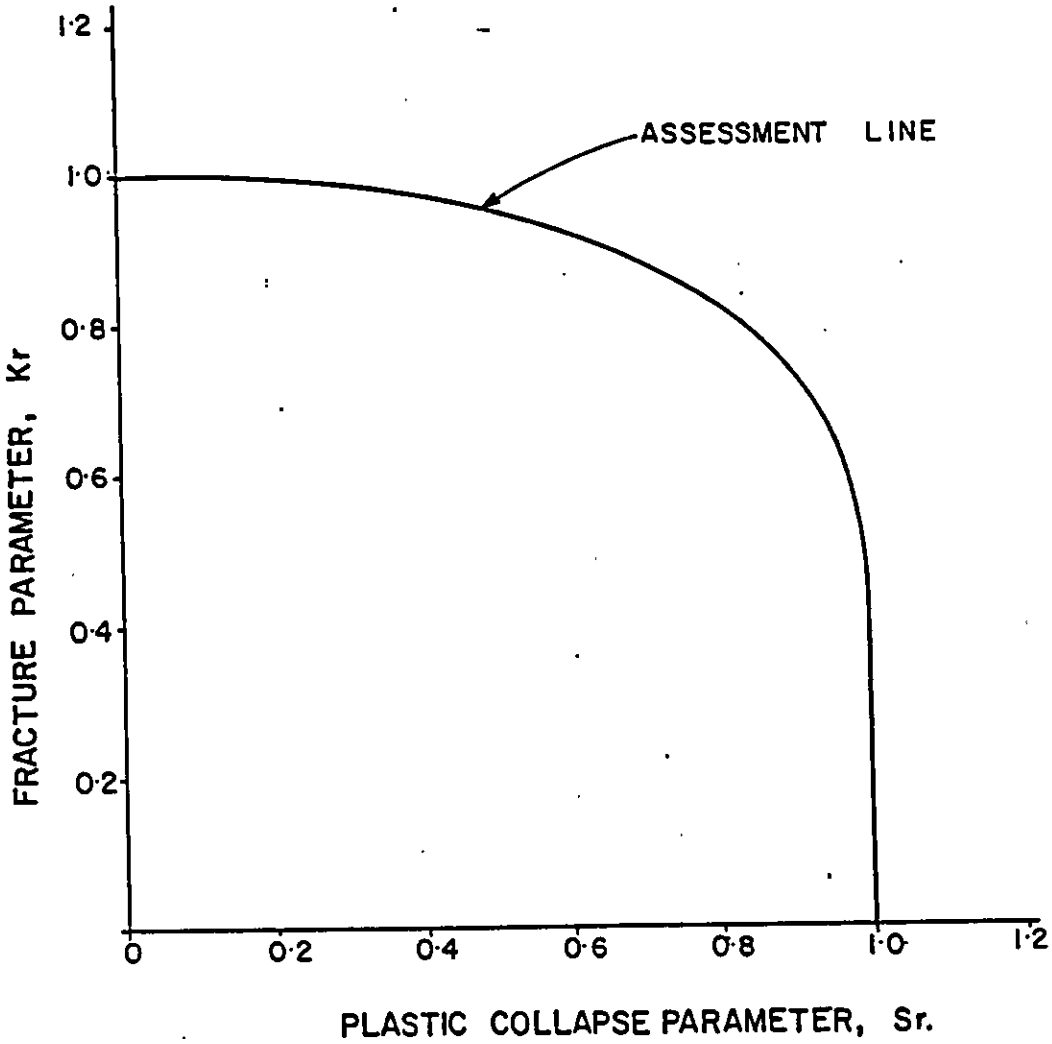

THE R6 FAILURE ASSESSMENT DIAGRAM (36)

PROJECT URP 72 : STUDY 4 INSPECTION PLANNING , THE ROLE OF DAMAGE ASSESSMENT	REPORT No. WOL109/86 FIG. 6.37

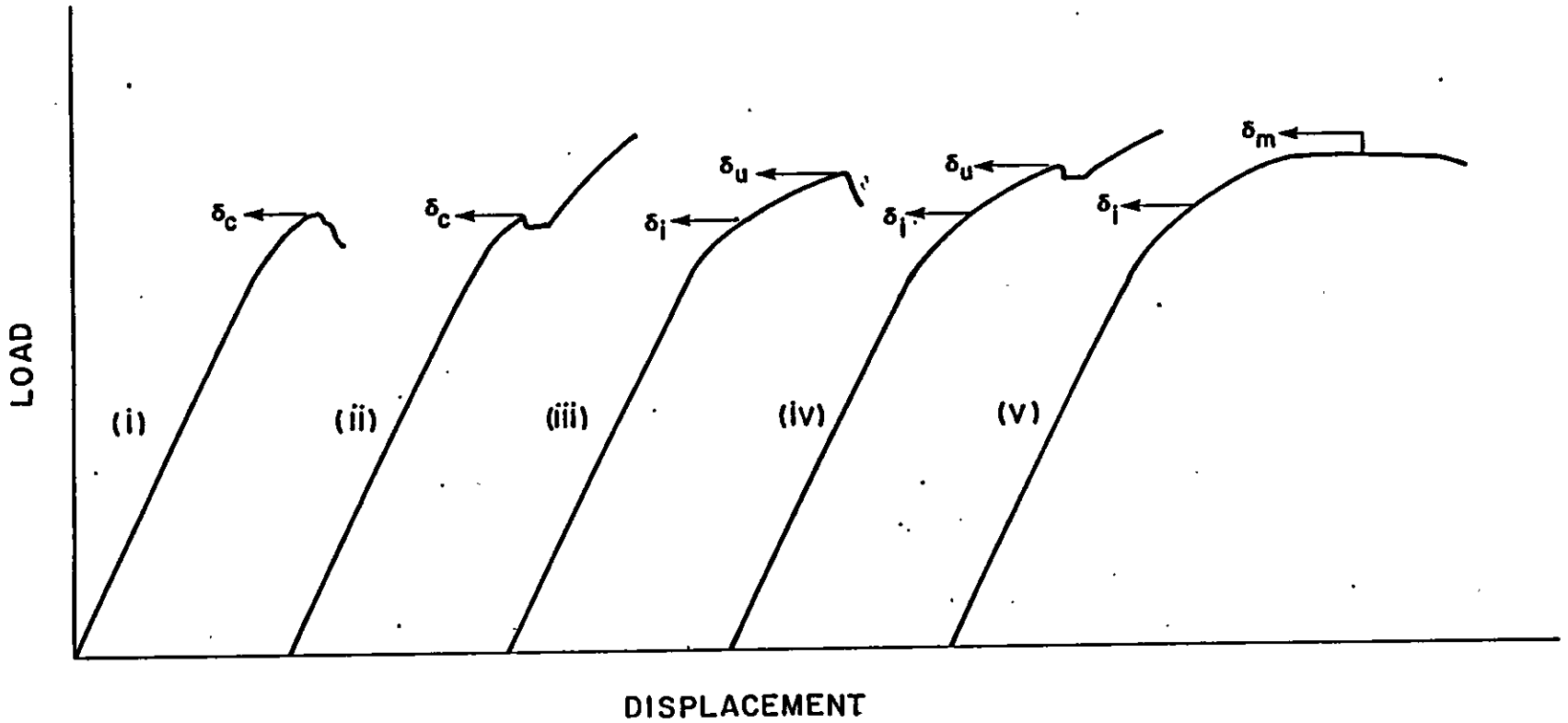

TYPES OF LOAD DISPLACEMENT GRAPHS FOR COD SHOWING VARIOUS TYPES OF BEHAVIOURS

PROJECT URP 72 : STUDY 4

INSPECTION PLANNING , THE ROLE OF DAMAGE ASSESSMENT

WIMPEY OFFSHORE
REPORT No. WOLI09/86

FIG. 6.38

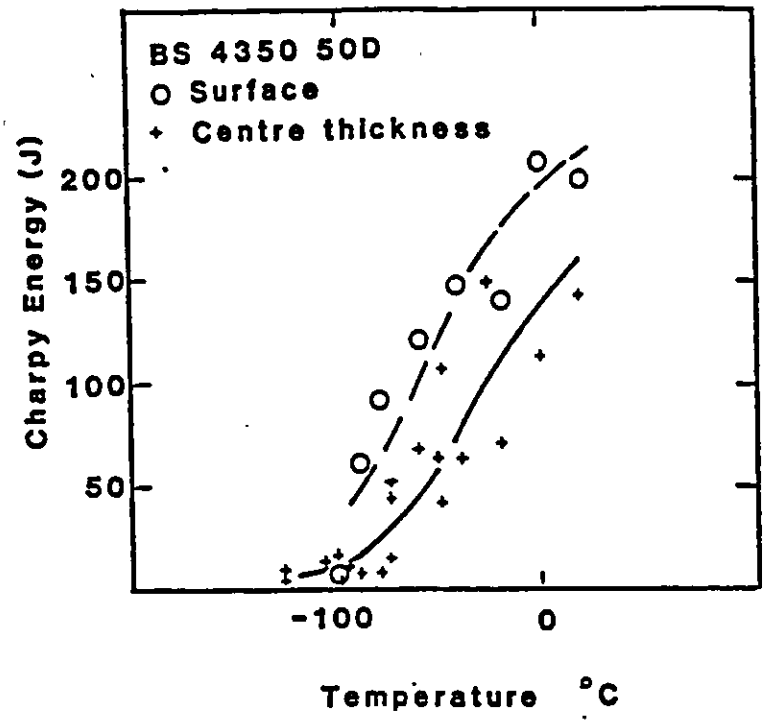

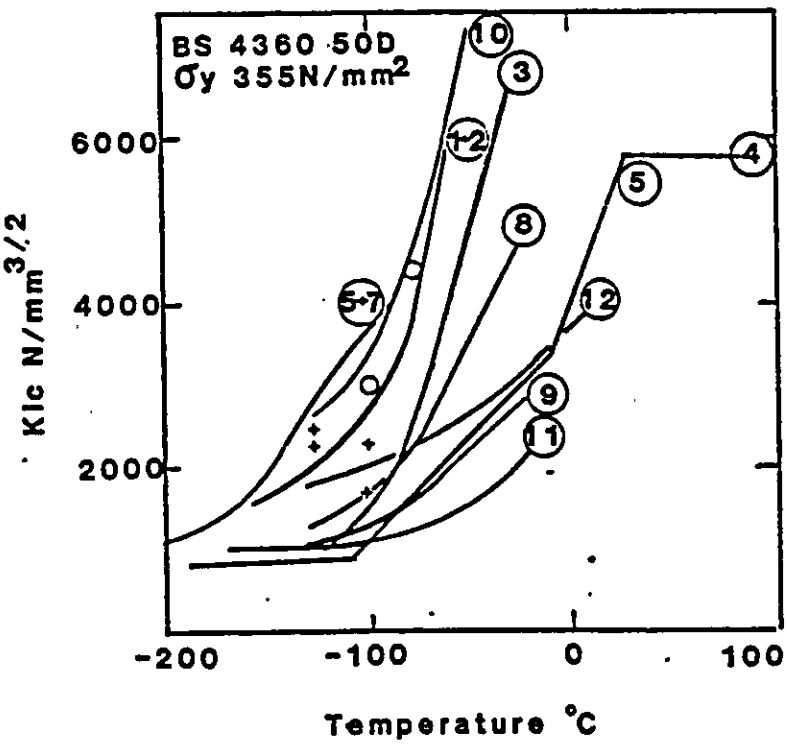

COMPARISON OF PREDICTED Klc CURVES WITH EXPERIMENTAL Klc VALUES FOR BS 4360 50D STEEL WITH CHARPY TRANSITION CURVE OF ABOVE (REF.53)

PROJECT URP 72 : STUDY 4 INSPECTION PLANNING , THE ROLE OF DAMAGE ASSESSMENT	REPORT No. WOLI09/86 FIG. 6.39

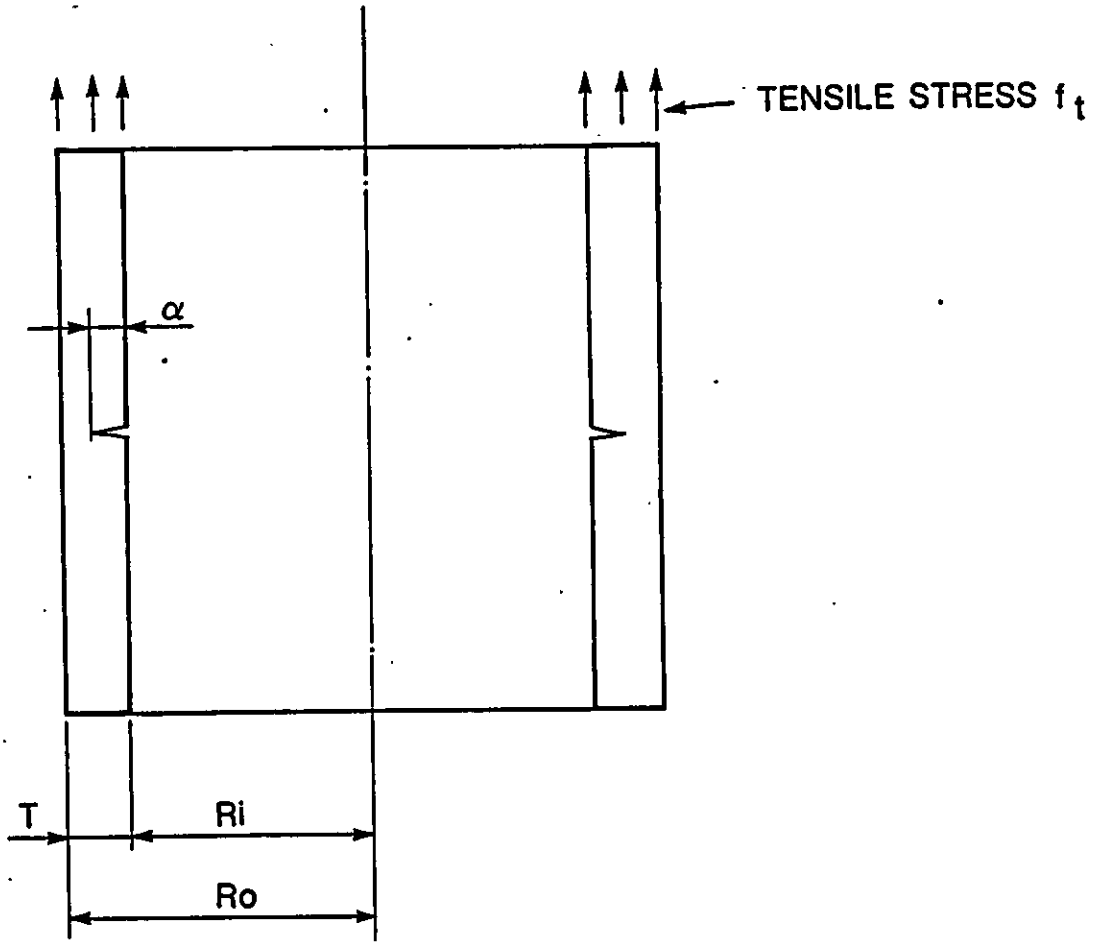

BENCHMARK PROBLEM-INTERNALLY CRACKED CYLINDER UNDER TENSION

PROJECT URP 72 : STUDY 4 INSPECTION PLANNING , THE ROLE OF DAMAGE ASSESSMENT	REPORT No. WOL109/86 FIG. 6.40

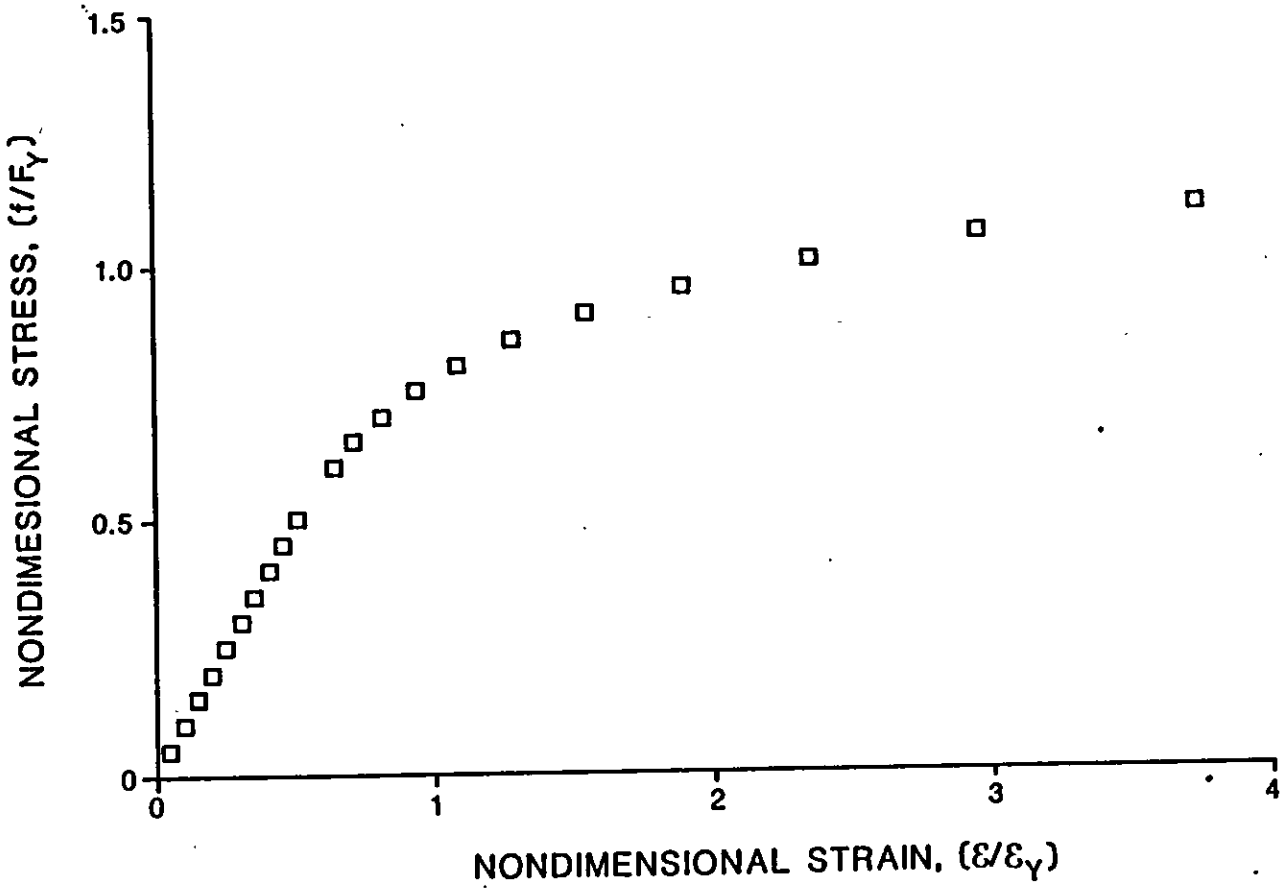

CRACK STABILITY BENCHMARK

STRESS - STRAIN CURVE (RAMBERG - OSGOOD MODEL)

PROJECT UPR 72 : STUDY 4

INSPECTION PLANNING, THE ROLE OF DAMAGE ASSESSMENT

REPORT No. WOL109/86

FIG. 6.41

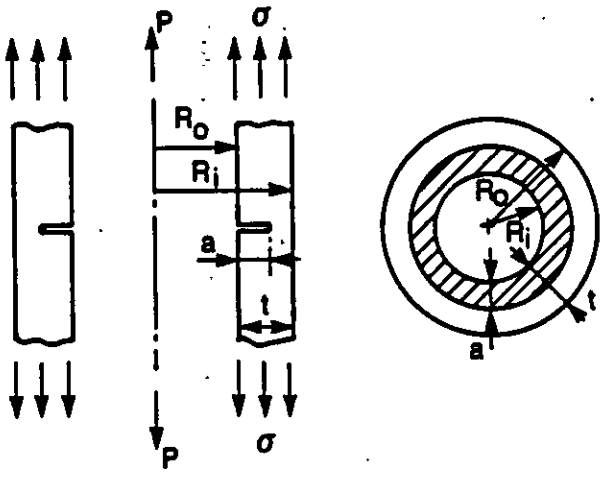

$$f_t = \frac{P}{\pi(r_o^2 - r_i^2)}$$

$$K_I = f_t\sqrt{\pi a} \cdot Y_t\left(\frac{r_i}{r_o}, \frac{a}{t}\right)$$

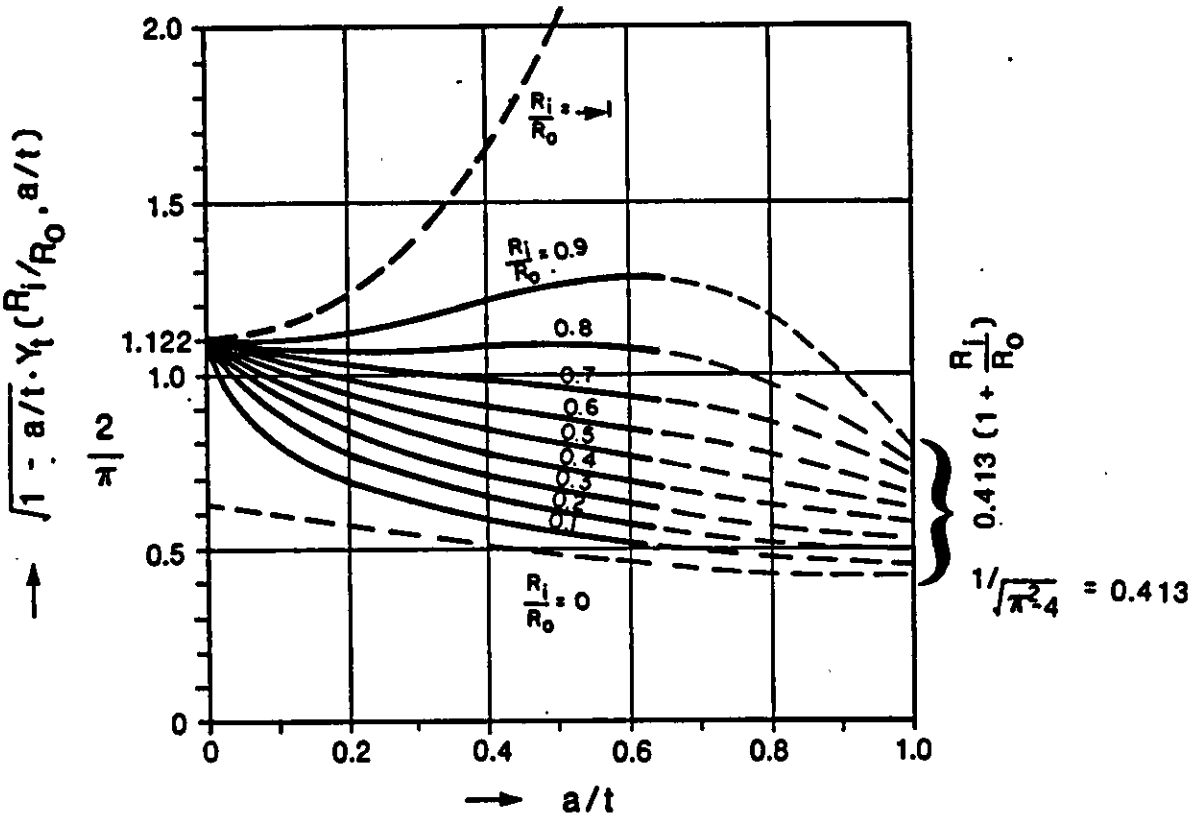

CRACK STABILITY BENCHMARK

STRESS INTENSITY FACTOR SOLUTION[29]

PROJECT URP 72 : STUDY 4 INSPECTION PLANNING THE ROLE OF DAMAGE ASSESSMENT	REPORT No. WOL109/86 FIG. 6.42

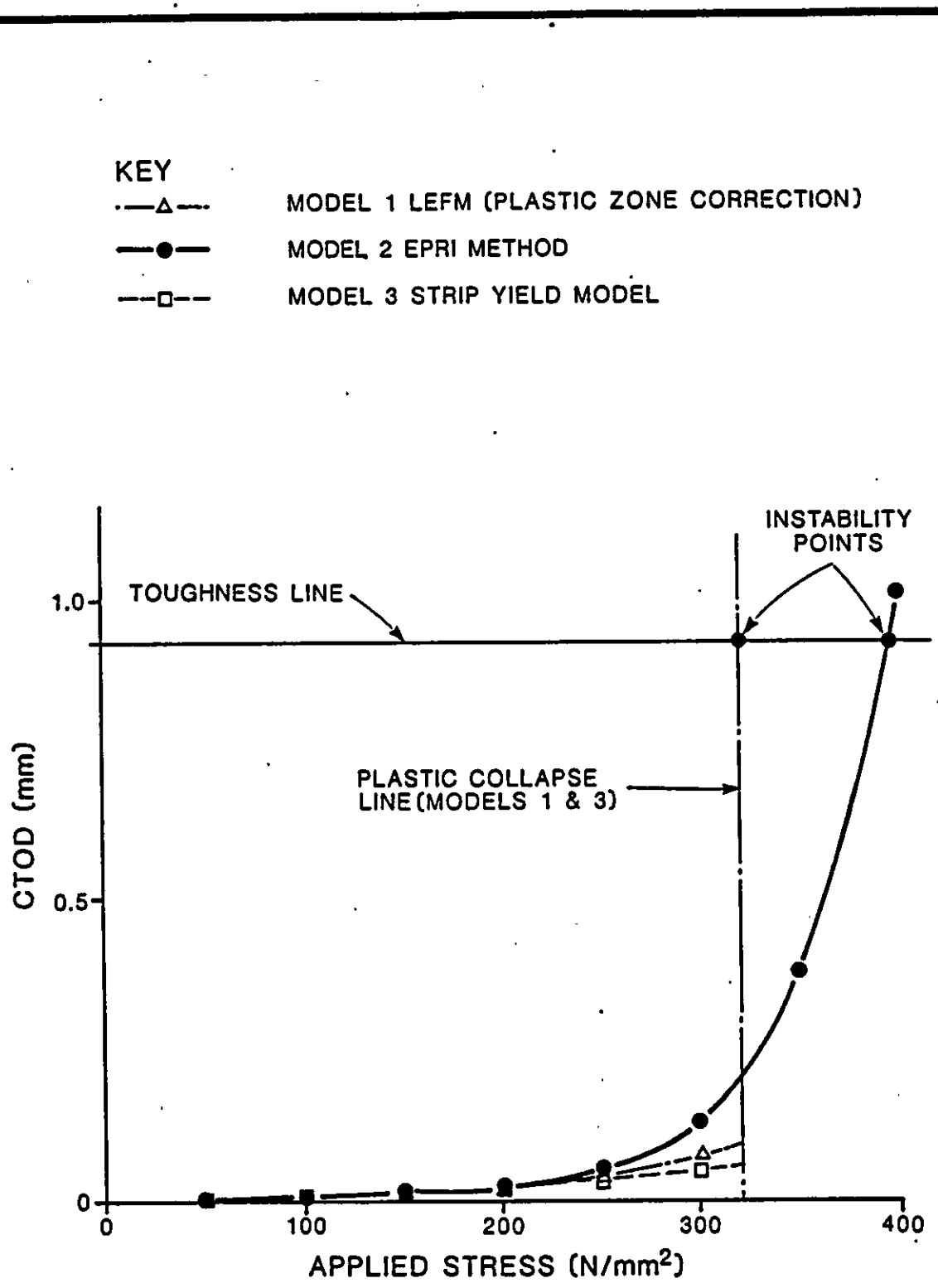

CRACK STABILITY BENCHMARK STABILITY DIAGRAM

PROJECT URP 72 : STUDY 4 INSPECTION PLANNING , THE ROLE OF DAMAGE ASSESSMENT	REPORT No. WOL109/86 FIG. 6.43

AARQUE 7865/84

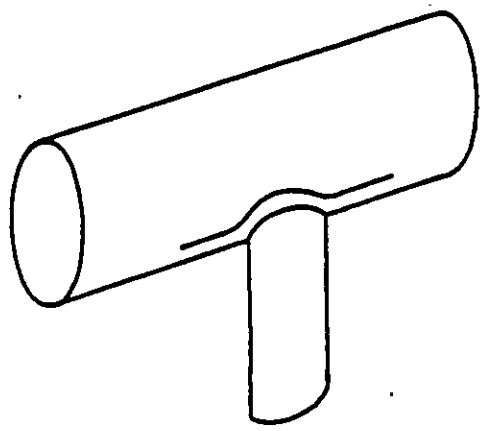

(a) AXIAL CRACK FAILURE

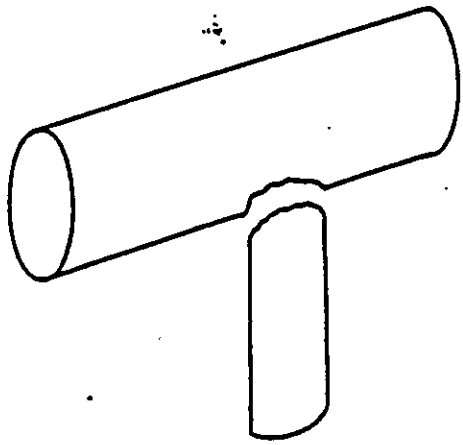

(b) FOOTPRINT FAILURE

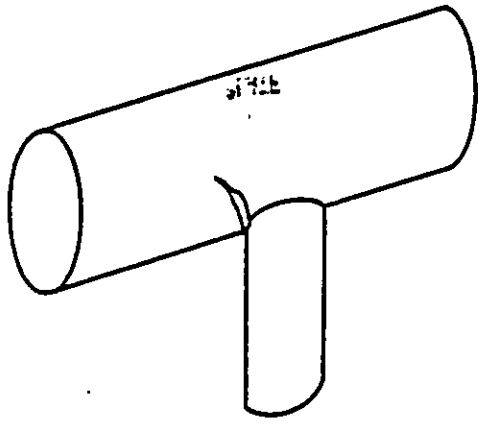

(c) CIRCUMFERENTIAL CRACK FAILURE

POSSIBLE FAILURE MODES AT TUBULAR JOINT

PROJECT URP 72 : STUDY 4 INSPECTION PLANNING , THE ROLE OF DAMAGE ASSESSMENT	REPORT No. WOL109/86 FIG. 6.44

7. DEVELOPMENT OF AN 'OPTIMISED' INSPECTION STRATEGY

7.1 Introduction

It was pointed out in Section 2 that alternative approaches to structural inspection are available which provide a greater degree of reliability than the traditional approach, which is primarily governed by statutory requirements, the nominal fatigue lives and the likelihood of ultimate failure of the components inspected.

In this section, an approach to the optimisation of underwater inspection is developed in some detail for a steel jacket structure, the most complex subsea item for which inspection plans are required. The principles can be adapted to other subsea items with appropriate simplifications and modifications (see Section 8.2). Although it is inevitable (for various reasons, discussed below) that some judgements will be subjective, the format adopted attempts to maximise objectivity in planning for inspection.

The approach presented aims to cover all of the major items having a bearing on underwater inspection, and as a result is rather complex. It is the intention that operators may, if desired, implement only those aspects of the approach deemed to be most important since this will, nonetheless, represent a considerable advance over current practice. There is then the option available to introduce progressively the other aspects, if desired, until the complete system is in place.

The system proposed requires a considerable quantity of data to be processed when planning the underwater inspection, and it is recommended that a computer database should be established to manage this. A microcomputer based system would be adequate for most structures if a simplified version of the total system were to be implemented. This would lend itself naturally to the points systems proposed for inspection priority ranking.

It is emphasised that this approach is for inspection planning. Damage discovered during an inspection would always be assessed using the methods described in Section 6. After assessment of damage, a decision on whether to repair and what revised inspection strategy should be adopted for future inspection of the component is fed back into the inspection planning database developed in this Section.

Use is also made in this Section of damage assessment techniques in rationalising inspection plans; components considered critical can be assessed to determine the effects of damage before damage occurs. An understanding of the development of a postulated defect in a component will have an important impact on the strategy adopted for its inspection.

Subsection 7.2 reiterates the objectives of inspection. The development of the overall approach, starting with overall philosophy and culminating in a detailed methodology is the subject of the following subsections. The methodology is illustrated by example in Section 8.1.

7.2 Inspection Objectives

The principal objective of an inspection plan is to provide a level of reliability which is commensurate with the consequences of failure. If a new inspection strategy is to be implemented, it must satisfy the following criteria:

1. There should be no reduction in the level of confidence in the integrity of the structure.

2. Either cost or risk should be reduced, compared to the conventional inspection strategy.

Little purpose is served in implementing an inspection plan which does not meet these objectives.

7.3 Development of the Overall Approach

7.3.1 General

The approach to optimisation of underwater inspection is shown as a flowchart in Figure 7.1. In this format it is possible to portray the principal considerations which have a bearing on the inspection programme, and their relationship with each other. In this section, the major concepts are introduced and discussed, and the method of incorporating them in the inspection plan is demonstrated.

7.3.2 Overall Strategy

The approach to development of an inspection strategy was discussed in Section 2 and it was concluded that an 'optimum' inspection plan would be based on consideration of the following criteria:

- Consequence of damage
- Failure mode
- Likelihood of damage
- Cost and reliability of inspection.

Attempts to be wholly objective in the design of an inspection programme encounter the following problems:

1. Size problem

   It is immediately apparent that an almost infinite set of damage scenarios, including combinations of different sorts of damage, could be postulated.

2. Loading regime

   The loading regime in each significant component would be generated as a matter of course during the design process but whether or not a component is 'fracture critical' may be a function of relevant loading combinations. For example, if a member acts in compression for 90% of its life, but comes into tension occasionally during storms from a particular direction, the member cannot be simply classified as a tension or compression member.

3. Practical considerations

   The practical considerations the inspection planners need to address include:

   - Specification and location of the DSV,
   - Diving requirements,

- Cleaning requirements and method,
- Inspection methods,
- Cleaning time,
- Time taken to inspect.

The realistic philosophy is to accept that, if the objectives set in Section 7.2 are to be met, a combination of objective and subjective decisions is inevitable in the design of a routine inspection plan.

Our aims in developing the plan must therefore be:

- to maximise the objectivity
- to use the best information possible in making subjective decisions.

In the following subsections, ways of achieving these aims are developed. The methodology is to develop an inspection priority ranking system to be used as a tool by the inspection programme designers. Before the techniques for developing the priority ranking are discussed, the needs and requirements of the user are discussed, and the idea of an expert 'review panel' is introduced.

7.3.3 Review Panel

Accepting that judgements are inevitable for the successful formalisation of the plan, an expert review panel is proposed. It should contain, as a minimum, representation by:

- Structural design specialists
- Quality assurance specialists
- Inspection specialists
- Diving specialists

It is probable that there would be specialist metallurgical and corrosion input and possibly input from the Certifying Authority.

The functions of the review panel would be:

- to provide, from calculations and experience, input into a logic plan for assessing the importance of inspection of each component,
- to make judgements on which items of a list of preferred items shall be inspected,
- to advise on inspection methods,
- to liaise with the Certifying Authority.

It would be very beneficial if the same group were responsible for the offshore inspection management. Suitable quality and reliability audit by outside specialists would also be appropriate.

7.3.4 Philosophy towards Inspection, Maintenance and Repair

Although the basic principles behind the optimisation of underwater inspection are relatively well defined, they may be implemented in a number of different ways, reflecting the operating procedures of the platform Operator. The Operator's approach to a number of different aspects should be clearly defined before attempting to implement an underwater inspection plan. Aspects to be considered include the following:

1. The degree of optimisation desired.

   The Operator should establish its position as to whether a highly optimised inspection plan is desired, or whether the level of inspection should be determined primarily by statutory requirements.

2. Balance between cost and reliability.

   The Operator should determine whether it wishes to implement the lowest cost scheme, or whether they are prepared to accept increased costs in exchange for additional reliability.

3. Importance attached to analytical predictions.

The inspection programme may be planned largely on the basis of analytical predictions of where to inspect, and with what frequency. Alternatively, the planning may be based primarily on empirical rules. The operator should establish the degree to which the results of analytical studies will be incorporated in the planning of the inspection programme.

4. Balance between planned and contingency inspections.

The total inspection effort will, in part, be planned in accordance with the predictions of where the effort should be directed, and in part on a contingency basis (ie. random inspections). The operator should establish the balance which it wishes to strike between these two approaches.

7.3.5 Inspection Priority Ranking

A rational basis is required for the review panel to be able to assess the importance of inspection of a given component.

The URP72 study 2[(1)] report Section 5.2.5, proposed a 'ranking tree' approach which indicated inspection priority for a component as a function of probability of failure and consequence of failure. This approach provides a useful method for the designer of a new structure to ensure IMR costs are minimised.

The in-service inspection planning for a real structure is more complex and a more sophisticated approach is required. The Study 2 ranking tree does not allow decisions to be taken on which components to inspect in a given year, as the inspection priorities will, on the ranking tree basis, vary very little from year to year. It is not to be implied that the operator can therefore justify a repeat performance of an almost identical inspection plan each year.

The assessment of importance of inspection of a component 'j' in a given year, 'n', is a function of:

- consequences of damage,

- mode of failure,
- likelihood of failure,
- cost and reliability of inspection,
- inspection history/certification requirements.

Although a ranking tree could be developed which accommodates all of the above, designing a points system would be difficult. As discussed in 7.3.2, the amount of analysis to define the relative importance of inspection for each component according to the above criteria would be impractical. In any event, judgement would have to be made on some aspects of the ranking (for example, the relative importance of when the component was last inspected) so that the outcome would be a mixture of objective analysis and subjective judgement. If all components were ranked on a single table, the review panel would be in danger of believing that it was making inspection decisions objectively, despite the fact that part of the input is initially subjective. Once a table was listed by computer there would be a temptation to believe that the input parameters were infallible.

Simplification is therefore proposed. Currently, Certification Authorities require a programme which is seen broadly to cover, as separate inspection areas:

- Corrosion condition
- Fatigue conditions (joints and members)
- Member condition
- Marine growth condition
- Scour

As a first stage in simplification, a set of subcategories, such as those above, would be defined and treated separately for review until the offshore work programme is assembled.

It is proposed that an inspection ranking be given on a conventional computer spread sheet database for each category. The subjective and objective weightings for each relevant parameter in the ranking would be exposed and effect of changes in the weightings could be assessed at the touch of a few buttons. Hence, we propose to provide the review panel with a simple working tool, defined as objectively as possible but which gives the review panel the opportunity of estimating the effect of 'judgements' they may be proposing to make in formulating the offshore inspection plan for a given season.

7.3.6 The Role of Detailed Studies in the Optimisation of the Inspection Plan

It may be appropriate to conduct detailed studies to assist in refining the underwater inspection programme. This should in particular be considered either for components which have a high criticality rating where the objective would be additional safety, or for components which are expensive to inspect, where the objective would be cost savings.

The studies discussed here would be based on postulated damage, performed for the purposes of optimisation, and would be undertaken before performing the inspection; these studies should not be confused with those conducted after inspection when a defect has been found, where the main objective would be to assist in a repair/no repair decision. Typical studies which might be performed are as follows:

1. Redundancy.

A preliminary assessment of redundancy would be performed on the basis of engineering judgement by an experienced jacket designer. More detailed studies would require a computer analysis - techniques for performing this have been discussed in Section 6.5. Redundancy studies have become common for bracing members in the splash zone which are vulnerable to boat impacts.

2. Preventative maintenance (strengthening).

Strengthening may be considered for marginal components where the cost of reliable inspection is high. If strengthening is to be performed, the decision should be taken early in the life of the structure, to reap the benefits of the reduced inspection requirements. If the strengthening is applied before any damage has occurred to the original structure, a full loadsharing design may be adopted, with consequent reductions in weight and cost. For this design approach, Certifying Authorities may require that the original structure remains unobscured by the strengthening so that it can be inspected during future inspections.

3. Refined fatigue analyses.

Refinements may be made to improve the accuracy of the S-N fatigue analysis. Typical measures would include finite element studies to determine SCFs for joints which are inadequately represented by parametric formulae, or the use of influence coefficients to account for the effects of the loading in all members meeting at a joint on the net stress. These detailed studies would typically also investigate the variation in fatigue life around the joint with a view to zoning the inspection.

4. Fracture mechanics studies.

Fracture mechanics studies could be conducted to investigate the crack growth and stability characteristics. The basis behind these methods, and the information obtainable from them, have been discussed in Sections 6.3-6.4.

5. Dented member studies.

Dented member studies are traditionally applied to perform an assesment of dents after they have been detected in a subsea inspection. However, there is a strong case for using these studies as a tool to identify those members in which the strength is reduced disproportionately by the introduction of minor dents. Suitable candidates would be compression members, with slenderness ratios in the imperfection sensitive range, in locations which exposed them to impacts from vessels or dropped objects. Methods of performing dented member studies are detailed in Section 6.2.

7.4 Factors Affecting Inspection Priority Ranking

7.4.1 General

The aim in deriving a priority ranking of components is to provide the inspection plan designers with a decision assisting tool. For the tool to be of use, as many input parameters as possible should be formulated on an objective basis. As discussed in 7.3, this is not wholly practicable. The following discussion presents the approach

recommended for each of the major input parameters. The way in which the approach would be used to formulate a real plan is the subject of Section 7.5.

7.4.2 Consequence of Failure

The concept of consequence of failure is closely associated with structural redundancy, and with other considerations which may be difficult to quantify. A points weighting scheme to assist in quantifying the consequences of failure, applicable to a joint, is tentively proposed in Figure 7.2 (2). A similar system could be developed for other classes of component.

The first action in applying this system is to classify the structural component under consideration as primary, secondary or tertiary according to its duty. Primary structure includes the main legs and piles, major bracing members and principal members in the module support frame. The conductor ladders and structure required for installation purposes (launch runners, etc.) would be classified as tertiary, and most of the remainder of the structure as secondary.

The next item in the weighting system is assessment of the redundancy. When applying the test to a brace member at a joint, it is important to assess the redundancy of both the brace member itself and, at the same time, of the chord. Both members should be considered together in this manner since loss of the brace may also involve significant damage in the chord.

The concept of 'likelihood of other short term losses' refers to the case where loss of a component immediately causes consequential damage, such as causing a portion of the structure to fall; this in turn might cause impact damage on lower portions of the structure, and would involve costs for recovery of the item involved.

The concepts of 'immediate risk to life' and 'risk to the environment' are probably more difficult than any other to quantify. Some guidance on the way in which this may be handled, in connection with the derivation of suitable factors of safety for design codes, may be found in Reference (2). The types of component which would involve a

risk to life are mainly associated with topsides structures, or with a significant release of energy (tethers, prestressing bars, high pressure lines, etc).

The items concerning 'risk of lost production' and 'cost of repair' are easier to quantify because they can be measured in financial terms.

7.4.3 Likelihood of Failure

A detailed discussion was given in Section 6 of methods of determining the likely modes and locations of structural failure. For each location, the relative likelihood of failure is quantified using the points system given in Figure 7.2 (3).

The likelihood of failure of a component is a function of:

- design life and time in service
- material quality
- fabrication quality
- rate of corrosion
- existing defects
- marine and platform operations.

7.4.3.1 Design Life: Use of conventional techniques

The following discussion is broken down into those factors which are functions of length of time in service (7.4.3.1 and 7.4.3.2) and those incidences of damage which might occur at any stage in a structure's lifetime, ie. random damage (7.4.3.3).

Most of the above factors are accounted for in design and, as a corollory, a well designed structure can expect no damage during its design life other than from random accidental damage. Of course, this expectation must not be taken too literally and studies prior to commencement of a lifetime inspection programme will be effective in identifying areas most worthy of attention (high consequence of failure components). Older structures in the North Sea encountered

damage, particularly from fatigue, which had not been anticipated in design. This led to improvements in approach to fatigue design and recent studies have shown that structures behave reasonably well according to S-N curve type reanalysis expectations. Nevertheless, the level of experience of the reanalysis contractor is crucial in designing a reanalysis model which will identify the areas susceptible to premature fatigue. Real fatigue cracks are often the result of poor fabrication practice, poor materials or at locations simplified in the fatigue analysis (eg. the parametric derivation of stress concentrations). Consequently fatigue analyses should only be taken to provide guidance.

Again, we must rationalise our problem to a manageable size. For fatigue consideration, the suggested first cut approach is:

- execute fatigue analysis of global structure
- identify other areas in the structure susceptible to fatigue but excluded from global analysis (eg. access windows in braces, appurtenance connections)
- categorise components into broad classes, eg:

  - class 1; fatigue life $< \frac{1}{2}$ x design life
  - class 2; $\frac{1}{2}$ x design life $<$ fatigue life < 5 x design life
  - class 3; fatigue life > 5 x design life

- carry out more detailed fatigue analyses (eg. FE shell analyses) on complex joints in class 1. It is worth remembering that if by so doing, a class 1 component can be reclassified, then the analysis cost will almost certainly be outweighed by savings of a single inspection of that component.

Hence it is proposed that FE studies are executed before planning future inspection, and certainly before damage is discovered.

7.4.3.2 Design life: Use of advanced techniques

The discussion above relates to computation of design life on an S-N curve basis. The actual development of a crack, usually developing from a surface defect or defects, does not cause 'failure' until it

has progressed to a point where the component can no longer sustain its required static loading, ie. until it is 'unstable'. Conventional techniques assume that the 'safe limit' (called the design life) of a crack is coincident with the crack propagating through the thickness of the component.

Techniques based on fracture mechanics (FM) discussed in Section 6, offer a more systematic approach to assessing the course of crack development.

The way in which cracks develop during different parts of their life cycles varies according to geometry, loading and material properties. What the inspection designer needs to know is 'when must I inspect to ensure that I identify a crack (and have time to execute remedial procedures) before component failure?' rather than 'when must I inspect to ensure I identify a crack before it goes through thickness?' Section 6 has demonstrated that confidence in FM is improving as the techniques are benchmarked against relevant test results, but that there is still a paucity of data on post through thickness behaviour of tubular joints.

It is impracticable to postulate all possible cracks and calculate probable growth rates and stability. It is proposed that the route taken as 'first cut' in 7.4.3.1 be followed and detailed FM analysis be carried out on components where premature cracks are anticipated and where the consequence of failure is serious.

Hence it is proposed that FE studies are executed before planning future inspection, and certainly before damage is discovered.

7.4.3.3 Other damage

Although much of the testing work to support the design of tubular structures has been retrospective, service experience of static load failure due to service loading is very small. This is no cause for complacency; the behaviour of tubular joints is complex and some early design assumptions have now been proven unconservative. Nevertheless, it is reasonable to assume that structures designed to

current standards are unlikely to fail under static loading other than from the following causes:

- exceptional loading (eg. earthquake, impact, temporary or permanent increases in topsides loading, unexpected marine growth).

- inadequate corrosion protection or allowance

- faulty materials or workmanship.

If the inspection designer has reason to doubt the quality of his structure, or components thereof, higher weighting can be given to their inspection priority. The most common damage problem offshore to date (excluding fatigue) has been damage from impact, either from floating vessels or from dropped objects, although other damage sources (eg. member crushing under the weight of drill cuttings) has also occurred.

Primary components susceptable to impact damage could be assessed for redundancy before planning inspection. This is discussed in Section 6.5. It is almost certain, in view of the infinite range of damage that could be caused in this category, that the inspection planners would opt to carry out systematic damage assessment only when a component is found to be damaged, with a view to planning subsequent inspection philosophy. Techniques for addressing minor and major damage are discussed in Section 6. The likelihood of failure in the light of the damage would be assessed as well as the consequence. The likelihood is a function of the type of damage, load regime and possible failure modes of the component.

For the case of ultimate load failure, there is generally little evidence of distress until a local failure has occurred, and this may be detected by general visual inspections or by structural monitoring. Failures of this type are usually caused by exceptional loadings, such as boat impact or from dropped objects; inspections should thus be carried out as soon as an incident is reported, or if other evidence is encountered, such as unexplained debris on the seabed.

7.4.3.4 Other considerations

There are statistical uncertainties associated with all the factors which contribute to the inspection programme. For example, the maximum load in a member may vary from the predicted maximum load and the strength of a member is also subject to variation about a mean calculated strength. There is a finite possibility that the actual maximum load may exceed the actual strength of a component, as shown in Figure 7.3. Computation of likely distributions for all variables represents an impractically large computing problem. In practice, finite values would have to be assigned to each parameter and an assessment made mathematically of the likely range of real fracture criticality based on sample data (benchmarking).

The problem can and should be handled practically by carrying out random inspections on non-critical components. This should be easy to accommodate in a real inspection programme; components would be selected on the basis of convenience to vessel location and inspection priorities on fracture critical components.

7.4.4 Inspection History and Certification Requirements

The considerations of certification requirements are, strictly, irrelevant to the development of an optimised inspection strategy. Nevertheless, the certification system is an important part of the quality plan and development of an optimised strategy in conjunction with the Certifying Authority would be rational.

The following historical information must be accounted for in developing an optimised plan:

- quality of records,
- inspection history and findings,
- when last inspected.

The quality of records and the inspection history will carry a fixed weighting through the life of the structure until such time as damage is identified.

It is obvious that, for two components with equal priority in a structure, it is preferable to examine in year (n) the component which was not inspected in year (n-1).

Bearing in mind that our aim is to give the review panel a ranking of components for inspection in year 'n' (ie. a ranking which changes from year to year), a simple weighting system is required according to historical inspection timescale. As a first cut, an additive factor is proposed to ensure that components for consideration in year 'n' which have not been inspected recently appear high on the list.

A possible ranking for components would be:

	Factor
• Inspected last year	add 0
• Inspected 2 years ago	add 1280
• Inspected 3 years ago	add 2560
• Inspected 4 years ago	add 3840
• Inspected 5 years ago	add 5120
• Inspected more than 5 years ago	add 6400 to cumulative ranking

The value of the weighting has been derived on the premise that the average component should be inspected every 5 years under normal circumstances. The 'average' score under likelihood of failure weighting, X, is 80, and similarly for the consequence of failure weighting Y. The value of 1280 is obtained from the product of $(X)_{ave}$ and $(Y)_{ave}$ divided by 5,

ie. $$\frac{80 \times 80}{5} = 1280$$

7.4.5 Cost and Reliability of Inspection

It is not the purpose of this report to assess the reliability of independent techniques but rather to highlight the importance of a thorough understanding of the reliability of techniques which are adopted and show how they should be treated. The reliability of both technique and operation must be considered.

Before choosing an inspection technique for a specific component, the planner must decide what quality of information he requires. For example, if he knows that a through-thickness crack can be tolerated in a specific component he may opt to use flooded member detection (FMD) with relatively low cost and high reliability rather than using MPI (high cost, low reliability). If loss of the components is not critical, visual inspection might be selected.

The questions which should be asked in applying a specific technique to a specific component are:

- what quality of information is required?
- what is the cost of inspecting by this technique?
- what is the reliability of this technique?
- what is the cost of inspecting to give a satisfactory confidence level that the findings are accurate?
- is this cost commensurate with the inspection priority for this location?
- what is the cost of repair/strengthening for a specific location?

If the cost of repair is lower than the cost of identifying a defect before failure and the component is non essential to overall integrity, it is self- evident that detailed inspection is not cost effective. Detailed NDE should be replaced by visual inspection (provided that failure will be manifest).

Strengthening should be considered where:

- cost of inspection is high
- reliability of inspection is low
- consequence and probability of failure are high.

Strengthening (preventative maintenance) is usually cheaper than repair.

In circumstances where inspection reliability is low in a component of interest, repeated inspection in a single inspection season should be considered, using different operators and techniques if possible. Usually a large fraction of cost of inspection is attributable to

cleaning. To clean once and inspect 5 times in a given year is likely to be more cost effective than cleaning 5 times and inspecting 5 times in successive years to give the same overall reliability. This expedient should only be used for components with a low likelihood but high consequence of failure, to minimise the chance of missing the complete development cycle of a critical crack.

As discussed in Section 6, historical work on crack growth has concentrated on crack development prior to through thickness. This is changing slowly as fracture mechanics approaches gain imputus from improved techniques and cheaper computing. This trend is of great interest to offshore operators, some of whom are already replacing expensive, less reliable MPI by cheap, reliable FMD methods, although this approach means that there is no chance of discovering crack-like defects before they are through-thickness. Nevertheless at least one operator (see Section 5) considers that his overall chance of discovering an important defect is greater using FMD as a far greater percentage of the overall structure can be covered for a given cost. This approach is particularly worth persuing on new structures, where crack like defects are not anticipated. More detailed inspection of joints is appropriate where reanalysis or service history indicates high likelihood of premature cracking and inspection is still cheaper than repair.

7.5 The Optimised Inspection Strategy

The approach that has been developed implies, rather than an inspection cycle, a unique programme each year designed on the basis of all available information.

During the design of the inspection plan for year 1 an initial ranking of components is carried out, which will highlight the components worthy of special consideration. The likelihood and consequence of failure of these components will be investigated immediately and, where appropriate, new rankings will be assigned. This revised ranking table will be used to design the first inspection programme and the rankings will alter thereafter in the light of inspection findings. In this way, new priorities will be highlighted each year.

The full procedure proposed is detailed below and is presented in a flowchart, figure 7.1.

Activity (1) formulate the IMR Strategy

The operator's overall approach to IMR should be formulated by the Review Panel, and this should be incorporated in a policy document which would act as a guide for the implementation of the inspection plan.

Activity (2); preliminary 'criticality' ranking

The optimised inspection programme is based on:

(1) consequence of damage
(2) likelihood of damage
(3) Cost and reliability of inspection
(4) inspection history.

The first step is to divide the components into inspection groups. For a jacket structure, these might be:

- inspection group 1: members
- inspection group 2: joints
- inspection group 3: foundations

For each group the next step is to obtain the inspection weighting for each component as a function of consequence and likelihood of damage. For a new structure there is no 'inspection history', so inspection weighting is identically equal to the 'criticality rating'.

The preliminary inspection ranking should be performed by evaluation of the weighting factor Z, as shown in Figure 7.2 (1). The first step in this is to identify potential failure modes and locations for each component. It is then possible to evaluate the weighting for likelihood of failure, X, from Figure 7.2 (3). Determination of the factors for consequences of failure (Figure 7.2 (2)) enables the preliminary ranking to be completed.

The reasoning behind the points systems has been given in Section 7.3, and notes on their application are given below:

It is noted in Section 7.4 above that for a first cut, consequence of failure (fracture criticality) would be assessed subjectively. Item A (Figure 7.2(2)) is linked strongly with items B, C and D to give the designer's assessment of the component's fracture criticality. Items D to G address risks other than structural as a result of damage to a specific component and would normally score average. Exceptions would be, for example, damage to risers, which would score high under F and G; loss of an MSF member which would score high under E.

An obvious danger is that different people will make different subjective judgements in identical situations. This must be minimised by:

- making written guidance on how to assess each consideration,
- ensuring that one person makes final judgement on all components, for each consideration.

For example, one engineer should make the assessments of the degree of redundancy of all components in a group. It is less important that another person makes all the judgements on, say, immediate risk of lost production; although this might sway the emphasis slightly towards or away from the importance of these risks relative to the structural considerations, the overall ranking will be little affected. The rules for ranking could form an annex to the policy document devised in Activity 1.

An 'average' component will score 80 on this table and the more critical components will score commensurately higher.

The likelihood of damage (figure 7.2(3)) can be assessed somewhat more objectively, which is probably why inspection is largely designed on this basis at present. For fatigue in joints, the approach of 7.4.3.1 is proposed as a first cut. For members, the fatigue class would be 'average' except for members with access windows or appurtenance connections, in which case they would be placed in class 1 (figure 7.2(3)). For a new structure, confidence in the assessment would be 'average' for all components until detailed studies (see below) are performed.

Items I_j and S_j (Figures 7.2(2) and (3), respectively) would be given a 'medium' or 'class 2' rating unless the component 'j' is not represented in the structural analysis model, in which case 'low' or 'class 3' rating would be applied.

For each inspection group, a ranking of component is computed by obtaining the product of consequence of failure (Y) and likelihood of failure (X) for each component.

First cut inspection priority ranking = (Y) x (X) = 'criticality rating'.

The assessments would be filled in on a proforma compatible with the spread sheet to be used. An example spread sheet layout is presented in Figure 7.4.

If this inspection procedure is to be applied to a new structure, there will be no in service inspection history and nominally no corrosion. Application to existing in service structures requires that the ranking be compiled using current knowledge of the structure. Time since last inspection W, would also have to be included (see 7.4.4) and the procedure that should be adopted is analagous to activity 6, inspection year 'n', hereunder.

Activity (3) assess inspection methods

For 'assessment of inspection methods' the following categories should be isolated:

CATEGORY	CONSEQUENCE OF FAILURE	LIKELIHOOD OF FAILURE
1	Low	Low
2	Low	High
3	High	Low
4	High	High

TABLE 7.1

This can be done automatically by computer once the information required in Figure 7.4 is complete.

Tables of possible inspection methods against categories would be devised, eg.

METHOD	CATEGORY			
	1	2	3	4
a; Visual Inspection, ROV	✓			
b; Close Visual Inspection, Diver	✓	✓		
c; *MPI Classification 1		✓	✓	✓
d; *MPI Classification 2			✓	✓
e; Flooded Member Detection	✓	✓		

TABLE 7.2a; Joints

*MPI Classification 1; clean and inspect once

*MPI Classification 2; clean, and inspect three or more times; different divers, modified procedures

METHOD	CATEGORY			
	1	2	3	4
a; Visual Inspection, ROV	✓	✓	✓	
b; Close Visual Inspection, Diver		✓	✓	✓
c; *MPI Classification 1				
d; *MPI Classification 2				
e; Flooded Member Detection	✓	✓		

TABLE 7.2b; Members

There is no difficulty in assigning a column in the database (see Figure 7.4) to the inspection category.

Desk and laboratory studies would then be undertaken (on selected components) for each method to assess the cost of using that technique to give suitable confidence that the inspection will identify defects. Characterisation of the defects is a separate topic; extra money would be justified inspecting a single defect in considerable detail to allow sensible damage assessment.

Although these studies on inspection techniques are outside the scope of this report, it is worth noting that the investigations would encompass:

- reliability of the techniques
- cleaning and inspection costs as a function of:
  - depth
  - access
  - temperature

Level of confidence required would increase from category 1 to 4; it is suggested that targets of 80%, 85%, 90% and 95% reliability be set for categories 1, 2, 3 and 4, respectively. This is independent of frequency of inspection and relates to reliability of inspection in a given season.

We now have the following information for each component:

- ranking as a function of consequence and likelihood of failure (Activity 2)
- inspection category (see above)
- cost weighting for inspection which accounts for:
  - inspection category
  - confidence level
  - depth
  - temperature
  - access.

The product of criticality rating and cost weighting is then computed. This 'compound weighting' gives a measure of the probable cost of inspection of each component during the lifetime of the structure.

Activity (4) Damage tolerance studies; undamaged structure

It is self evident that those components with very high 'compound weighting' (ie. those with a very high life time inspection cost expectancy) are likely to benefit most from detailed assessment. There are two reasons for carrying out further studies before damage occurs on components with high weightings:

- to increase the level of confidence in a judgement which has been largely subjective
- to reduce overall inspection cost by reassessing the inspection category (with implications on selected inspection method and therefore on compound weighting).

Sections 6 and 7.4.3.2 describe methods which could be applied. Damage tolerance studies are likely to be cost effective in terms of inspection savings for category 4 components. The rate of return on investment in study would decrease with the lower categories. It is suggested that the cost effectiveness of studies in category 4 be assessed on realistic case studies before progressing to lower categories.

Activity (5) Revised ranking

Following detailed studies on specific components (or like sets of components) revised input parameters are entered onto the main spread sheet (see Figure 7.4). Components covered by detailed assessment now have the 'confidence' penalty of "I" and "S" (figures 7.2(2) and (3)) reduced to 'high' or 'class 2' rating respectively.

The ranking for each inspection group is then recomputed.

Activity (6) Inspection, year 1

For new structures, no weighting according to previous history is required. Hence, the inspection priority ranking (Y) x (X) gives the order of priority for inspection in each inspection group. Practical considerations will prevail on the decisions taken by the review panel on components which are to be inspected. It is to be expected that, in early years, high priority will be given to ensuring that:

- damage from installation operations is identified
- all appurtenances pertaining to fabrication, erection and installation are identified and recorded on as 'installed' drawings.

This represents a considerable volume of work and will almost certainly limit the amount of routine inspection as a consequence. On the other hand, damage relating to life in service (fatigue life) should not yet be evident and the emphasis of inspection need only be on category 4 components. If it can be shown that components with high consequence and likelihood of failure can tolerate through thickness cracking, the approach of using FMD (or some other technique which only identifies through thickness cracking) could be used although this should be treated cautiously; a crack which has developed so quickly to through thickness is almost certain to exhibit a short life to component failure. Detailed inspection of the most critical joints might be considered in preference to FMD; the ideal would be to use both approaches.

Inspection, year 2

The design of the routine part of the inspection plan for year 2 uses the ranking (Y) x (X), modified by the findings from year 1 and by the fact that inspection of certain components took place in year 1. Firstly, all priority scores used in year 1 will be raised by 1280 in year 2 (see 7.4.4) except for those components that were inspected in year 1.

Secondly, findings from components inspected in the first year would be incorporated into the spread sheet rankings by changing the relevant weightings. For instance, a component showing unexpectedly high marine growth might be reassessed under item R; (Figure 7.2 (3)).

Hence, when the computer is asked to rank components for inspection in year 2, difference priorities will be identified, on which the inspection designers can make judgement.

Inspection, year 'n'

In general, the rankings performed each year identify the components requiring inspection, with rankings from 'mandatory' to 'desirable'. An operational review should be conducted to determine possible execution plans

to perform the required inspections. A flowchart for this, which assumes the use of a DSV for diving operations, is given in Figure 7.5. The result of this review will be an execution plan which permits inspection of all components with a mandatory inspection requirement, and which gives the widest possible coverage of other locations with a high ranking, and for contingency inspections.

Let us suppose that inspection according to the methodology developed above has progressed smoothly with changed database priority ratings selected in the light of experience of a number of years. Some minor defects come to light. Damage assessment now comes in to play in the more straightforward sense. The stages are:

- characterisation of the damage (by practical measurement and reference to historical data).

- analytical appraisal of the damage and its effect on the structure (damage assessment).

- decision on whether or not to repair immediately. The decision will be based on

  - expected time to component failure
  - consequence of component failure
  - comparison cost of reliable inspection against cost of repair.

If the damage does not need immediate repair, the component's ranking will be reappraised. Category 'N' (Figure 7.2 (3)) will increase to ensure that the component has high visibility on the ranking, even though 'I' and 'S' (confidence) on Figures 7.2 (2) and 7.2 (3), respectively, will have lower values.

If a component or group of components annually appears near the top of the priority rankings and yet no damage is discovered during inspections, it can be considered a candidate for assessment studies, to ensure that its ranking is, indeed appropriate. Review of the rankings table (Figure 7.4) will reveal which parameter is giving rise to the high ranking and a change in parameter importance may be required. In this way, the ranking procedure itself is refined and tuned in the light of operational experience.

Practical Considerations

It has been emphasised that the ranking procedure is a tool for the inspection review panel, not a list of instructions. The actual steps in designing an inspection plan for a given year are:

- computer rankings.
- identify components which must be inspected.
- decide DSV locations and timescales to allow those components to be inspected.
- determine likely additional dive time that will be available.
- select other components with high ranking which are convenient to the DSV programme (these are the 'should inspect' components on Figure 2.2).
- select other components to inspect which are not deemed critical, but are convenient to the overall programme (see Section 7.6.4). Simple techniques will be adequate (eg. visual, FMD) unless unexpected damage is identified.

The methodology described above is not intended to be definitive. The aim is to show how inspection planning taking into account cost savings which could be made might be tackled by assessing the importance that damage would have before damage is located.

Strengthening before damage is identified might also be cost effective in areas which are critical and expensive to inspect reliably.

REFERENCES

1. CIRIA UEG
Project URP 72/S2 Implications of Design to Inspection and Maintenance of Offshore Installations and Pipelines. September 1985.

2. Baker M J
'Rationalisation of safety and serviceability factors in structural codes' CIRIA Report 63, July 1977.

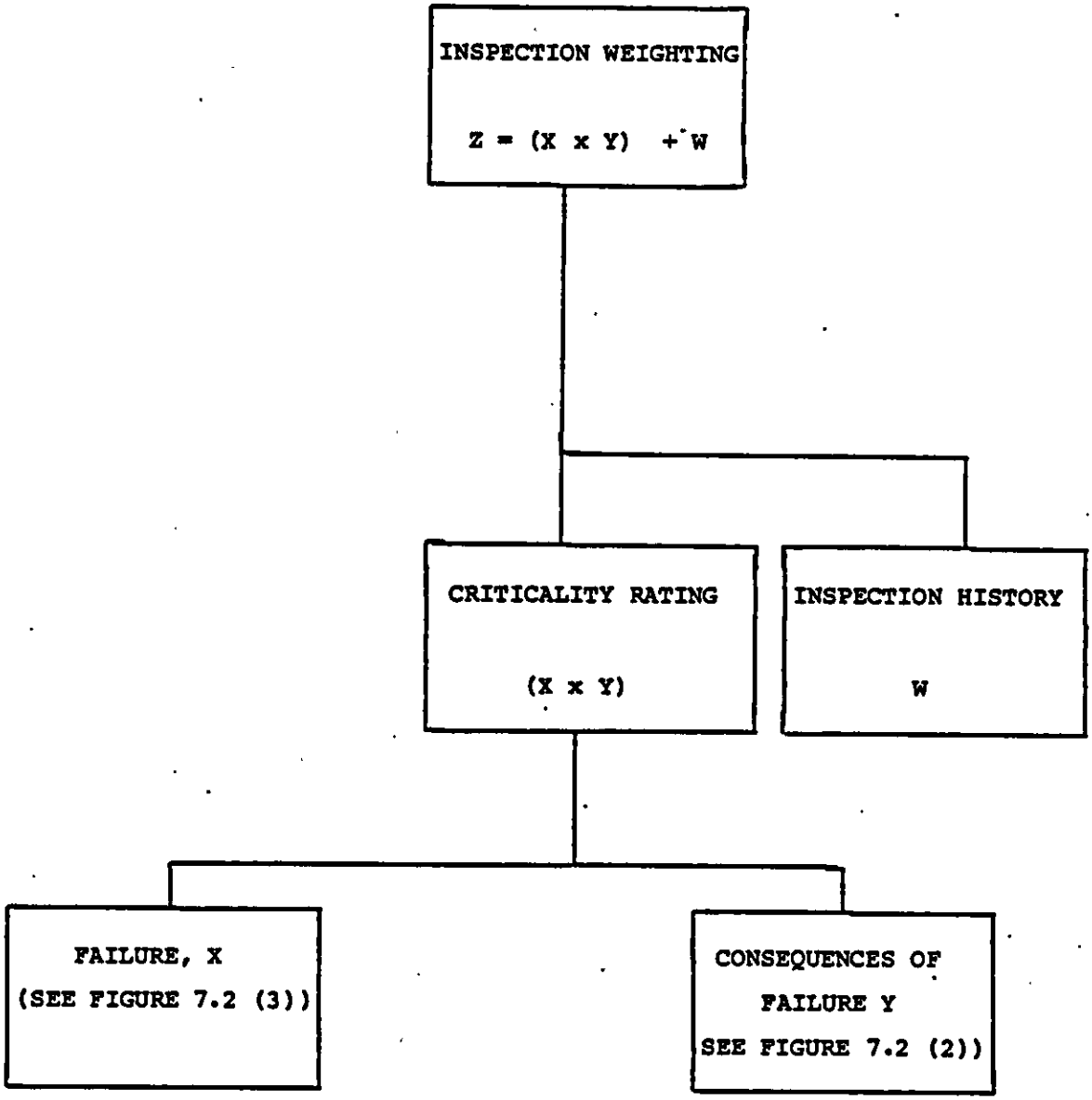

COMPUTATION OF INSPECTION WEIGHTING, Z.

URP 72; S4 DAMAGE ASSESSMENT

FIGURE 7.2 (1)

For joint 'j' CONSEQUENCES OF FAILURE, $y_j = A_j + B_j + \ldots\ldots + I_j$

Where:

SYMBOL	INFLUENCING ITEM	RATING VALUE		
		HIGH	MEDIUM	LOW
A_j	is component • primary (high) • secondary (medium) • tertiary (low)	40	10	1
B_j	Redundancy of brace	1	10	40
C_j	Redundancy of chord	1	10	40
D_j	Likelihood of other short term losses	20	5	1
E_j	Immediate risk to life	100	10	1
F_j	Immediate risk to environment	100	10	1
G_j	Immediate risk of lost production	50	10	1
H_j	Cost of repair	20	5	1
I_j	Confidence in assessment	2	10	40
y_j	(Medium rating)		80	

TENTATIVE WEIGHTINGS
URP 72; S4 DAMAGE ASSESSMENT

FIGURE 7.2(2)

For joint 'j' LIKELIHOOD OF FAILURE, $X_j = K_j + M_j + \ldots\ldots + S_j$

Where:

SYMBOL	INFLUENCING ITEM	RATING VALUE		
		CLASS 1	CLASS 2	CLASS 3
K_j	Fatigue category	40	10	1
M_j	Susceptibility to damage	20	5	1
N_j	Defect known to exist*	100	35	5
O_j	Corrosion condition at last inspection	20	5	1
P_j	Material	20	5	1
Q_j	Fabrication quality	20	5	1
R_j	Excessive marine growth	10 high	5 med	1 low
S_j	Confidence in assessment	2	10	20
			—	
X_j	(medium rating)		80	
			=	

*Damage assessment studies in addition to reclassification

TENTATIVE WEIGHTINGS
URP 72; S4 DAMAGE ASSESSMENT

FIGURE 7.2(3)

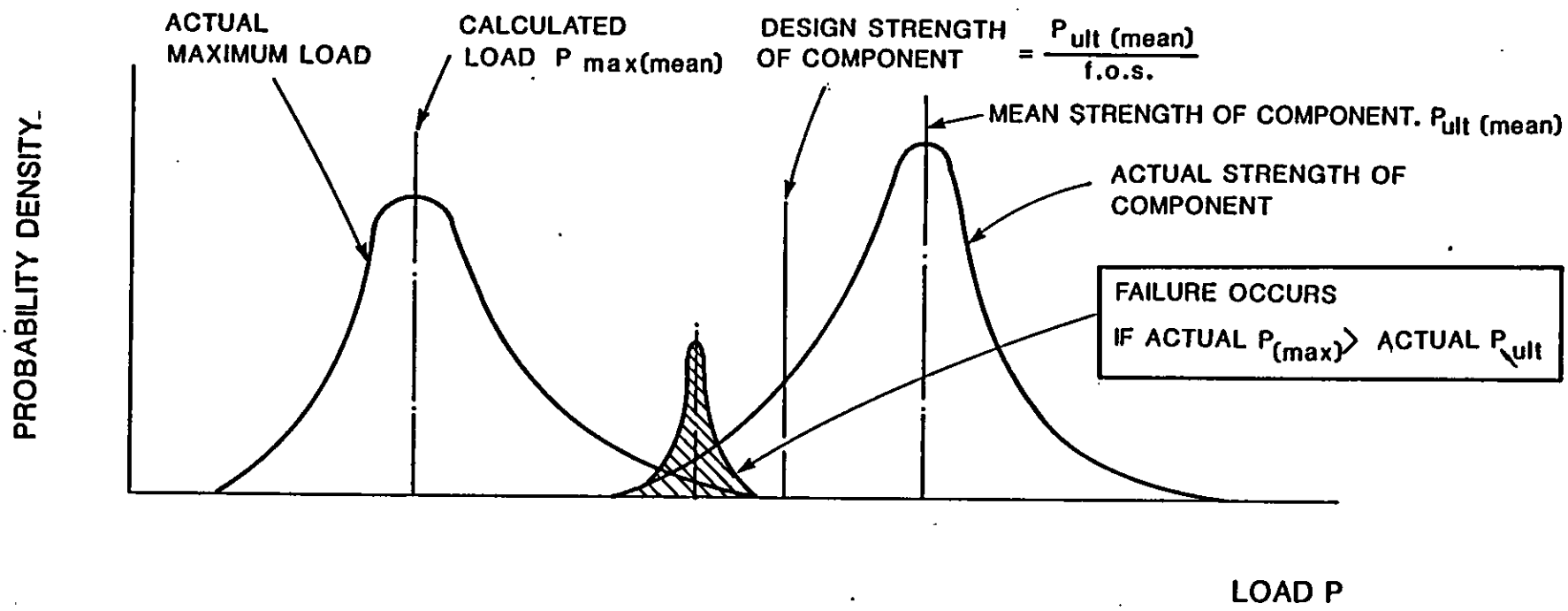

RELATIONSHIP BETWEEN LOAD CARRYING CAPACITY AND LOAD IN A COMPONENT

PROJECT UPR 72 : STUDY 4

INSPECTION PLANNING , THE ROLE OF DAMAGE ASSESSMENT

WIMPEY OFFSHORE REPORT No. WOLI09/86

FIG. 7.3

JOINTS - END OF INSPECTION YEAR 19 9

JOINT	DESIGN	REFERENCE DRAWING	ACCESS (1-5)	LAST INSPECTED W	CONSEQUENCE OF FAILURE										LIKELIHOOD OF FAILURE									RANK (Y) x (X) + W	INSPECTION CATEGORY	NOMINAL PRIORITY
					A	B	C	D	E	F	G	H	I	Y	K	M	N	O	P	Q	R	S	X			

URP 72; S4 INSPECTION PLANNING

THE ROLE OF DAMAGE ASSESSMENT

FIGURE 7.4

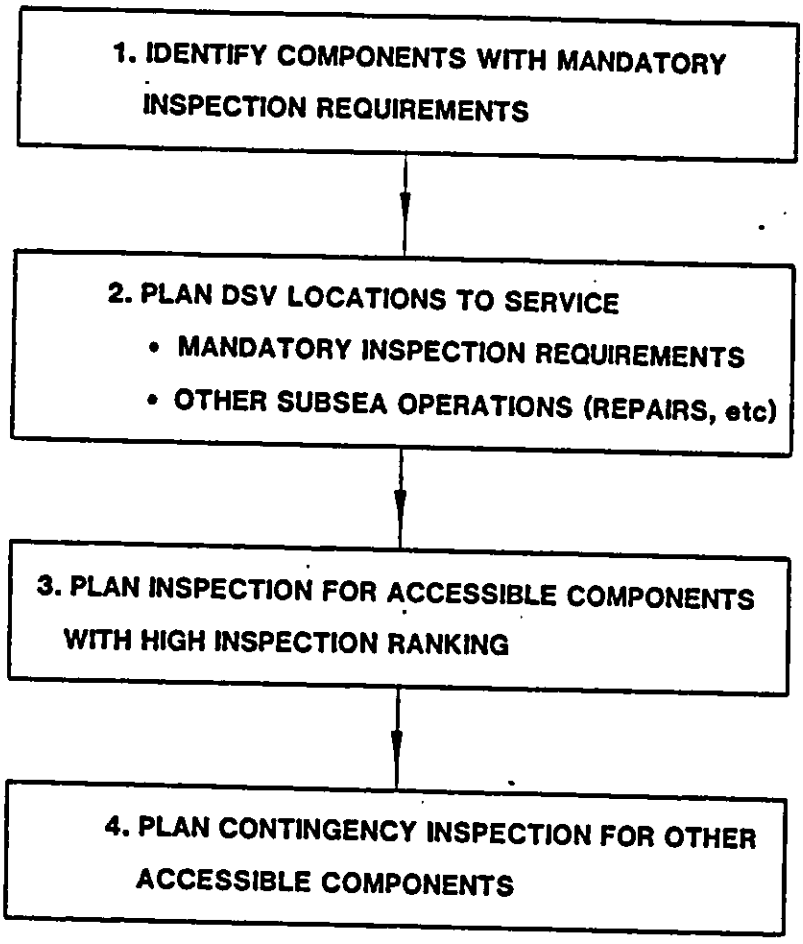

FLOWCHART FOR OPERATIONAL REVIEW

PROJECT URP 72 : STUDY 4 INSPECTION PLANNING THE ROLE OF DAMAGE ASSESSMENT	REPORT No. WOL 109/86 FIG. 7.5

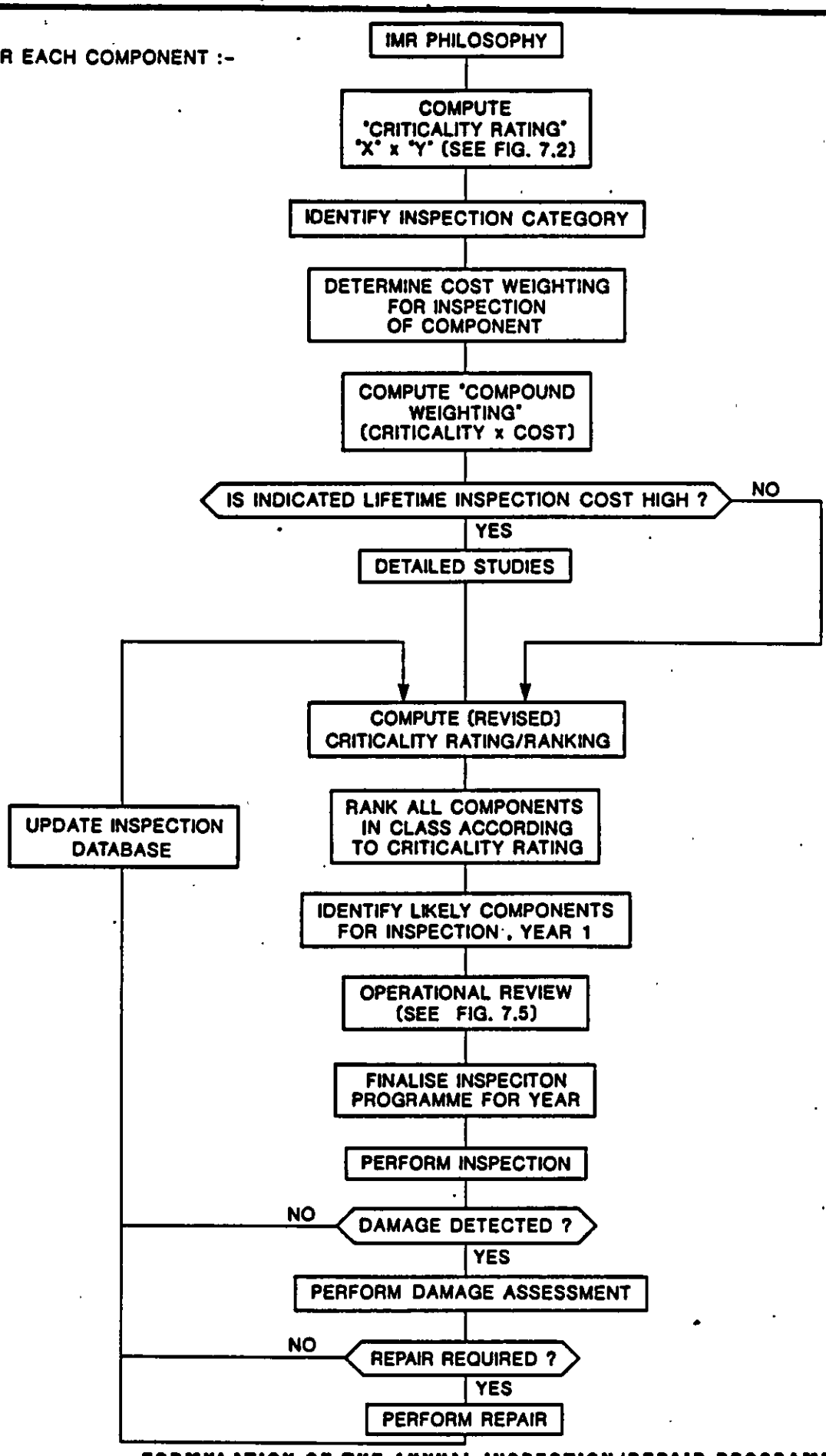

FORMULATION OF THE ANNUAL INSPECTION/REPAIR PROGRAMME

PROJECT URP 72 : STUDY 4 **INSPECTION PLANNING** **THE ROLE OF DAMAGE ASSESSMENT**	**REPORT No. WOL 109/86**
	FIG. 7.1

8. APPLICATION OF AN OPTIMISED STRATEGY

8.1 Implementation of the strategy

Section 7 shows how a system of inspection planning could be developed from the philosophy described in this document. The influencing items and, more importantly, the rating value (reference figures 7.2(2) and (3)) require much more systematic review before adoption to a real structure to be inspected.

Nevertheless, the approach could be valid and its effectiveness is illustrated in the following example.

8.1.1 Worked example

For the purposes of this exercise, part of a steel jacket first subsea horizontal framing panel has been selected. This is an area of great inspection interest as it may well suffer, during the lifetime of the structure, both fatigue damage and impact damage from dropped objects or ship collision.

The frame is shown in Figure 8.1 and some of the joints, as indicated, have been selected for ranking.

Figure 8.2 shows the rankings which would be applied to each joint on completion of inspection in year 'n'. The 'last inspected' column has already been amended to give priorities for next years inspection. Before looking at the ranking, it is worthwhile reviewing the numbers which have contributed to it.

Firstly for the components considered in the example (joints) it is assumed that loss of the chord as a result of joint failure would be serious, as each chord member is primary (item C) at the joints under consideration. Where the brace is secondary, in the conductor guide frame area, a lower rating is given (item B). Item A is based on the subjective decision of an experienced designer and concerns the role of the component in the overall frame work of the jacket. The time

taken to further losses, which would result from failure of a component are given a weighting under item D. E, F and G are assessments of the possible consequences, other than structural, due to failure of a component. For example, a failed riser support or conductor guide frame member increases the risk of lost production and environmental damage. Cost of repair (H) would be assessed subjectively. Much more detailed attention would be given to components which would be very expensive to inspect and which have a high likelihood of failure (see Section 7). Items I and S refer to the confidence made in the assessment. A rating of 10 implies a subjective assessment supported by representation in the structural model. A higher rating implies that the component is not accurately represented in the structural model. When a detailed assessment of a particular component is undertaken (finite element analysis, redundancy analysis) the confidence in the assessment increases and a low weighting is given.

Likelihood of failure, X, can be assessed more objectively on the 'first cut' than the consequence of damage. Item M refers to susceptibility to accidental damage. Item N, 'defect known to exist' gives a very high weighting to X. It is proposed that whenever N is 100, an asterisk (flag) appears in the 'inspection category' column. A damage assessment is almost certain to follow; if remedial action (eg. crack grinding) is undertaken as a consequence, the 'N' rating will reduce to 35. This is illustrated by joint 31 in the example and its inspection priority is higher than the almost identical joint 29. P and Q refer to the quality of available data as well as the content of that data - ie. scant records will confer a higher rating than well documented evidence. R will only be given a non-average weighting if the marine growth is different from expectations. Normally, marine growth assumptions are incorported in design and these should be understood and taken into account by the inspection designer.

The ranking is computed as (Y) x (X) + (W) (see Section 7) and is listed in descending priority order. The inspection category was defined in Section 7, Activity (2).

Let us examine the frame of our example in Figure 8.1. The year now is 19 x 8 and the structure was installed in 19x0. A reassessment of the structure was carried out in late 19x6 and new weightings were allocated to all components. Part of the reassessment involved detailed appraisal of critical joints at legs. Hence joints 1 and 2 carry high confidence in categories I and S. Reappraisal of the conductor guide frames gave the model shown in Figure 8.1 after indications were discovered in joints 26 and 29 in year 19x6. The cracks were ground out and the reanalysis shows that there is no reason to expect premature failure. Poor fabrication quality was the likely cause of the defect in joint 31. The indication at joint 26 may have been erroneous as surface grinding and repeat MPI gave a clean bill of health.

Last year, (19x7), joints 1 and 2 were inspected and found to be free from damage. This year joints 37, 39, 47 and 48 were inspected. 47 and 48 were of particular interest as the reanalysis indicated low fatigue lives (less than half the design life). Modelling in the reanalysis made conservative assumptions but inspection was carried out nonetheless, under the 'should inspect' criterion. A crack indication was found in joint 47 late in the season.

At the end of the 19x8 inspection season, the 'W' ratings were increased to give next years values and reranked in the order shown on Figure 8.2.

The first action to be taken is a review of items justifying further study. Joints 31, 33, 35 are adjacent (inspection ease) and earlier damage in joint 29 will not discourage the panel from inspecting these components next year. Joints 47 and 48, however, would be expensive to inspect regularly and it is decided to undertake a detailed study to assess the inspection priority. This study is shown in Example 2 Appendix 2. The presence of a crack indication in joint 47 highlights a possible requirement for action before the winter. Fortunately, the study is able to demonstrate that the small crack is stable under all loading conditions and will propogate only very slowly.

The working (unshown) also demonstrates that joint 48 has a fatigue life in category 2. Joint 26 is held near the top of the ranking as a defect is known to have existed. Its position alerts the review panel to the increased likelihood of further damage. Joints 3 and 4 are primary and are due for inspection in 19x9. It can easily be seen that the lowest inspection priorities are those with low consequence and low likelihood of failure (category 1). In the middle of the table are those joints in inspection categories 2 and 3 and the decisions on which joints to inspect will be a function of both required confidence and cost.

In the event, the review panel selects joints 47, 48, 31, 33 and 35 and 4 for inspection in 19x9.

The defect at joint 47 showed no discernable size increase and was removed by light grinding. 48 showed no defect. 31, 33 and 35 received a clean bill of health. The area around joint 4 had experienced exceptional marine growth. The changes at the end of 19x9 are shown on Figure 8.3. Studies in the winter following 19x9 might concentrate on the conductor guide frames; no significant damage is materialising yet the frame joints have high rankings. An assessment which will allow reduction in the column 'I' would be worthwhile. If this were done before the next inspection season commenced a modified listing could be used.

8.1.2 Comment

It is evident that the subjective weightings suggested in this exercise can have profound influence on the rankings. The keys to using this methodology would be:

- consistency of interpretation; all rules for allocation of numbers must be written. The review panel personnel will change!
- centralisation of data input; a single micro based record with password access to a single user would be best

- review periodically to ensure that the weightings of relevant factors are realistic

- Recognition of status of the rankings; that it is a tool not a dictator

- Systematic update.

Of course, a real structure would have a much larger number of joints. Likewise, similar lists would exist for members, foundation condition, corrosion condition. It may well be that further simplification of the system shown above would be required. Nevertheless, the absolute ranking of a component is less important than its approximate position in the list; the ranking will be pointing to groups of components which the review body should be reviewing.

Actual damage would, in practice, be dealt with in a much more systematic way than is apparent here. A column 'N' rating of 100 automatically highlights a problem. If, for example, inspection of the crack and grinding had not solved the crack problem on joint 47, then the rating would stay at 100 and the joint would still be a special case for consideration, even if the review panel are confident of the crack's stability (as demonstrated in Example 2).

8.2 Application to other subsea components

Jackets are fairly defect tolerant; even if prediction errors are made in the likelihood of component failure, there is not necessarily an important consequence before remedial action can be taken. Hence, the strategy for inspection planning described above can be used cost effectively.

On the other hand pipelines, remote completions, templates, tethers etc. have little or no redundancy; the consequence of damage is likely to be serious whether or not the likelihood of damage is high.

How, then, can damage assessment be applied to non-redundant subsea installations? There are two scenarios:

- installation undamaged
- one or more installation components damaged.

For undamaged installations the approach postulated in Section 2, and shown in Figure 2.2 is proposed, ie;

1. identify fracture criticality of a component

2. assess relative costs of inspection and protection to give required confidence levels for fracture critical items.

Unlike jackets, this methodology is simple to apply as components are much less likely to suffer from widely fluctuating loads. On the other hand, almost all components are likely to be found fracture critical and the inspection designer is still faced with item 2. Non-fracture critical items can be inspected on a component failure basis, eg. visual inspection, FMD or load indicator (tethers).

The relative cost of inspection and protection is likely to be taken into account by the installation designer. He must also investigate the cost of repair of a protected component as against an unprotected component in the event that failure arises from an unexpected cause. For example, a pipeline may be buried in a shipping lane to protect it from damage from dragnets, anchor chains, dropped debris etc., but a pin hole leak in that pipeline will be more expensive to repair as a consequence.

Unfortunately, there is insufficient data available to make an objective assessment of these considerations for a given location and the judgement of the designer and preference of his client will prevail; a subjective assessment is inevitable.

There have been recent efforts to protect subsea wellheads in the North Sea, but again the design premise for the wellhead protector is likely to be subjective. The problem is akin to that of ship impact on structures; there is a small risk of enormous damage, and the cost of protection against serious damage (particularly from impact) at some point becomes prohibitive. Some techniques are, however, available from risk evaluation specialists. A more detailed appraisal is beyond the scope of this report.

The analytical treatment of damage that has been detected is likely to be little used on fracture critical components. For overriding safety and public confidence reasons, remedial action would always be taken. If a

component is not fracture critical, then failure tests might be preferable to detailed inspection (visual, FMD, load indicator etc.).

It is concluded that, for installations of low redundancy, damage assessment techniques can assist the inspection designers only thus far:

- in identifying criticality of components
- in deciding on inspection frequency on fracture critical components where damage is likely to be progressive.

In the latter case, the techniques described in Section 6 apply.

In summary, the methodology is easier to apply but is likely to be of less benefit than to jacket structures.

8.3 Value of Adopting the Proposed Optimised Inspection Planning Methodology

It is well nigh impossible to made a realistic commercial assessment of the impact that the adoption of the proposed methodology would have on inspection costs of a structure without carrying out a detailed, structure specific study.

To assist in making an assessment, an unsupported scenario is developed in 8.3.2, below, to show how a financial appraisal could be approahced.

8.3.1 Technical review

In adopting the proposed methodology, the operator finds himself with a model of his installation which provides the following:

- A basis for assessing inspection priority which integrates the importance of fatigue and static damage considerations.
- A rational basis on which to decide which components justify detailed studies.
- A basis for assessing whether strengthening is cheaper txan repair.

- An indication of which parameters are governing the inspection frequency of a given component.

This model is an important and versatile tool which the operator can use to assess his immediate and future inspection costs.

The power of the model is further increased if it is integrated with a computerised inspection history database. The latter are already under development with some operators. In addition, he will have established a team of experts to advise on all aspects of inspection and which will set up the model and support it with the necessary detailed studies. The costs of establishing the methodology will not be cheap but the potential payback is considerable.

Consider the following example. Let us assume that the model and studies prove that the cost of strengthening a component is likely to cost the same as two detailed inspections and thus that strengthening is the cost effective option. It could be argued that this conclusion could be drawn from independent studies on single components perceived as expensive to inspect based purely on 'engineers judgement'. What is also possible, however, if the full system is adopted, is an appraisal of the impact of specific reduced inspection requirements on overall inspection costs. Perhaps by obviating, or dramatically reducing inspection requirements on a few key components, the operator can obviate two complete inspection seasons in every five, whilst ensuring that his confidence in overall integrity is not diminished. The likelihood of this dramatic option could be tested by altering parameters arbitarily in the model prior to the expense of detailed studies.

8.3.2 Cost consideration

In adopting the methodology, the operator is faced with the following costs:

1. hardware
2. software development
3. setting up the system
4. detailed studies
5. review panel
6. ongoing system support costs

These will only be justified against one or both of the following criteria:

a. increased integrity assurance
b. reduced inspection cost without loss of integrity assurance.

The following breakdown, with unsupported estimates of implication costs, are provided solely to assist in making a rational assessment for a real installation:

A. Costs

Item	Description	Allow (£)
1, 2	hardware, software development	10,000
	*obtain/programme 'cost of reliable inspection' model	100,000
3	• subdivide structure • design proformas • learning curve • preliminary ranking (say 200 member structure) • obtain compound rankings • postulate initial detailed studies Allow 1 senior engineer and 1 junior engineer for 6 months	32,000
3, 5	• review initial recommendations Allow 4 consultants, 2 days and 4 x 1 day sessions @ £250	6,000
3, 4	• define studies, appoint and monitor contractor Allow 1 senior engineer, 2 months	7,000

Item		Description	Allow (£)
4	•	5 initial detailed studies	125,000
3, 5	•	reassess priorities, define further studies	10,000
4	•	10 further detailed studies	200,000
3, 5	•	reassess, define inspection priorities	20,000
		allow	£500,000

(Only those costs additional to standard inspection design practice are allowed for)

*Outwith the scope of this study..

Ongoing costs, 6, are likely to be of a similar magnitude to those for a manual inspection design process.

B. Return

Assume five node inspections at depth are saved per year. Assume diving costs are £30,000 per day. Allowing inspection rate of 1 node per day, savings would be:

		£
1.	Offshore costs, 5 x £30,000	£150,000
2.	Inspection planning, allow 2 engineers x 4 weeks	£10,000
3.	Reporting costs	£10,000
	Total saving, per annum	£170,000

8.3.3 Conclusion

It is immediately apparant that the potential for financial return on the high initial outlay may be easily justified, particularly if the zero inspection option can be used in, say, one year in five.

The additional benefit of using the integrated inspection system is that a consistent approach to decision making is used throughout the lifetime of the structure. It is not practicable to assess the impact that this will have on increased safety assurance, but in any event, the system will be at least as safe as current methods.

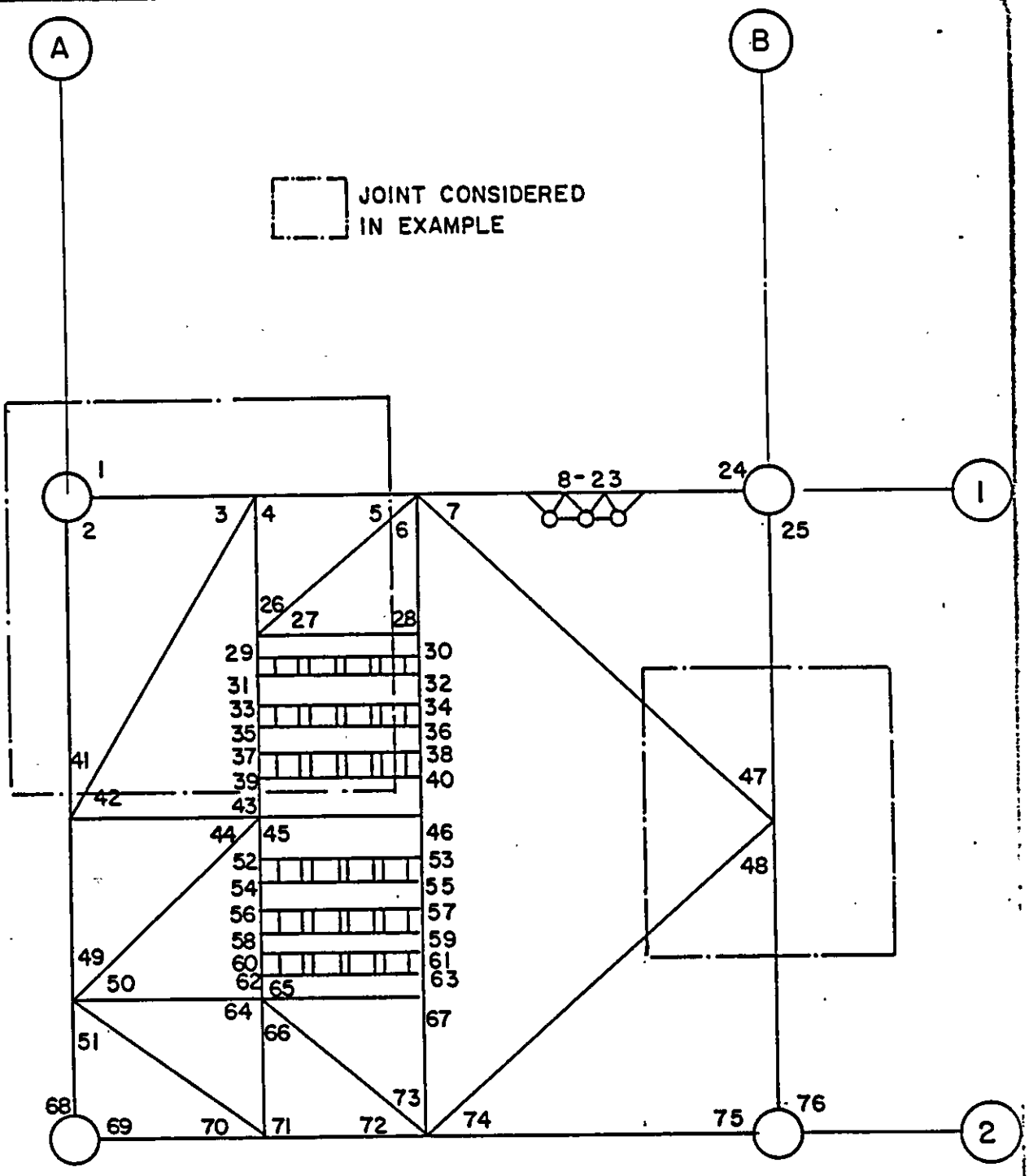

CONDUCTOR GUIDE FRAME AT EL (-) 38'-0"

WORKED EXAMPLE : JOINTS SKETCH 1

PROJECT URP 72 : STUDY 4 INSPECTION PLANNING , THE ROLE OF DAMAGE ASSESSMENT	REPORT No. WOL109/86 FIG. 8·1

JOINTS - END OF INSPECTION YEAR 19 8

JOINT	DESIGN	REFERENCE DRAWING	ACCESS (1-5)	LAST INSPECTED	CONSEQUENCE OF FAILURE										LIKELIHOOD OF FAILURE										RANK (Y) x (X) + W	INSPECTION CATEGORY	NOMINAL PRIORITY
				W	A	B	C	D	E	F	G	H	I	Y	K	M	N	O	P	Q	R	S	X				
47	-38	Sketch 1	1	1280	40	40	40	20	10	1	1	5	10	159	40	20	100	5	5	5	1	10	178	29582	4	1
31	-38	Sketch 1	4	3840	10	10	40	20	1	10	10	5	40	146	10	5	35	5	5	20	10	20	110	19900	2	2
33	-38	Sketch 1	4	7680	10	10	40	20	1	10	10	5	40	146	10	5	5	1	5	20	10	20	76	18776	2	3
35	-38	Sketch 1	4	7680	10	10	40	20	1	10	10	5	40	146	10	5	5	1	5	20	10	20	76	18776	2	4
48	-38	Sketch 1	1	1280	40	40	40	20	10	1	1	5	10	159	40	20	5	1	5	1	1	10	91	15749	4	5
26	-38	Sketch 1	2	3840	40	40	40	1	10	1	1	5	10	148	10	5	35	1	5	5	5	10	76	15088	2	6
3	-38	Sketch 1	1	7680	40	40	40	5	10	1	1	5	10	152	1	20	5	1	5	1	5	10	48	14976	3	7
4	-38	Sketch 1	1	7680	40	40	40	5	10	1	1	5	10	152	1	20	5	1	5	1	5	10	48	14976	3	8
29	-38	Sketch 1	4	3840	10	10	40	20	1	10	10	5	40	146	10	5	5	1	5	20	10	20	76	14936	2	9
1	-38	Sketch 1	1	2560	40	40	40	20	100	1	50	20	2	313	1	20	5	1	1	1	5	2	36	13776	3	10
2	-38	Sketch 1	1	2560	40	40	40	20	100	1	50	20	2	313	1	20	5	1	1	1	5	2	36	13776	3	11
37	-38	Sketch 1	4	1280	10	10	40	20	1	10	10	5	40	146	10	5	5	1	5	20	10	20	76	12376	2	12
39	-38	Sketch 1	4	1280	10	10	40	20	1	10	10	5	40	146	10	5	5	1	5	20	10	20	76	12376	2	13
27	-38	Sketch 1	2	3840	10	10	40	1	10	1	1	5	10	88	10	5	5	1	5	5	10	10	51	8328	1	14

URP 72; S4 INSPECTION PLANNING

THE ROLE OF DAMAGE ASSESSMENT

FIGURE 8.2

JOINTS - END OF INSPECTION YEAR 19 9

JOINT	DESIGN	REFERENCE DRAWING	ACCESS (1-5)	LAST INSPECTED	CONSEQUENCE OF FAILURE										LIKELIHOOD OF FAILURE									RANK (Y) x (X)	INSPECTION CATEGORY	NOMINAL PRIORITY
				W	A	B	C	D	E	F	G	H	I	Y	K	M	N	O	P	Q	R	S	X	+ W		
31	-38	Sketch 1	4	1280	10	10	40	20	1	10	10	5	40	146	10	5	35	5	5	20	10	20	110	17340	2	1
47	-38	Sketch 1	1	1280	40	40	40	20	10	1	1	5	2	151	40	20	35	5	5	5	1	2	105	17135	4	2
26	-38	Sketch 1	2	5120	40	40	40	1	10	1	1	5	10	148	10	5	35	1	5	5	5	10	76	16368	2	3
29	-38	Sketch 1	4	5120	10	10	40	20	1	10	10	5	40	146	10	5	5	1	5	20	10	20	76	16216	2	4
3	-38	Sketch 1	1	7680	40	40	40	5	10	1	1	5	10	152	1	20	5	1	5	1	10	10	53	15736	3	5
1	-38	Sketch 1	1	3840	40	40	40	20	100	1	50	20	2	313	1	20	5	1	1	1	5	2	36	15108	3	6
2	-38	Sketch 1	1	3840	40	40	40	20	100	1	50	20	2	313	1	20	5	1	1	1	5	2	36	15108	3	7
37	-38	Sketch 1	4	2560	10	10	40	20	1	10	10	5	40	146	10	5	5	1	5	20	10	20	76	13656	2	8
39	-38	Sketch 1	4	2560	10	10	40	20	1	10	10	5	40	146	10	5	5	1	5	20	10	20	76	13656	2	9
33	-38	Sketch 1	4	1280	10	10	40	20	1	10	10	5	40	146	10	5	5	1	5	20	10	20	76	12376	2	10
35	-38	Sketch 1	4	1280	10	10	40	20	1	10	10	5	40	146	10	5	5	1	5	20	10	20	76	12376	2	11
4	-38	Sketch 1	1	1280	40	40	40	5	10	1	1	5	10	152	1	20	5	1	5	1	10	10	53	9336	3	12
27	-38	Sketch 1	2	5120	10	10	40	1	10	1	1	5	10	88	10	5	5	1	5	5	10	10	51	9608	1	13
48	-38	Sketch 1	1	1280	40	40	40	20	10	1	1	5	2	151	10	20	5	1	5	1	1	2	45	8075	3	14

URP 72; S4 INSPECTION PLANNING

THE ROLE OF DAMAGE ASSESSMENT

FIGURE 8.3

APPENDICES

WIMPEY OFFSHORE ENGINEERS & CONSTRUCTORS LIMITED
140 CAUSEWAYEND
ABERDEEN AB2 3TN

TELEPHONE 0224 637755
TELEX 739180

CALCULATIONS

CLIENT: CIRIA UEG
CONTRACT:
CONTRACT/ACCOUNT NO:

VOLUME:
SHEET:
MADE BY: JRF
CHKD. BY:

PAGE: 1.
OF:
DATE: JUNE 86
DATE:

LOCATION:
ITEM:
REF./DWG NO:

EXAMPLE 1 – FATIGUE CRACK GROWTH ASSESSMENT FOR A CIRCUMFERENTIAL PART-THROUGH CRACK IN A RING STIFFENED TUBULAR JOINT

A joint on a typical northern North Sea jacket, shown below, is found to have a low fatigue life from the results of an S-N fatigue analysis. In order to help optimise the inspection period for the joint a fracture mechanics fatigue crack growth assessment can be carried out.

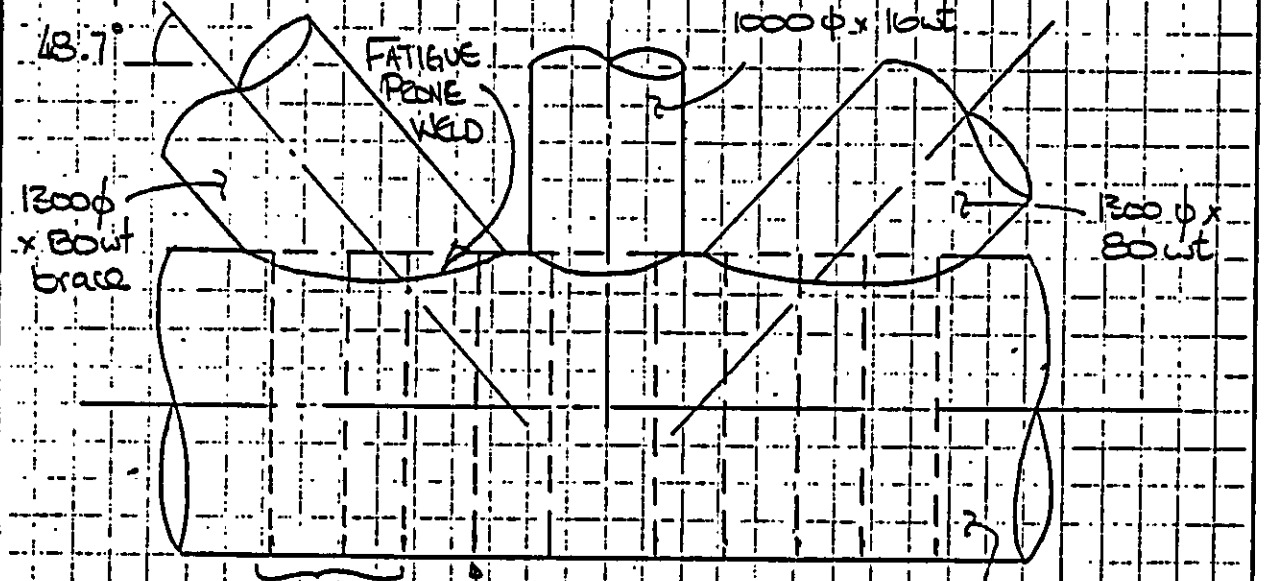

JOINT 'A' – RING STIFFENED KT TUBULAR JOINT

WIMPEY OFFSHORE ENGINEERS & CONSTRUCTORS LIMITED
140 CAUSEWAYEND
ABERDEEN AB2 3TN

TELEPHONE 0224 637755
TELEX 739180

CALCULATIONS

CLIENT: CIRIA UEG | VOLUME: | PAGE: 2
SHEET: | OF:
CONTRACT: | MADE BY: JEF | DATE: JUNE 86
CONTRACT/ACCOUNT NO: | CHKD. BY: | DATE:
LOCATION: | ITEM: | REF./DWG NO:

The maximum fatigue damage was located, from the SN analysis results, at the crown position of the brace/chord weld adjacent to the T brace. The fatigue damage was primarily due to high axial and in-plane brace loading. The chord-side weld toe was found to be the most susceptible location for fatigue crack growth due to the chord wall being thicker than the brace wall.

The geometric parameters for the joint are found to be :-

$\tau = t/T = 0.80$

$\beta = d/D = 0.65$

$\gamma = R/T = 10.0$

$\zeta = g/D = 0.663$

$\theta = 48.7°$

Substituting the above parameters into the modified Smedley/Wordsworth equations (Reference (1)) for a KT joint, with

WIMPEY OFFSHORE ENGINEERS & CONSTRUCTORS LIMITED
140 CAUSEWAYEND
ABERDEEN AB2 3TN

TELEPHONE 0224 637755
TELEX 739180

CALCULATIONS

CLIENT: CIRIA UEG | VOLUME: | PAGE: 3

CONTRACT: | SHEET: | OF:

CONTRACT/ACCOUNT NO: | MADE BY: JRF | DATE: JUNE 80

LOCATION: | ITEM: | REF./DWG NO: | CHKD. BY: | DATE:

No ring stiffening gives:-

LOAD COMPONENT	SCF			
	CHORD SIDE		PLACE SIDE	
	SADDLE	CROWN	SADDLE	CROWN
AXIAL	4.06	3.22	3.56	3.03
IPB	-	2.50	-	2.57
OPB	4.98	-	4.14	-

The reduction of the above SCFs due to internal ring stiffeners can be estimated from the following equation from Reference (2).

$$SCF_{(\text{ring stiffened})} = SCF_{(\text{unstiffened})} \times K_z^{-m}$$

where $K_z = \gamma\tau\left(12\frac{I_{xx}}{\ell}\right)^{1/3}$

$m = m(\rho/D, \tau, \beta, \gamma)$ is tabulated in reference 2

I_{xx} is the inertia of the shaded area in the sketch below

ℓ is defined in the sketch below

WIMPEY OFFSHORE ENGINEERS & CONSTRUCTORS LIMITED
140 CAUSEWAYEND
ABERDEEN AB2 3TN

TELEPHONE 0224 637755
TELEX 739180

CALCULATIONS

CLIENT: CIRIA JEG | VOLUME: | PAGE: 4.
SHEET: | OF:
CONTRACT: | MADE BY: JEF | DATE: JUNE 86
CONTRACT/ACCOUNT NO: | CHKD. BY: | DATE:
LOCATION: | ITEM: | REF./DWG NO:

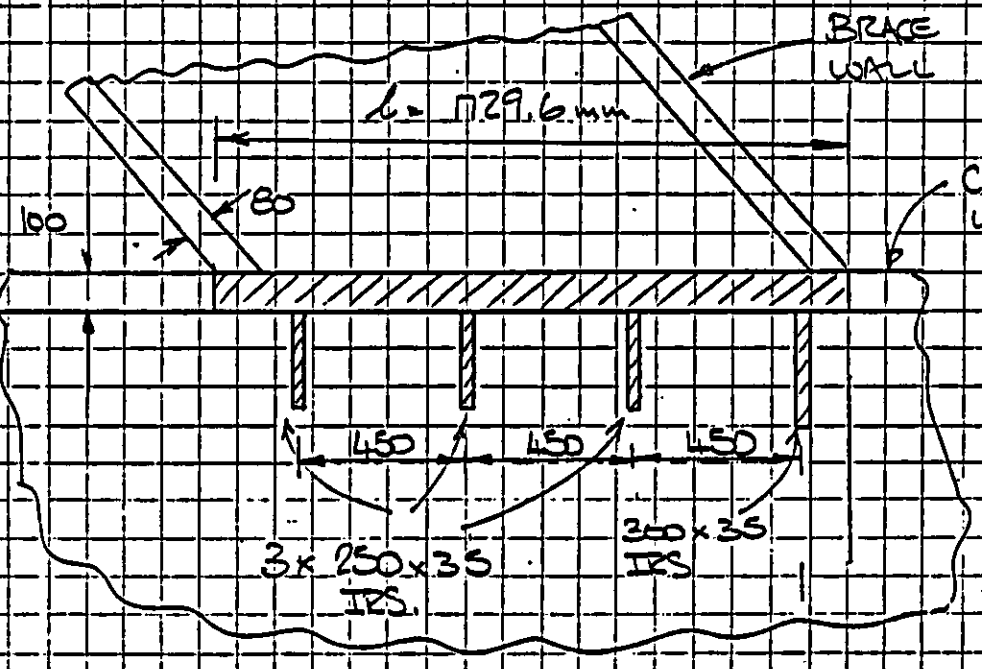

SECTION THROUGH ℄ OF BRACE AND CHORD

I_{xx} is calculated to be 1.37×10^9 mm⁴

This results in a value of K_2 of

$$K_2 = 1/T \left(\frac{12\, I_{xx}}{L} \right)^{1/3}$$

$$= 1/100 \left(\frac{12 \times 1.37 \times 10^9}{1729.16} \right)$$

$$= 2.12$$

To establish m, p/D is required where p is the pitch of the internal ring stiffeners

WIMPEY OFFSHORE ENGINEERS & CONSTRUCTORS LIMITED
140 CAUSEWAYEND
ABERDEEN AB2 3TN

TELEPHONE 0224 637755
TELEX 739180

CALCULATIONS

CLIENT: CIRIA JEG | VOLUME: | PAGE: 5
SHEET: | OF:
CONTRACT: | MADE BY: JEF | DATE: June 86
CONTRACT/ACCOUNT NO: | CHKD. BY: | DATE:
LOCATION: | ITEM: | REF./DWG NO:

$D/D = 450/2000 = 0.225$

From reference 2 the following values of m can be established:

LOAD COMPONENT	m
AXIAL	0.49
IPB	0.032
OPB	0.87

Thus, modifying the unstiffened SCFs from page 3 gives:-

LOAD COMPONENT	SCF			
	CHORD SIDE		BRACE SIDE	
	SADDLE	CROWN	SADDLE	CROWN
AXIAL	2.81	2.23	2.46	2.10
IPB	–	2.44	–	2.5
OPB	2.59	–	2.15	–

The fracture mechanics fatigue crack growth computation requires a knowledge of the stress distribution through the wall thickness on the plane of the crack. Assuming a linear variation of stress, typical distributions can be represented

WIMPEY OFFSHORE ENGINEERS & CONSTRUCTORS LIMITED
140 CAUSEWAYEND
ABERDEEN AB2 3TN

TELEPHONE 0224 637755
TELEX 739180

CALCULATIONS

CLIENT: CIRIA UEG | VOLUME: | PAGE: 6
SHEET: | OF:
CONTRACT: | MADE BY: JEF | DATE: JUNE 86
CONTRACT/ACCOUNT NO: | CHKD. BY: | DATE:
LOCATION: | ITEM: | REF./DWG NO:

as follows :-

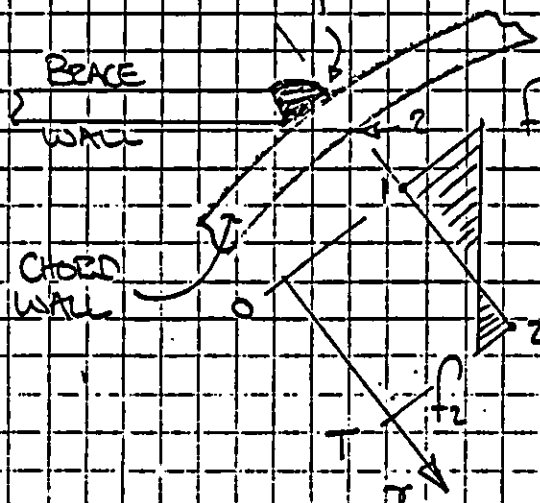

Distributions of this nature are characterised by f_{HS} (the 'hot-spot' stress on the outer surface) and λ_s the stress distribution factor where :-

$$\lambda_s = f_m / f_{HS}$$

with $f_m = (f_1 + f_2)/2$

The stress distribution is computed for each fatigue wave position by factoring the brace member fatigue forces by influence coefficients as follows :-

WIMPEY OFFSHORE ENGINEERS & CONSTRUCTORS LIMITED
140 CAUSEWAYEND
ABERDEEN AB2 3TN

TELEPHONE 0224 637755
TELEX 739180

CALCULATIONS

CLIENT: CIRIA UEG | VOLUME: | PAGE: 7
SHEET: | OF:
CONTRACT: | MADE BY: JEF | DATE: June 86
CONTRACT/ACCOUNT NO: | CHKD. BY: | DATE:
LOCATION: | ITEM: | REF./DWG NO:

$$f_1 = \alpha_{11} P \pm \alpha_{12} M_{ip} + \alpha_{13} M_{op}$$

$$f_2 = \alpha_{21} P \pm \alpha_{22} M_{ip} + \alpha_{23} M_{op}$$

and $f = f(x) = f_1 - f_1 x/T + f_2 x/T$

where P, M_{ip} and M_{op} are the axial, in-plane and out-of-plane brace loads for a particular wave position — obtained from a jacket analysis.

The influence coefficients have the forms:-

$$\alpha_{11} = \frac{SCF_{axial}}{A} \qquad \alpha_{12} = \frac{SCF_{ipb}}{Z} \qquad \alpha_{13} = \frac{SCF_{opb}}{Z}$$

$$\alpha_{21} = -(1 - 2(\lambda_s)_a)\,\alpha_{11}$$

$$\alpha_{22} = -(1 - 2(\lambda_s)_{ipb})\,\alpha_{12}$$

$$\alpha_{23} = -(1 - 2(\lambda_s)_{opb})\,\alpha_{13}$$

where A = area of brace member
Z = modulus of brace member

WIMPEY OFFSHORE ENGINEERS & CONSTRUCTORS LIMITED
140 CAUSEWAYEND
ABERDEEN AB2 3TN

TELEPHONE 0224 637755
TELEX 739180

CALCULATIONS

CLIENT: CIRIA. JEG | VOLUME: | PAGE: 8
SHEET: | OF:
CONTRACT: | MADE BY: JEF | DATE: JUNE 86
CONTRACT/ACCOUNT NO: | CHKD. BY: | DATE:
LOCATION: | ITEM: | REF./DWG NO:

It should be noted that the SCF's together with the λ_s are functions of location of the centre of the crack on the brace/chord intersection.

The λ_s values for the crown toe position of this particular joint have been determined by consulting Wimpey Offshore's database of results from previous finite element analyses of tubular joints. From the database, results from F.E. models with similar geometric parameters to this joint gave the following λ_s values at the crown toe:-

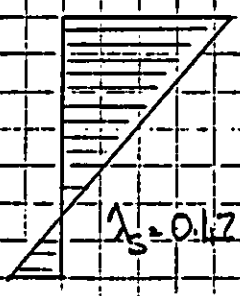

DISTRIBUTION DUE TO AXIAL BRACE LOAD

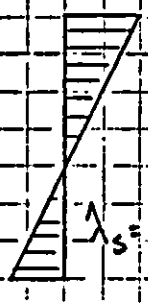

DISTRIBUTION DUE TO IPB BRACE LOAD

DISTRIBUTION DUE TO OPB BRACE LOAD

WIMPEY OFFSHORE ENGINEERS & CONSTRUCTORS LIMITED
140 CAUSEWAYEND
ABERDEEN AB2 3TN

TELEPHONE 0224 637755
TELEX 739180

CALCULATIONS

CLIENT: CIRIA UEG

CONTRACT:

CONTRACT/ACCOUNT NO:

VOLUME:

SHEET:

MADE BY: JBF

CHKD. BY:

PAGE: 9.

OF:

DATE: JUNE 86

DATE:

LOCATION:

ITEM:

REF./DWG NO:

Calculation of the influence coefficients can now be completed as follows:-

$\Delta = 306619 \text{ mm}^2$

$Z_1 = 8.814 \times 10^7 \text{ mm}^3$ (outside surface)

$Z_2 = 1.005 \times 10^8 \text{ mm}^3$ (inside surface)

$\alpha_{11} = 223 / 306619 = 7.27 \times 10^{-6} \text{ mm}^{-2}$

$\alpha_{12} = 2.44 / 8.814 \times 10^7 = 2.77 \times 10^{-8} \text{ mm}^{-3}$

$\alpha_{13} = 0.0$

$\alpha_{21} = -(1-2\times0.42) \times 7.27 \times 10^{-6} = -1.16 \times 10^{-6} \text{ mm}^{-2}$

$\alpha_{22} = -(1-2\times0.22) \times 2.77 \times 10^{-8} = -1.36 \times 10^{-8} \text{ mm}^{-2}$

$\alpha_{23} = 0.0$

These coefficients have been used to process the fatigue forces from the jacket analysis and thus determine the loading on the crack plane for all phase angles of all fatigue waves.

Wimpey Offshores fracture mechanics software has processed this load information together with the appropriate data defining crack growth rate in terms of stress intensity range to produce the crack growth characteristic given overleaf.

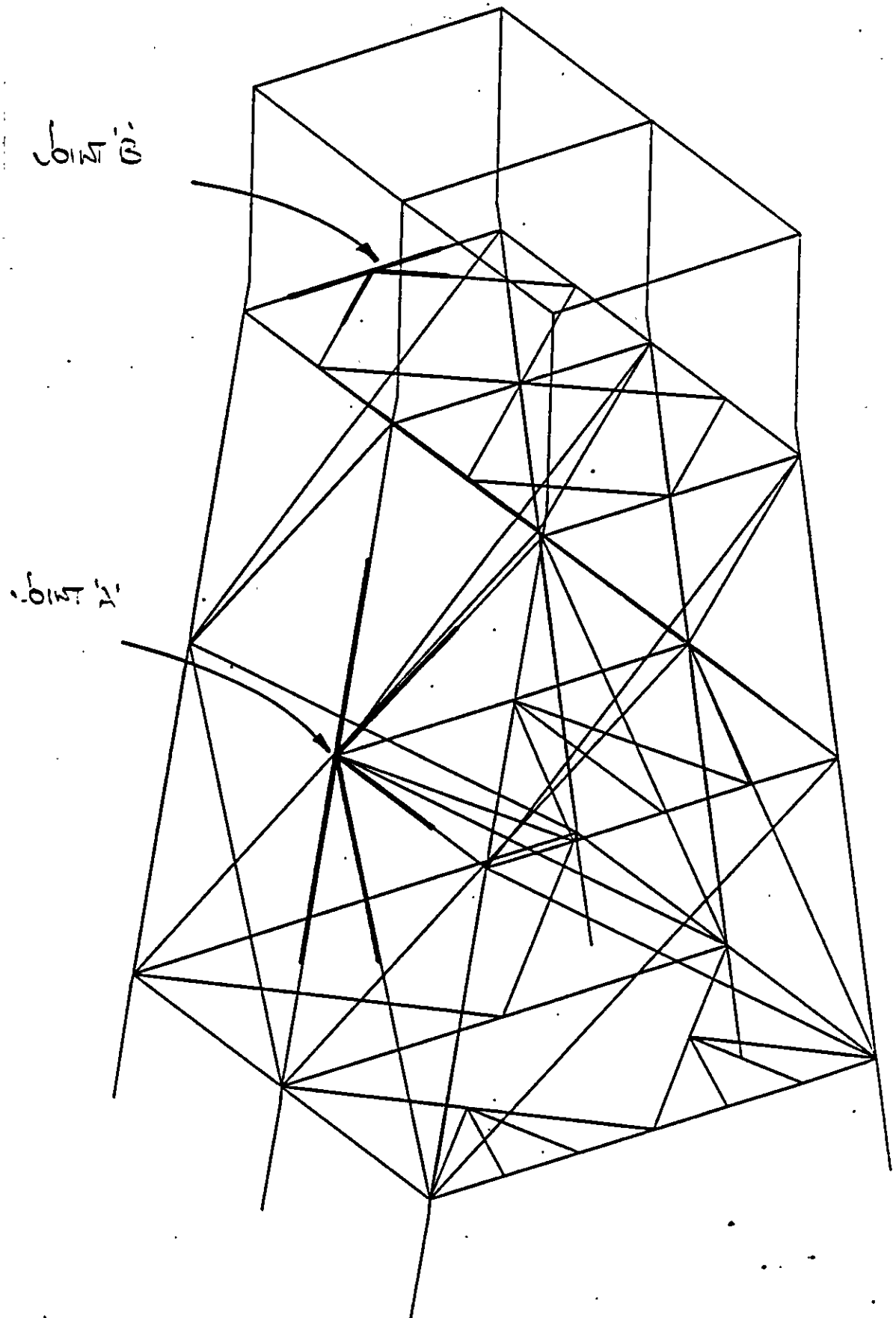

JACKET STRUCTURE SHOWING JOINTS FOR ASSESSMENT.

WIMPEY OFFSHORE
REPORT No. WOL /

FIG. A5.1

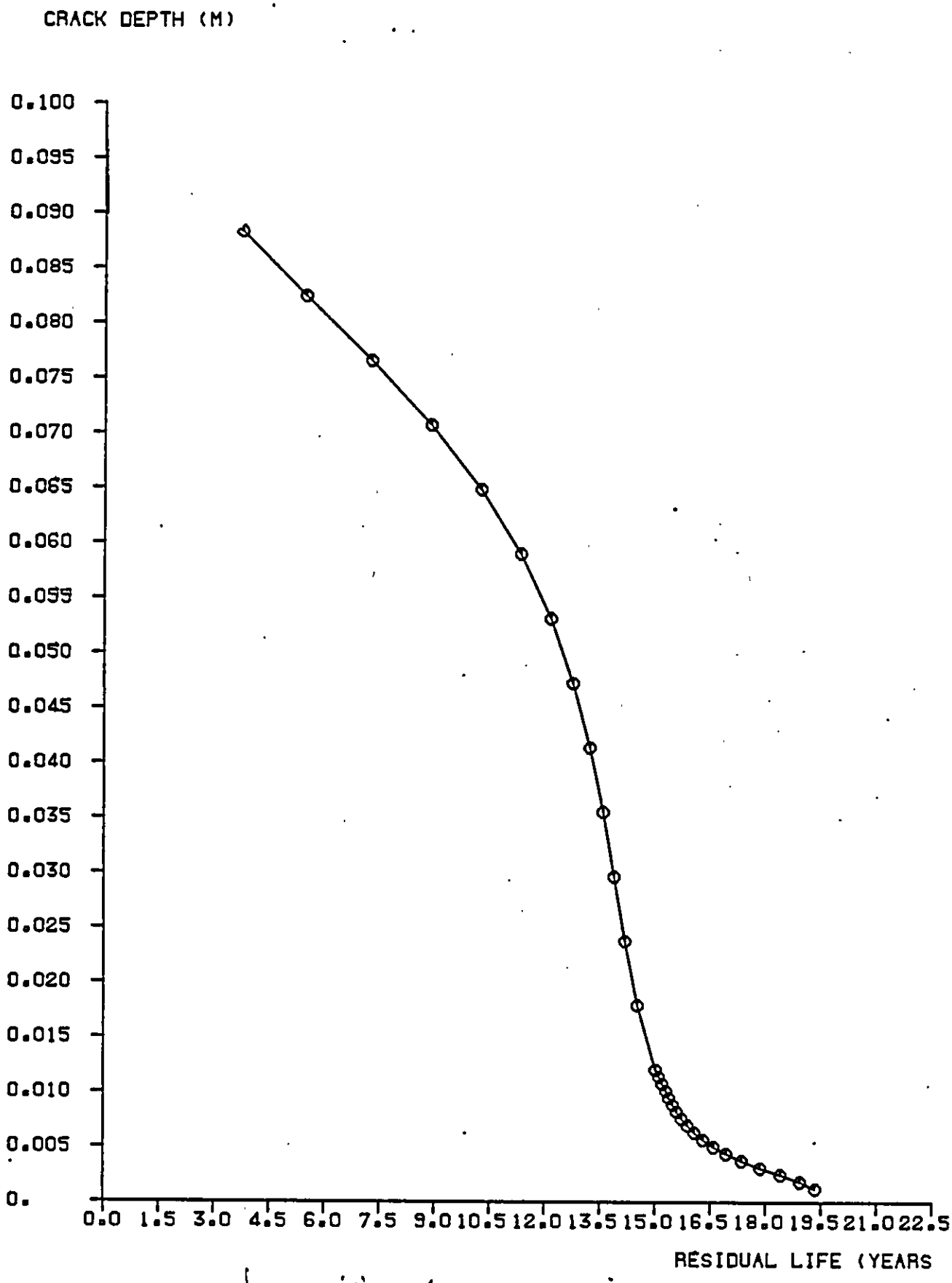

Joint 'A' (12 o'clock)

WIMPEY OFFSHORE
REPORT No. WOL /

FIG. A3.2

WIMPEY OFFSHORE LIMITED.

WIMPEY OFFSHORE ENGINEERS & CONSTRUCTORS LIMITED
140 CAUSEWAYEND
ABERDEEN AB2 3TN

TELEPHONE 0224 637755
TELEX 739180

CALCULATIONS

CLIENT: CIRIA . UEG
CONTRACT:
CONTRACT/ACCOUNT NO:

VOLUME:
SHEET:
MADE BY: JEF
CHKD. BY:

PAGE: 10
OF:
DATE: JUNE 86
DATE:

LOCATION:
ITEM:
REF./DWG NO:

EXAMPLE 2 – FATIGUE CRACK GROWTH ASSESSMENT FOR A LONGITUDINAL PART-THROUGH CRACK IN A SIMPLE TUBULAR JOINT.

- Joint 47 on the jacket structure (shown in figure 8.1) is found to have a low fatigue life from the results of an S-N fatigue analysis. An indication is found in year 19x8 has accelerated the need for an appraisal of this joint; to ensure that future inspection is optimised. A fracture mechanics crack-growth assessment is to be carried out.

The joint forms part of a simple K tubular joint as shown below.

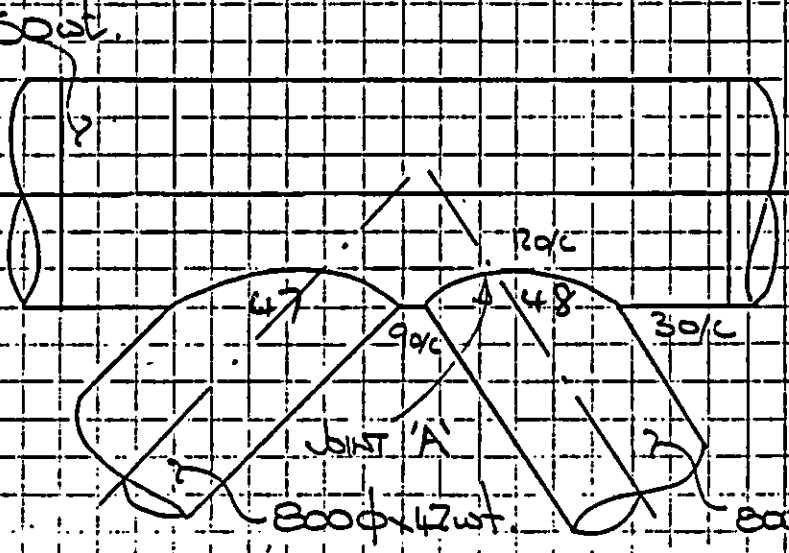

JOINT B – SIMPLE K TUBULAR JOINT

WIMPEY OFFSHORE ENGINEERS & CONSTRUCTORS LIMITED
140 CAUSEWAYEND
ABERDEEN AB2 3TN

TELEPHONE 0224 637755
TELEX 739180

CALCULATIONS

CLIENT: CDIA VEG | VOLUME: | PAGE: 11
SHEET: | OF:
CONTRACT: | MADE BY: JEF | DATE: June 86
CONTRACT/ACCOUNT NO: | CHKD. BY: | DATE:
LOCATION: | ITEM: | REF./DWG NO:

The maximum fatigue damage was located from the S-N analysis at the 12 o'clock position at the saddle position of joint 'B'. The fatigue damage is maximum at the chord side weld toe due to a combination of high notch and geometric stress concentration factor and high out-of-plane bending loads from vertical water particle motion.

The geometric parameters of the joint are :-

$\alpha = t/T = 0.84$

$\beta = d/D = 0.67$

$\gamma = R/T = 12.0$

$\theta = 56.6°$

$\tau = \zeta/D = 0.02$

Substituting these parameters in the Efthymiou Durkin equations (Reference (3)) for a K joint give the following SCFs :-

WIMPEY OFFSHORE ENGINEERS & CONSTRUCTORS LIMITED
140 CAUSEWAYEND
ABERDEEN AB2 3TN

TELEPHONE 0224 637755
TELEX 739180

CALCULATIONS

CLIENT: CIRIA OEG | VOLUME: | PAGE: 12
CONTRACT: | SHEET: | OF:
CONTRACT/ACCOUNT NO: | MADE BY: JRF | DATE: June 86
LOCATION: | ITEM: | CHKD. BY: | DATE: | REF./DWG NO:

Load component	Stress Concentration Factors			
	Chord		Brace	
	Saddle	Crown	Saddle	Crown
Axial	4·9	3·65	3·75	3·3
IPB	–	3·49	–	2·92
OPB	8·82	–	6·56	–

Following the same procedure outlined in Example 1 the stress distribution on the plane of the crack at the saddle position is found from the influence coefficients which are function of SCF and λ_s

Inspection of Wimpey Offshore's database on stress distributions for previous FE models gave the following stress distributions at a similar position on a similar tubular joint to joint 'B'.

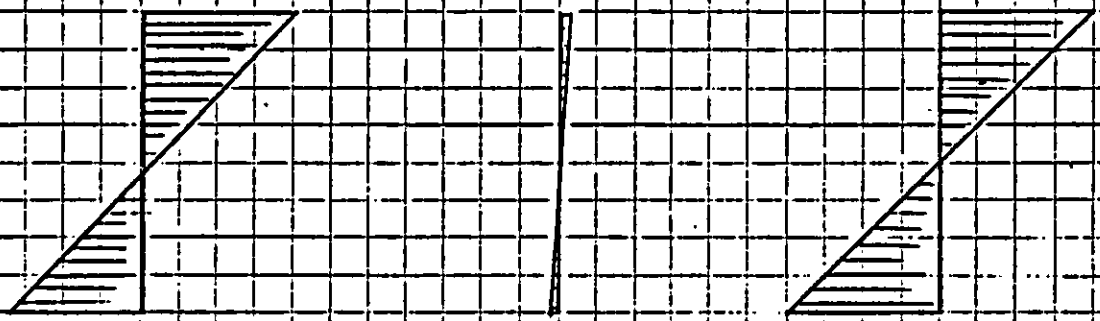

Distribution due to Axial brace load $\lambda_s = 0.113$ | Distribution due to IPB brace load $\lambda_s = 0.0$ | Distribution due to OPB brace load $\lambda_s = 0.084$

WIMPEY OFFSHORE ENGINEERS & CONSTRUCTORS LIMITED
140 CAUSEWAYEND
ABERDEEN AB2 3TN

TELEPHONE 0224 637755
TELEX 739180

CALCULATIONS

CLIENT: CIRIA UEG | VOLUME: | PAGE: 13
CONTRACT: | SHEET: | OF:
CONTRACT/ACCOUNT NO: | MADE BY: JEF | DATE: June 86
LOCATION: | ITEM: | REF./DWG NO: | CHKD. BY: | DATE:

Calculation of the influence coefficients can now be completed as follows:-

brace area $A = 10.0016\ mm^2$

brace modulus $Z_1 = 1.801 \times 10^7\ mm^3$ (outside surface)

brace modulus $Z_2 = 2.013 \times 10^7\ mm^3$ (inside surface)

$\alpha_{11} = 4.9 / 10.0016 = 4.899 \times 10^{-3}\ mm^{-2}$

$\alpha_{12} = 0.0$

$\alpha_{13} = 8.82 / 1.801 \times 10^7 = 4.897 \times 10^{-7}\ mm^{-3}$

$\alpha_{21} = -(1-2 \times 0.113) \times 4.9 / 10.0016 = -3.792 \times 10^{-3}\ mm^{-2}$

$\alpha_{22} = 0.0$

$\alpha_{23} = -(1-2 \times 0.113) \times 8.82 / 2.013 \times 10^7 = -3.666 \times 10^{-7}\ mm^{-3}$

These coefficients were used to process the fatigue forces from the jacket analysis and thus determine the loading on the crack plane for all fatigue loads.

The fracture mechanics software then produced the plot shown on figure A2.3 which gives the crack depth against time before through thickness failure.

WIMPEY OFFSHORE ENGINEERS & CONSTRUCTORS LIMITED
140 CAUSEWAYEND
ABERDEEN AB2 3TN

TELEPHONE 0224 637755
TELEX 739180

CALCULATIONS

CLIENT: CIRIA UEG | VOLUME: | PAGE: 14
CONTRACT: | SHEET: | OF:
CONTRACT/ACCOUNT NO: | MADE BY: JBF | DATE: June 86
| CHKD. BY: | DATE:
LOCATION: | ITEM: | REF./DWG NO:

Comparison of figures A3.2 and A3.3 clearly shows that although both joints have similar through thickness fatigue lives, the rate of crack growth is entirely different. Obviously the joint in example 1 can tolerate a relatively deeper crack than joint 'B' for the same residual life. (Residual life is defined as the time for a crack to propagate from a given depth to through thickness.) Thus, for the purpose of an optimised inspection plan, joint 'B' requires more frequent inspection than joint 'A'.

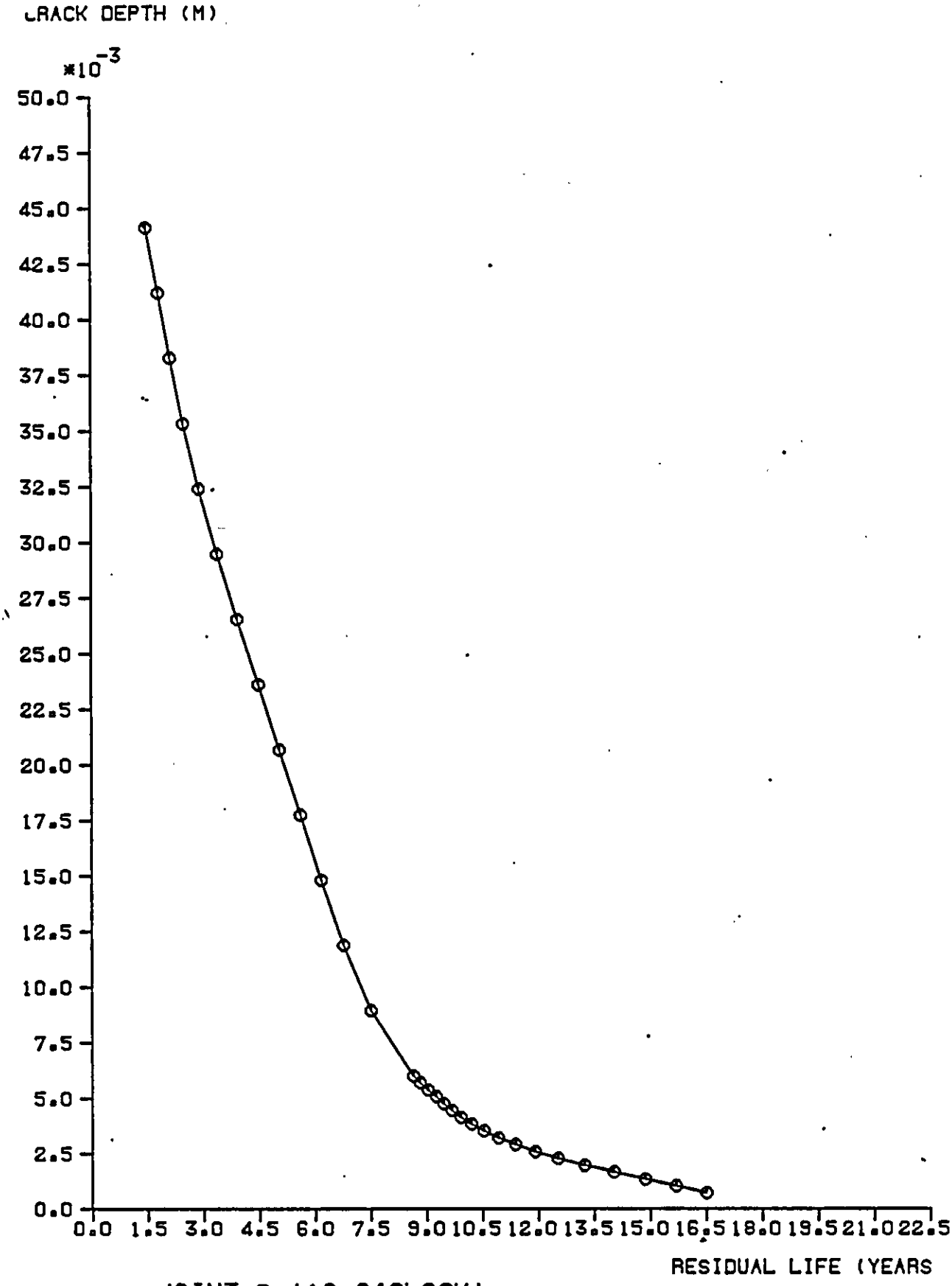

JOINT B (12 O'CLOCK)

WIMPEY OFFSHORE
REPORT No. WOL /

FIG. A3.3

WIMPEY OFFSHORE LIMITED

WIMPEY OFFSHORE ENGINEERS & CONSTRUCTORS LIMITED
FLYOVER HOUSE
GREAT WEST ROAD
BRENTFORD MIDDLESEX TW8 9AR

TELEPHONE 01-560 3100
TELEX 933851

CALCULATIONS

CLIENT: CIRIA UEG
CONTRACT:
CONTRACT/ACCOUNT NO:

VOLUME:
SHEET:
MADE BY: RNH.
CHKD. BY: DGS

PAGE:
OF:
DATE: 29/5
DATE: 1/6

LOCATION:
ITEM:
REF./DWG NO:

Example 3 - STABILITY ASSESSMENT FOR A LONGITUDINAL PART-THROUGH CRACK IN A SIMPLE TUBULAR JOINT

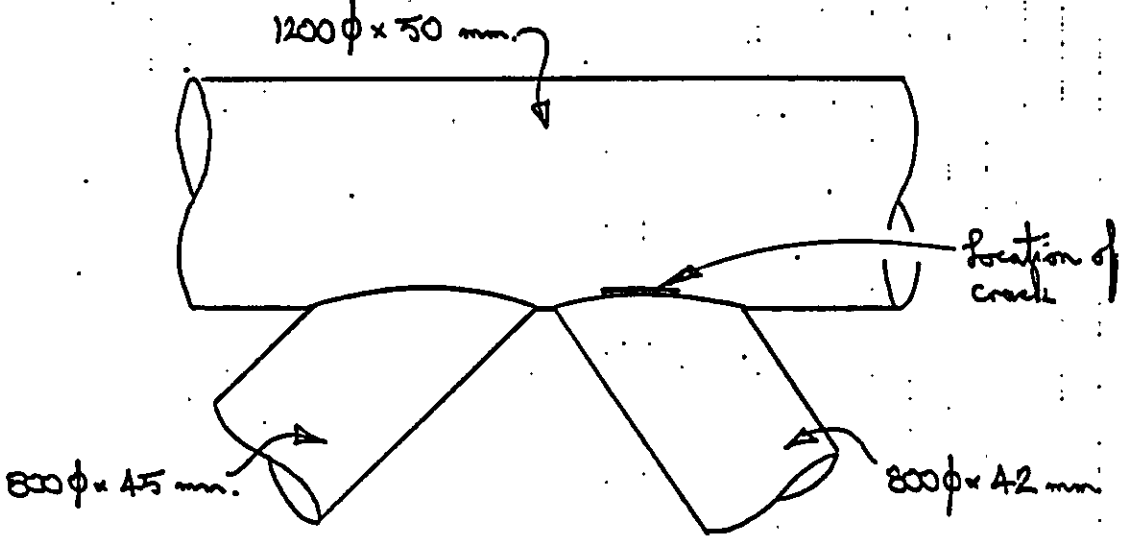

Plan view (N.B. same joint as Example 2)

Material Properties:

The following properties have been derived for the steel.

Yield stress $F_y = 364$ N/mm². UTS $F_u = 554$ N/mm²

Flow stress $F_{fl} = \frac{1}{2}(F_y + F_u) = 459$ N/mm²

CTOD in HAZ: $\delta_c =$ 0.03 mm

CTOD in parent plate: $\delta_c =$ 0.14 mm

WIMPEY OFFSHORE ENGINEERS & CONSTRUCTORS LIMITED
FLYOVER HOUSE
GREAT WEST ROAD
BRENTFORD MIDDLESEX TW8 9AR

TELEPHONE 01-560 3100
TELEX 933861

CALCULATIONS

CLIENT: CIRIA UEG
CONTRACT:
CONTRACT/ACCOUNT NO:

VOLUME:
SHEET:
MADE BY: RWH
CHKD. BY:

PAGE:
OF:
DATE: 29/5
DATE:

LOCATION:
ITEM:
REF/DWG NO:

Example 3 (cont'd)

Applied stress:

Based on the SCFs developed within Example 2, the max stress under storm loading is as follows:

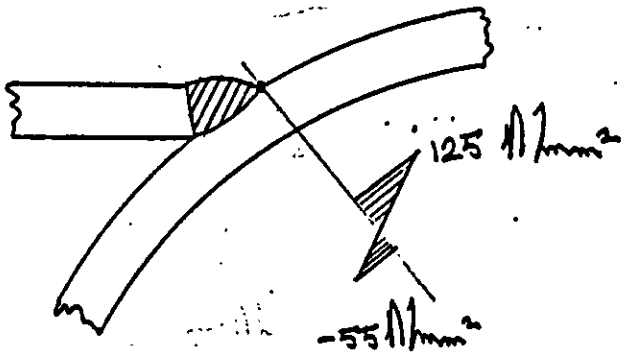

Residual stress:

This joint has been stress relieved ∴ assume that

$f_{res}^{(max)} = 0.25 F_y$

$= 0.25 \times 364 = 91$ N/mm².

It is assumed that the residual stress field has the following distribution (ref. Section ?).

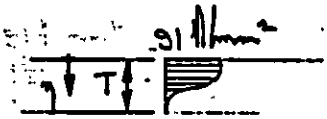

$$f_{res} = \frac{1}{2} f_{res}^{(max)} \left[1 + \cos\left(\frac{\pi y}{2T}\right)\right]$$

$$= 45.5 \left[1 + \cos\left(\frac{\pi y}{2T}\right)\right]$$

WIMPEY OFFSHORE ENGINEERS & CONSTRUCTORS LIMITED
FLYOVER HOUSE
GREAT WEST ROAD
BRENTFORD MIDDLESEX TW8 9AR

TELEPHONE 01-560 3100
TELEX 933861

CALCULATIONS

CLIENT: CIRIA UEG.
CONTRACT:
CONTRACT/ACCOUNT NO:

VOLUME:
SHEET:
MADE BY: RW
CHKD. BY:

PAGE:
OF:
DATE: 29/5
DATE: 10/6

LOCATION: ITEM: REF./DWG NO:

Example 3 (cont'd)

The applied CTOD may be calculated from

$$\delta = \frac{\pi F_y a}{E} \left\{ \frac{f_p}{f_n} \left[\frac{8}{\pi^2} \ln \sec\left(\frac{\pi}{2} \frac{f_n}{F_y} \right) \right]^{1/2} + \frac{f_s}{F_y} \right\}^2 \quad \ldots (1)$$

where: δ = applied CTOD
E = Young's modulus
F_y = yield stress
a = crack depth
f_p = effective primary stress = $\frac{K_I^p}{\sqrt{\pi a}}$ ... (2)
(K_I^p is the SIF from the actual primary stress)

f_s = effective secondary stress = $\frac{K_I^s}{\sqrt{\pi a}}$ ... (3)
(K_I^s is the SIF from the actual secondary stress)

f_n = effective net section stress
$$= \frac{f_t + \sqrt{f_t^2 + 3 f_b^2 (1 - a/T)^2}}{3(1 - a/T)^2} \quad \ldots (4)$$

(f_t and f_b are the tension and bending components of the primary stresses).

WIMPEY OFFSHORE ENGINEERS & CONSTRUCTORS LIMITED
FLYOVER HOUSE
GREAT WEST ROAD
BRENTFORD MIDDLESEX TW8 9AR

TELEPHONE 01-560 3100
TELEX 933861

CALCULATIONS

CLIENT: CIRIA UEG
CONTRACT:
CONTRACT/ACCOUNT NO:

VOLUME:
SHEET:
MADE BY: RWH
CHKD. BY:

PAGE:
OF:
DATE: 29/5
DATE: 16/6

LOCATION: ITEM: REF./DWG NO:

Example 3 (cont'd)

The applied CTOD will be calculated for $a = 0.005$ m. Running the program KTUBE for the primary and the residual stresses depicted on p. gives:

$K_I^p = 16.4$ MPa $m^{1/2}$; $K_{I_r} = 14.2$ MPa $m^{1/2}$.

$$\therefore f_p = \frac{16.4}{\sqrt{\pi \times 0.005}} = 130.6 \text{ MPa}$$

$$f_r = \frac{14.2}{\sqrt{\pi \times 0.005}} = 113.1 \text{ MPa}.$$

Dividing the primary stress into tension and bending components: $f_t = 35$ N/mm^2; $f_b = \pm 90$ N/mm^2

Hence, the effective net section stress is (equation (4))

$$f_n = \frac{90 + \sqrt{90^2 + 9 \times 35^2 (1 - 0.1)^2}}{3(1 - 0.1)^2}$$

$$= 90.7 \text{ N/mm}^2$$

From equation (1), the applied CTOD is

$$\delta = \frac{\pi \times 459 \times 0.005}{2.1 \times 10^5} \left\{ \frac{130.6}{90.7} \left[\frac{8}{\pi^2} \ln \sec \left(\frac{\pi}{2} \frac{90.7}{459} \right) \right]^{1/2} + \frac{113.1}{459} \right\}^2$$

$$= 3.433 \times 10^{-5} \{0.2869 + 0.2464\}^2 = 9.76 \times 10^{-6} \text{ m}.$$

i.e. $\delta = 0.0098$ mm.

WIMPEY OFFSHORE

WIMPEY OFFSHORE ENGINEERS & CONSTRUCTORS LIMITED
FLYOVER HOUSE
GREAT WEST ROAD
BRENTFORD MIDDLESEX TW8 9AR

TELEPHONE 01-560 3100
TELEX 933861

CALCULATIONS

CLIENT: CIRIA UEG
CONTRACT:
CONTRACT/ACCOUNT NO:

VOLUME: | PAGE:
SHEET: | OF:
MADE BY: RWH | DATE: 29/5
CHKD. BY: [illegible] | DATE: [illegible]

LOCATION: | ITEM: | REF./DWG NO:

Example 3 (cont'd)

Note that in the above calculation, the flow stress (F_{μ}) has been substituted for the yield stress (F_y) to allow for strain hardening.

The CTOD has been calculated at other depths, in increments of $a/T = 0.05$. The crack driving force characteristic is illustrated overleaf. [illegible] the figure have been the CTOD [illegible] for HAZ and parent plate. The HAZ has been [illegible] weld – thus [illegible] HAZs [illegible] parent [illegible]. The crack driving force for small crack [illegible] crack [illegible] for the HAZ. For the parent plate, the crack driving force [illegible] 27.5 mm [illegible] [illegible] 3 [illegible] Thus [illegible]

WIMPEY OFFSHORE ENGINEERS & CONSTRUCTORS LIMITED
FLYOVER HOUSE
GREAT WEST ROAD
BRENTFORD MIDDLESEX TW8 9AR

TELEPHONE 01-560 3100
TELEX 933861

CALCULATIONS

CLIENT: China Ocj

CONTRACT:

CONTRACT/ACCOUNT NO:

VOLUME:

SHEET:

MADE BY:

CHKD. BY:

PAGE:

OF:

DATE:

DATE:

LOCATION:

ITEM:

REF./DWG NO:

satisfactorily be demonstrated that work in the type of joint under study dictates a minimum overlap length to wall depth ratio of 7:1, then a minimum wall of 140 mm is required to be detailed.

WIMPEY OFFSHORE ENGINEERS & CONSTRUCTORS LIMITED
140 CAUSEWAYEND
ABERDEEN AB2 3TN

TELEPHONE 0224 637755
TELEX 739180

CALCULATIONS

CLIENT: CIRIA VEG

CONTRACT:		VOLUME:	PAGE:
CONTRACT/ACCOUNT NO:		SHEET:	OF:
		MADE BY:	DATE:
		CHKD. BY:	DATE:
LOCATION:	ITEM:	REF./DWG NO:	

Example 3!

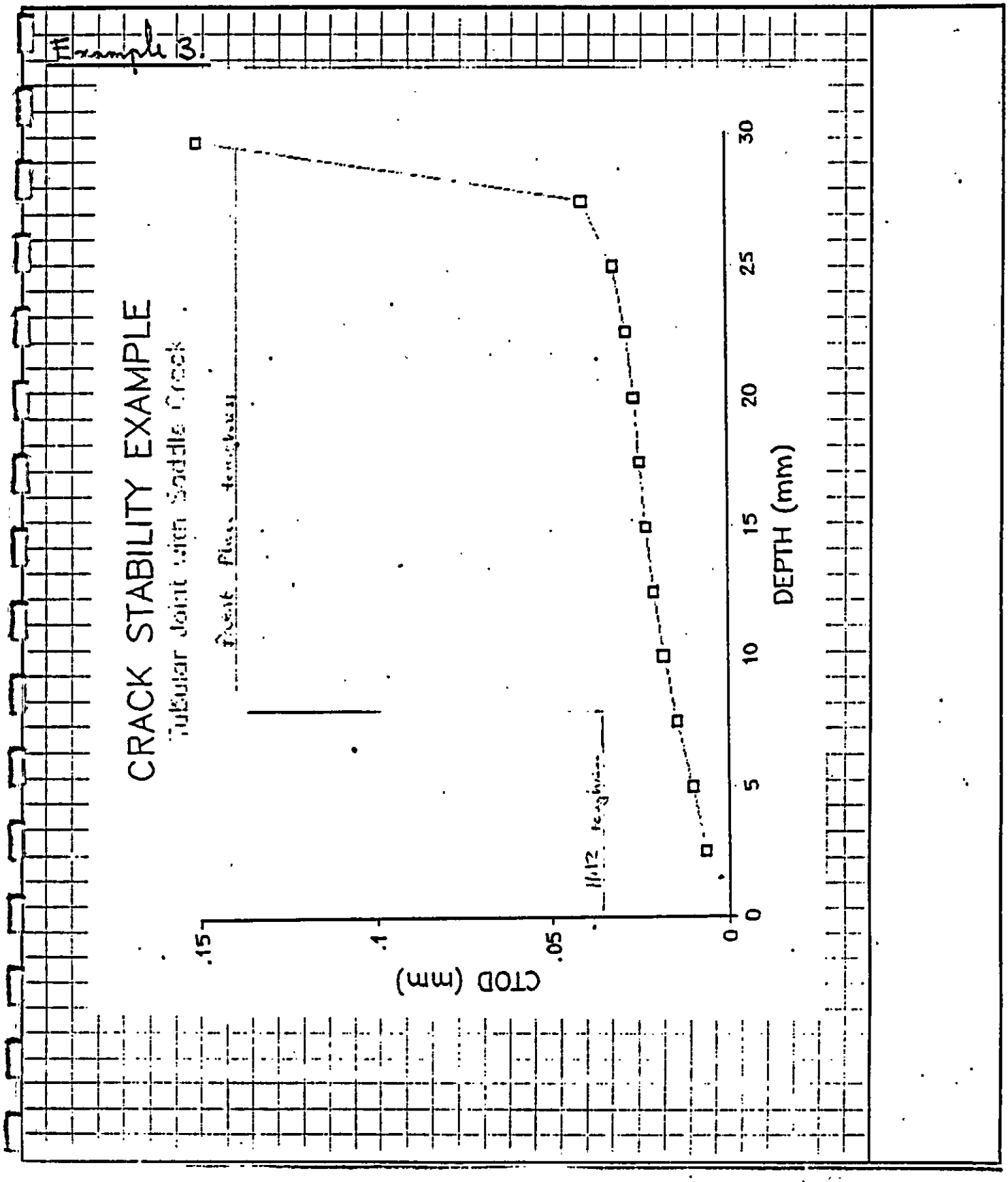

WIMPEY OFFSHORE ENGINEERS & CONSTRUCTORS LIMITED
140 CAUSEWAYEND
ABERDEEN AB2 3TN

TELEPHONE 0224 637755
TELEX 739190

CALCULATIONS

CLIENT: CIRIA JEG

CONTRACT:

CONTRACT/ACCOUNT NO:

VOLUME: PAGE: 15

SHEET: OF:

MADE BY: JEF DATE: JUNE 80

CHKD. BY: DATE:

LOCATION: ITEM: REF/DWG NO:

EXAMPLE 4 - DAMAGED MEMBER ASSESSMENT

The jacket structure shown on Figure A3.4 is considered to have a damaged diagonal brace due to impact from a dropped object. The damage to the member is assumed to take the form of bending damage with a bilinear deflected shape with $\delta_0/L = 0.04$. The member is also assumed to have been deflected downwards in the vertical plane. The residual strength and stiffness of the member are to be assessed, based on the methods discussed in section 6.1, and the effect on the structural integrity of the jacket quantified. The reference number of the damaged member in the jacket computer model is 83, surrounding members on the jacket computer model are identified on Figure A3.5

WIMPEY OFFSHORE ENGINEERS & CONSTRUCTORS LIMITED
140 CAUSEWAYEND
ABERDEEN AB2 3TN

TELEPHONE 0224 637755
TELEX 739180

CALCULATIONS

CLIENT: CIRIA UEG

CONTRACT:

CONTRACT/ACCOUNT NO:

VOLUME:

SHEET:

MADE BY: JBF

CHKD. BY:

PAGE: 16

OF:

DATE: JUNE 86

DATE:

LOCATION:

ITEM:

REF./DWG NO:

The damaged member properties are:-

outer diameter	D =	457.2 mm
wall thickness	t =	23.8 mm
length	L =	18.39 m
yield stress	F_y =	350 N/mm^2
Young's modulus	E =	2.1×10^5 N/mm^2

Analysis of the jacket for storm loading with member B3 in an undamaged state gives the following bending moment distribution:-

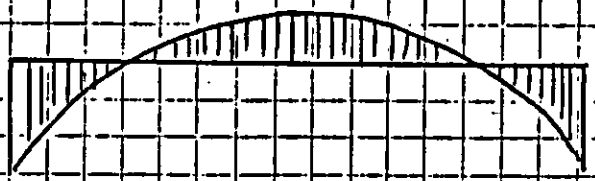

BM distribution for member B3 co-existing with the maximum axial compressive load

This shows the member to behave approximately as a fully fixed beam under the action of a lateral load. Therefore an effective length factor, K, of 0.6 (based on Figures 6.10 and 6.11) can be assumed.

WIMPEY OFFSHORE ENGINEERS & CONSTRUCTORS LIMITED
140 CAUSEWAYEND
ABERDEEN AB2 3TN

TELEPHONE 0224 637755
TELEX 739180

CALCULATIONS

CLIENT: CIRIA JEG
CONTRACT:
CONTRACT/ACCOUNT NO:
LOCATION:
ITEM:
VOLUME:
SHEET:
MADE BY: JEF
CHKD. BY:
REF./DWG NO:
PAGE: 17
OF:
DATE: JUNE 86
DATE:

The effect of the lateral load coexisting with the maximum axial compression is neglected. This is due to the ratio of applied to collapse lateral load being 0.1 and thus has a negligible reduction on ultimate axial compression. Having established the effective length factor the reduced slenderness can be calculated

$$\lambda = \left(\frac{F_y}{\pi^2 E}\right)^{\frac{1}{2}} \times \left(\frac{L}{r}\right) \times \left(\frac{K}{\pi}\right)$$

$$= \left(\frac{350}{2.1 \times 10^5}\right)^{\frac{1}{2}} \times \frac{1839 \times 10^3}{153.46} \times \frac{0.6}{\pi}$$

$$= 0.93$$

The member is therefore in the imperfection sensitive range with Euler and squash loads almost equal.

Two non-linear, elasto-plastic, large displacement analyses of the member were performed with the bending damage excluded and included respectively. The models is shown below and selected output

WIMPEY OFFSHORE ENGINEERS & CONSTRUCTORS LIMITED
140 CAUSEWAYEND
ABERDEEN AB2 3TN

TELEPHONE 0224 637755
TELEX 739180

CALCULATIONS

CLIENT: CIRIA UEG
CONTRACT:
CONTRACT/ACCOUNT NO:
LOCATION:
ITEM:
REF./DWG NO:

VOLUME:
SHEET:
MADE BY: JBF
CHKD. BY:
PAGE: 18.
OF:
DATE: JUNE 86
DATE:

from the computer analysis is given at the end of the example.

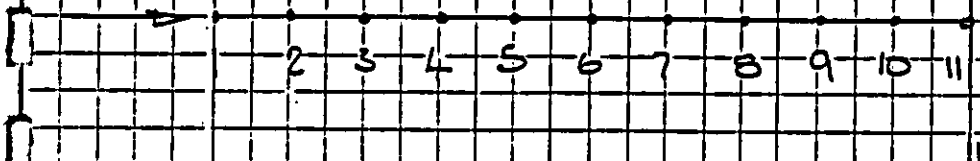

Node 1 is fixed vertically and rotationally. Node 11 is fixed horizontally and rotationally.

The results of the computer analysis are plotted on Figure A3.6, as axial load factor against axial shortening, for member 83 in its damaged and undamaged states respectively.

The jacket was then analysed with member 83 removed for storm load and unit load respectively. The storm load (loadcase 1) was chosen as the wave direction and phase angle which maximised the axial compression in member 83. The unit load (loadcase 2) was calculated as follows :-

WIMPEY OFFSHORE ENGINEERS & CONSTRUCTORS LIMITED
140 CAUSEWAYEND
ABERDEEN AB2 3TN

TELEPHONE 0224 637755
TELEX 739180

CALCULATIONS

CLIENT: CIRIA JEG

CONTRACT:

CONTRACT/ACCOUNT NO:

VOLUME:

SHEET:

MADE BY: JEF

CHKD. BY:

PAGE: 19.

OF:

DATE: JUNE 86

DATE:

LOCATION:

ITEM:

REF./DWG NO:

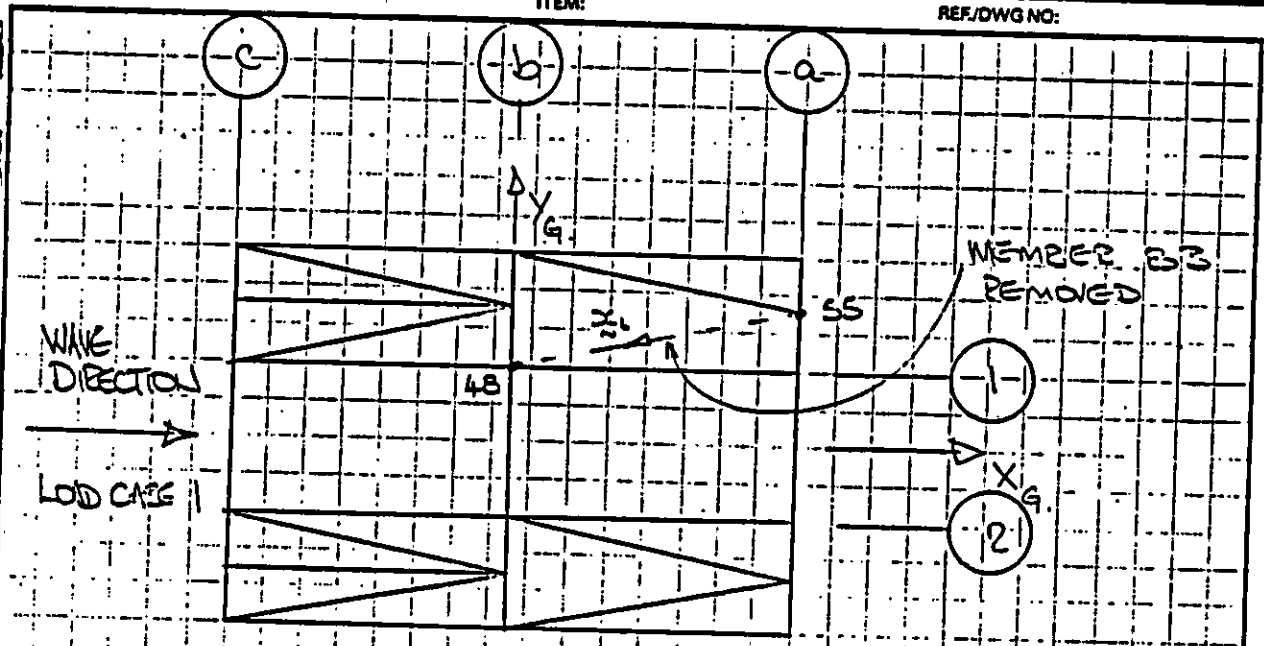

PLAN VIEW ON JACKET.

$$\underset{\sim}{x}_L = (\underset{\sim}{x}_{48} - \underset{\sim}{x}_{55}) / |\underset{\sim}{x}_{48} - \underset{\sim}{x}_{55}|$$

$$\underset{\sim}{x}_{48} - \underset{\sim}{x}_{55} = \begin{bmatrix} 0.0 \\ 6.299 \\ 30.176 \end{bmatrix} - \begin{bmatrix} 10.688 \\ 8.610 \\ 15.393 \end{bmatrix}$$

$$= \begin{bmatrix} -10.688 \\ -2.312 \\ 14.783 \end{bmatrix}$$

$$|\underset{\sim}{x}_{48} - \underset{\sim}{x}_{55}| = 18.39 \text{ m}$$

+ ms

$$\underset{\sim}{x}_L = \begin{bmatrix} -0.518 \\ -0.126 \\ 0.804 \end{bmatrix}$$

WIMPEY OFFSHORE ENGINEERS & CONSTRUCTORS LIMITED
140 CAUSEWAYEND
ABERDEEN AB2 3TN

TELEPHONE 0224 637755
TELEX 739180

CALCULATIONS

CLIENT: CIRIA UEG | VOLUME: | PAGE: 20
CONTRACT: | SHEET: | OF:
CONTRACT/ACCOUNT NO: | MADE BY: JEF | DATE: JUNE 86
| CHKD. BY: | DATE:
LOCATION: | ITEM: | REF./DWG NO:

Thus, for unit loads of 1000 N

$$\underset{\sim}{P}_{48} = \begin{bmatrix} -581.0 \\ -126.0 \\ 804.0 \end{bmatrix} \text{ N.}$$

$$\underset{\sim}{P}_{55} = \begin{bmatrix} 581.0 \\ 126.0 \\ -804.0 \end{bmatrix} \text{ N.}$$

The shortening of the gap between nodes 48 and 55 in the direction of the axis of member 83 was found from the displacements for loadcase 1 as:-

$$d_1 = \underset{\sim}{u}_{55} \cdot \underset{\sim}{x}_L - \underset{\sim}{u}_{48} \cdot \underset{\sim}{x}_L$$

where

$$\underset{\sim}{u}_{48} = \begin{bmatrix} 147.81 \\ 1.897 \\ -12.541 \end{bmatrix} \times 10^{-3} \text{ m}$$

$$\underset{\sim}{u}_{55} = \begin{bmatrix} 91.856 \\ 1.352 \\ -11.571 \end{bmatrix} \times 10^{-3} \text{ m}$$

Thus $d_1 = -62.869 + 96.243$

$= 33.373$ mm

WIMPEY OFFSHORE ENGINEERS & CONSTRUCTORS LIMITED
140 CAUSEWAYEND
ABERDEEN AB2 3TN

TELEPHONE 0224 637755
TELEX 739180

CALCULATIONS

CLIENT: CBIA UEG | VOLUME: | PAGE: 21
CONTRACT: | SHEET: | OF:
CONTRACT/ACCOUNT NO: | MADE BY: JCF | DATE: June 86
CHKD. BY: | DATE:
LOCATION: | ITEM: | REF./DWG NO:

The extension of the gap between nodes 48 and 55 in the direction of the axis of member B3 was found from the displacements for loadcase 2 as:-

$$d_2 = \underset{\sim}{u}_{48} \cdot \underset{\sim}{x}_1 - \underset{\sim}{u}_{55} \cdot \underset{\sim}{x}_1$$

where $\underset{\sim}{u}_{48} = \begin{bmatrix} -12.683 \\ -1.5772 \\ 3.1661 \end{bmatrix} \times 10^{-6}$ m

$\underset{\sim}{u}_{55} = \begin{bmatrix} 4.355 \\ 0.3962 \\ -2.7975 \end{bmatrix} \times 10^{-6}$ m

Thus $d_2 = (10.116 - 10.643) \times 10^{-3}$ mm/KN.

$= 20.76 \times 10^{-3}$ mm/KN

For compatibility between the damaged member and the remainder of the jacket structure to be achieved the following equation must be satisfied

$$e(P) = d_1 - P d_2$$

where $e(P)$ is the function describing the non-linear curve for the damaged

WIMPEY OFFSHORE ENGINEERS & CONSTRUCTORS LIMITED
140 CAUSEWAYEND
ABERDEEN AB2 3TN

TELEPHONE 0224 637755
TELEX 739180

CALCULATIONS

CLIENT: CIRIA UEG

VOLUME: PAGE: 22
SHEET: OF:
MADE BY: JBF DATE: JUNE 86
CHKD. BY: DATE:
CONTRACT:
CONTRACT/ACCOUNT NO:
LOCATION: ITEM: REF./DWG NO:

member shown on Figure A3.6. This equation can be solved iteratively by expressing ε as

$$\varepsilon_i = P_i a_i$$

where a_i is a linear flexibility coefficient

A first approximation of a_i is taken from Figure A3.6 as:-

$$a_1 = 8.376 \times 10^{-3} \text{ mm/KN}$$

thus

$$P_1 = d_1 / (d_2 + a_1)$$

$$= 33.373 / (20.76 \times 10^{-3} + 8.376 \times 10^{-3})$$

$$= 1145.4 \text{ KN}$$

thus $\varepsilon_1 = P a_1 = 9.59$ mm

load factor $= P_1 / P_{ult}$

$$= 1145.4 \times 10^3 / (350 \times 3240.5)$$

$$= 0.101$$

From Figure A3.6 the initial assumption for a_i is therefore satisfactory and the load in the damaged member to maintain compatibility is 1145 KN.

WIMPEY OFFSHORE ENGINEERS & CONSTRUCTORS LIMITED
140 CAUSEWAYEND
ABERDEEN AB2 3TN

TELEPHONE 0224 837755
TELEX 739180

CALCULATIONS

CLIENT: CIRIA UEG

CONTRACT:

CONTRACT/ACCOUNT NO:

VOLUME:

SHEET:

MADE BY: JEF

CHKD. BY:

PAGE: 23

OF:

DATE: JUNE 86

DATE:

LOCATION:

ITEM:

REF./DWG NO:

Results for a third loadcase were then created by factoring the results of loadcase 1 with 1.45 times the results of loadcase 2. The members on Frame 1 were then code checked to API / ASC by the jacket analysis computer program. The resulting utilisation values are shown on Figures A3.7 and A3.8 for loadcase 1 and 3 respectively. The computer output for the code checking is included at the end of this example.

The utilisation ratios show that an assumption of zero residual stiffness is conservative, in this case, leading to most utilisations exceeding unity and some exceeding the API / ASC factor of safety. However, by considering the residual stength and stiffness of the damaged member the utilisations of adjacent members are reduced to a safe level. This indicates that imediate repair is not necessary.

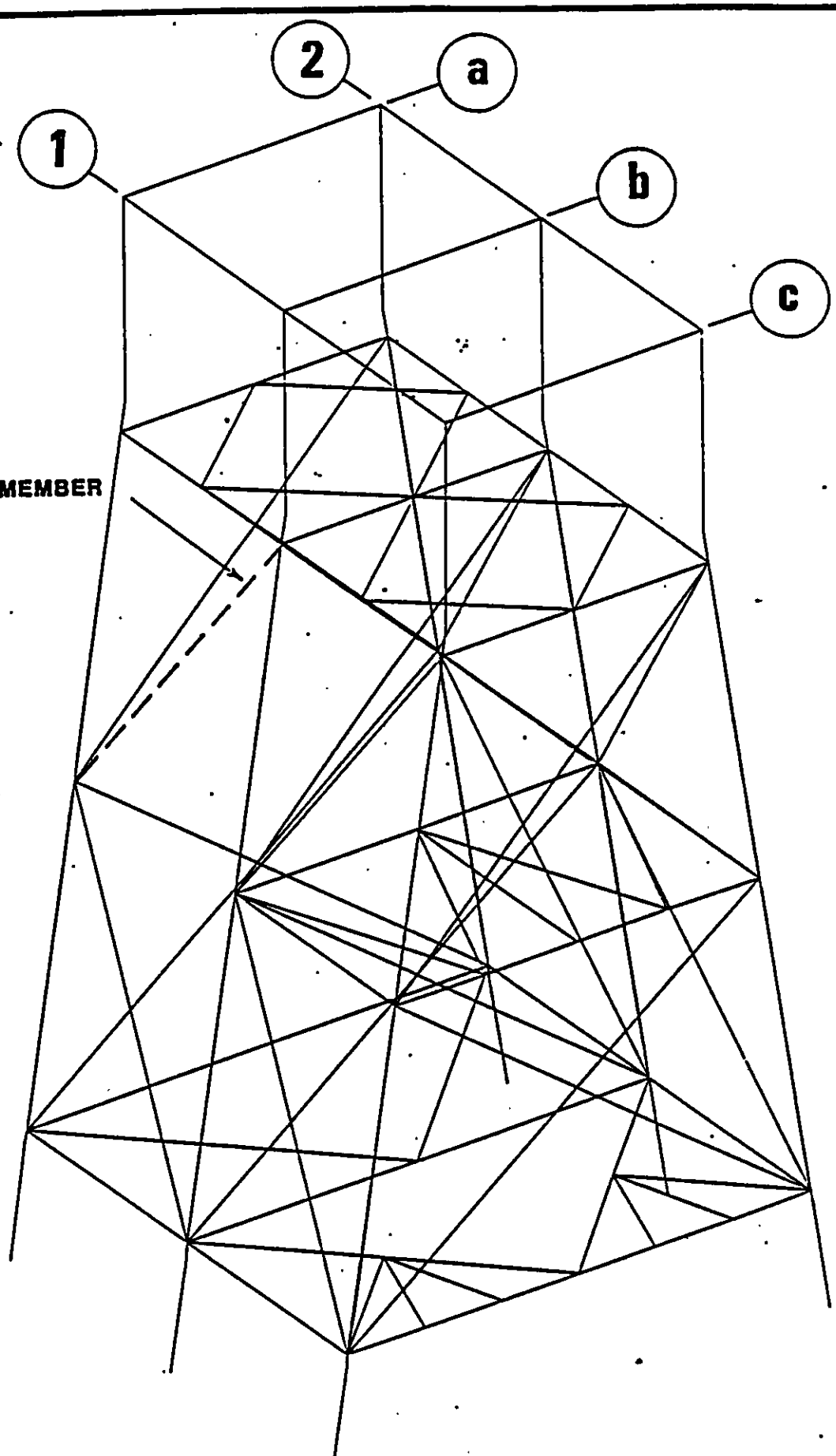

JACKET WITH DAMAGED MEMBER

WIMPEY OFFSHORE
REPORT No. WOL /

WIMPEY OFFSHORE

FIG. A3.4

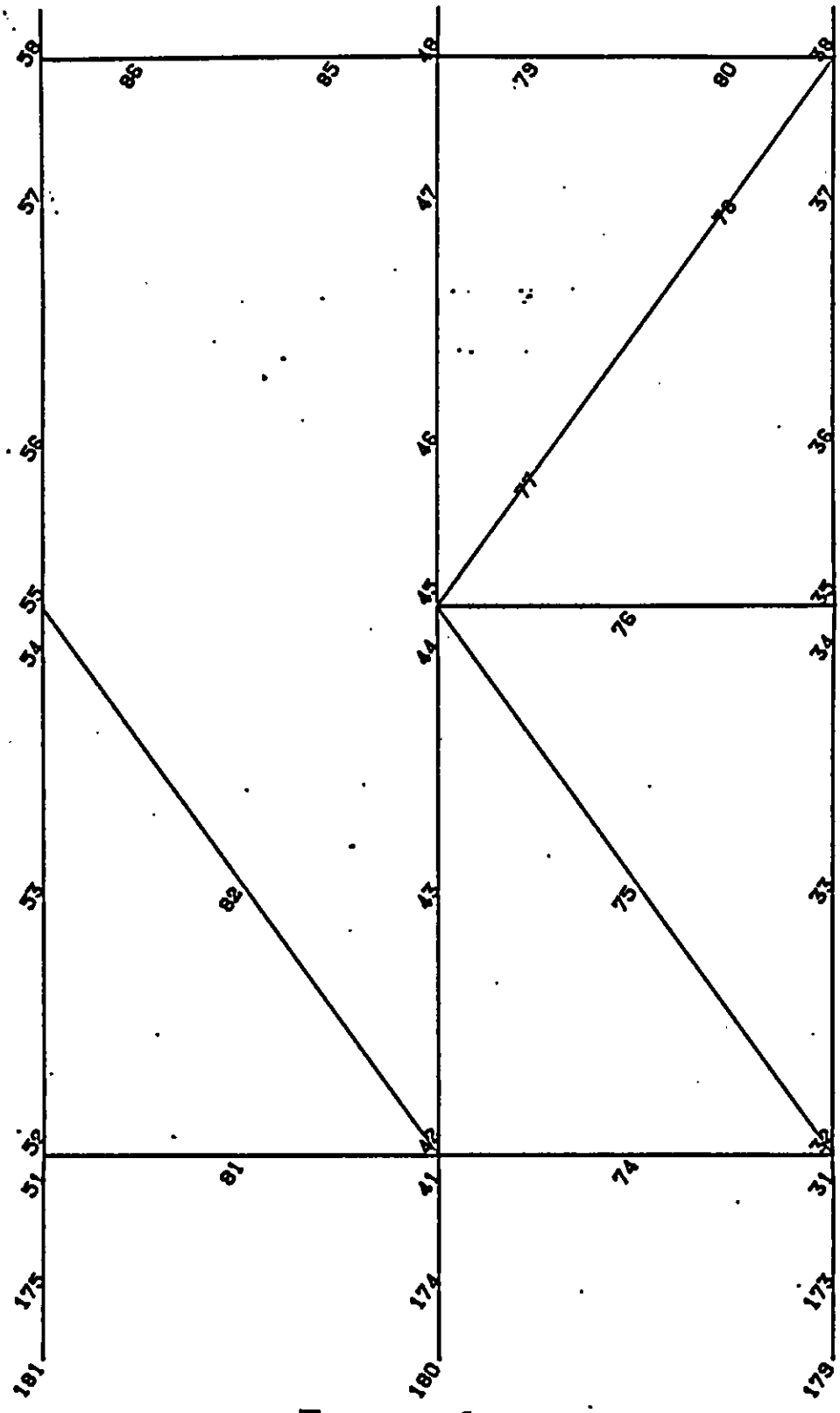

Frame 1
member numbering

WIMPEY OFFSHORE
REPORT No. WOL /

WIMPEY OFFSHORE

FIG. A3.5

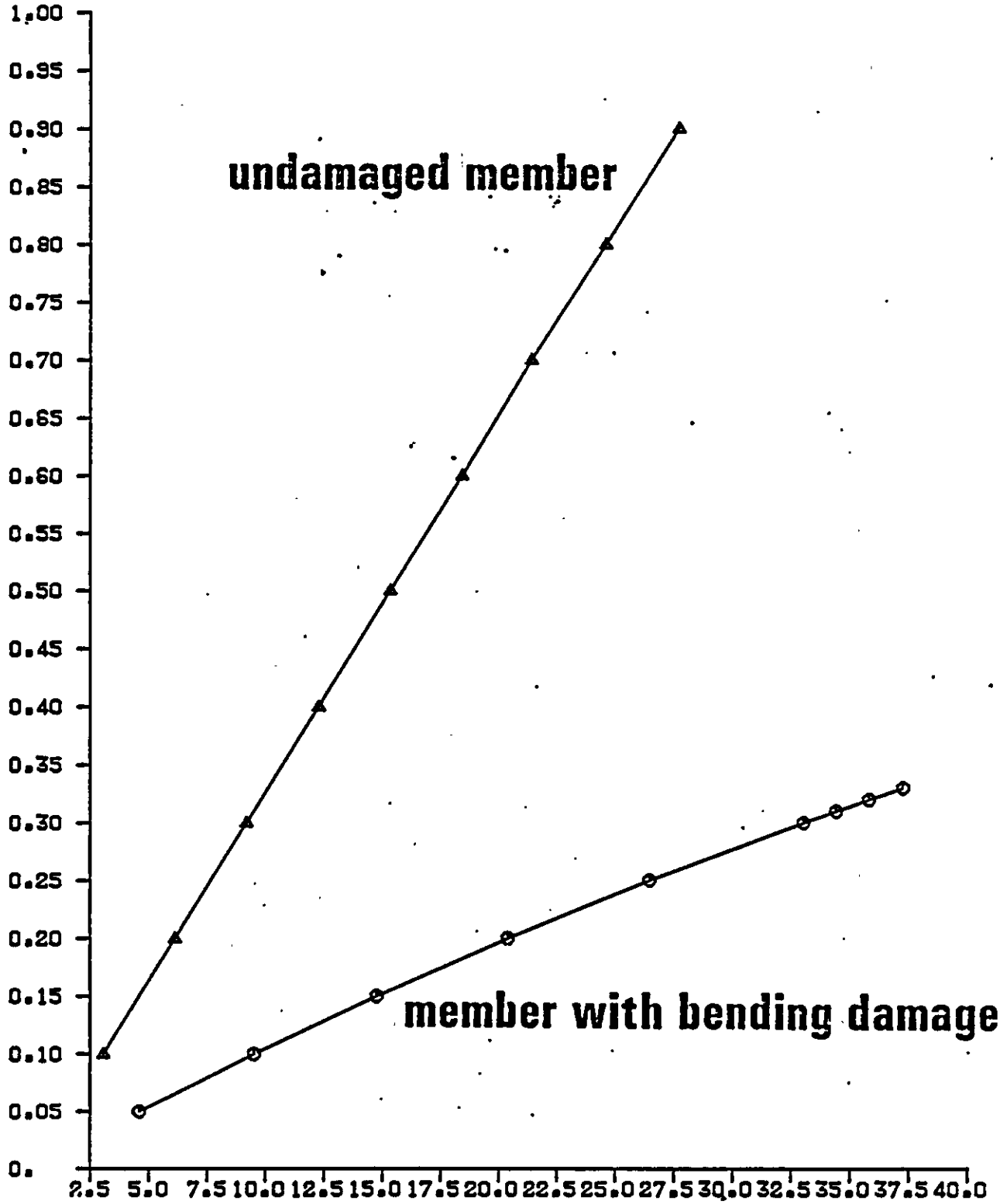

STIFFNESS OF DAMAGED TUBULAR

WIMPEY OFFSHORE
REPORT No. WOL /

FIG. A3.6

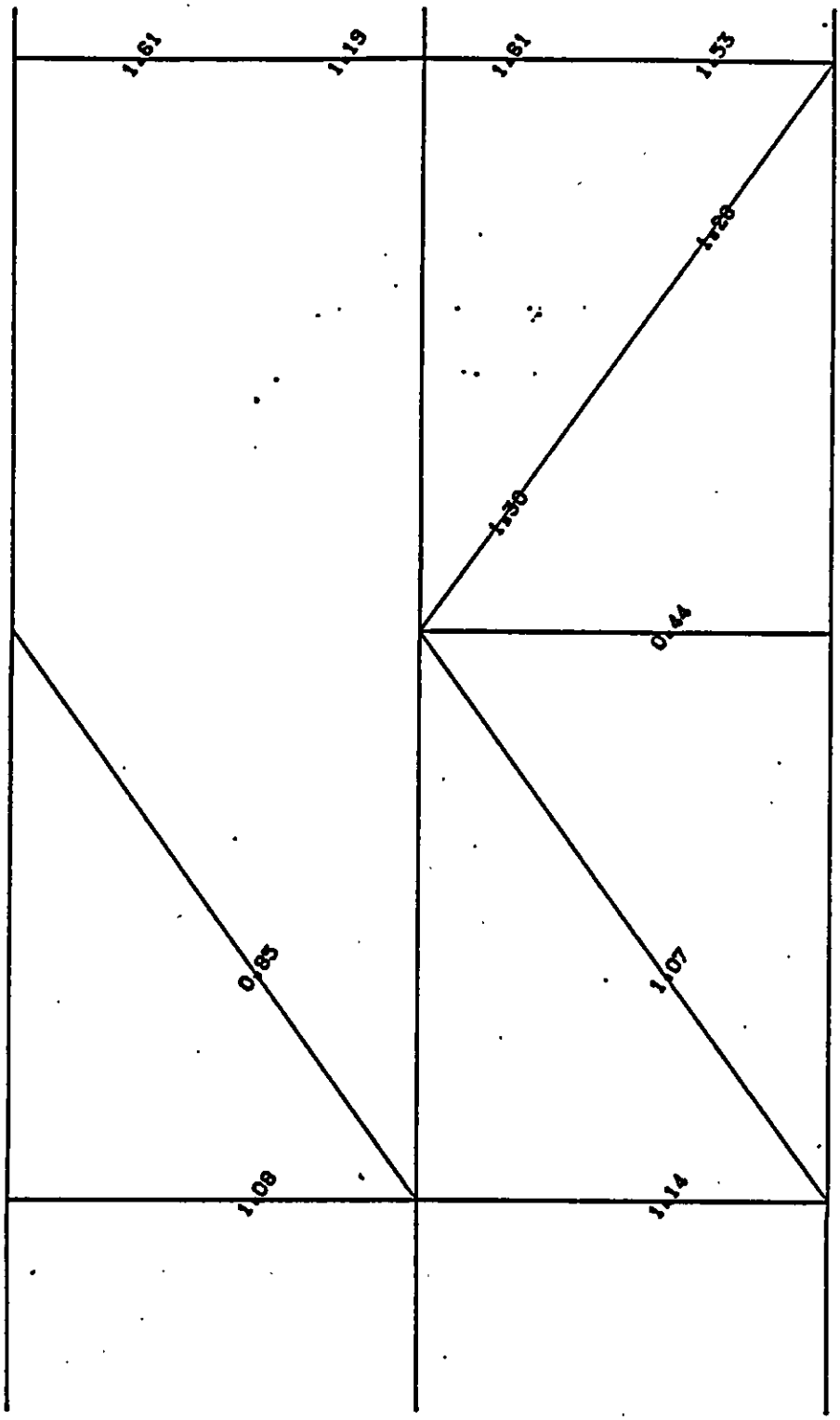

Frame 1

AISC utilisations with damaged member removed

WIMPEY OFFSHORE
REPORT No. WOL /

WIMPEY OFFSHORE

FIG. A3.7

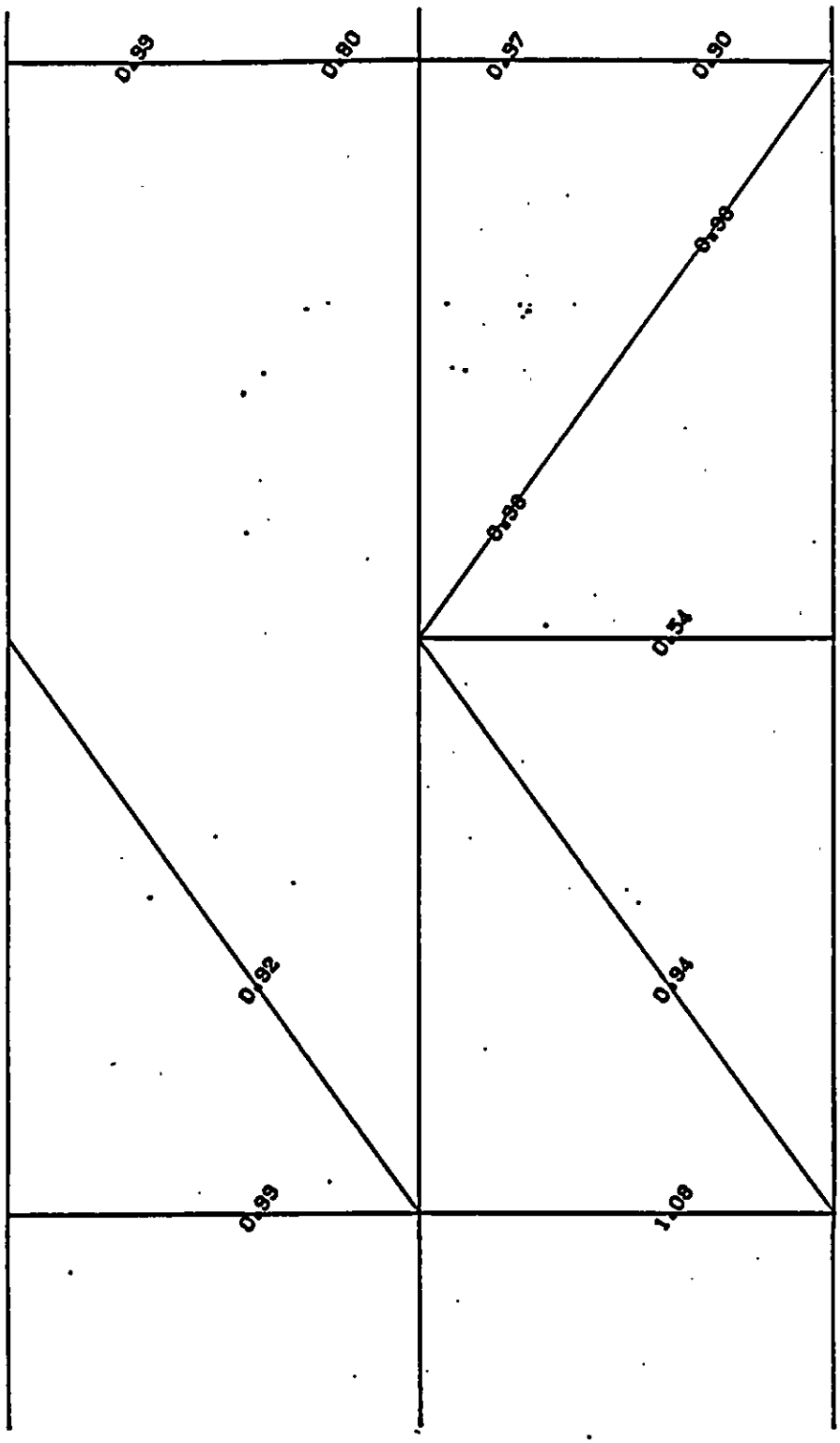

Frame 1

AISC utilisations with residual stiffness from damaged member

	WIMPEY OFFSHORE REPORT No. WOL /
	WIMPEY OFFSHORE FIG. A3-8

WIMPEY OFFSHORE ENGINEERS & CONSTRUCTORS LIMITED
140 CAUSEWAYEND
ABERDEEN AB2 3TN

TELEPHONE 0224 637755
TELEX 739180

CALCULATIONS

CLIENT: CIRIA UEG

VOLUME: | PAGE: 24.
SHEET: | OF:
MADE BY: JF | DATE: June 86
CHKD. BY: | DATE:
CONTRACT:
CONTRACT/ACCOUNT NO:
LOCATION: | ITEM: | REF./DWG NO:

REFERENCES.

(1) Design of tubular joints for offshore structures
CIRIA UEG, 1985

(2) Stress concentration factors for tubular complex joints
Lloyds Register 1985

(3) Efthymiou M. and Durkin S.
Stress concentrations in T/Y and gap/overlap K-joints
Behaviour of Offshore Structures,
Amsterdam 1985